องค์ประกอบทางเคมีที่มีฤทธิ์ทางชีวภาพจากพีพวนน้อยและนางแดง

นางสาวขนิษฐา ดีประหลาด

BIOACTIVE CHEMICAL CONSTITUENTS FROM *UVARIA RUFA* AND

MITREPHORA MAINGAYI

Miss Khanittha Deepralard

A Dissertation Submitted in Partial Fulfillment of the Requirements

for the Degree of Doctor of Philosophy Program in Pharmaceutical Chemistry and Natural Products

Faculty of Pharmaceutical Sciences

Chulalongkorn University

Academic Year 2006

ISBN 974-14-3463-4

Copyright of Chulalongkorn University

Thesis Title	BIOACTIVE CHEMICAL CONSTITUENTS FROM *UVARIA RUFA* AND *MITREPHORA MAINGAYI*
By	Miss Khanittha Deepralard
Field of Study	Pharmaceutical Chemistry and Natural Products
Thesis Advisor	Associate Professor Rutt Suttisri, Ph.D.
Thesis Co-Advisor	Associate Professor Thitima Pengsuparp, Ph.D.

Accepted by the Faculty of Pharmaceutical Sciences, Chulalongkorn University in Partial Fulfillment of the Requirements for the Doctoral Degree

............Pornpen Pramyoth............Dean of the Faculty of Pharmaceutical Sciences

(Associate Professor Pornpen Pramyothin, Ph.D.)

THESIS COMMITTEE

....Chairman

(Associate Professor Ekarin Saifah, Ph.D.)

....Thesis Advisor

(Associate Professor Rutt Suttisri, Ph.D.)

....Thesis Co-Advisor

(Associate Professor Thitima Pengsuparp, Ph.D.)

....Member

(Associate Professor Amorn Petsom, Ph.D.)

....Member

(Witchuda Thanakijcharoenpath, Ph.D.)

ขนิษฐา ดีประหลาด: องค์ประกอบทางเคมีที่มีฤทธิ์ทางชีวภาพจากพีพวนน้อยและนางแดง (BIOACTIVE CHEMICAL CONSTITUENTS FROM *UVARIA RUFA* AND *MITREPHORA MAINGAYI*)

อ. ที่ปรึกษา: รศ.ดร.รุทธ์ สุทธิศรี, อ. ที่ปรึกษาร่วม: รศ.ดร.ธิติมา เพ็งสุภาพ 244 หน้า. ISBN 974-14-3463-4.

การศึกษาองค์ประกอบทางเคมีจากพีพวนน้อย (วงศ์ Annonaceae) สามารถแยกสารบริสุทธิ์ได้ 18 ชนิด เป็นสารกลุ่มอนุพันธ์ของ cyclohexene, triterpenoid, flavonoid และสาร aromatic ester โดยสารอนุพันธ์ของ cyclohexene 5 ชนิด ได้แก่ (-)-pipoxide, 1-epizeylenol, ellipeiopsol B, zeylenol และ microcarpin B รวมทั้งสารกลุ่ม flavonoid glycoside 5 ชนิด ได้แก่ rutin, isoquercitrin, kaempferol 3-*O*-β-D-glucopyranoside, astragalin และ quercetin 3-*O*-β-D-glucopyranoside-6-acetate แยกได้จากส่วนใบ ส่วนสารอีก 8 ชนิด คือสารกลุ่ม flavone 3 ชนิด ได้แก่ tectochrysin, 7-*O*-methylwogonine และ 6,7-*O*,*O*-dimethylbaicalein สารกลุ่ม flavonone 2 ชนิด ได้แก่ 2,5-dihydroxy-7-methoxyflavanone และ eriodictyol สารกลุ่ม triterpenoid 2 ชนิด ได้แก่ glut-5(6)-ene-3β-ol และ taraxerol รวมทั้ง benzyl benzoate ถูกสกัดแยกได้จากส่วนลำต้น สำหรับการศึกษาองค์ประกอบทางเคมีของพืชวงศ์ Annonaceae อีกชนิดหนึ่ง คือนางแดง สามารถแยกสารได้ 10 ชนิด โดยเป็นสารกลุ่ม sesquiterpenoid คือ spathulenol สารกลุ่ม diterpenoid 2 ชนิด คือ kaurenoic acid และ didymooblongin กับสารกลุ่ม lignan 3 ชนิด คือ(+)-epieudesmin, (±)-eudesmin และ magnone A แยกได้จากส่วนใบ ส่วนอีก 4 ชนิด คือ สารกลุ่ม diterpene คือ pimaric acid สารกลุ่ม oxoaporphine alkaloid คือ liriodenine และ oxostephanine กับสารกลุ่ม flavanone คือ pinocembrin สกัดแยกได้จากส่วนลำต้น

สาร tectochrysin มีความเป็นพิษอย่างอ่อนต่อ human small cell lung carcinoma (NCI-H187) cell line ในขณะที่สาร 6,7-*O*,*O*-dimethylbaicalein มีความเป็นพิษต่อ breast cancer (BC) cell line kaurenoic acid มีความเป็นพิษอย่างอ่อนต่อ BC cell line ในขณะที่ oxoaporphine alkaloid ทั้ง 2 ชนิดคือ liriodenine และ oxostephanine มีความเป็นพิษอย่างแรงต่อ KB และ BC cell line มีสารหลายกลุ่มจากพืชทั้ง 2 ชนิดที่แสดงฤทธิ์ด้านเชื้อวัณโรค (*Mycobacterium tuberculosis* H37Ra) ได้แก่ zeylenol, taraxerol, benzyl benzoate, 6,7-*O*,*O*-dimethylbaicalein และ eriodictyol ซึ่งสกัดได้จากพีพวนน้อย และ kaurenoic acid, (+)-epieudesmin, liriodenine, oxostephanine และ pinocembrin ซึ่งสกัดได้จากนางแดง นอกจากนี้ยังพบว่า zeylenol, 6,7-*O*,*O*-dimethylbaicalein และ oxostephanine แสดงฤทธิ์ด้าน herpes simplex virus ส่วน quercetin 3-*O*-β-D-glucopyranoside-6-acetate และ isoquercitrin มีฤทธิ์ยับยั้งการสร้าง Advanced Glycation End-product (AGE) ได้ดีกว่า quercetin ซึ่งใช้เป็น positive control

สาขาวิชา ภสัชเคมีและผลิตภัณฑ์ธรรมชาติ ลายมือชื่อนิสิต......................

ปีการศึกษา 2549 ลายมือชื่ออาจารย์ที่ปรึกษา......................

  ลายมือชื่ออาจารย์ที่ปรึกษาร่วม......................

Investigation of the chemical constituents of *Uvaria rufa* (family Annonaceae) led to the isolation of eighteen compounds including cyclohexene derivatives, triterpenoids, flavonoids and an aromatic ester. From the leaves of this plant, five cyclohexene derivatives including (-)-pipoxide, 1-epizeylenol, ellipeiopsol B, zeylenol and microcarpin B, were isolated together with a series of flavonoid glycosides including rutin, isoquercitrin, kaempferol 3-*O*-β-D-glucopyranoside, astragalin and quercetin 3-*O*-β-D-glucopyranoside-6-acetate. From the stems, three flavones including tectochrysin, 7-*O*-methylwogonine, and 6,7-*O,O*-dimethylbaicalein, two flavanones (2,5-dihydroxy-7-methoxyflavanone and eriodictyol), two triterpenoids [glut-5(6)-ene-3β-ol and taraxerol] and benzyl benzoate were isolated. Similar study on another annonaceous plant, *Mitrephora maingayi*, afforded ten of its constituents including one sesquiterpenoid (spathulenol), two diterpenoids (kaurenoic acid and didymooblongin) and three lignans [(+)-epieudesmin, (±)-eudesmin and magnone A] from the leaves, whereas a diterpene acid (pimaric acid), two oxoaporphine alkaloids (liriodenine and oxostephanine), and a flavanone (pinocembrin) were obtained from the extraction of its stems.

Tectochrysin was mildly toxic against human small cell lung carcinoma (NCI-H187) cell line, whereas 6,7-*O,O*-dimethylbaicalein was cytotoxic to breast cancer (BC) cell line. Kaurenoic acid was weakly active against BC cell line, while both oxoaporphine alkaloids, liriodenine and oxostephanine, were strongly cytotoxic against KB and BC cell lines. Diverse types of compounds from these two plants were active against *Mycobacterium tuberculosis* H37Ra. Zeylenol, taraxerol, benzyl benzoate, 6,7-*O,O*-dimethylbaicalein and eriodictyol from *U. rufa*, together with kaurenoic acid, (+)-epieudesmin, liriodenine, oxostephanine and pinocembrin from *M. maingayi* exhibited antituberculosis activity. Zeylenol, 6,7-*O,O*-dimethylbaicalein and oxostephanine showed certain degrees of anti-herpes simplex activity. Quercetin 3-*O*-β-D-glucopyranoside-6-acetate and isoquercitrin were shown to be more potent inhibitors of Advanced Glycation End-product (AGE) formation than quercetin as the positive control.

Field of Study: Pharmaceutical Chemistry and Natural Products   Student's Signature............................

Academic Year: 2006   Advisor's Signature............................

Co-advisor's Signature............................

ACKNOWLEDGEMENTS

CONTENTS

5. Evaluation of Biological Activities

IV RESULTS AND DISCUSSION

Page

สถาบันวิทยบริการ

จุฬาลงกรณ์มหาวิทยาลัย

LIST OF TABLES

Page

LIST OF FIGURES

Page

Page

LIST OF SCHEMES

LIST OF ABBREVIATIONS AND SYMBOLS

$[\alpha]^{25}_{D}$	=	Specific rotation at 25 ^{o}C and sodium D line (589 nm)
µl	=	Microlitre
^{13}C NMR	=	Carbon-13 nuclear magnetic resonance
^{1}H-NMR	=	Proton magnetic resonance
acetone-d_6	=	Deuterated acetone
AGEs	=	Advanced glycation end-products
c	=	Concentration
CD$_3$OD	=	Deuterated methanol
CDCl$_3$	=	Deuterated chloroform
CFU	=	Colony forming unit
CH$_2$Cl$_2$	=	Dichloromethane
CHCl$_3$	=	Chloroform
cm	=	Centimetre
cm^{-1}	=	Reciprocal centimeter (unit of wave number)
DEPT	=	Distortionless enhancement by polarization transfer
DMSO-d_6	=	Deuterated dimethyl sulfoxide
ED$_{50}$	=	Effective dose 50 %
ESITOFMS	=	Electrospray ionized time of flight mass spectrometry
EtOAc	=	Ethyl acetate
G	=	Gram
KBr	=	Potassium bromide
Kg	=	Kilogram
L	=	Litre
m	=	Metre
M^{+}	=	Molecular ion
MeCN	=	Acetonitrile
MeOH	=	Methanol
MHz	=	Megahertz
MIC	=	Minimum inhibitory concentration

min	=	Minute
mm	=	Millimetre
mM	=	Millimolar
Mp	=	Melting point
nm	=	Nanometre
$^{\circ}$C	=	Degree celcius
α	=	Alpha
β	=	Beta
δ	=	Chemical shift

CHAPTER I

INTRODUCTION

The family Annonaceae, also called custard apple family or soursop family, is a flowering plant family consisting of trees, shrubs and climbers. With about 2,300-2,500 species in 120-130 genera, this is the largest family of the order Magnoliales. Annonaceous plants are concentrated in the tropics, with only one genus, *Asimina*, found in temperate regions. About 900 species are found in American continent, 450 species in Africa and the rest occur in Asia and Australia. Members of the Annonaceae are recognized by their alternate, exstipulate leaves, mostly trimerous flowers, numerous and often truncate free stamens, free carpels and seeds with ruminate endosperm (Hutchinson, 1964; Takhtajan, 1969; Leboeuf *et al.*, 1982).

Economically, this family is important as a source of edible fruits, for examples, the pawpaw (*Asimina*), cherimoya, sweetsop, soursop, custard apple and ilama (*Annona*), and plants in the genus *Cananga* and *Rollinia* are also grown for their edible fruits (Heywood, 1978). Oils from the seeds of some plants are used for the production of edible oil and soap, whereas woods are employed to produce the alcohol. Fragrant flowers of ylang ylang (*Cananga odorata*) are an important raw material in perfume industries. Moreover, the barks, leaves and roots of many species are used in folk medicine for various purposes. The spectrum of the compounds isolated from annonaceous species covers primary metabolites such as carbohydrates, lipids amino acids and proteins, and secondary metabolites such as essential oils, terpenes, polyhydroxy cyclohexene derivatives, alkaloids, dihydrochalcones, lactones, and phenolics. A large number of these compounds display biological activities i.e. anticancer, antimalarial, antimicrobial, antiprotozoal, antituberculosis and pesticidal activities (Leboeuf *et al.*, 1982).

The genus *Uvaria* and *Mitrephora* belonging to the family Annonaceae are distributed throughout tropical Asia, Africa and Australia. The genus *Uvaria* comprises 150 species, fourteen of which can be found in Thailand, as follows: *Uvaria cordata* (นมช้าง), *U. dac* (กล้วยอีเห็น), *U. fauveliana* (เงาะพวงผลกลม), *U. grandiflora* (ย่านนมควาย), *U. grandiflora* var. *grandiflora* (กล้วยหมูสัง), *U. grandiflora* var. *flava* (กล้วยหมูสังสีนวล), *U. hahnii* (นมควายน้อย), *U. hamiltonii* (กล้วยพังพอน), *U. hamiltonii* var. *kurzii* (นมแมวป่า), *U. leptopoda*

(กล้วยหมูสังเล็ก), *U. lurida* (กล้วยไอ้พอน), *U. microcarpa* (ก้นปิ๊ง), *U. pierrei* (พีพวน), and *U. rufa* (พีพวน น้อย). There are about 40 species in the genus *Mitrephora*, and 11 species are reportedly found in Thailand, as follows: *Mitrephora alba* (พรหมขาวพรม), *M. collinsae* (กิ่งขึ้น), *M. javanica* (สังหยู), *M. keithii* (กลาย), *M. maingayi* (นางแดง), *M. siriketiae* (มหาพรมราชินี), *M. thorelii* (ลำดวนดง), *M. tomentosa* (ดงคำขาว), *M. vandaeflora* (มะป่วน), *M. wangii* (ลำดวนดอย) and *M. winitii* (มหาพรม) (ปิยะ เฉลิมกลิ่น, 2544).

Various *Uvaria* species have been used as medicaments and tonics. A decoction of the root bark of *U. narum* is used to control fits in pregnant women at the time of delivery and also used for treating rheumatism, bowel complaints and eczema, whereas the leaves are recommended for jaundice, biliousness and fever (Parmar *et al*., 1994). *U. pandensis* (Nkunya, *et al.*, 1997) and *U. scheffleri* (Nkunya *et al.*, 1990) are used for the treatment of fever and stomach disorders. The roots of *U. chamae* growing in the tropical rain forest of Western Africa are reported to have purgative and febrifugal properties. A decoction of the root is drunk to ease severe abdominal pains and fever. Moreover, the ethanolic extract from the stem bark of this plant showed *in vivo* activity against P-388 lymphocytic leukemia in mouse and *in vitro* against nasopharynx human carcinoma cell line (Hufford and Lasswell Jr., 1976). The extracts of *U. afzelii* displayed potent antimicrobial activity against gram-positive and acid-fast bacteria (Hufford, Oguntimein and Baker, 1981). *U. elliotiana*, an African medicinal plant, possessed antibiotic activity against some fungi (Achenbach, 1986). Antimicrobial and cytotoxic activities were also present in the root extract of *U. angolensis* (Hufford and Oguntimein, 1980). There are many reports showing the activity against the multidrug-resistant K1 strain of *Plasmodium falciparum* of various *Uvaria* extracts, namely *U. dependens*, *U. faulknearae, U. kirkii, U. laptocladon, U. lucida, U. scheffleri* and *U. tanzaniae* (Weenen *et al.*, 1990; Weenen, Nkunya and Mgani, 1991; Nkunya, Waibel and Achenbach, 1993).

The first phytochemical study on the genus *Uvaria* was presented in 1968 (Holland *et al.*, 1968), and during the past three decades numerous chemical studies on this plant genus have revealed the presence of various types of compounds. Physiologically active compounds isolated from *Uvaria* species are terpenoids, polyhydroxy cyclohexene derivatives, alkaloids, acetogenins and flavonoids. These compounds displayed both potent bioactivities and interesting chemical structures (Parmar *et al*., 1994).

On the other hand, there are currently only 6 records of the phytochemical and

pharmacological investigations on the plants of the genus *Mitrephora*. A number of aporphine alkaloids were isolated from *M. maingayi*, some of which showed cytotoxicity and anticancer activity (Lee, Xu, and Goh, 1999; Yu *et al.*, 2005). Two polyacetylene carboxylic acids and two diterpenoids from *M. celebica* demonstrated significant activity against methicillin-resistant *Staphylococcus aureus* and *Mycobacterium smegmatis* (Zgoda *et al.*, 2001; 2002). Pimarane and kaurane diterpenoids were reported as the constituents of *M. tomentosa* (Supudompol *et al.*, 2004), whereas three cytotoxic trachylobane diterpenoids were found from *M. glabra* (Li *et al.*, 2005). Recently, an alkaloid with novel skeleton, maingayinine, was isolated from *M. maingayi* (Yu *et al.*, 2005).

Uvaria rufa Blume or "Phi Phuan Noi" is a climbing shrub, often 5-9 m in height, growing in deciduous and evergreen forest of Thailand. The younger parts and lower surfaces of the leaves are rather hairy, with stellately arranged, rusty, short hairs. The leaves, borne on very short stalks, are alternate, oblong-ovate to oblong-lanceolate, 8-16 cm long, with pointed tip and rounded or heart-shaped base. The flowers are extra-axillary, solitary or 2 or 3 in depauperate cymes, usually about 1.5-2 cm in diameter. Its red fruit is edible, and has an agreeable flavor. It is oval or kidney-shaped, hairy and usually about 4-5 cm in length and 3.5-4 cm in diameter, borne in rounded clusters. The rind is about 6.8 cm thick and inside of this is a whitish, sub-acid, translucent, somewhat aromatic pulp. There are 2 rows of seeds, which are flattened, oblong, shiny smooth and about 1-2 cm long by 0.7-0.9 cm wide (ปิยะ เฉลิมกลิ่น, 2544).

Preliminary bioactivity screening has revealed that the hexane and dichloromethane extracts of the leaves of *U. rufa* exhibited cytotoxicity against human small cell lung cancer (NCI-H187) at the IC_{50} values of 1.03 and 3.98 µg/ml, respectively, as well as antimycobacterial activity against *Mycobacterium tuberculosis* with the MIC values of 50 and 12.5 µg/ml, respectively. The hexane and dichloromethane extracts of its stem also exhibited cytotoxic activity against NCI-H187 cancer cell line at the IC_{50} values of 0.09 and 1.18 µg/ml, respectively, as well as antimycobacterial activity with the MIC values of 25 and 50 µg/ml, respectively.

Another annonaceous plant investigated in this study, *Mitrephora maingayi* Hook. F. & Thomson or "Nang Dang", is an erect tree, 20-30 m in height. Its shining leaves are elliptic-ovate-oblong-lanceolate, 4-6.5 cm by 14-20 cm, with their midrib raised on the upper surface. The petiole is 4-7 cm in length. Its monoecious flowers are yellow cream

with red-purple stripes. The pedicels are 2 cm in length. Each flower has three sepals and two whorls of three petals, showing valvate aestivation. The outer petals are large, free and spreading, whereas the inner petals are smaller, rhombic, clawed and are apically connivent to form a mitriform dome over the reproductive organs. The fruits are aggregate, broadly rounded, 4-5 cm in diameter, with 10-12 seeds. This plant can be found growing in deciduous forest in the north and south of Thailand (ปิยะ เฉลิมกลิ่น, 2544).

Preliminary bioactivity screening has revealed the hexane and dichloromethane extracts of its leaves as exhibiting cytotoxic activity against human small cell lung cancer (NCI-H187) at the IC_{50} values of 11.94 and 14.03 µg/ml, respectively, as well as antituberculosis activity at the MIC values of 25 and 200 µg/ml, respectively. The dichloromethane extract of the stem exhibited cytotoxicity against lung cancer (NCI-H187) cell line at the IC_{50} value of 8.10 µg/ml, whereas both hexane and dichloromethane extracts of the stem were active against *Mycobacterium tuberculosis* at the same MIC value of 100 µg/ml.

Therefore, these plants were selected for further investigation of their bioactive chemical constituents. The purposes of this research are as follows:

1.   Isolation and purification of compounds from the stems and leaves of *Uvaria rufa* and *Mitrephora maingayi*.

2.   Determination of chemical structures of the isolated compounds.

3.   Evaluation of biological activities of the isolated compounds.

Figure 1. *Uvaria rufa* Blume

Figure 2. *Mitrephora maingayi* Hook. F. & Thomson

CHAPTER II

HISTORICAL

Chemical studies on the family Annonaceae which have intensified in the past three decades revealed various compound types of both the primary metabolites such as carbohydrates, lipids, amino acids and proteins, and the secondary metabolites such as acetogenins, alkaloids, flavonoids, polyhydroxy cyclohexene derivatives and terpenoids (Leboeuf *et al.*, 1982; Parmar *et al.*, 1994). A large number of these compounds displayed biological activities i.e. anticancer, antimalarial, antimicrobial, antiprotozoal, antituberculosis and pesticidal activities, and several of them were shown to have unique and interesting skeletons as well. Acetogenins, oxoaporphine alkaloids and *C*-benzylated flavonoids are compound types which seem to be limited mostly to the genus *Uvaria,* whereas the diterpenoid derivatives of the kaurane series which richly occur in the genera *Annona* and *Xylopia,* can certainly be used as chemotaxonomic markers to illustrate the relationships among annonaceous species or the ones belonging to phylogenetically related families such as those of the order Magnoliales, Laurales, Piperales, Aristolochiales, Ranunculales and Papaverales (Leboeuf *et al.*, 1982).

In this chapter, reviews of diterpenoids (labdane, halimane, clerodane, pimarane, kaurane, beyerane, atisane and trachylobane-type diterpenoids) and flavonoids (focusing on flavanone, flavone and flavonol) obtained from annonaceous plants, as well as a summary of the search for active natural compounds which inhibited advanced glycation end-product (AGE) formation, are presented below.

Diterpenoids of the family Annonaceae

Being the well-known source of bioactive acetogenins, alkaloids and dihydrochalcones, the Annonaceae is also a source of diterpenoids, several of which displayed interesting bioactivities such as cytotoxicity against cancer cell lines, antifeedant, antimicrobial and anti-HIV activities.

Two labdane diterpenes, 17-*O*-acetylacuminolide **(1.1)** and acuminolide **(1.2)**, obtained from *Neouvaria acuminatissima,* were reported to be cytotoxic (Lee *et al.*, 1995).

16-Oxo-cleroda-3,13-dien-15-oic acid **(1.25)** and 16α-Hydroxy-cleroda-3,13*Z*-

dien-15,16-olide **(1.27)**, isolated from the leaves of *Polyalthia longifolia,* exhibited antifeedant activity against casterlooper (*Achaea janata*) (Phadnis *et al.*, 1988). Several clerodane-type diterpenoids found as the constituents of *P. barnesii* (Ma *et al.*, 1994) and *P. longifolia* var. *pendula* (Chen *et al.*, 2000b) were also reported to be cytotoxic.

Activity-guided fractionation of the stem bark of *Annona senegalensis* gave a series of bioactive *ent*-kaurenoids. Kaurenoic acid **(1.101)** showed selective and significant cytotoxicity against MCF-7 (breast cancer) cells (ED_{50} 1 µg/ml), whereas 16β,17-diacetoxy-*ent*-kauran-19-oic acid **(1.55)** and *ent*-19-carbomethoxy-kauran-19-oic acid **(1.89)** exhibited selective cytotoxicity against PC-3 (prostate cancer) cells with weaker potency (ED_{50} 17-18 µg/ml) (Fatope *et al.*, 1996). 16β,17-Dihydroxy-*ent*-kauran-19-oic acid **(1.57)**, isolated from the fresh fruits of *A. squamosa* and methyl-16α-hydro-19-al-*ent*-kauran-17-oate **(1.102)** furnished from another species, *A. glabra,* inhibited HIV replication in H9 lymphocyte cells (Chang *et al.*, 1998; Wu *et al.*, 1996). In addition, 16α,17-dihydroxy-*ent*-kauran-19-oic acid **(1.47)** obtained from the fruits of *A. glabra* potently inhibited HIV-reverse transcriptase (Chang *et al.*, 1998). The same compound and kaurenoic acid **(1.101)** isolated from *A. squamosa* stem were also able to completely inhibit rabbit platelet aggregation (Yang *et al.*, 2002).

Investigation of the extract from *Mitrephora celebica* revealed two diterpenoids, *ent*-trachyloban-19-oic acid **(1.112)** and kaurenoic acid **(1.101)**. Both compounds were found to be active against methicillin-resistant *Staphylococcus aureus* and *Mycobacterium smegmatis* (Zgoda *et al.*, 2001; Zgoda-Pols *et al.*, 2002). Recently, an interesting series of *ent*-trachylobane diterpenoids, mitrephorones A-C **(1.120)**-**(1.122)**, isolated from *Mitrephora glabra,* displayed cytotoxic and antimicrobial activities. Mitrephorone A **(1.120)** possessed a hexacyclic ring system with adjacent ketone moieties and an oxetane ring, both of which are unprecedented among trachylobanes (Li *et al.*, 2005).

The diterpenoid types reported as constituents within this family are labdanes, halimanes, clerodanes, pimaranes, kauranes, beyeranes, atisanes and trachylobanes. The distribution of these compounds in the family Annonaceae is presented in **Table 1** and their chemical structures are shown in **Figure 3**.

Table 1. Diterpenoids in the family Annonaceae

Compound Name	Sources	Plant Part	References
Labdanes 17-*O*-Acetylacuminolide (**1.1**)	*Neouvaria acuminatissima*	Stem bark	Lee *et al.*, 1995
Acuminolide (**1.2**)	*N. acuminatissima*	Stem bark	Lee *et al.*, 1995
ent-13′-Nor-13′-oxomethylisoozate dimer (**1.3**)	*Xylopia aromatica*	Bark	Martin *et al.*, 1999
ent-Labda-8(17),13(16),14-trien-18-oic acid (**1.4**)	*X. aromatica*	Bark	Martin *et al.*, 1999
ent-Labdan-13,16-diol-8(17),14-dien-18-oic acid (**1.5**)	*X. aromatica*	Fruit	Moraes and Roque, 1988
ent-Methylisoozate dimer (**1.6**)	*X. aromatica*	Bark	Martin *et al.*, 1999
Labd-13*E*-en-8-ol-15-oic acid (**1.7**)	*Polyalthia longifolia* var. *pendula*	Leaves	Chen *et al.*, 2000b
Spiroacuminolide (**1.8**)	*N. acuminatissima*	Stem bark	Lee *et al.*, 1995
Halimanes 16-Hydroxy-*ent*-halima-5(10),13-dien-15,16-olide (**1.9**)	*P. longifolia*	Stem bark	Hara *et al.*, 1995
16-Oxo-*ent*-halima-5(10),13-dien-15-oic acid (**1.10**)	*P. longifolia*	Stem bark	Hara *et al.*, 1995
3β,5β,16α-Trihydroxyhalima-13(14)-en-15,16-olide (**1.11**)	*P. longifolia* var. *pendula*	Leaves	Chen *et al.*, 2000b
ent-Halima-1(10),13-dien-15,16-olide (**1.12**)	*P. longifolia*	Stem bark	Hara *et al.*, 1995
ent-Halima-1(10),13*E*-dien-15-oic acid (**1.13**)	*P. longifolia*	Stem bark	Hara *et al.*, 1995
ent-Halima-5(10),13-dien-15,16-olide (**1.14**)	*P. longifolia*	Stem bark	Hara *et al.*, 1995

Table 1. Diterpenoids in the family Annonaceae (continued)

Compound Name	Sources	Plant Part	References
ent-Halima-5(10),13-dien-15-oic acid (**1.15**)	*P. longifolia*	Stem bark	Hara *et al*., 1995
Clerodanes (4→2)-*abeo*-16(*R*)-2,3Z-Kolavadien-15,16-olide-3-al (**1.16**)	*P. viridis*	Bark	Kijjoa *et al.*, 1990; 1993
(4→2)-*abeo*-16(*S*)-2,3Z-Kolavadien-15,16-olide-3-al (**1.17**)	*P. viridis*	Bark	Kijjoa *et al.*, 1990; 1993
14,15-Bisnor-3,11*E*- kolavadien-13-one (**1.18**)	*P. viridis*	Bark	Kijjoa *et al.*, 1990
16(*R*)-3,13Z-Kolavadien-15,16-olide (**1.19**)	*P. viridis*	Bark	Kijjoa *et al.*, 1990
16(*R*)-3,13Z-Kolavadien-15,16-olide-2-one (**1.20**)	*P. viridis*	Bark	Kijjoa *et al.*, 1990; 1993
16(*S*)-3,13Z-Kolavadien-15,16-olide-2-one (**1.21**)	*P. viridis*	Bark	Kijjoa *et al.*, 1990; 1993
16-Acetoxy-cleroda-3,13-dien-15,16-olide (**1.22**)	*Cyathocalyx zeylanica*	Stem bark	Wijeratne *et al.*, 1995
16-Hydroxy-cleroda-3,13-dien-15,16-olide (**1.23**)	*P. longifolia*	Stem bark	Hara *et al.*, 1995
16-Hydroxy-cleroda-4(18),13-dien-15,16-olide (**1.24**)	*P. longifolia*	Stem bark	Hara *et al.*, 1995
16-Oxo-cleroda-3,13-dien-15-oic acid (**1.25**)	*P. longifolia*	Stem bark	Hara *et al.*, 1995
	P. longifolia	Leaves	Phadnis *et al.*, 1988
16-Oxo-cleroda-4(18),13-dien-15-oic acid (**1.26**)	*P. longifolia*	Stem bark	Hara *et al.*, 1995
16α-Hydroxy-cleroda-3,13Z-dien-15,16-olide (**1.27**)	*P. longifolia*	Leaves	Phadnis *et al.*, 1988; Chakrabarty and Nath, 1992
	P. cheliensis	Stem bark	Hao *et al.*, 1995

Table 1. Diterpenoids in the family Annonaceae (continued)

Compound Name	Sources	Plant Part	References
16α-Hydroxy-cleroda-4(18),13(14)*Z*-dien-15,16-olide **(1.28)**	*P. cheliensis*	Stem bark	Hao *et al.*, 1995
16α-Methoxy-cleroda-3,13*Z*-dien-15,16-olide **(1.29)**	*P. longifolia*	Leaves	Chakrabarty and Nath, 1992
2,18,19-Triacetoxy-(-)-cleroda-13(16),14-diene-18,19-oxide **(1.30)**	*Monodora brevipes*	Seed	Etse *et al.*, 1989
2-Isobutoxy-18,19-diacetoxy-(-)-cleroda-13(16),14-diene-18,19-oxide **(1.31)**	*M. brevipes*	Seed	Etse *et al.*, 1989
2-Oxo-18-acetoxy-10α,17α,19α,20β-(-)-cleroda-3,13(16),14-triene **(1.32)**	*M. brevipes*	Seed	Etse *et al.*, 1989
2-Oxokolavenic acid **(1.33)**	*X. acutiflora*	Stem bark	Hasan, Healey and Waterman, 1985
3,12*E*-Kolavadien-15-oic acid-16-al **(1.34)**	*P. viridis*	Bark	Kijjoa *et al.*, 1993
3,13*E*-Kolavadien-15-oic acid **(1.35)**	*P. viridis*	Bark	Kijjoa *et al.*, 1990
3,13-Kolavadien-15-oic acid-16-al **(1.36)**	*P. viridis*	Bark	Kijjoa *et al.*, 1993
3-Hydroxy-cleroda-4(18),13*Z*-dien-15-oic acid **(1.37)**	*Cyathocalyx zeylanica*	Stem bark	Wijeratne *et al.*, 1995
Cleroda-3,13-dien-15,16-olide **(1.38)**	*P. longifolia*	Stem bark	Hara *et al.*, 1995
Cleroda-3,13*E*-dien-15-oic acid **(1.39)**	*P. cheliensis*	Stem bark	Hao *et al.*, 1995
	P. longifolia	Stem bark	Hara *et al.*, 1995
Cleroda-4(18),13(14)*E*-dien-15-oic acid **(1.40)**	*P. cheliensis*	Stem bark	Hao *et al.*, 1995
Cleroda-4(18),13-dien-15,16-olide **(1.41)**	*P. longifolia*	Stem bark	Hara *et al.*, 1995
Cleroda-4(18),13*E*-dien-15-oic acid **(1.42)**	*P. longifolia*	Stem bark	Hara *et al.*, 1995
(1.43)	*P. viridis*	Bark	Kijjoa *et al.*, 1993
(1.44)	*P. viridis*	Bark	Kijjoa *et al.*, 1993

Table 1. Diterpenoids in the family Annonaceae (continued)

Compound Name	Sources	Plant Part	References
Kauranes 15-Oxo-*ent*-kaur-16-en-19-oic acid **(1.45)**	*X. aethiopica*	Fruit	Ekong, Olagbemi and Odutola, 1969
	X. aethiopica	Stem bark	Harrigan *et al.*, 1994
	X. sericea	Seed	Takahashi *et al.*, 2001
16α,17-Dihydroxy-*ent*-kauran-19-al **(1.46)**	*A. squamosa*	Stem	Yang *et al.*, 2002
16α,17-Dihydroxy-*ent*-kauran-19-oic acid **(1.47)**	*A. squamosa*	Fruit	Wu *et al.*, 1996
	A. squamosa	Stem	Yang *et al.*, 2002
	A. glabra	Fruit	Chang *et al.*, 1998
16α-Hydro-19-al-*ent*-kauran-17-methyl ester **(1.48)**	*A. glabra*	Stem	Chen *et al.*, 2000a
16α-Hydro-19-al-*ent*-kauran-17-oic acid **(1.49)**	*A. glabra*	Fruit	Chang *et al.*, 1998
	A. glabra	Stem	Chen *et al.*, 2000a
	A. squamosa	Stem	Yang *et al.*, 2002
16α-Hydro-*ent*-kauran-17,19-dimethyl ester **(1.50)**	*A. glabra*	Stem	Chen *et al.*, 2000a
16α-Hydro-*ent*-kauran-17,19-dioic acid **(1.51)**	*A. glabra*	Stem	Chen *et al.*, 2000a
	A. squamosa	Stem	Yang *et al.*, 2002
16α-Hydro-*ent*-kauran-17-oic acid **(1.52)**	*A. glabra*	Fruit	Chang *et al.*, 1998
	A. glabra	Stem	Chen *et al.*, 2000a
16α-Hydroxy-*ent*-kauran-19-oic acid **(1.53)**	*A. glabra*	Stem	Chen *et al.*, 2000a
	X. sericea	Seed	Takahashi *et al.*, 2001
16α-Methoxy-*ent*-kauran-19-oic acid **(1.54)**	*A. glabra*	Stem	Chen *et al.*, 2000a
16β,17-Diacetoxy-*ent*-kauran-19-oic acid **(1.55)**	*A. glabra*	Stem	Chen *et al.*, 2000a
	A. senegalensis	Stem bark	Fatope *et al.*, 1996
16β,17-Dihydroxy-*ent*-kauran-19-al **(1.56)**	*A. squamosa*	Fruit	Wu *et al.*, 1996
	A. squamosa	Stem	Yang *et al.*, 2002

Table 1. Diterpenoids in the family Annonaceae (continued)

Compound Name	Sources	Plant Part	References
16β,17-Dihydroxy-*ent*-kauran-19-oic acid (**1.57**)	*A. glabra*	Stem	Chen *et al.*, 2000a
	A. squamosa	Fruit	Wu *et al.*, 1996
	A. squamosa	Stem	Yang *et al.*, 2002
16β-Hydro-*ent*-kauran-17,19-dioic acid (**1.58**)	*A. squamosa*	Stem	Yang *et al.*, 2002
16β-Hydro-*ent*-kauran-17-oic acid (**1.59**)	*A. glabra*	Fruit	Chang *et al.*, 1998
16β-Hydroxy-17-acetoxy-*ent*-kauran-19-oic acid (**1.60**)	*A. glabra*	Fruit	Chang *et al.*, 1998
	A. squamosa	Stem	Yang *et al.*, 2002
16β-Hydroxy-17-acetoxy-*ent*-kauran-19-al (**1.61**)	*A. glabra*	Fruit	Chang et al., 1998
16β-Hydroxy-*ent*-kauran-19-oic acid (**1.62**)	*X. sericea*	Seed	Takahashi *et al.*, 2001
17-Acetoxy-16β-*ent*-kauran-19-oic acid (**1.63**)	*A. squamosa*	Fruit	Wu *et al.*, 1996
17-Hydroxy-16α-*ent*-kauran-19-oic acid (**1.64**)	*A. squamosa*	Fruit	Wu *et al.*, 1996
	A. squamosa	Stem	Yang *et al.*, 2002
17-Hydroxy-16β-*ent*-kauran-19-al (**1.65**)	*A. squamosa*	Fruit	Wu *et al.*, 1996
	A. squamosa	Stem	Yang *et al.*, 2002
17-Hydroxy-16β-*ent*-kauran-19-oic acid (**1.66**)	*A. squamosa*	Fruit	Wu *et al.*, 1996
	A. squamosa	Stem	Yang *et al.*, 2002
19-Formyl-*ent*-kauran-17-oic acid (**1.67**)	*A. squamosa*	Fruit	Wu *et al.*, 1996
19-Nor-*ent*-kauran-4α-ol-17-oic acid (**1.68**)	*A. glabra*	Fruit	Chang et al., 1998
	A. glabra	Stem	Chen *et al.*, 2000a
4α-Hydroxy-19-nor-*ent*-kauran-17-oic acid (**1.69**)	*A. squamosa*	Fruit	Wu *et al.*, 1996
	A. squamosa	Stem	Yang *et al.*, 2002
7-Oxo-*ent*-kaur-16-en-19-oic acid (**1.70**)	*X. aethiopica*	Stem bark	Hasan *et al.*, 1982a
Acutifloric acid (**1.71**)	*X. acutiflora*	Stem bark	Hasan *et al.*, 1985
Annoglabasin A (**1.72**)	*A. glabra*	Fruit	Chang *et al.*, 1998

Table 1. Diterpenoids in the family Annonaceae (continued)

Compound Name	Sources	Plant Part	References
Annoglabasin B (**1.73**)	*A. glabra*	Fruit	Chang *et al.*, 1998
Annoglabasin C (**1.74**)	*A. glabra*	Stem	Chen *et al.*, 2000a
Annoglabasin D (**1.75**)	*A. glabra*	Stem	Chen *et al.*, 2000a
Annoglabasin E (**1.76**)	*A. glabra*	Stem	Chen *et al.*, 2000a
Annoglabasin F (**1.77**)	*A. glabra*	Stem	Chen *et al.*, 2000a
Annomosin A (**1.78**)	*A. squamosa*	Stem	Yang *et al.*, 2002
Annosquamosin A (**1.79**)	*A. squamosa*	Fruit	Wu *et al.*, 1996
Annosquamosin B (**1.80**)	*A. squamosa*	Fruit	Wu *et al.*, 1996
Annosquamosin C (**1.81**)	*A. squamosa*	Stem	Yang *et al.*, 2002
Annosquamosin D (**1.82**)	*A. squamosa*	Stem	Yang *et al.*, 2002
Annosquamosin E (**1.83**)	*A. squamosa*	Stem	Yang *et al.*, 2002
Annosquamosin F (**1.84**)	*A. squamosa*	Stem	Yang *et al.*, 2002
Annosquamosin G (**1.85**)	*A. squamosa*	Stem	Yang *et al.*, 2002
ent-15α-Acetoxy-kaur-16-en-19-oic acid (**1.86**)	*X. sericea*	Seed	Takahashi *et al.*, 2001
ent-15α-Hydroxy-kaur-16-en-19-oic acid (**1.87**)	*X. aethiopica*	Fruit	Ekong, *et al.*, 1969
ent-15β-Hydroxy-kaur-16-en-19-oic acid (**1.88**)	*X. aethiopica*	Stem bark	Harrigan *et al.*, 1994
ent-19-Carbomethoxy-kauran-19-oic acid (**1.89**)	*A. senegalensis*	Stem bark	Fatope *et al*, 1996
ent-3β-Hydroxy-kaur-16-ene (**1.90**)	*A. senegalensis*	Stem bark	Fatope *et al.*, 1996
ent-7β-Acetoxy-kaur-16-en-19-oic acid (**1.91**)	*X. acutiflora*	Stem bark	Takahashi *et al.*, 2001
ent-7β-Hydroxy-kaur-16-en-19-oic acid (**1.92**)	*X. aethiopica*	Stem bark	Hasan, *et al.*, 1982
ent-Kaur-15-ene-17,19-diol (**1.93**)	*A. glabra*	Fruit	Chang *et al.*, 1998
	A. glabra	Stem	Chen *et al.*, 2000a
ent-Kaur-15-ene-17-al-19-oic acid (**1.94**)	*X. aethiopica*	Stem bark	Harrigan *et al.*, 1994

Table 1. Diterpenoids in the family Annonaceae (continued)

Compound Name	Sources	Plant Part	References
ent-Kaur-15-ene-17-ol-19-oic acid (**1.95**)	*A. glabra*	Stem	Chen *et al.*, 2000a
ent-Kaur-16-en-19-ol (**1.96**)	*A. glabra*	Fruit	Chang *et al.*, 1998
	A. squamosa	Fruit	Wu *et al.*, 1996
ent-Kauran-16α,19-diol (**1.97**)	*X. aethiopica*	Fruit	Ekong, *et al.*, 1969
ent-Kauran-16α-ol (**1.98**)	*X. aethiopica*	Fruit	Ekong, *et al.*, 1969
ent-Kauran-16β,17,19-triol (**1.99**)	*A. squamosa*	Fruit	Wu *et al.*, 1996
ent-Kauran-16β-ol (**1.100**)	*X. acutiflora*	Stem bark	Hasan *et al.*, 1985
	X. sericea	Seed	Takahashi *et al.*, 2001
Kaurenoic acid (**1.101**)	*A. glabra*	Fruit	Chang *et al.*, 1998
	A. glabra	Stem	Chen *et al.*, 2000
	A. senegalensis	Stem bark	Fatope *et al.*, 1996
	A. squamosa	Fruit	Wu *et al.*, 1996
	A. squamosa	Stem	Yang *et al.*, 2002
	Mitrephora tomentosa	Bark	Supudompol *et al.*, 2004
	M. celebica	Stem bark	Zgoda-Pols *et al.*, 2002
	X. aethiopica	Fruit	Ekong, *et al.*, 1969
	X. aethiopica	Stem bark	Hasan, *et al.*, 1982
	X. sericea	Seed	Takahashi *et al.*, 2001
Methyl-16α-hydro-19-al-*ent*-kauran-17-oate (**1.102**)	*A. glabra*	Fruit	Chang *et al.*, 1998
Beyeranes Methyl *ent*-beyer-15-ene-19-oate (**1.103**)	*X. sericea*	Seed	Takahashi *et al.*, 2001
Atisanes *ent*-Atisan-16α,18-diol (**1.104**)	*X. aromatica*	Fruit	Moraes and Roque, 1988
ent-Atisan-16α-ol-18-oic acid (**1.105**)	*X. aromatica*	Fruit	Moraes and Roque, 1988

Table 1. Diterpenoids in the family Annonaceae (continued)

Compound Name	Sources	Plant Part	References
Methyl *ent*-15-atisene-19-oate (**1.106**)	*X. sericea*	Seed	Takahashi *et al.*, 2001
Trachylobanes 15-Hydroxy-*ent*-trachyloban-19-oic acid (**1.107**)	*X. aethiopica*	Stem bark	Harrigan *et al.*, 1994
15-Oxo-*ent*-trachyloban-19-oic acid (**1.108**)	*X. aethiopica*	Stem bark	Harrigan *et al.*, 1994
7β-Acetoxy-trachyloban-18-oic acid (**1.109**)	*X. quintasii*	Stem bark	Hasan *et al.*, 1982a
7β-Hydroxy-trachyloban-19-oic acid (**1.110**)	*X. aethiopica*	Stem bark	Ngouela *et al.*, 1998
ent-15α-Hydroxy-trachyloban-19-oic acid (**1.111**)	*X. aethiopica*	Stem bark	Harrigan *et al.*, 1994
	X. sericea	Seed	Takahashi *et al.*, 2001
ent-Trachyloban-19-oic acid (**1.112**)	*Mitrephora celebica*	Stem bark	Zgoda-Pols *et al.*, 2002
	X. sericea	Seed	Takahashi *et al.*, 2001
ent-Trachyloban-3β-ol (**1.113**)	*X. aromatica*	Fruit	Moraes and Roque, 1988
Methyl *ent*-15α-acetoxy-trachyloban-19-oate (**1.114**)	*X. sericea*	Seed	Takahashi *et al.*, 2001
Methyl *ent*-trachyloban-18-oate (**1.115**)	*X. sericea*	Seed	Takahashi *et al.*, 2001
Methyl *ent*-trachyloban-19-oate (**1.116**)	*X. sericea*	Seed	Takahashi *et al.*, 2001
Pimaranes 7,15-Pimaradien-18-oic acid (**1.117**)	*M. celebica*	Stem bark	Zgoda-Pols *et al.*, 2002
8(14),15-Pimaradien-18-oic acid (**1.118**)	*M. celebica*	Stem bark	Zgoda-Pols *et al.*, 2002
8-Hydroxypimar-15-en-18-oic acid (**1.119**)	*M. tomentosa*	Bark	Supudompol *et al.*, 2004
Mitrephorone A (**1.120**)	*M. glabra*	Bark	Li *et al.*, 2005
Mitrephorone B (**1.121**)	*M. glabra*	Bark	Li *et al.*, 2005
Mitrephorone C (**1.122**)	*M. glabra*	Bark	Li *et al.*, 2005
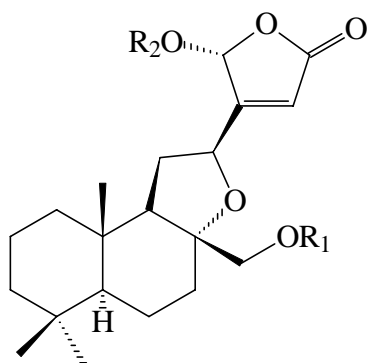
17-*O*-Acetylacuminolide (**1.1**)　　: R₁ = Ac, R₂ = H

Acuminolide (**1.2**)　　　　　　　: R₁ = H, R₂ = H
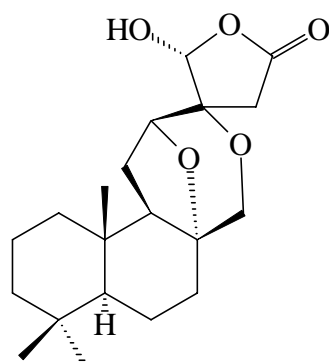
Spiroacuminolide (**1.8**)
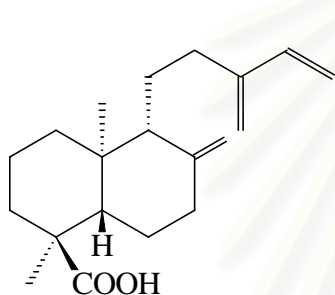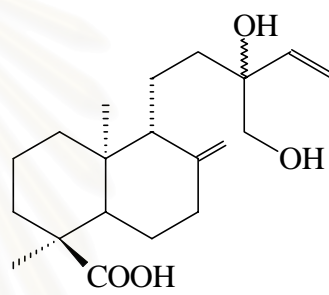
ent-Labda-8(17),13(16),14-trien-18-oic acid (**1.4**)　　*ent*-Labdan-13,16-diol-8(17),14-dien-18-oic acid (**1.5**)
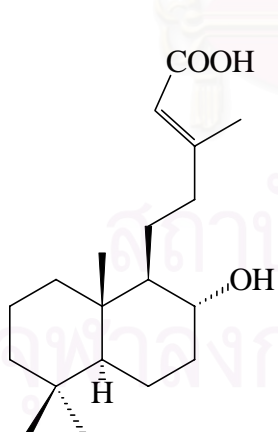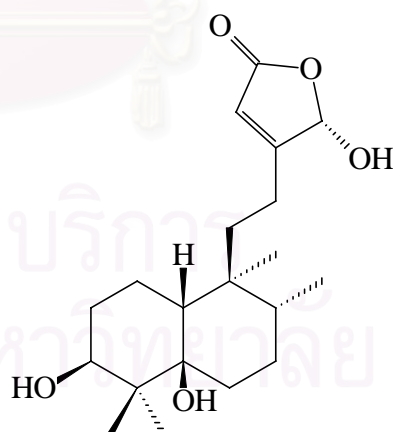
Labd-13*E*-en-8-ol-15-oic acid (**1.7**)　　　3β,5β,16α-trihydroxyhalima-13(14)-en-15,16-olide (**1.11**)

Figure 3.　Chemical structures of diterpenoids in the family Annonaceae
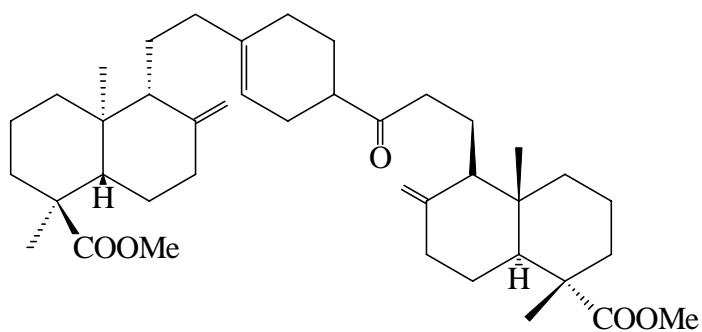
ent-13′-Nor-13′-oxomethylisoozate dimer **(1.3)**
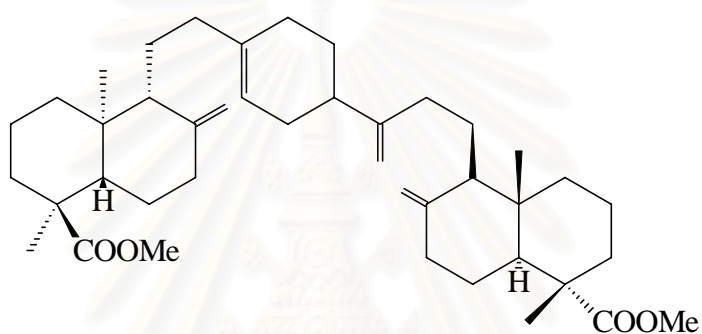
ent-Methylisoozate dimer **(1.6)**

16-Hydroxy-*ent*-halima-5(10),13-dien-15,16-olide : R =

(1.9)
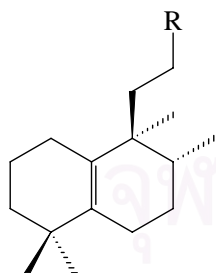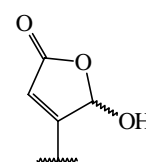
ent-Halima-5(10),13*E*-dien-15-oic acid **(1.15)** : R =
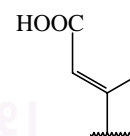
16-Oxo-*ent*-halima-5(10),13-dien-15-oic acid : R =

(1.10)
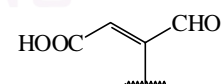
ent-Halima-5(10),13-dien-15,16-olide **(1.14)** : R =
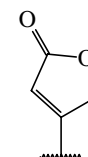
Figure 3. Chemical structures of diterpenoids in the family Annonaceae (continued)
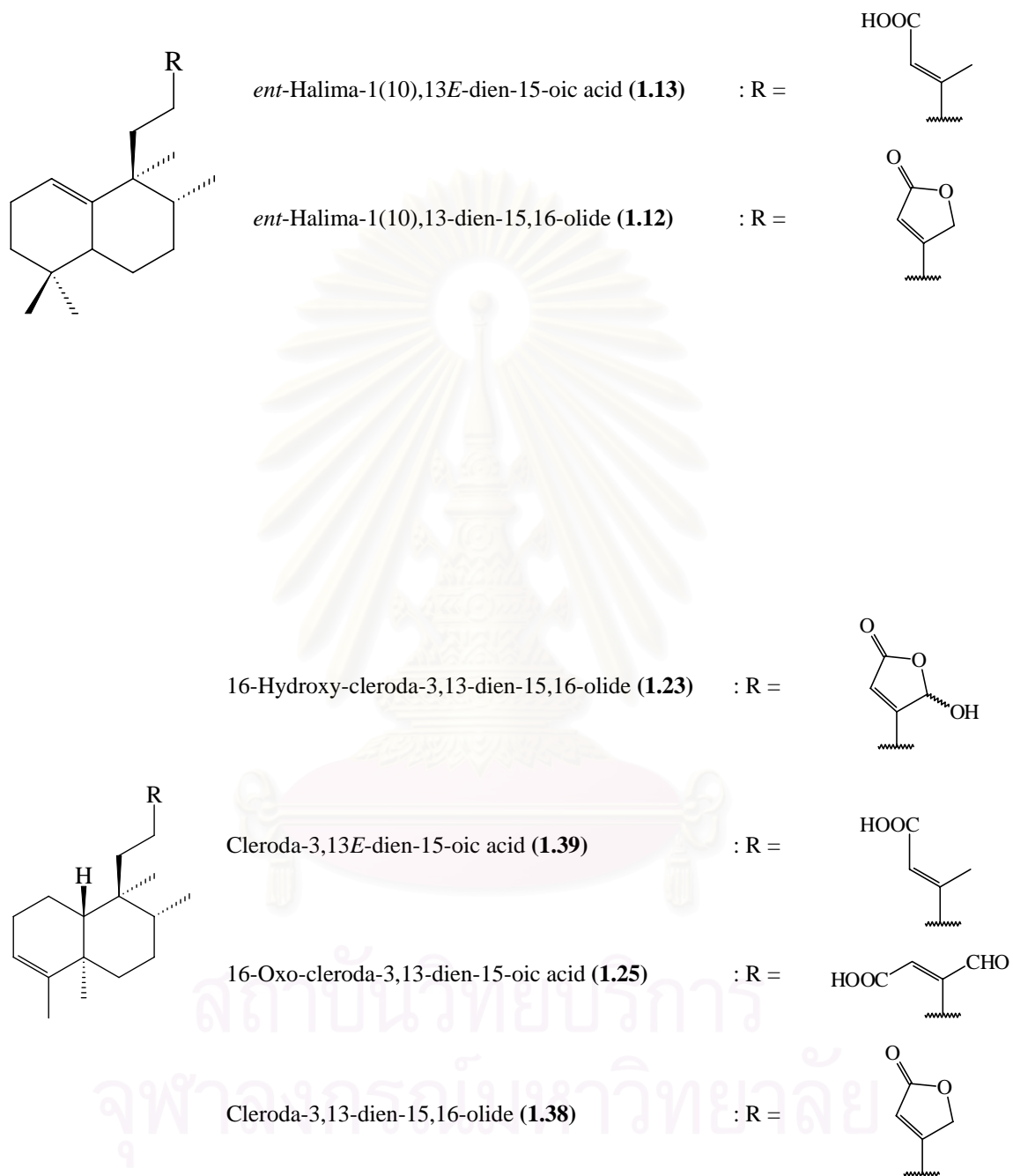
ent-Halima-1(10),13*E*-dien-15-oic acid **(1.13)**   : R =

ent-Halima-1(10),13-dien-15,16-olide **(1.12)**   : R =

16-Hydroxy-cleroda-3,13-dien-15,16-olide **(1.23)**   : R =

Cleroda-3,13*E*-dien-15-oic acid **(1.39)**   : R =

16-Oxo-cleroda-3,13-dien-15-oic acid **(1.25)**   : R =

Cleroda-3,13-dien-15,16-olide **(1.38)**   : R =
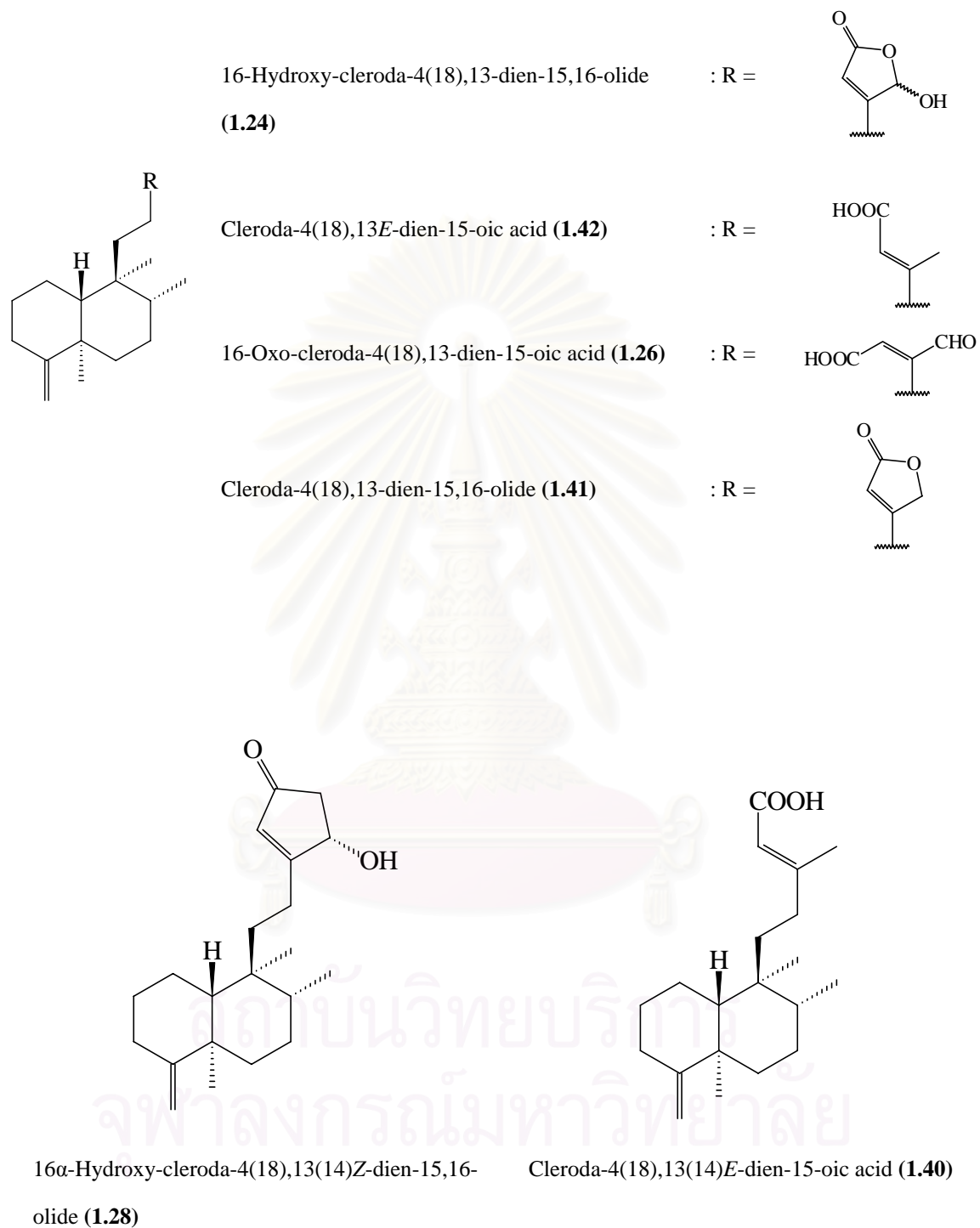
Figure 3. Chemical structures of diterpenoids in the family Annonaceae (continued)

16-Hydroxy-cleroda-4(18),13-dien-15,16-olide : R =

(1.24)

Cleroda-4(18),13*E*-dien-15-oic acid **(1.42)** : R =

16-Oxo-cleroda-4(18),13-dien-15-oic acid **(1.26)** : R =

Cleroda-4(18),13-dien-15,16-olide **(1.41)** : R =

16α-Hydroxy-cleroda-4(18),13(14)*Z*-dien-15,16-olide **(1.28)**

Cleroda-4(18),13(14)*E*-dien-15-oic acid **(1.40)**

Figure 3. Chemical structures of diterpenoids in the family Annonaceae (continued)
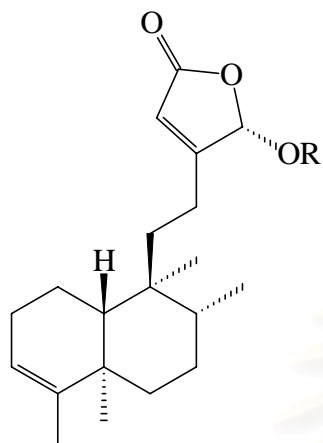
16α-Hydroxy-cleroda-3,13Z-dien-15,16-olide **(1.27)** : R = H

16α-Methoxy-cleroda-3,13Z-dien-15,16-olide **(1.29)** : R = Me
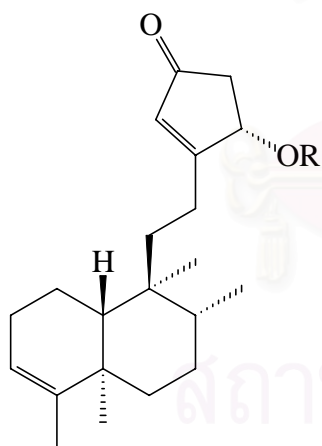
16(*R*)-3,13Z-Kolavadien-15,16-olide : R = H **(1.19)**

16-acetoxy-cleroda-3,13-dien-15,16-olide : R = Ac **(1.25)**
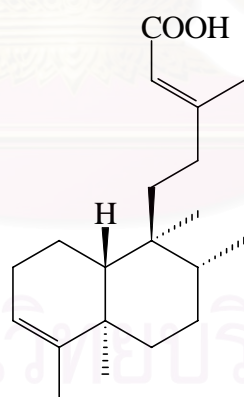
3,13*E*- Kolavadien-15-oic acid **(1.35)**
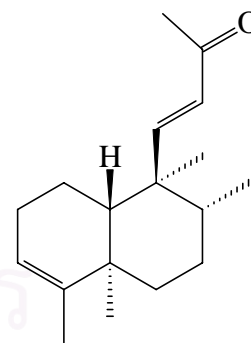
14,15-Bisnor-3,11*E*-kolavadien-13-one **(1.18)**

Figure 3. Chemical structures of diterpenoids in the family Annonaceae (continued)
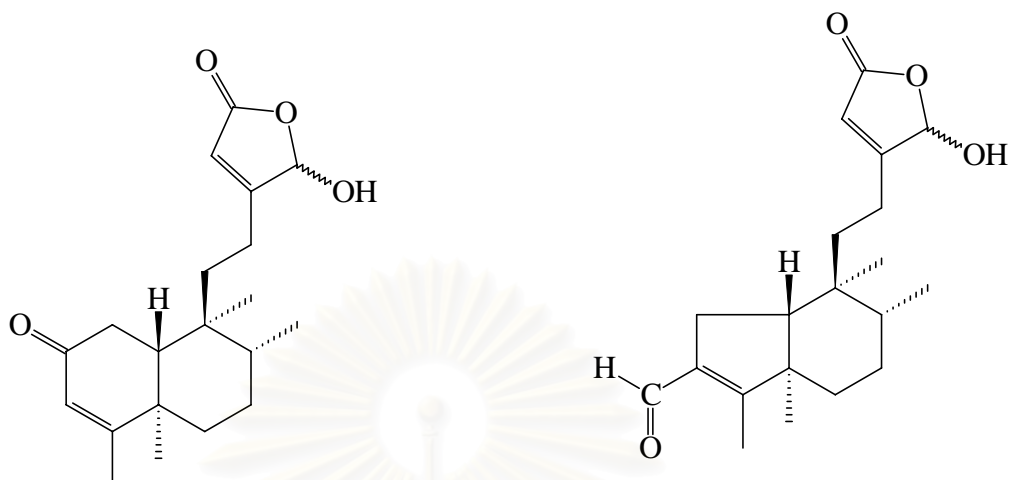
16(*R*)-3,13*Z*-Kolavadien-15,16-olide-2-one :16*R* (**1.20**)

16(*S*)-3,13*Z*-Kolavadien-15,16-olide-2-one :16*S* (**1.21**)

(4→2)-*abeo*-16(*R*)-2,3*Z*-Kolavadien-15,16-olide-3-al :16*R* (**1.16**)

(4→2)-*abeo*-16(*S*)-2,3*Z*-Kolavadien-15,16-olide-3-al :16*S* (**1.17**)
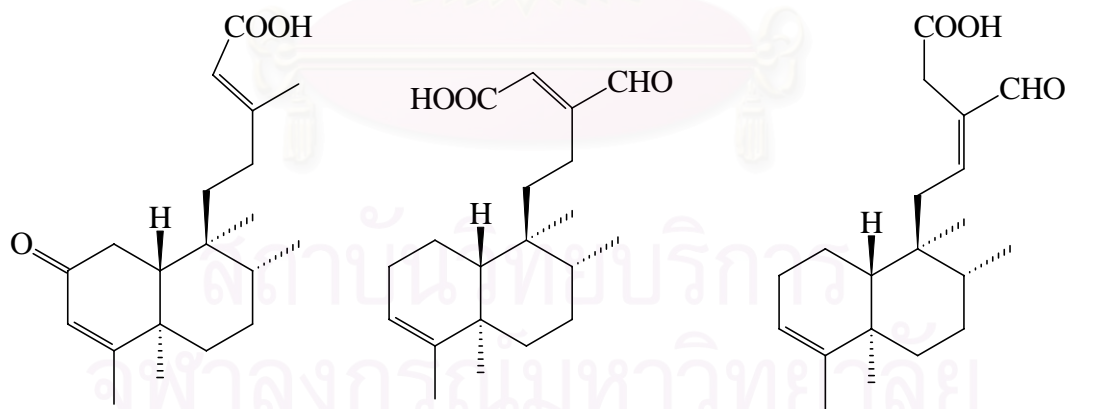
(**1.43**)

3,13-Kolavadien-15-oic acid-16-al (**1.36**)

3,12*E*-Kolavadien-15-oic acid-16-al (**1.34**)

Figure 3. Chemical structures of diterpenoids in the family Annonaceae (continued)
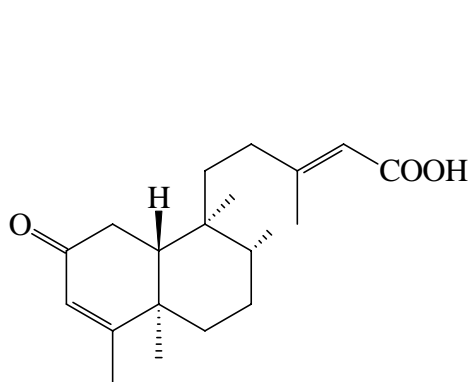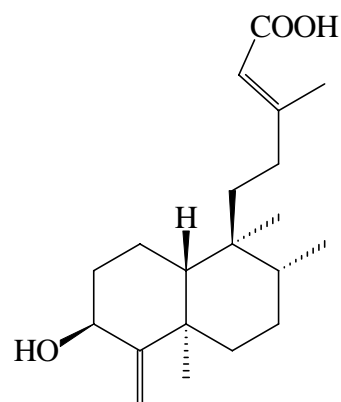
2-Oxokolavenic acid **(1.33)**   3-Hydroxy-cleroda-4(18),13Z-dien-15-oic acid **(1.37)**
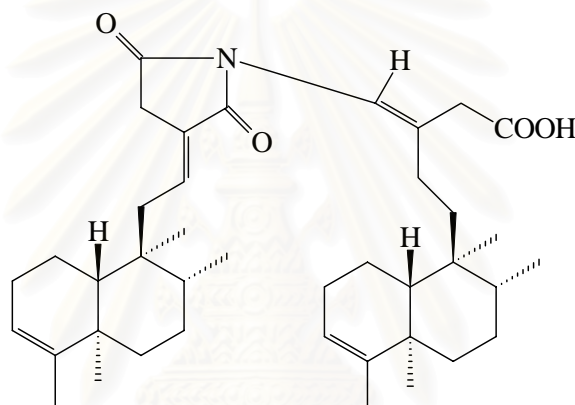
(1.44)
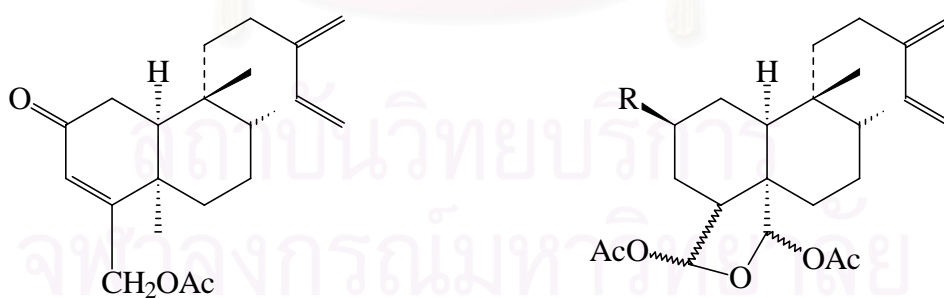
2-Oxo-18-acetoxy-10α,17α,19α,20β-(-)-cleroda-3,13(16),14-triene **(1.32)**

2,18,19-Triacetoxy-(-)-cleroda-13(16),14-diene-18,19-oxide : R = OAc **(1.30)**

2-Isobutoxy-18,19-diacetoxy-(-)-cleroda-13(16),14-diene-18,19-oxide : R = OCOCH(CH₃)₂ **(1.31)**

Figure 3. Chemical structures of diterpenoids in the family Annonaceae (continued)
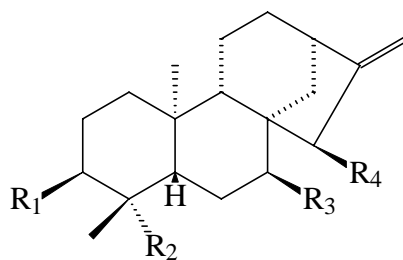
	R_1	R_2	R_3	R_4
Kaurenoic acid **(1.101)**	H	COOH	H	H
ent-Kaur-16-en-19-ol **(1.96)**	H	CH$_2$OH	H	H
ent-3β-Hydroxy-kaur-16-ene **(1.90)**	OH	CH$_3$	H	H
ent-15β-Hydroxy-kaur-16-en-19-oic acid **(1.88)**	H	COOH	H	OH
ent-7β-Hydroxy-kaur-16-en-19-oic acid **(1.92)**	H	COOH	OH	H
ent-7β-Acetoxy-kaur-16-en-19-oic acid **(1.91)**	H	COOH	OCOCH$_3$	H
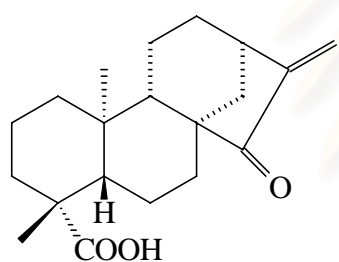
15-Oxo-*ent*-Kaur-16-en-19-oic acid **(1.45)**
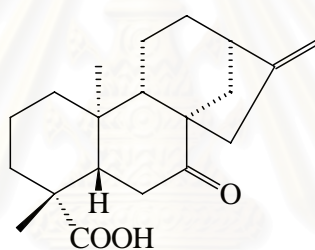
7-Oxo-*ent*-Kaur-16-en-19-oic acid **(1.70)**
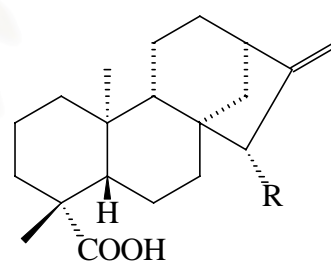
ent-15α-Acetoxy-kaur-16-en-19-oic acid **(1.86)**   : R = OCOCH$_3$

ent-15α-Hydroxy-kaur-16-en-19-oic acid **(1.87)**   : R = OH
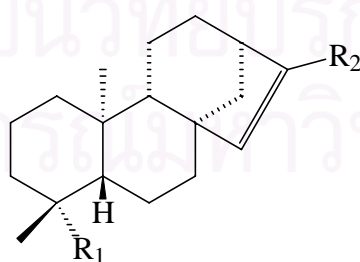
ent-Kaur-15-ene-17,19-diol **(1.93)**   : R$_1$ = CH$_2$OH, R$_2$ = CH$_2$OH

ent-Kaur-15-ene-17-al-19-oic acid **(1.94)**   : R$_1$ = COOH, R$_2$ = CHO

ent-Kaur-15-ene-17-ol-19-oic acid **(1.95)**   : R$_1$ = COOH, R$_2$ = CH$_2$OH

Figure 3. Chemical structures of diterpenoids in the family Annonaceae (continued)
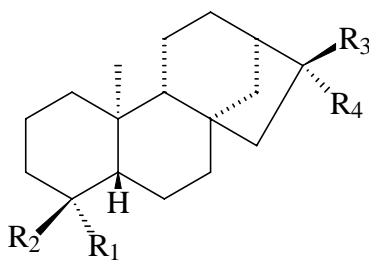
	R_1	R_2	R_3	R_4
Annosquamosin A (**1.79**)	CHO	CH$_3$	OH	CH$_2$OCOCH$_3$
Annosquamosin B (**1.80**)	OH	CH$_3$	OH	CH$_2$OH
Annosquamosin C (**1.81**)	OH	CH$_3$	CH$_2$OH	H
Annosquamosin D (**1.82**)	OH	CH$_3$	OCOCH$_3$	CH$_2$OH
Annosquamosin E (**1.83**)	OCHO	CH$_3$	OH	CH$_2$OCOCH$_3$
Annosquamosin F (**1.84**)	CH$_3$	COOH	OH	CH$_2$OCOCH$_3$
Annosquamosin G (**1.85**)	CH$_3$	COOH	OH	CH$_2$OH
4α-Hydroxy-19-nor-*ent*-kauran-17-oic acid (**1.69**)	OH	CH$_3$	COOH	H
16α-Hydro-*ent*-kauran-17,19-dioic acid (**1.51**)	COOH	CH$_3$	COOH	H
16β-Hydro-*ent*-kauran-17,19-dioic acid (**1.58**)	COOH	CH$_3$	H	COOH
17-Hydroxy-16α-*ent*-kauran-19-oic acid (**1.64**)	COOH	CH$_3$	CH$_2$OH	H
17-Hydroxy-16β-*ent*-kauran-19-oic acid (**1.66**)	COOH	CH$_3$	H	CH$_2$OH
16α,17-Dihydroxy-*ent*-kauran-19-oic acid (**1.47**)	COOH	CH$_3$	CH$_2$OH	OH
16β,17-Dihydroxy-*ent*-kauran-19-oic acid (**1.57**)	COOH	CH$_3$	OH	CH$_2$OH
16β-Hydroxy-17-acetoxy-*ent*-kauran-19-oic acid (**1.60**)	COOH	CH$_3$	OH	CH$_2$OCOCH$_3$
16α-Hydro-19-al-*ent*-kauran-17-oic acid (**1.49**)	CHO	CH$_3$	COOH	H
17-Hydroxy-16β-*ent*-kauran-19-al (**1.65**)	CHO	CH$_3$	H	CH$_2$OH
16α,17-Dihydroxy-*ent*-kauran-19-al (**1.46**)	CHO	CH$_3$	CH$_2$OH	OH
16β,17-Dihydroxy-*ent*-kauran-19-al (**1.56**)	CHO	CH$_3$	OH	CH$_2$OH
ent-Kauran-16α-ol (**1.98**)	CH$_3$	CH$_3$	CH$_3$	OH
ent-Kauran-16β-ol (**1.100**)	CH$_3$	CH$_3$	OH	CH$_3$
ent-Kauran-16α,19-diol (**1.97**)	CH$_2$OH	CH$_3$	CH$_3$	OH
ent-Kauran-16β,17,19-triol (**1.99**)	CH$_2$OH	CH$_3$	OH	CH$_2$OH
17-Acetoxy-16β-*ent*-kauran-19-oic acid (**1.62**)	COOH	CH$_3$	H	CH$_2$OCOCH$_3$
19-Formyl-*ent*-kauran-17-oic acid (**1.67**)	CHO	CH$_3$	H	COOH

Figure 3. Chemical structures of diterpenoids in the family Annonaceae (continued)
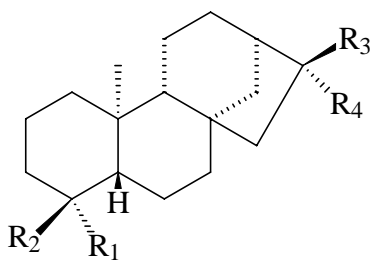
	R$_1$	R$_2$	R$_3$	R$_4$
Annoglabasin A **(1.72)**	CHO	CH$_3$	OCOCH$_3$	COOCH$_3$
Annoglabasin B **(1.73)**	CH$_2$OCOCH$_3$	CH$_3$	COOH	H
Annoglabasin C **(1.74)**	COOH	CH$_3$	COOCH$_3$	OCOCH$_3$
Annoglabasin D **(1.75)**	CHO	CH$_3$	COOCH$_3$	OCOCH$_3$
Annoglabasin E **(1.76)**	CH$_2$OH	CH$_3$	COOH	H
Annoglabasin F **(1.77)**	OH	CH$_3$	COOCH$_3$	OCOCH$_3$
16α-Hydro-*ent*-kauran-17-oic acid **(1.52)**	CH$_3$	CH$_3$	COOH	H
16β-Hydro-*ent*-kauran-17-oic acid **(1.59)**	CH$_3$	CH$_3$	H	COOH
Methyl-16α-hydro-19-al-*ent*-kauran-17-oate **(1.102)**	CHO	CH$_3$	OCOCH$_3$	H
16β-Hydroxy-17-acetoxy-*ent*-kauran-19-al **(1.61)**	CHO	CH$_3$	OH	CH$_2$OCOCH$_3$
19-Nor-*ent*-kauran-4α-ol-17-oic acid **(1.68)**	OH	CH$_3$	COOH	H
16α-Methoxy-*ent*-kauran-19-oic acid **(1.54)**	COOH	CH$_3$	CH$_3$	OCH$_3$
16α-Hydro-*ent*-kauran-17,19-dimethyl ester **(1.50)**	COOCH$_3$	CH$_3$	COOCH$_3$	H
16α-Hydro-19-al-*ent*-kauran-17-methyl ester **(1.48)**	CHO	CH$_3$	COOCH$_3$	H
16β,17-Diacetoxy-*ent*-kauran-19-oic acid **(1.55)**	COOH	CH$_3$	OCOCH$_3$	OCOCH$_3$
16α-Hydroxy-*ent*-kauran-19-oic acid **(1.53)**	COOH	CH$_3$	OH	CH$_3$
16β-Hydroxy-*ent*-kauran-19-oic acid **(1.62)**	COOH	CH$_3$	CH$_3$	OH
ent-19-Carbomethoxy-kauran-19-oic acid **(1.89)**	COOCH$_3$	CH$_3$	COOH	OH
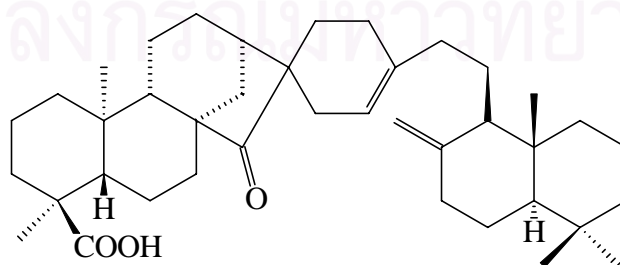
Acutifloric acid **(1.71)**

Figure 3. Chemical structures of diterpenoids in the family Annonaceae (continued)

Annomosin A (**1.78**)

Methyl *ent*-beyer-15-ene-19-

oate (**1.103**)

ent-Atisan-16α,18-diol (**1.104**)

: R = CH₂OH

ent-Atisan-16α-ol-18-oic acid (**1.105**)

: R = COOH

Methyl *ent*-15-atisene-19-oate

(**1.106**)

ent-Trachyloban-3β-ol (**1.113**)

15-Oxo-*ent*-trachyloban-19-oic acid (**1.108**)   : R = O

15-Hydroxy-*ent*-trachyloban-19-oic acid (**1.107**) : R = α-H, β-OH
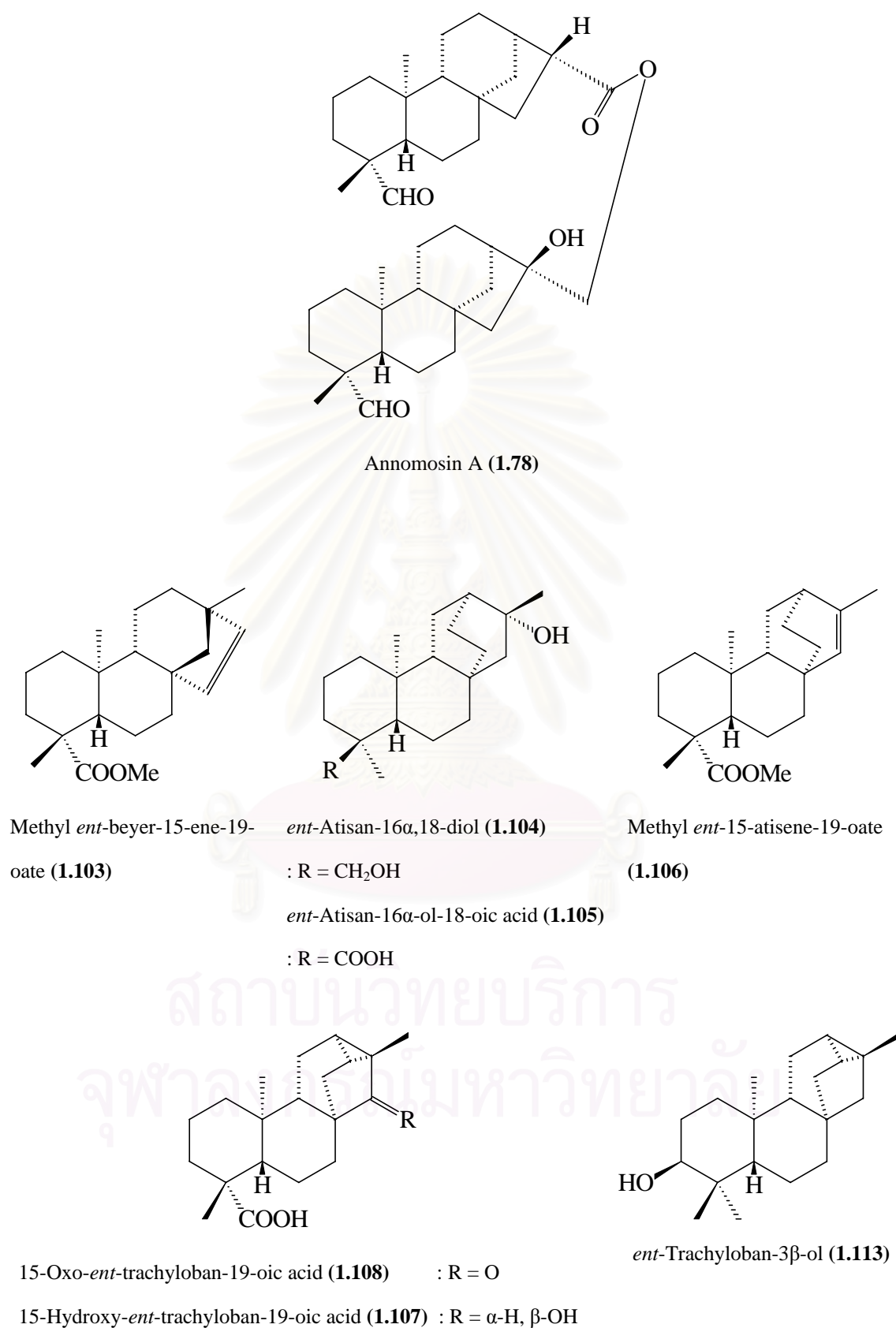
Figure 3. Chemical structures of diterpenoids in the family Annonaceae (continued)
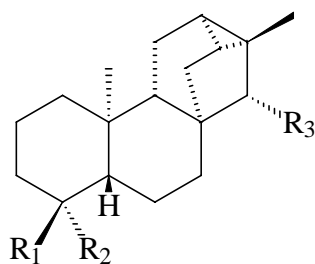
	R_1	R_2	R_3
ent-15α-Hydroxy-trachyloban-19-oic acid **(1.111)**	CH₃	COOH	OH
Methyl *ent*-15α-acetoxy-trachyloban-19-oate **(1.114)**	CH₃	COOCH₃	OCOCH₃
ent- trachyloban-19-oic acid **(1.112)**	CH₃	COOH	H
Methyl *ent*-trachyloban-19-oate **(1.116)**	CH₃	COOCH₃	H
Methyl *ent*- trachyloban-18-oate **(1.115)**	COOCH₃	CH₃	H
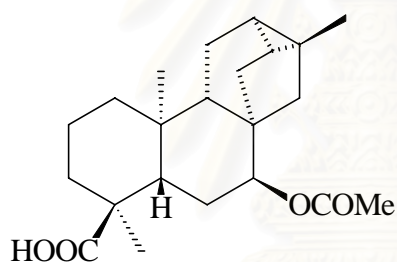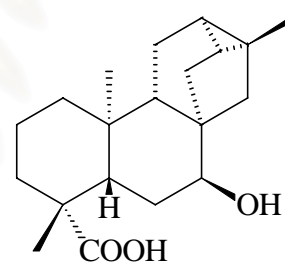
7β-Acetoxy-trachyloban-18-oic acid **(1.109)**   7β-Hydroxy-trachyloban-19β-oic acid **(1.110)**
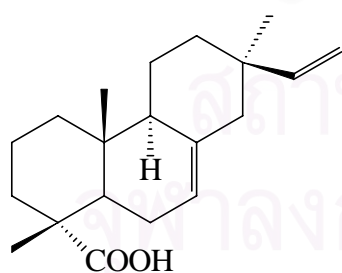
7,15-Pimaradien-18-oic acid   8(14),15-Pimaradien-18-oic acid   8β-Hydroxypimar-15-en-18-oic
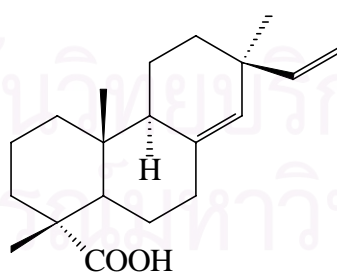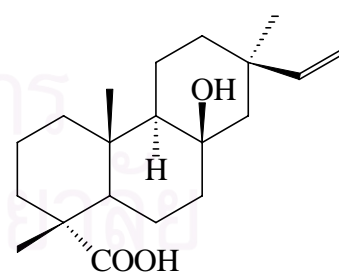
(1.117)   **(1.118)**   acid **(1.119)**

Figure 3. Chemical structures of diterpenoids in the family Annonaceae (continued)

Mitrephorone A (**1.120**)   Mitrephorone B (**1.121**)   Mitrephorone C (**1.122**)
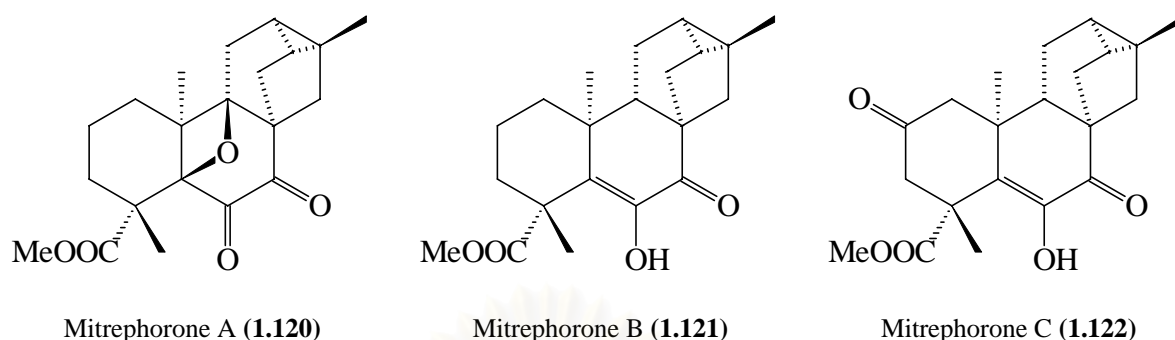
Figure 3. Chemical structures of diterpenoids in the family Annonaceae (continued)

Flavonoids of the family Annonaceae

The Annonaceae is one of the plant families rich in flavonoids which displayed interesting bioactivities and unique chemical structures. Most studies of annonaceous flavonoids dealt with those isolated from the stem bark and root of *Uvaria* species, which to date have yielded mainly flavanones and chalcones. Although flavanones and chalcones are widespread in higher plants, the addition of benzyl groups in their main skeletons is quite rare and seems to be limited to this family, especially the genus *Uvaria*. *Uvaria* flavonoids possess a number of distinctive characteristics, such as their association with benzyl groups and the absence of B-ring substitution (Leboeuf *et al*., 1982; Parmar *et al*., 1994). Several annonaceous flavonoids have been reported as displaying cytotoxic, antitumor and antimicrobial properties. The review of flavonoids in the Annonaceae presented below will focus on three flavonoid subgroups: flavanones, flavones and flavonols.

In addition to their use as chemotaxonomic markers, *C*-benzylated flavanones mainly obtained from the genus *Uvaria* are also important pharmacologically. Chamanetin (**2.20**) and isochamanetin (**2.30**) isolated from the stem bark of *U. chamae* exhibited cytotoxic activity (Hufford and Lasswell Jr., 1976), whilst uvarinol (**2.40**) from the same species showed cytotoxicity (ED_{50}) against both KB cell line at the ED_{50} value of 5.9 μg/ml and PS cell line at the ED_{50} value of 9.7 μg/ml cultures, and also antimicrobial activity against *Staphylococcus aureus*, *Bacillus subtilis* and *Mycobacterium smegmatis* (Hufford and Lasswell Jr., 1979). A phytochemical study of the dichloromethane extract of *Xylopia africana* root revealed the presence of four tetra *C*-benzylated flavanones (**2.8**)-(**2.10**), (**2.18**), which possessed significantly antibacterial

activities against various microbial strains (Anam, 1994a; 1994b). Another *C*-benzylated flavanone, dichamanetin **(2.27)**, isolated from a rare plant, *Melodorum fruticosum,* exhibited cytotoxicity against KBMRI (human nasopharyngeal carcinoma) and HT-29 (human nasopharyngeal carcinoma) cell lines with moderate potency (ED_{50} values of 5.38 and 5.1 μg/ml, respectively) (Jung *et al.*, 1990).

Examination of *Uvaria chamae* stem bark (Lasswell Jr. and Hufford, 1977) and *Melodorum fruticosum* bark (Jung *et al.*, 1990) afforded pinocembrin **(2.37)**, a flavanone having selective cytotoxicity to 9PS (chemically-induced murine lymphocytic leukemia) cells, *in vitro* antimicrobial activity (Metzner *et al.*, 1979), local anesthetic effect in rabbits and mice (Paintz and Metzner, 1979) and inhibitory effect against the enzyme tyrosine kinase (Geahlen *et al.*, 1989). Two flavanones, hamiltone A **(2.28)** and B **(2.29)**, with DNA strand-scission activity were obtained from the combined leaves and stems of *U. hamiltonii* (Huang *et al.*, 1998). A very uncommon flavanone, leiocarpin B **(2.36)**, isolated from the stem bark of *Goniothalamus leiocarpus,* displayed *in vitro* anticancer activity (Mu *et al*., 2002).

Desmos chinensis is a medicinal plant used as antimalarial, insecticidal, antirheumatic, antispasmodic and analgesic in folk medicine (Chi, 1997; Loi, 2001). Investigation of its bioactive metabolites revealed interesting flavonoids such as the flavanone lawinal **(2.35)** with anti-HIV activity against HIV-1 replication in H9 lymphocytes (Wu *et al*., 2003). Another flavanone, desmal **(2.23)**, was a tyrosine kinase inhibitor (Kakeya *et al.*, 1993), whereas the flavone negletein **(2.50)** exhibited potent inhibitory activity against nuclear factor of activated T cells (NFAT) transcription factor (Kiem *et al*., 2005).

Guiding by the brine shrimp bioassay, fractionation of the roots of a Malaysian plant, *Cyathostemma argenteum*, used traditionally for the treatment of breast cancer, yielded two uncommon flavanones: 2,5-dihydroxy-6,7-dimethoxyflavanone **(2.4)** and 2,5-dihydroxy-7-methoxyflavanone **(2.7)**. Both flavonoids exhibited cytotoxic activities against MCF-7 cells (Khamis, 2004).

The distribution of flavanones, flavone and flavonol in the family Annonaceae is presented in **Table 2** and their chemical structures are shown in **Figure 4**. In addition, flavonoid glycosides reported from annonaceous plants (Leboeuf *et al.*, 1982; Sinz *et al.*, 1998) are summarized in **Table 3**.

Table 2. Distributions of flavanones and flavones in the family Annonaceae

Compounds	Sources	Part	References
Flavanones (+)-6,8-Dimethylpinocembrin 5-methyl ether (**2.1**)	*Uvaria angolensis*	Root	Hufford and Oguntimein, 1982
(±)-Chamanetin 5-methyl ether (**2.2**)	*U. angolensis*	Root	Hufford and Oguntimein, 1982
	U. chaemae	Root bark	El-Sohly, Lasswell and Hufford, 1979
(±)-Dichamanetin 5-methyl ether (**2.3**)	*U. chaemae*	Root bark	El-Sohly *et al.*, 1979
2,5-Dihydroxy-6,7-dimethoxyflavanone (**2.4**)	*Cyathostemma argenteum*	Root	Khamis *et al.*, 2004
2,5-Dihydroxy-7-methoxy-6-methylflavanone (**2.5**)	*Friesodielsia enghiana*	Stem bark	Fleischer, Waigh and Waterman, 1997
2,5-Dihydroxy-7-methoxy-8-methylflavanone (**2.6**)	*F. enghiana*	Stem bark	Fleischer *et al.*, 1997
2,5-Dihydroxy-7-methoxyflavanone (**2.7**)	*C. argenteum*	Root	Khamis *et al.*, 2004
2′′′′′-Hydroxy-3′′′′-benzyluvarinol (**2.8**)	*Xylopia africana*	Root	Anam, 1994a
2′′′′′-Hydroxy-5′′′′–benzylisouvarinol-A (**2.9**)	*X. africana*	Root	Anam, 1994a
2′′′′′-Hydroxy-5′′′′–benzylisouvarinol-B (**2.10**)	*X. africana*	Root	Anam, 1994a
2′-Hydroxydemethoxymatteucinol (**2.11**)	*Uvaria afzelii*	Stem	Hufford and Oguntimein, 1981
5,6,7-Trimethoxyflavanone (**2.12**)	*Oxymitra velutina*	Twig	Achenbach and Hemrich, 1991
5,6-Dihydroxy-7-methoxy-dihydroflavone (**2.13**)	*Desmos chinensis*	Leaves	Kiem *et al.*, 2005
5,7,8-Trimethoxyflavanone (**2.14**)	*Popowia cauliflora*	Stem	Panichpol and Waterman, 1978

Table 2. Distributions of flavanones and flavones in the family Annonaceae (continued)

Compounds	Sources	Part	References
5-Hydroxy-7-methoxyflavanone (**2.15**)	*Friesodielsia enghiana*	Stem bark	Fleischer *et al*., 1997
6-Formyl-5-hydroxy-7-methoxy-8-methylflavanone (**2.16**)	*D. chinensis*	Leaves	Hao *et al*., 1993
6-Hydroxy-5,7,8-trimethoxyflavanone (**2.17**)	*Fissistigma polyanthoides*	Bark	Jongbunprasert *et al*., 2000
7-*O*-Methylchamanetin (**2.18**)	*X. africana*	Root	Anam, 1994b
7-*O*-Methylisochamanetin (**2.19**)	*X. africana*	Root	Anam, 1994b
Chamanetin (**2.20**)	*Uvaria chamae*	Stem bark	Hufford and Lasswell Jr., 1976; Lasswell Jr. and Hufford, 1977
	U. ferruginea	Stem	Kodpinid, Thebtaranonth and Thebtaranonth, 1985
Chamanetin 5-methyl ether (**2.21**)	*U. chaemae*	Stem	Kodpinid *et al*., 1985
Demethoxymatteucinol (**2.22**)	*U. afzelii*	Stem	Hufford, Oguntimein and Baker, 1981
Desmal (**2.23**)	*D. chinensis*	Leaves	Kakeya *et al*., 1993
Desmethoxymatteucinol (**2.24**)	*U. lawii*	Stem	Joshi and Gawad, 1974
Desmethoxymatteucinol-7-methyl ether (**2.25**)	*U. lawii*	Stem	Joshi and Gawad, 1974
Desmosflavanone II (**2.26**)	*D. cochinchinensis*	Root	Wu *et al*., 1997
Dichamanetin (**2.27**)	*U. chamae*	Stem bark	Lasswell Jr. and Hufford, 1977
	Melodorum fruticosum	Bark	Jung *et al*., 1990
Hamiltone A (**2.28**)	*U. hamiltonii*	Stem and leaves	Huang *et al*., 1998

Table 2. Distributions of flavanones and flavones in the family Annonaceae (continued)

Compounds	Sources	Part	References
Hamiltone B (**2.29**)	*U. hamiltonii*	Stem and leaves	Huang *et al.*, 1998
Isochamanetin (**2.30**)	*U. chamae*	Stem bark	Hufford and Lasswell Jr., 1976; Lasswell Jr. and Hufford, 1977
Isouvaretin (**2.31**)	*U. chamae*	Stem bark	Franz and Pearl, 1976
Iso-uvarinol (**2.32**)	*X. africana*	Root	Ekpa and Anam, 1993
Kanakugin (**2.33**)	*P. cauliflora*	Fruit	Waterman and Pootakahm, 1979
Kwangsienin A (**2.34**)	*Fissistigma kwangsiense*	Bark	Shang, Zhao and Hao, 1994
Lawinal (**2.35**)	*Unona lawii*	Stem	Joshi and Gawad, 1974
	Desmos chinensis	Leaves	Wu *et al.*, 2003
Leiocarpin B (**2.36**)	*Goniothalamus leiocarpus*	Bark	Mu *et al.*, 1999
Pinocembrin (**2.37**)	*Uvaria chamae*	Stem bark	Lasswell Jr. and Hufford, 1977
	Melodorum fruticosum	Bark	Jung *et al.*, 1990
Pinostrobin (**2.38**)	*Uvaria chamae*	Root bark	Lasswell Jr. and Hufford, 1977
Uvaretin (**2.39**)	*U. chamae*	Stem bark	Franz and Pearl, 1976
Uvarinol (**2.40**)	*U. chaemae*	Stem bark	Hufford and Lasswell Jr., 1979
	X. africana	Root	Ekpa and Anam, 1993
Flavones 5,8-Dihydroxy-6,7-dimethoxyflavone (**2.41**)	*Fissistigma polyanthoides*	Bark	Jongbunprasert *et al.*, 2000

Table 2. Distributions of flavanones and flavones in the family Annonaceae (continued)

Compounds	Sources	Part	References
5-Hydroxy-7-methoxy-6-methylflavone **(2.42)**	*F. enghiana*	Stem bark	Fleischer *et al.*, 1997
5-Hydroxy-7-methoxy-8-methylflavone **(2.43)**	*F. enghiana*	Stem bark	Fleischer *et al.*, 1997
6,7-*O,O*-Dimethylbaicalein **(2.44)**	*C. argenteum*	Stem bark	Khamis *et al.*, 2004
	Popowia cauliflora	Stem	Panichpol and Waterman, 1978
	Uvaria rufa	Bark	Lojanapiwatna *et al.*,1981
7-*O*-Methylwogonine **(2.45)**	*U. rufa*	Bark	Lojanapiwatna *et al.*,1981
Baicalein trimethyl ether **(2.46)**	*P. cauliflora*	Stem	Panichpol and Waterman, 1978
	P. cauliflora	Fruit	Waterman and Pootakahm, 1979
Desmosdumotin B (Dasytrichone) **(2.47)**	*Dasymaschalon trichophorum*	Stem and leaves	Liu *et al.*, 1992
	Desmos dumosus	Root	Wu *et al.*, 2001
Desmosflavone **(2.48)**	*D. cochinchinensis*	Root	Wu *et al.*, 1994
	Friesodielsia enghiana	Stem bark	Fleischer *et al.*, 1997
Isounonal **(2.49)**	*Unona lawii*	Stem	Joshi and Gawad, 1976
Negletein **(2.50)**	*D. chinensis*	Leaves	Kiem *et al.*, 2005
	D. dumosus	Root	Wu *et al.*, 2001
Tectochrysin **(2.51)**	*Cyathostemma argenteum*	Stem bark	Khamis *et al.*, 2004
	F. enghiana	Stem bark	Fleischer *et al.*, 1997
	Uvaria rufa	Bark	Lojanapiwatna *et al.*, 1981

Table 2. Distributions of flavanones and flavones in the family Annonaceae (continued)

Compounds	Sources	Part	References
Unonal (**2.52**)	*Unona lawii*	Stem	Joshi and Gawad, 1976
Unonal-7-methyl ether (**2.53**)	*U. lawii*	Stem	Joshi and Gawad, 1976
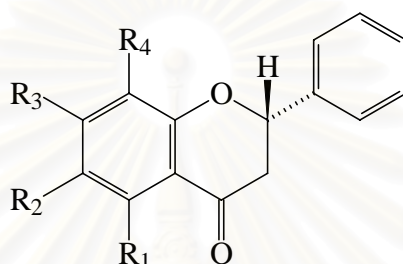
	R_1	R_2	R_3	R_4
Lawinal (**2.35**)	OH	CH_3	OH	CHO
Desmethoxymatteucinol (**2.24**)	OH	CH_3	OH	CH_3
Desmethoxymatteucinol-7-methyl ether (**2.25**)	OH	H	OCH_3	CH_3
Pinocembrin (**2.37**)	OH	H	OH	H
Pinostrobin (**2.38**)	OH	H	OCH_3	H
(+)-6,8-Dimethylpinocembrin 5-methyl ether (**2.1**)	OCH_3	CH_3	OH	OCH_3
Kwangsienin A (**2.34**)	OCH_3	OCH_3	OCH_3	OH
5,6-Dihydroxy-7-methoxy-dihydroflavone (**2.13**)	OH	OH	OCH_3	H
5,6,7-Trimethoxyflavanone (**2.12**)	OCH_3	OCH_3	OCH_3	H
5,7,8-Trimethoxyflavanone (**2.14**)	OCH_3	H	OCH_3	OCH_3
6-Hydroxy-5,7,8-trimethoxyflavanone (**2.17**)	OCH_3	OH	OCH_3	OCH_3
Kanakugin (**2.33**)	OCH_3	OCH_3	OCH_3	OCH_3
6-Formyl-5-hydroxy-7-methoxy-8-methylflavanone (**2.16**)	OH	CHO	OCH_3	CH_3
Desmosflavanone II (**2.26**)	OCH_3	CH_3	OH	CHO

Figure 4. Chemical structures of flavonoids in the family Annonaceae
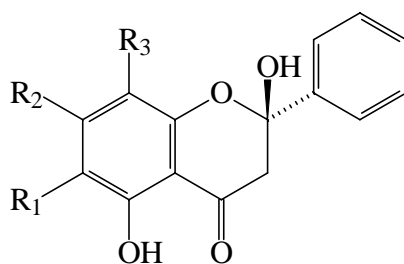
	R_1	R_2	R_3
Desmal **(2.23)**	CH_3	OH	CHO
2,5-Dihydroxy-7-methoxy-8-methylflavanone **(2.6)**	H	OCH_3	CH_3
2,5-Dihydroxy-7-methoxy-6-methylflavanone **(2.5)**	CH_3	OCH_3	H
2,5-Dihydroxy-7-methoxyflavanone **(2.7)**	H	OCH_3	H
2,5-Dihydroxy-6,7-dimethoxyflavanone **(2.4)**	OCH_3	OCH_3	H
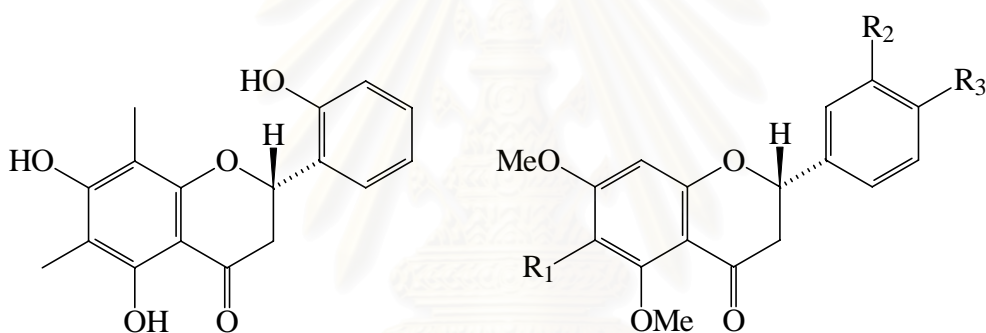
2′-Hydroxydemethoxymatteucinol **(2.11)**

Hamiltone A **(2.28)** : R_1 = OH, R_2 = H, R_3 = OMe

Hamiltone B **(2.29)** : R_1 = OMe, R_2 = R_3 = OH
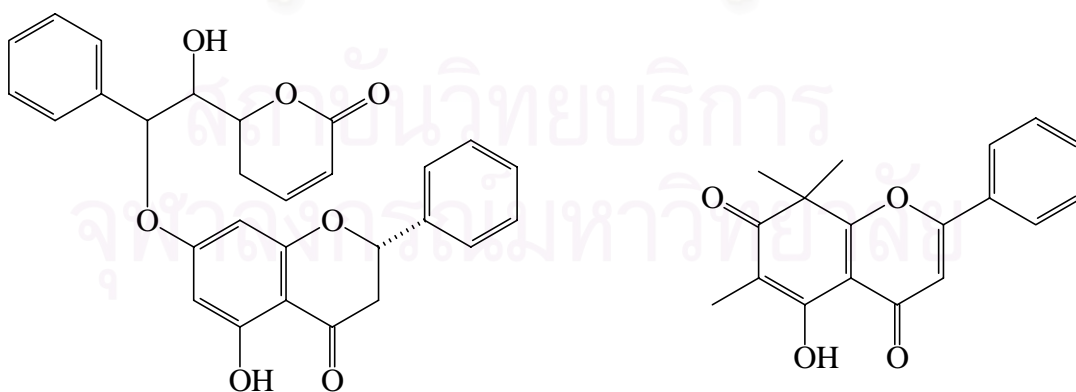
Leiocarpin B **(2.36)**

Desmosdumotin B (Dasytrichone) **(2.47)**

Figure 4. Chemical structures of flavanones and flavones in the family Annonaceae (continued)
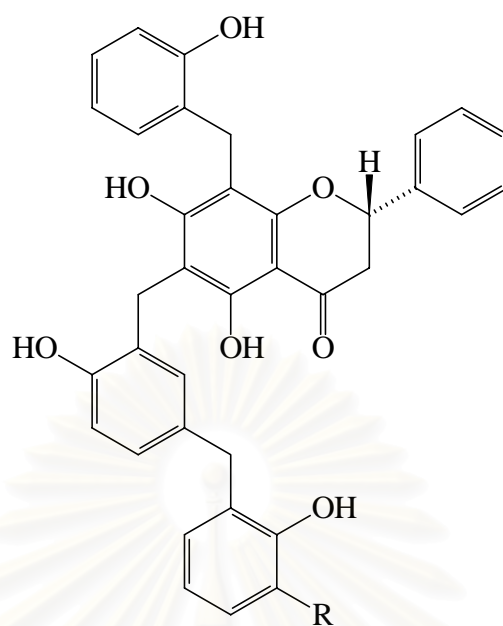
Uvarinol **(2.40)**   : R = H

2''''-Hydroxy-3''''-benzyluvarinol **(2.8)** : R = ξ—CH$_2$
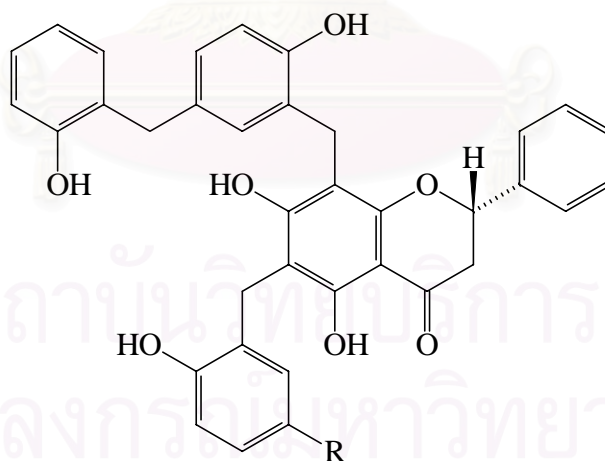
Iso-uvarinol **(2.32)**   : R = H

2''''-Hydroxy-5''''–benzylisouvarinol-B **(2.10)** : R = ξ—CH$_2$

Figure 4. Chemical structures of flavanones and flavones in the family Annonaceae
(continued)
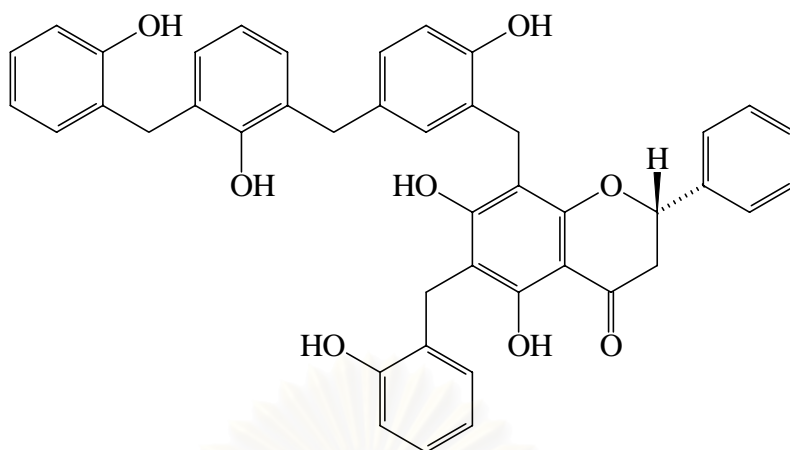
2′′′′′-Hydroxy-5′′′′–benzylisouvarinol-A **(2.9)**
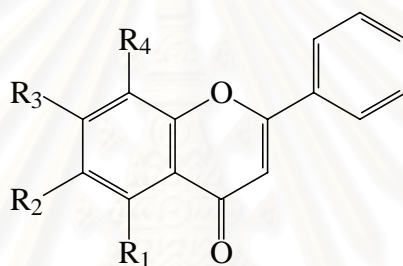
	R₁	R₂	R₃	R₄
Unonal **(2.52)**	OH	CH₃	OH	CHO
Isounonal **(2.49)**	OH	CHO	OH	CH₃
Unonal-7-methyl ether **(2.53)**	OH	CH₃	OCH₃	CHO
5-Hydroxy-7-methoxy-6-methylflavone **(2.42)**	OH	CH₃	OCH₃	H
5-Hydroxy-7-methoxy-8-methylflavone **(2.43)**	OH	H	OCH₃	CH₃
5,8-Dihydroxy-6,7-dimethoxyflavone **(2.41)**	OH	OCH₃	OCH₃	OH
Tectochrysin **(2.51)**	OH	H	OCH₃	H
7-*O*-Methylwogonine **(2.45)**	OH	H	OCH₃	OCH₃
6,7-*O,O*-Dimethylbaicalein **(2.44)**	OH	OCH₃	OCH₃	H
Baicalein trimethyl ether **(2.46)**	OCH₃	OCH₃	OCH₃	H
Desmosflavone **(2.48)**	OH	CH₃	OCH₃	CH₃
Negletein **(2.50)**	OH	OH	OCH₃	H

Figure 4. Chemical structures of flavanones and flavones in the family Annonaceae

(continued)

	R₁	R₂	R₃	R₄
Chamanetin (**2.20**)	OH	H	OH	—CH₂(2-hydroxyphenyl)
Isochamanetin (**2.30**)	OH	—CH₂(2-hydroxyphenyl)	OH	H
Dichamanetin (**2.27**)	OH	—CH₂(2-hydroxyphenyl)	OH	—CH₂(2-hydroxyphenyl)
Chamanetin 5-methyl ether (**2.21**)	OCH₃	H	OH	—CH₂(2-hydroxyphenyl)
(±)-Dichamanetin 5-methyl ether (**2.3**)	OCH₃	—CH₂(2-hydroxyphenyl)	OH	—CH₂(2-hydroxyphenyl)
7-*O*-Methylchamanetin (**2.18**)	OH	H	OCH₃	—CH₂(2-hydroxyphenyl)
7-*O*-Methylisochamanetin (**2.19**)	OH	—CH₂(2-hydroxyphenyl)	OCH₃	H
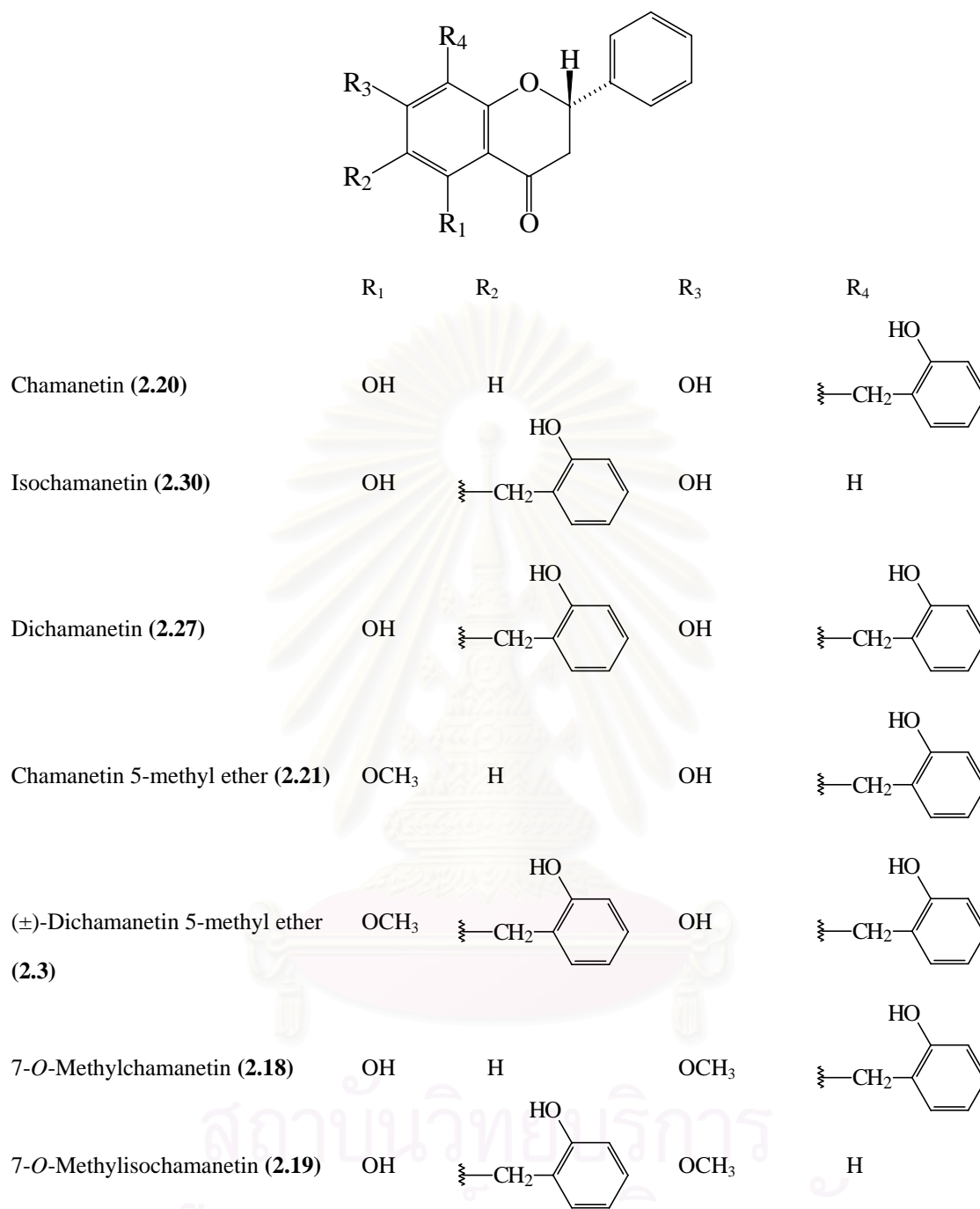
Figure 4. Chemical structures of flavanones and flavones in the family Annonaceae
(continued)

Table 3. Flavonoid glycosides reported from annonaceous plants

Flavones	
Apigenin-6-C-glucoside (vitexin)	6-Hydroxyrhamnocitrin-3-O-glucoside
Apigenin-7-O-glucoside	6-Hydroxyrhamnocitrin-3-O-(glucose-rhamnose)*
Apigenin-7-O-glucosylglucoside	
Apigenin-8-C-glucoside (isovitexin)	Quercetin-3-O-arabinoside
Hispidulin-7-O-glucosylglucoside	Quercetin-3-O-galactoside
Luteolin-6-hydroxy-7-O-rhamnosylglucoside	Quercetin-3-O-glucoside
Luteolin-7-O-glucoside	Quercetin-3-O-rhamnoside
Scutellarein-6-O-galactoside	Quercetin-3-O-arabinosylarabinoside
Scutellarein-6-O-glucosylglucoside	Quercetin-3-O-arabinosylgalactoside
	Quercetin-3-O-arabinosylglucoside
Flavonols	Quercetin-3-O-arabinosylglucuronide
	Quercetin-3-O-arabinosylrhamnoside
Kaempferol-3-O-arabinoside	Quercetin-3-O-arabinosylxyloside
Kaempferol-3-O-galactoside	Quercetin-3-O-galactosylglucoside
Kaempferol-3-O-glucoside	Quercetin-3-O-galactosylrhamnoside
Kaempferol-3-O-rhamnoside	Quercetin-3-O-glucosylglucoside
Kaempferol-3-O-arabinosylarabinoside	Quercetin-3-O-glucosylrhamnoside
Kaempferol-3-O-(arabinose-glucose)*	Quercetin-3-O-rhamnosylgalactoside
Kaempferol-3-O-arabinosylrhamnoside	Quercetin-3-O-rhamnosylglucoside
Kaempferol-3-O-(galactose-glucuronic acid)*	Quercetin-3-O-rhamnosylrhamnoside
Kaempferol-3-O-galactosylgalactoside	Quercetin-3-O-(xylose-glucuronic acid)*
Kaempferol-3-O-galactosylglucoside	Quercetin-3-O-arabinoside-7-O-arabinoside
Kaempferol-3-O-galactosylrhamnoside	Quercetin-3-O-galactoside-7-O-galactoside
Kaempferol-3-O-glucosylglucoside	Quercetin-3-O-glucoside-7-O-glucoside
Kaempferol-3-O-glucosylrhamnoside	Quercetin-3-O-glucoside-7-O-rhamnoside
Kaempferol-3-O-rhamnosylarabinoside	Quercetin-3-O-rhamnoside-7-O-arabinoside
Kaempferol-3-O-rhamnosylgalactoside	Quercetin-3-O-rhamnoside-7-O-glucoside
Kaempferol-3-O-rhamnosylglucoside	Quercetin-3-O-rhamnoside-7-O-rhamnoside
Kaempferol-3-O-rhamnosylrhamnoside	Quercetin-3-7-O-(arabinose-glucose)*
Kaempferol-3-O-(xylose-glucuronic acid)*	Quercetin-3-7-O-(arabinose-xylose)*
Kaempferol-3-O-glucosylglucosilglucoside	Quercetin-3-O-rhamnoside-7-O-rhamnoside-30-O-rhamnoside
Kaempferol-3-O-(glucose-glucose-rhamnose)*	
Kaempferol-3-O-(glucose-rhamnose-rhamnose)*	Isorhamnetin-3-O-galactoside
Kaempferol-3-O-(rhamnose-galactose)*glucoside	Isorhamnetin-3-O-glucoside
Kaempferol-3-O-glucoside-7-O-rhamnoside	Isorhamnetin-3-O-galactosylgalactoside
Kaempferol-3-O-rhamnoside-7-O-arabinoside	Isorhamnetin-3-O-galactosylrhamnoside
Kaempferol-3-O-glucoside-7-O-glucosylrhamnoside	Isorhamnetin-3-O-glucosylglucoside
Kaempferol-3-O-rhamnoside-7-O-glucosylglucoside	Isorhamnetin-3-O-rhamnosylglucoside
Rhamnocitrin-3-O-glucoside (7-O-methylkaempferol-3-O-glucoside)*	Rhamnetin-3-O-glucosylglucoside
Rhamnocitrin-3-O-rhamnosylglucoside	Rhamnetin-3-O-glucosylrhamnoside
	Rhamnetin-3-O-rhamnosylglucoside

* Relative position of sugar not determined

Natural inhibitors of advanced glycation end-products (AGE) formation

Accumulation of the products of non-enzymatic reaction between reducing sugars and proteins (protein glycation), known as advanced glycation end-products (AGEs), in the body leads to structural and functional modifications of tissue proteins. Many studies have shown glycation to play important roles in the progress of normal aging and the pathogenesis of diabetic complications. Therefore, the investigations to find agents capable of inhibiting the formation of AGEs are purposed to have therapeutic potentials in patients with diabetes or other age-related diseases (Singh *et al*., 2001).

Non-enzymatic reaction between reducing sugar and free amino group of proteins, also known as Maillard reaction, leads to the formation of glycated protein termed Amadori product. Further rearrangement, oxidation and reduction of the Amadori product result in the formation of several complex, irreversible and fluorescent products which are named advanced glycation end-products. Examples of these AGEs are pentosidine, carboxymethyllysine, crossline and pyralline. Some of these compounds can react with a free amino group nearby and form cross-linking between proteins (Ulrich and Cerami, 2001). The cross-linked protein, e.g. cross-linked collagen, are postulated to confer pathological conditions found in diabetic patients and aging, such as arterial stiffness and decreased myocardial compliance, resulting from the loss of collagen elasticity (Singh *et al*., 2001; Aronson, 2003).

The oxidation process is believed to play an important role in AGEs formation. Further oxidation of Amadori product leads to the formation of intermediate carbonyl compounds that can react with the nearby lysine or arginine residues to form protein crosslink or AGEs. These reactive carbonyl compounds may also be generated from the metal ion-catalyzed autooxidation of glucose (Rahbar and Figarola, 2003; Voziyan *et al*., 2003). Therefore, agents with antioxidative or metal-chelating properties may retard the process of AGEs formation by preventing further oxidation of Amadori product and metal-catalyzed glucose oxidation.

Aminoguanidine (pimagedine) (**3.1**), a small hydrazine-like compound, has been synthesized and become one of the most promising pharmacological interventions for glycation inhibition. This agent prevents AGE formation by blocking the carbonyl groups of Amadori products (Edelstein and Brownlee, 1992; Thornalley, 2003). Aspirin (acetylsalicylic acid) (**3.2**), with its ability to act as a free radical scavenger and metal ion chelator, is another pharmacological agent which was demonstrated to reduce glycation *in*

vitro and in animal experiments. However, these compounds can cause unwanted side effects in patients, such as gastrointestinal disturbances, flu-like symptoms and anemia (Fu, Thorpe and Baynes, 1994).

In addition to the development of synthetic compounds as inhibitors of AGE formation, there has been a growing interest in anti-glycation natural products which might be less toxic. Most of these active phytochemicals are polyphenolic metabolites. The flavonoid quercetin (**3.3**), eriodictyol (**3.4**), 5,6,4'-trihydroxy-7,8,3'-trimethoxyflavone (**3.5**) and cirsilineol (**3.6**) obtained from *Thymus vulgaris* leaves were active inhibitors, and both quercetin and eriodictyol were more potent than aminoguanidine, a known glycation inhibitor, in the inhibition of AGEs (Morimitsu *et al.*, 1995). Curcumin (**3.7**), a principal constituent of *Curcuma longa*, can prevent the accumulation of AGEs and cross-linking collagen in diabetic rats (Sajithlal, Chithra and Chandrakasan, 1998). Examination of the fruit rind extract from *Garcinia indica* revealed an active AGE inhibitor, garcinol (**3.8**), which is a polyisoprenylated benzophenone derivative (Yamaguchi *et al.*, 2000). Plantagoside (**3.9**) from the seeds of *Plantago asiatica* (Matsuura *et al.*, 2002b), as well as two flavone C-glycosides, altheranthin (**3.10**) and chrysoeriol 6-*C*-β-boivinopyranosyl-7-*O*-β-glucopyranoside (**3.11**), from the style of *Zea mays* (Suzuki, Okada and Okuyama, 2003) exhibited significant inhibitory activity against AGE formation *in vitro*.

A series of tannins (**3.12**-**3.18**) isolated from Luobuma tea (*Apocynum venetum*) strongly inhibited AGE formation (Yokozawa and Nakagawa, 2004). Further investigation for anti-AGE agents from natural products led to the isolation of three flavonol glycosides, astragalin (**3.19**), isoquercitrin (**3.20**) and quercetin 3-*O*-α-L-arabinopyranosyl-(1→2)-β-D-glucopyranoside (**3.21**) from the leaves of *Eucommia ulmoides*, a plant which is a folk remedy for the treatment of diabetes in Korea (Kim *et al.*, 2004). All of these compounds exhibited glycation inhibitory activity comparable to aminoguanidine. An extract of *Cratoxylum cochinchinensis* containing at least 90% mangiferin (**3.22**) was particularly potent in inhibiting the formation of AGEs on proteins (Tang *et al.*, 2004). Recently, activity-guided fractionation of the ethyl acetate extract of an annonaceous tropical tree, *Stelechocarpus cauliflorus,* yielded astilbin (**3.23**), a dihydroflavonol glycoside, as an AGE inhibitor (Wirasathien *et al.*, 2006).
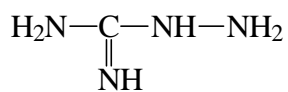
Aminoguanidine (pimagedine) **(3.1)**
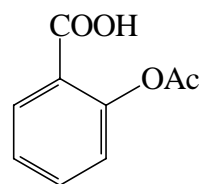
Aspirin (acetylsalicylic acid) **(3.2)**
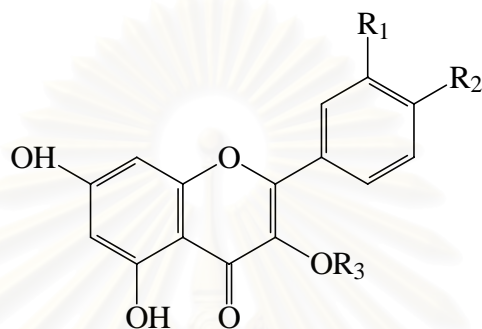
	R_1	R_2	R_3
Quercetin **(3.3)**	OH	OH	H
Astragalin **(3.19)**	H	OH	Glucose
Isoquercitrin **(3.20)**	OH	OH	Glucose
Quercetin 3-*O*-α-L-arabinopyranosyl-	OH	OH	Arabinose(1→2)Glucose
(1→2)-β-D-glucopyranoside **(3.21)**			

Curcumin **(3.7)**
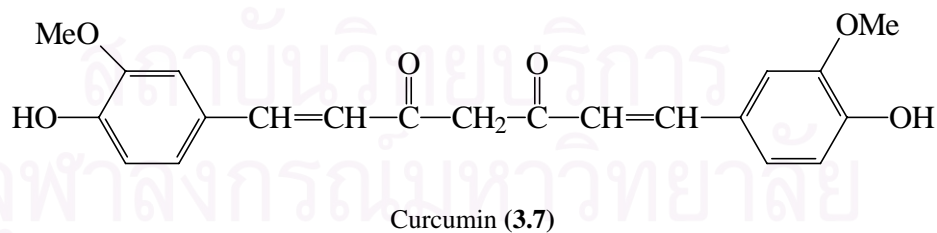
Figure 5. Inhibitors of advanced glycation end-products (AGE) formation

	R_1	R_2	R_3	R_4	R_5
5,6,4′-Trihydroxy-7,8,3′-trimethoxyflavone **(3.5)**	OH	CH$_3$	OCH$_3$	OCH$_3$	OH
Cirsilineol **(3.6)**	OCH$_3$	CH$_3$	H	OCH$_3$	OH
Altheranthin **(3.10)**	Boivinose	H	H	OH	OCH$_3$
Chrysoeriol 6-*C*-β-boivinopyranosyl-7-*O*-β-glucopyranoside **(3.11)**	Boivinose	Glucose	H	OH	OCH$_3$
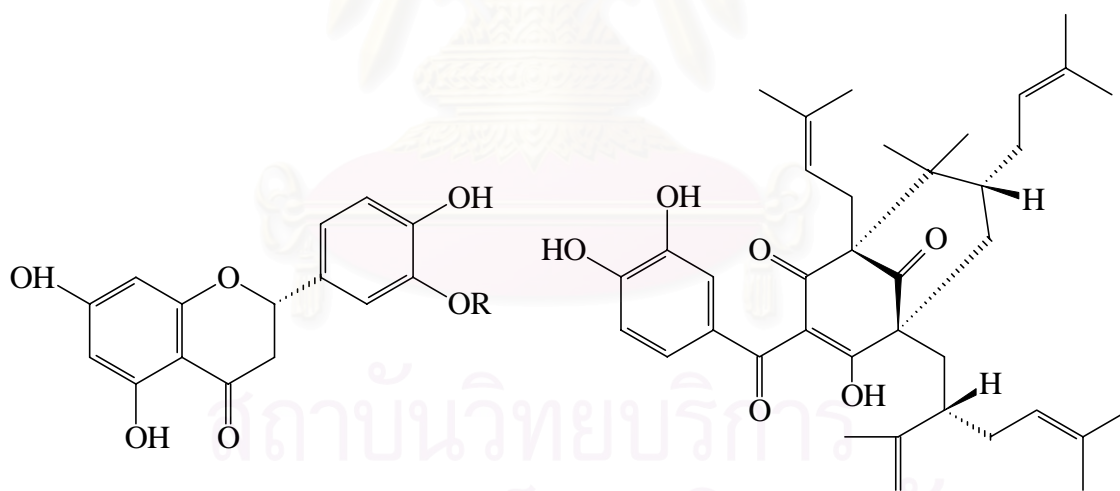
Eriodictyol **(3.4);**   R = H   Garcinol **(3.8)**

Plantagoside **(3.9);**   R = Glucose

Figure 5. Inhibitors of advanced glycation end-products (AGE) formation (continued)
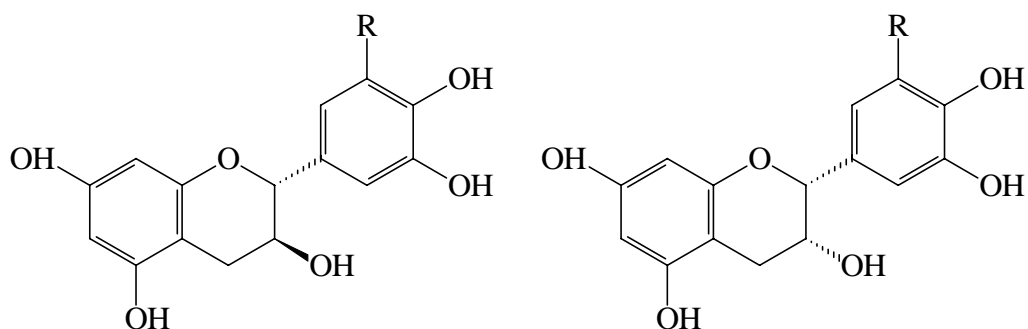
Gallocatechin (**3.12**)   : R = OH

Catechin (**3.13**)   : R = H

Epigallocatechin (**3.14**)   : R = OH

Epicatechin (**3.15**)   : R = H
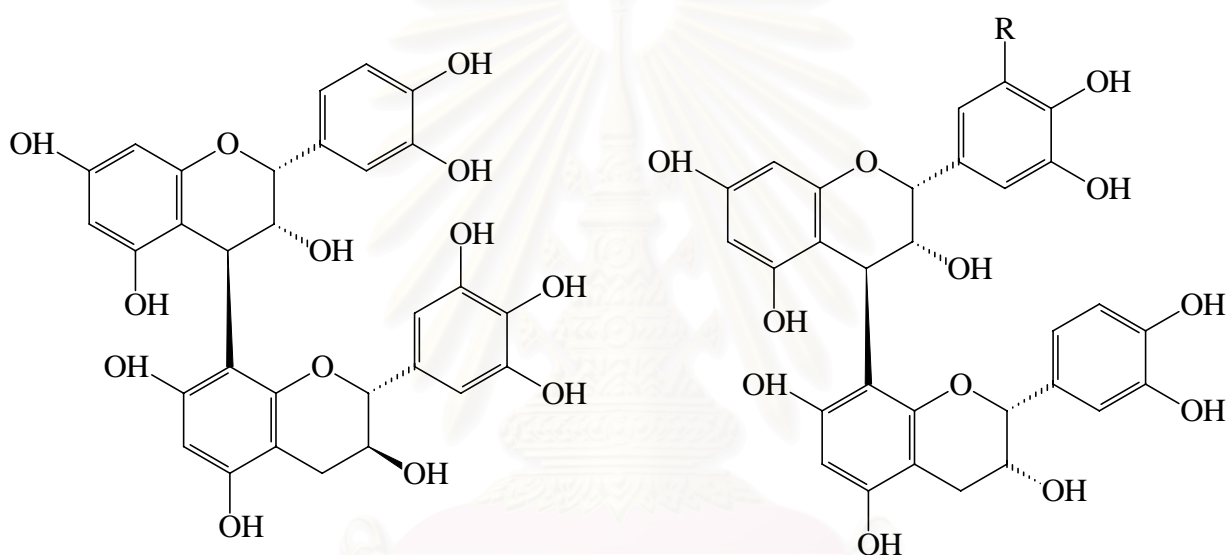
Epicatechin-(4β-8)-gallocatechin (**3.16**)

Epigallocatechin-(4β-8)-epicatechin (**3.17**)   : R = OH

Procyanidin B-2 (**3.18**)   : R = H
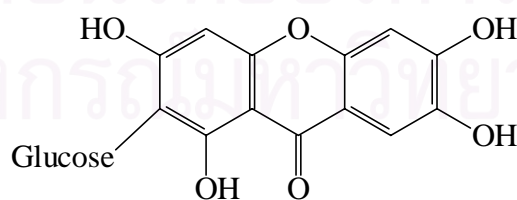
Mangiferin (**3.22**)

Figure 5. Inhibitors of advanced glycation end-products (AGE) formation (continued)
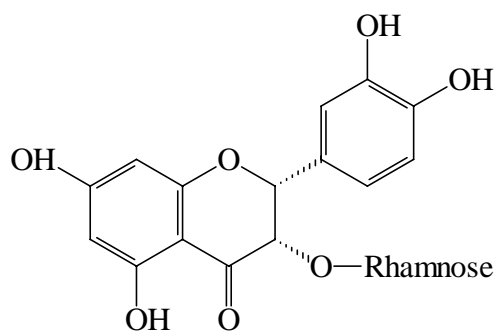
Astilbin **(3.23)**

Figure 5. Inhibitors of advanced glycation end-products (AGE) formation (continued)

CHAPTER III

EXPERIMENTAL

1. Sources of Plant Materials

The leaves and stems of *Mitrephora maingayi* Hook. F. & Thomson were collected from Khao Chong, Trang, Thailand in March, 2003. The leaves and stems of *Uvaria rufa* Blume were collected from Chachoengsao, Thailand in April of the same year. Voucher specimens of both plants have been deposited at the herbarium of the Department of Pharmaceutical Botany, Faculty of Pharmaceutical Sciences, Chulalongkorn University, Bangkok, Thailand.

2. General Techniques

2.1 Solvents

Throughout this work, all organic solvents were of commercial grade and were redistilled prior to use.

2.2 Analytical Thin-Layer Chromatography (TLC)

Technique	:	One dimension, ascending
Adsorbent	:	Silica gel 60 F_{254} (E. Merck) pre-coated plate
Layer thickness	:	0.2 mm
Distance	:	5.0 cm
Temperature	:	Laboratory temperature (25-30 ℃)
Detection	:	1) Ultraviolet light (254 and 365 nm)
		2) Spraying with anisaldehyde-sulfuric acid solution and
		heating at 100-110 ℃ for 10 min

2.3 Column Chromatography

2.3.1 Quick Column Chromatography

Column	:	Sintered glass filter column
Adsorbent	:	Silica gel 60 (No. 7734) particle size 0.063-0.200 mm
		(E. Merck)
Solvent	:	Various solvent systems depending on materials

Packing method	:	Adsorbent was wet-packed. The slurry of adsorbent in the solvent was poured into the column. The solvent was sucked out by vacuum pump and the adsorbent was pressed tightly.
Sample loading	:	The sample extract was dissolved in a small amount of the organic solvent, mixed with a small quantity of the adsorbent, triturated, dried and then placed gently on top of the column.
Detection	:	Fractions were examined by TLC technique in the same manner as described in section 2.2

2.3.2 Flash Column Chromatography

Column size	:	The glass columns, 1.5-5.0 cm in diameter, were used depending on the quantity of the sample to be separated.
Adsorbent	:	Silica gel 60 (No. 9385) particle size 0.040-0.063 mm (E. Merck)
Solvent	:	Various solvent systems depending on the materials
Packing method	:	Adsorbent was wet-packed. The slurry of adsorbent in the eluent was poured into the column and allowed to set.
Sample loading	:	The sample was dissolved in a small amount of the eluent and then applied gently on top of the column.
Detection	:	Fractions were examined by TLC technique in the same manner as described in section 2.2

2.3.3 Gel Filtration Chromatography

Column size	:	Glass columns, 2.2 cm in diameter
Gel Filter	:	Sephadex LH-20 (Pharmacia Biotech AB)
Solvent	:	$CHCl_3$-MeOH (2:1) and MeOH
Packing method	:	Gel filter was suspended in the eluent and left standing to swell for 24 hours prior to use, then poured into the column and allowed to set tightly.
Sample loading	:	The sample was dissolved in a small amount of the eluent and then applied gently on top of the column.
Detection	:	Fractions were examined by TLC technique in the same manner as described in section 2.2

2.3.4 Medium Pressure Liquid Chromatography (MPLC)

Column	:	Pre-packed column Licroprep RP-18 (30 x 250 mm)
Flow rate	:	5 ml/min
Mobile Phase	:	MeOH-water gradient (0:1 to 4:1)
Injection volume	:	5 ml
Pump	:	Buchi 681
Detector	:	996 Photodiode-array
Temperature	:	25 ℃

2.3.5 High Pressure Liquid Chromatography (HPLC)

Column

(Semi-preparative)	:	Cosmosil C18-AR II (20 × 250 mm)
(Analytical)	:	Cosmosil C18 AR II (4.6 × 15 mm)

Flow rate

(Semi-preparative)	:	2 ml/min
(Analytical)	:	1 ml/min

Mobile Phase

(Semi-preparative)	:	MeCN-water gradient (10:9 to 8:2)
(Analytical)	:	MeCN-water (15:85)

Injection volume

(Semi-preparative)	:	2 ml
(Analytical)	:	1 µl
Pump	:	Gilson 445
Detector	:	996 Photodiode-array
Temperature	:	25 ℃

2.4 Spectroscopy

2.4.1 Ultraviolet (UV) Absorption Spectra

UV absorption spectra were obtained on a Shimadzu UV-160A spectrophotometer (Pharmaceutical Research Instrument Center, Faculty of Pharmaceutical Sciences, Chulalongkorn University)

2.4.2 Infrared (IR) Absorption Spectra

IR absorption spectra (KBr disc and film) were recorded on a Perkin Elmer

FT-IR 1760X spectrometer (Scientific and Technological Research Equipment Center, Chulalongkorn University).

2.4.3 Mass Spectra (MS)

Electrospray Ionization Time of Flight (ESI-TOF) mass spectra were obtained on a Micromass LCT mass spectrometer (National Center for Genetic Engineering and Biotechnology, BIOTEC, Thailand).

2.4.4 Proton and Carbon-13 Nuclear Magnetic Resonance (^{1}H and ^{13}C NMR) Spectra

1) ^{1}H (300 MHz) and ^{13}C (75 MHz) NMR spectra were obtained on a Bruker DPX-300 FT-NMR spectrometer (Pharmaceutical Research Instrument Center, Faculty of Pharmaceutical Sciences, Chulalongkorn University).

2) ^{1}H (500 MHz) and ^{13}C (125 MHz) NMR spectra were obtained on a JEOL JMN-A 500 spectrometer (Scientific and Technological Research Equipment Center, Chulalongkorn University).

The solvents for NMR spectra were deuterated chloroform ($CDCl_3$), deuterated methanol (CD_3OD), deuterated acetone (acetone-d_6) and deuterated dimethylsulfoxide (DMSO-d_6). The chemical shifts were reported in ppm scale using the chemical shift of the solvent as the reference signal.

2.4.5 Fluorescence Spectrophotometer

Fluorescence spectra were measured on a Hitachi F-2000 fluorescence spectrophotometer (Kobe Pharmaceutical University).

2.5 Physical Properties

2.5.1 Melting Points

Melting points were obtained on a Fisher-John melting point apparatus (Department of Pharmaceutical Botany, Faculty of Pharmaceutical Sciences, Chulalongkorn University).

2.5.2 Optical Rotations

Optical rotations were measured on a Perkin-Elmer 341 polarimeter using a sodium lamp operating at 589 nm (Pharmaceutical Research Instrument Center, Faculty of Pharmaceutical Sciences, Chulalongkorn University).

3. Extraction and Isolation

3.1 Extraction and Isolation of Compounds from the Leaves of *Uvaria rufa*

3.1.1 Extraction

Dried leaves of *Uvaria rufa* (290 g) were ground then macerated with hexane (5 x 1.5 L), EtOAc (5 x 1.5 L) and MeOH (5 x 1.5 L), successively. Each filtrate was pooled and evaporated to dryness under reduced pressure at temperature not exceeding 40 ℃ to yield the hexane extract (8.10 g, 2.79 % based on dried weight of leaves), EtOAc extract (9.61 g, 3.31 % of dried weight) and MeOH extract (29.94 g, 10.32 % of dried weight).

3.1.2 Isolation of Compounds from the Hexane Extract of *U. rufa* Leaves

The hexane extract (7.0 g) was subjected to quick column chromatography. The extract was dissolved in a small amount of hexane, triturated with kieselguhr, dried at room temperature and then applied to the top of a silica gel column (400 g, 13 x 6 cm). Elution was performed in polarity gradient manner with mixtures of hexane and acetone (99:1 to 0:1). The collected fractions (300 ml each) were examined by TLC, with hexane-acetone (9:1) as the developing solvent system. Sixty-five fractions were collected and combined according to their TLC profiles into 5 major fractions (A1-A5) as shown in **Table 4**.

Table 4. Combined fractions from the hexane extract of *U. rufa* leaves

Fraction Code	Number of Eluates	Weight (g)
A1	1-15	2.74
A2	16-22	0.91
A3	23-38	1.14
A4	39-49	0.77
A5	50-65	0.68

3.1.2.1 Isolation of Compound URL-1

When developed with hexane-acetone (7:3), fraction A4 (0.77 g) displayed one main spot, which appeared as an orange-brown spot on TLC plate after being sprayed with anisaldehyde-sulfuric acid solution and heated for 5 min. Recrystallization of

A4 with MeOH gave the compound URL-1 as white amorphous powder (188 mg, 0.075 % of dried weight). Isolation of this compound from the hexane extract of *U. rufa* leaves was summarized in **Scheme 1**.

3.1.3 Isolation of Compounds from the EtOAc Extract of *U. rufa* Leaves

The EtOAc extract (7.0 g) was separated by quick column chromatographic technique. The extract was dissolved in a small volume of EtOAc, triturated with kieselguhr and dried at room temperature, then applied to the top of a column of silica gel (400 g, 13 x 6 cm). A gradient of hexane-acetone (9:1 to 0:1) was used to elute the column, yielding 59 fractions of 300 ml each. MeOH was then used to wash down the column. The collected fractions were monitored and combined according to their TLC patterns (solvent system: hexane-acetone = 2:1) to give 7 major fractions (B1-B7) as shown in **Table 5**.

Table 5. Combined fractions from the EtOAc extract of *U. rufa* leaves

Fraction Code	Number of Eluates	Weight (g)
B1	1-12	1.86
B2	13-22	0.71
B3	23-34	2.28
B4	35-41	0.62
B5	42-55	0.55
B6	56-58	0.47
B7	59	0.38

3.1.3.1 Isolation of Compound URL-1

Fraction B3 (2.28 g) was fractionated on a silica gel column. The fraction was dissolved in a small volume of hexane-EtOAc (20:1) and applied to the top of a column (4.5 x 10 cm) already packed with a slurry of silica gel (75 g) in the same solvent system. The mixture was also employed as the eluting solvent and the collected fractions were examined by TLC, with hexane-EtOAc (15:1) as the developing system. The volume

of each fraction was approximately 50 ml. Eighty-three fractions were collected. The fractions were pooled according to their TLC patterns into 6 combined fractions (B31-B36) as presented in **Table 6**.

Table 6. Combined fractions from the fraction B3

Fraction Code	Number of Eluates	Weight (g)
B31	1-22	0.51
B32	23-29	0.33
B33	30-45	0.28
B34	46-53	0.79
B35	54-64	0.23
B36	65-83	0.11

Fraction B34 (0.79 g), which appeared as an orange-brown spot on the TLC plate after being sprayed with anisaldehyde-sulfuric acid solution and heated, was further purified on a Sephadex LH-20 column (2.2 x 85 cm). The fraction was dissolved in a small volume of CHCl$_3$-MeOH (2:1) and loaded on the top of the column. The same solvent mixture was employed as the eluting solvent. The fractional volume was about 15 ml. All 20 collected fractions were examined by TLC with hexane-EtOAc (2:1) as the developing solvent, then combined into 5 fractions (B341-B345, **Table 7**)

Table 7. Combined fractions from the fraction B34

Fraction Code	Number of Eluates	Weight (mg)
B341	1-6	432.6
B342	7-11	205.0
B343	12-14	86.0
B344	15-16	48.1
B345	17-20	16.4

Recrystallization of fraction B344, which appeared as an orange-brown spot on the TLC plate after being sprayed with anisaldehyde-sulfuric acid solution and heated for 5 min, afforded compound URL-1 as white needles (35 mg, 0.0166 % of dried weight). The isolation of URL-1 from the EtOAc extract of *U. rufa* leaves can be summarized as shown in **Scheme 2**.

3.1.3.2 Isolation of Compound URL-2

Fraction B4 (0.62 g) was subjected to silica gel column chromatography (75 g, 3 x 25 cm) using gradient solvent mixture of cyclohexane and acetone (5:1 to 0:1) as the mobile phase, to give 51 fractions (50 ml each). These fractions were collected and combined based on their TLC patterns (solvent system: cyclohexane-acetone = 3:1) to give 5 fractions (B41 –B45) as shown in **Table 8**.

Table 8. Combined fractions from the fraction B4

Fraction Code	Number of Eluates	Weight (mg)
B41	1-8	311.0
B42	9-20	77.4
B43	21-25	16.0
B44	26-32	25.8
B45	33-51	174.0

Fraction B43 appeared as one orange-brown spot on the TLC plate sprayed with anisaldehyde-sulfuric acid solution and heated for 5 min. Recrystallization of the fraction gave 11 mg of compound URL-2 (0.0052 % yield) as white amorphous powder. The isolation of URL-2 from the EtOAc extract of *U. rufa* leaves was also presented in **Scheme 2**.

3.1.3.3 Isolation of Compound URL-3, URL-4 and URL-5

Fraction B44 (25.8 mg) was repeatedly purified on a silica gel column (40 g, 2.3 x 20 cm) using a solvent mixture of cyclohexane and EtOAc (3:1) as the eluent, to

afford 30 fractions (50 ml each). These fractions were collected and combined according to their TLC profiles (solvent system: cyclohexane-EtOAc = 1:1) to give 4 fractions (B441 – B444) as shown in **Table 9**.

Table 9. Combined fractions from the fraction B44

Fraction Code	Number of Eluates	Weight (mg)
B441	1-9	8.8
B442	10-21	10.6
B443	22-24	4.0
B444	25-30	2.1

Fraction B442, recrystallized with MeOH, gave 6.4 mg of white amorphous powder, named compound URL-3 (0.0030 % yield). The isolation of this compound from the EtOAc extract of *U. rufa* leaves can be summarized as presented in **Scheme 2**.

Fraction B443, evaporated to dryness, yielded 4 mg of white amorphous powder, named compound URL-4 (0.0019 % yield), whereas recrystallization of fraction B444 with MeOH afforded compound URL-5 as white amorphous powder (1.9 mg, 0.0009 % of dried weight) **(Scheme 2)**.

3.2 Extraction and Isolation of Compounds from the Stems of *U. rufa*
3.2.1 Extraction

The dried stems of *U. rufa* (1.6 kg) were chopped into small pieces, then successively macerated with hexane (5 x 10 L), EtOAc (5 x 10 L) and MeOH (5 x 10 L). The filtrate was pooled and evaporated under reduced pressure at temperature not exceeding 40 ºC to obtain the hexane extract (6.47 g, 0.40% of dried weight), EtOAc extract (9.95 g, 0.62% of dried weight) and MeOH extract (31.50 g, 1.97% of dried weight).

3.2.2 Isolation of Compounds from the Hexane Extract of *U. rufa* Stems

The hexane extract (6.0 g) was subjected to quick column chromatography. The extract was dissolved in a small amount of hexane, triturated with

kieselguhr, dried at room temperature, then applied to the top of a column of silica gel (400 g, 13 x 6 cm). Elution was performed in polarity gradient manner with mixtures of hexane and acetone (99:1 to 0:1). Each collected fraction (approximately 300 ml) was examined by TLC, with hexane-acetone (19:1) as the developing system. Fifty-two fractions were collected and combined according to their TLC profiles into 5 major fractions (C1-C5) as presented in **Table 10**.

Table 10. Combined fractions from the hexane extract of *U. rufa* stems

Fraction Code	Number of Eluates	Weight (g)
C1	1-19	2.15
C2	20-28	2.07
C3	29-34	1.10
C4	35-45	0.38
C5	46-52	0.14

3.2.2.1 Isolation of Compound URS-1

Fraction C2 (2.07 g) was fractionated by silica gel column chromatography. The fraction was dissolved in a small volume of hexane-EtOAc (9:1) and applied to the top of a column (4.5 x 20 cm) already packed with slurry of silica gel (150 g) in the same solvent system, which was employed as the eluting solvent. The collected fractions were checked on TLC, with hexane-EtOAc (4:1) as the developing system. The volume of each fraction was approximately 50 ml. Fifty fractions were collected and pooled according to their TLC patterns into 5 fractions (C21-C25) as shown in **Table 11**.

Table 11. Combined fractions from the fraction C2

Fraction Code	Number of Eluates	Weight (g)
C21	1-17	1.02
C22	18-29	0.56
C23	30-33	0.30

Table 11. Combined fractions from the fraction C2 (continued)

Fraction Code	Number of Eluates	Weight (g)
C24	34-35	0.01
C25	36-50	0.06

When developed with hexane-EtOAc (4:1), fraction C23 (0.30 g) displayed one main spot, which appeared dark purple on TLC plate after spraying with anisaldehyde-sulfuric acid solution and heating for 5 min. Recrystallization of fraction C23 in acetone gave compound URS-1 as a white amorphous powder (22 mg, 0.0015 % of dried weight). Isolation of compound URS-1 from the hexane extract of *U. rufa* stem was shown in **Scheme 3**.

3.2.2.2 Isolation of Compound URS-2

In addition to fraction C23, TLC profiles of fraction C24, another combined fraction from the fraction C2, also showed a major purple spot. Recrystallization of fraction C24 in MeOH yielded 5 mg of a white amorphous powder, named compound URS-2.

This compound URS-2 was also isolated from the nearby fraction C3. Fraction C3 (1.10 g) was purified using gel filtration method. It was dissolved in a small volume of CHCl$_3$-MeOH (2:1) and loaded on the top of a Sephadex LH-20 column (2.2 x 85 cm). This same solvent mixture was employed as the eluting solvent. The volume of each collected fraction was approximately 15 ml. Nineteen fractions were collected and combined, following TLC examination with hexane-EtOAc (4:1) as the developing solvent, into 4 fractions (C31-C34, **Table 12**).

Table 12. Combined fractions from C3

Fraction Code	Number of Eluates	Weight (mg)
C31	1-7	460.3
C32	8-11	518.0

Table 12. Combined fractions from C3 (continued)

Fraction Code	Number of Eluates	Weight (mg)
C33	12-16	61.0
C34	17-19	58.0

Recrystallization of fraction C33 in MEOH afforded another quantity of compound URS-2 (45 mg, 0.0030 % of dried weight). The isolation of compound URS-2 from the hexane extract of *U. rufa* stem can be summarized as shown in **Scheme 3**.

3.2.3 Isolation of Compounds from the EtOAc Extract of *U. rufa* Stems

The EtOAc extract (9 g) was separated by quick column chromatographic technique. Elution was performed in a polarity gradient manner with mixtures of hexane and acetone (9:1 to 0:1) to give 95 fractions (300 ml each). These fractions were combined according to their TLC patterns (solvent system: hexane-acetone = 4:1) to yield 8 fractions (D1-D8, **Table 13**).

Table 13. Combined fractions from the EtOAc extract of *U. rufa* stem

Fraction Code	Number of Eluates	Weight (g)
D1	1-35	2.97
D2	36-47	1.14
D3	48-52	0.07
D4	53-60	0.08
D5	61-72	1.77
D6	73-79	0.27
D7	80-86	0.18
D8	87-95	2.36

3.2.3.1 Isolation of Compound URS-3

Fraction D1 (2.97 g) was fractionated on a silica gel column (75 g, 3 x 25 cm) using gradient mixtures of hexane-EtOAc (19:1 to 0:1) to give 52 fractions. The collected fractions (50 ml each) were examined by TLC, with hexane-EtOAc (9:1) as the developing solvent system, then pooled according to their TLC profiles into 7 major fractions (D11-D17) as shown in **Table 14**.

Table 14. Combined fractions from the fraction D1

Fraction Code	Number of Eluates	Weight (g)
D11	1-11	0.83
D12	12-18	0.55
D13	19-25	0.36
D14	26-37	0.90
D15	38-40	0.13
D16	41-43	0.04
D17	44-52	0.13

Examination of fraction D14 (0.9 g) revealed a blue spot on TLC plate after being sprayed with anisaldehyde-sulfuric acid solution and heated for 5 min. This fraction was repeatedly chromatographed on a silica gel column (75 g, 3 x 25 cm) using hexane-acetone (20:1) as the eluent. Fifty-four fractions (50 ml each) were collected and combined, based on their TLC patterns, to afford 4 main fractions (D141-D144) as presented in **Table 15**. Compound URS-3 (17 mg, 0.0012 % yield of dried weight) was obtained as colorless oil from fraction D143. Its isolation was summarized in **Scheme 4**.

Table 15. Combined fractions from the fraction D14

Fraction Code	Number of Eluates	Weight (mg)
D141	1-18	412.1
D142	19-25	38.9

Table 15. Combined fractions from the fraction D14 (continued)

Fraction Code	Number of Eluates	Weight (mg)
D143	26-28	17.0
D144	29-54	402.6

3.2.3.2 Isolation of Compound URS-4

Fraction D3, which appeared as a yellow powder (70 mg), was further purified on a Sephadex LH-20 column with $CHCl_3$-MeOH (2:1) as the eluent. Ten fractions (15 ml per fraction) were collected, then combined based on their TLC patterns (solvent system: hexane-EtOAc = 4:1) into 3 fractions (D31-D33) as shown in **Table 16**. Compound URS-4 (27 mg, 0.0019 % yield) precipitated as yellow amorphous powder from the fraction D32.

Table 16. Combined fractions from the fraction D3

Fraction Code	Number of Eluates	Weight (mg)
D31	1-6	31.4
D32	7-9	30.0
D33	10	7.7

3.2.3.3 Isolation of Compound URS-5

Fraction D5 (1.77 g), which was another yellow powder fraction and showed three yellow spots on TLC, was further separated on a silica gel column (75 g, 3 x 25 cm) eluted with a gradient mixture of $CHCl_3$-acetone (19:1 to 9:1) to give 64 fractions (50 ml each). Similar fractions were combined, after being examined by TLC (solvent system: $CHCl_3$-acetone = 10:1), into 6 fractions (D51-D56, **Table 17**). Recrystallization of the fraction D52 (13.4 mg) with a mixture of $CHCl_3$-acetone (1:1) afforded compound URS-5 as pale yellow powder (12 mg, 0.0008 % yield) (**Scheme 4**).

Table 17. Combined fractions from the fraction D5

Fraction Code	Number of Eluates	Weight (mg)
D51	1-16	805.8
D52	17-19	13.4
D53	20-42	311.8
D54	43-46	15.0
D55	47-50	18.9
D56	51-64	557.2

3.2.3.4 Isolation of Compound URS-6

Following the purification of the less polar, yellow-colored constituent of the fraction D5 as compound URS-5, the second, more polar one was further isolated. Fraction D54 (15 mg) was subjected to a Sephadex LH-20 column using MeOH as the eluent. Twelve fractions (15 ml each) were collected and combined according to their TLC patterns (solvent system: CHCl$_3$-acetone = 9:1) into 3 fractions (D541-D543) as shown in **Table 18**. Compound URS-6 (10 mg, 0.0007 % yield) was obtained as yellow amorphous powder from the fraction D543.

Table 18. Combined fractions from the fraction D54

Fraction Code	Number of Eluates	Weight (mg)
D541	1-6	2.6
D542	7-9	2.0
D543	10-12	10.2

3.2.3.5 Isolation of Compound URS-7

The third yellow compound, the most polar, from fraction D5 (1.77 g) appeared as main component in fraction D55 (18.9 mg). After recrystallization D55 by using the mixture of CHCl$_3$-acetone (1:1), compound URS-7 as yellow powder (14.4 mg, 0.0008 %

yield) was obtained (**Scheme 4**).

3.2.3.6 Isolation of Compound URS-8

Fraction D8 (2.36 g) was fractionated on a silica gel column. The fraction was dissolved in a small volume of CHCl$_3$-MeOH (9:1) and applied to the top of a column (4.5 x 20 cm) already packed with slurry of silica gel (150 g) in the same solvent. A gradient mixture of CHCl$_3$-MeOH (9:1 to 8:2) was employed as the eluting solvent. The collected fractions were monitored by TLC, with CHCl$_3$-MeOH (4:1) as the developing system. The fractional volume was approximately 50 ml. Fifty-five fractions were collected and pooled according to their TLC patterns into 7 fractions (D81-D87) as presented in **Table 19**.

Table 19. Combined fractions from the fraction D8

Fraction Code	Number of Eluates	Weight (g)
D81	1-22	1.19
D82	23-25	0,02
D83	26-30	0.12
D84	31-41	0.49
D85	42-50	0.46
D86	51-53	0.01
D87	54-55	0.05

Recrystallization of fraction D82 (20 mg) in CHCl$_3$ afforded compound URS-8 as yellow plates (16 mg, 0.0011 % of dried weight). The isolation of URS-8 from the EtOAc extract of *U. rufa* stem was summarized in **Scheme 4**.

3.3 Extraction and Isolation of Compounds from the Leaves of *Mitrephora maingayi*

3.3.1 Extraction

Dried *M. maingayi* leaves (500 g) were ground, then macerated with

hexane (5 x 3 L), CHCl$_3$ (5 x 3 L) and MeOH (5 x 3 L), respectively. The filtrate was pooled and evaporated under reduced pressure at temperature not exceeding 40 ℃ to afford the hexane extract (5.7 g, 1.14 % based on dried weight of leaves), CHCl$_3$ extract (10.0 g, 2.0% of dried weight) and MeOH extract (24.0 g, 4.8 % of dried weight).

3.3.2 Isolation of Compounds from the Hexane Extract of *M. maingayi* Leaves

The hexane extract (5.7 g) was dissolved in a small amount of hexane, triturated with kieselguhr, dried at room temperature, then applied on the top of a silica gel column (400 g, 13 x 6 cm) and separated by quick column chromatography. Elution was performed in polarity gradient manner with mixtures of hexane and acetone (99:1 to 0:1). Sixty fractions (300 ml per fraction) were collected. Fractions with similar TLC patterns (solvent system: hexane-EtOAc = 19:1) were combined to give 7 major fractions (E1-E7, **Table 20**).

Table 20. Combined fractions from the hexane extract of *M. maingayi* leaves

Fraction Code	Number of Eluates	Weight (g)
E1	1-10	0.98
E2	11-15	0.12
E3	16-28	1.62
E4	29-35	0.44
E5	36-49	2.23
E6	50-58	0.15
E7	59-60	0.09

3.3.2.1 Isolation of Compound MML-1

Fraction E2 (0.12 g) was subjected to silica gel column chromatography (80 g, 2.4 x 25 cm). A mixture of hexane-EtOAc (9:1) was used as the eluent. All of 22 collected fractions (50 ml each) were examined and combined based on their similar TLC profiles (solvent system: hexane-EtOAc = 9:1) into 4 fractions (E21-E24, **Table 21**).

Table 21. Combined fractions from the fraction E2

Fraction Code	Number of Eluates	Weight (mg)
E21	1-7	46.2
E22	8-11	21.0
E23	12-20	18.1
E24	21-22	33.3

Fraction E22 (21 mg) was further purified on a Sephadex LH-20 column (2.2 x 85 cm). The fraction was dissolved in a small volume of CHCl$_3$-MeOH (2:1) and loaded on the top of the column. This same solvent mixture was employed as the eluting solvent. The volume of each fraction was approximately 15 ml. Thirteen fractions were collected and combined according to their TLC profiles, with hexane-acetone (19:1) as the developing solvent, into 3 fractions (E221-E223, **Table 22**). Compound MML-1, which appeared as a purple spot when fraction E222 was detected on TLC plate with anisaldehyde-sulfuric acid solution and heated, was obtained as colorless oil (8 mg, 0.0016 % yield). The isolation of MML-1 was summarized as shown in **Scheme 5**.

Table 22. Combined fractions from the fraction E22

Fraction Code	Number of Eluates	Weight (mg)
E221	1-8	10.5
E222	9-10	8.0
E223	11-13	1.3

3.3.2.2 Isolation of Compound MML-2

Fraction E5 (2.23 g), which exhibited one main purple spot on TLC after spraying with anisaldehyde-sulfuric acid solution and heating for 5 min, was recrystallized in MeOH. Compound MML-2 was collected as colorless needles (430 mg,

0.086 % of dried weight). The isolation of this compound was also presented in **Scheme 5**.

3.3.3 Isolation of Compounds from the CHCl₃ Extract of *M. maingayi* Leaves

The CHCl₃ extract (10 g) was dissolved in a small amount of CHCl₃, triturated with kieselguhr and dried at room temperature. It was then applied on top of a silica gel column (400 g, 13 x 6 cm) and fractionated by quick column chromatography. Elution was performed in a polarity gradient manner with mixtures of hexane and acetone (9:1 to 0:1). Fifty fractions (300 ml each) were collected and pooled according to their TLC patterns (solvent system: hexane-acetone = 4:1), into 5 fractions (F1-F5, **Table 23**).

Table 23. Combined fractions from the CHCl₃ extract of *M. maingayi* leaves

Fraction Code	Number of Eluates	Weight (g)
F1	1-17	3.16
F2	18-22	1.25
F3	23-30	1.89
F4	31-48	3.27
F5	49-50	0.26

3.3.3.1 Isolation of Compound MML-2

Fraction F2 (1.25 g) was separated on a Sephadex LH-20 column (2.2 x 85 cm). A mixture of CHCl₃-MeOH (2:1) was employed as the eluting solvent. The fractional volume was approximately 15 ml. Eleven collected fractions were combined, upon TLC examination with hexane-acetone (9:1) as the developing solvent, into 3 fractions (F21-F23, **Table 24**). Compound MML-2 (13.0 mg, 0.0026 % yield) was obtained after fraction F23 was recrystallized in MeOH (**Scheme 6**).

Table 24. Combined fractions from the fraction F2

Fraction Code	Number of Eluates	Weight (g)
F21	1-8	1.10
F22	9-10	0.13
F23	11	0.02

3.3.3.2 Isolation of Compound MML-3

Fraction F4 (3.27 g), which displayed three pale purple spots on TLC plate after being sprayed with anisaldehyde-sulfuric acid solution and heated, was fractionated by silica gel column chromatography (150 g, 4.4 x 20 cm) eluted with gradient mixtures of CH_2Cl_2 and acetone (19:1 to 0:1). Sixty-five fractions (50 ml each) were collected and combined based on their TLC profiles (solvent system: CH_2Cl_2-acetone = 9:1) to give 5 major fractions (F41-F44, **Table 25**).

Table 25. Combined fractions from the fraction F4

Fraction Code	Number of Eluates	Weight (g)
F41	1-20	0.44
F42	21-24	0.01
F43	25-31	0.12
F44	32-45	1.98
F45	46-65	0.69

Fraction F41 (0.44 g) was further separated on a Sephadex LH-20 column (2.2 x 85 cm). A mixture of $CHCl_3$-MeOH (2:1) was employed as the eluting solvent. The volume of each fraction was 15 ml. Twenty-nine fractions were collected and pooled upon TLC examination, with hexane-acetone (9:1) as the developing solvent, into 5 fractions (F411-F415, **Table 26**). Recrystallization of fraction F413 in MeOH gave compound MML-3 as colorless needles (18.5 mg, 0.0037% yield). The isolation of

compound MML-3 can be summarized as shown in **Scheme 6**.

Table 26. Combined fractions from the fraction F41

Fraction Code	Number of Eluates	Weight (mg)
F411	1-8	210.6
F412	9-12	87.1
F413	13-14	24.0
F414	15-18	25.6
F415	19-29	86.9

3.3.3.3 Isolation of Compound MML-4

Similar to fraction F413, the subsequent fraction F414 (25.6 mg), which also appeared as a pale purple spot on TLC when sprayed with anisaldehyde-sulfuric acid solution, was recrytallized in MeOH. Compound MML-4 (13.6 mg, 0.0027% yield) was obtained as colorless needles. The isolation of this compound was also shown in **Scheme 6**.

3.3.3.4 Isolation of Compound MML-5

Fraction F42 (10 mg), which was another fraction showing up as a pale purple spot on TLC plate after being sprayed with anisaldehyde-sulfuric acid solution, was recrytallized in MeOH. Compound MML-5 (8.1 mg, 0.0016% yield) was obtained as colorless rod-shaped crystals. The isolation of this compound was also displayed in **Scheme 6**.

3.3.3.5 Isolation of Compound MML-6

Fraction F43 (120 mg) was applied on the top of a Sephadex LH-20 column (2.2 x 85 cm) and eluted with a mixture of CHCl$_3$ and MeOH (2:1). The volume of each collected fraction was 15 ml. Twelve fractions were collected, combined according to TLC examination with hexane-EtOAc (4:1) as the developing solvent, into 3 fractions (F431-F433, **Table 27**). After removal of the solvent from the fraction F432, compound MML-6 was afforded as white powder (7.7 mg, 0.0015% yield).

Table 27. Combined fractions from the fraction F43

Fraction Code	Number of Eluates	Weight (mg)
F431	1-7	96.3
F432	8-9	7.7
F433	10-12	14.9

3.4 Extraction and Isolation of Compounds from the Stems of *M. maingayi*

3.4.1 Extraction

Dried, chopped stems of *M. maingayi* (3 kg) were successively macerated with hexane (5 x 8 L), CHCl$_3$ (5 x 8 L) and MeOH (5 x 8 L). The filtrates were pooled and evaporated under reduced pressure at temperature not exceeding 40 ºC to afford the hexane extract (10 g, 0.33 % based on dried weight of stems), CHCl$_3$ extract (30 g, 1.00 % of dried weight) and MeOH extract (41 g, 1.37 % of dried weight).

3.4.2 Isolation of Compounds from the Hexane Extract of *M. maingayi* Stems

The hexane extract (10 g) was dissolved in a small amount of hexane, triturated with kieselguhr, dried at room temperature, then separated by silica gel quick column chromatography (400 g, 13 x 6 cm) eluted stepwise with mixtures of hexane and acetone (99:1 to 0:1). Fifty fractions (300 ml each) were collected and combined according to their TLC patterns (solvent system: hexane-acetone = 19:1) to yield 4 major fractions (G1-G4, **Table 28**).

Table 28. Combined fractions from the hexane extract of *M. maingayi* stems

Fraction Code	Number of Eluates	Weight (g)
G1	1-17	3.22
G2	18-28	2.76

Table 28. Combined fractions from the hexane extract of *M. maingayi* stems (Continued)

Fraction Code	Number of Eluates	Weight (g)
G3	29-33	0.45
G4	34-50	3.49

3.4.2.1 Isolation of Compound MML-2

Fraction G3 (0.45 g) was separated on a Sephadex LH-20 column (2.2 x 85 cm) eluted with a mixture of CHCl$_3$ and MeOH (2:1). The volume of each fraction was 15 ml. Twenty fractions were collected and combined, after TLC examination using hexane-EtOAc (9:1) as the developing solvent, into 4 fractions (G31-G34, **Table 29**). Compound MML-2 (7.9 mg, 0.0016 % yield) was obtained from the fraction G32.

Table 29. Combined fractions from the fraction G3

Fraction Code	Number of Eluates	Weight (mg)
G31	1-11	222.7
G32	12-13	8.2
G33	14-17	15.1
G34	18-20	199.8

3.4.2.2 Isolation of Compound MMS-1

Fraction G4 (3.49 g) was subjected to a silica gel column (150 g, 4.5 x 20 cm) eluted with a mixture of cyclohexane-EtOAc (9:1). Forty-five collected fractions (50 ml each) were combined based on their similar TLC patterns (solvent system: cyclohexane-EtOAc = 9:1) into 6 fractions (G41-G46, **Table 30**).

Table 30. Combined fractions from the fraction G4

Fraction Code	Number of Eluates	Weight (g)
G41	1-14	1.04

Table 30. Combined fractions from the fraction G4 (Continued)

Fraction Code	Number of Eluates	Weight (g)
G41	1-14	1.04
G42	15-17	0.09
G43	18-27	0.92
G44	28-35	0.68
G45	36-42	0.41
G46	43-45	0.29

Fraction G42 (90 mg) was further purified on a Sephadex LH-20 column (2.2 x 85 cm). A mixture of $CHCl_3$ and MeOH (2:1) was employed as the eluting solvent. The fractional volume was 15 ml. Twelve fractions were collected and pooled according to their TLC profiles with hexane-acetone (9:1) as the developing solvent into 4 fractions (G421-G424, **Table 31**). Eight milligram (0.0016 % yield) of compound MMS-1 was recrystallized as white needles from the fraction G423, which appeared as a blue spot on TLC sprayed with anisaldehyde-sulfuric acid solution and heated. The isolation of compound MMS-1 was summarized as shown in **Scheme 7**.

Table 31. Combined fractions from the fraction G42

Fraction Code	Number of Eluates	Weight (mg)
G421	1-5	55.6
G422	6-8	19.3
G423	9-10	9.7
G424	11-12	4.9

3.4.3 Isolation of Compounds from the CHCl₃ Extract of *M. maingayi* Stems

The CHCl₃ extract (20 g) was dissolved in a small amount of hexane, triturated with kieselguhr and dried at room temperature. It was then fractionated by quick column chromatography using a column of silica gel (400 g, 13 x 6 cm). Elution was performed in a polarity gradient manner with mixtures of CHCl₃ and MeOH (99:1 to 0:1). Seventy-two fractions (300 ml each) were collected and examined by TLC (solvent system: CHCl₃-MeOH = 20:1). Fractions with similar chromatographic profiles were combined to yield six fractions (H1-H6, **Table 32**).

Table 32. Combined fractions of the CHCl₃ extract from *M. maingayi* stems

Fraction Code	Number of Eluates	Weight (g)
H1	1-30	5.77
H2	31-42	3.09
H3	43-50	1.66
H4	51-58	0.37
H5	59-62	0.41
H6	63-72	8.50

3.4.3.1 Isolation of Compound MMS-2

Fraction H3 (1.66 g) was fractionated on a silica gel column (150 g, 4.5 x 20 cm), eluted with a mixture of hexane-acetone (2:1). Thirty-three fractions (100 ml each) were collected, then combined based on their TLC patterns (solvent system: hexane-acetone = 1:1) into 5 fractions (H31-H35) as presented in **Table 33**.

Table 33. Combined fractions from the fraction H3

Fraction Code	Number of Eluates	Weight (g)
H31	1-13	0.44
H32	14-18	0.05

Table 33. Combined fractions from the fraction H3 (Continued)

Fraction Code	Number of Eluates	Weight (g)
H33	19-25	0.21
H34	26-31	0.83
H35	32-33	0.11

Fraction H32 (50 mg), which showed a major yellow spot on TLC plate (UV$_{366}$), was further purified on a Sephadex LH-20 column (2.2 x 72 cm) using MeOH as the eluent to yield 15 fractions. TLC examination (solvent system: hexane-acetone = 1:1) led to the combination of these into 3 fractions (H321-H323, **Table 34**). Compound MMS-2 was obtained as yellow needles (21.0 mg, 0.0010% yield) after recrystallyzation of the fraction H322 in MeOH.

Table 34. Combined fractions from the fraction H32

Fraction Code	Number of Eluates	Weight (mg)
H321	1-10	20.3
H322	11-14	25.0
H323	15	4.4

3.4.3.2 Isolation of Compound MMS-3

Fraction H4 (370 mg) was separated on a Sephadex LH-20 column (2.2 x 72 cm) using MeOH as the eluent to yield 25 fractions. TLC examination (solvent system: hexane-acetone = 1:1) led to the combination of these collected fractions into 4 fractions (H41-H44, **Table 35**). Compound MMS-3, which appeared as an orange spot on TLC plate (UV$_{366}$), was obtained as yellow powder (18.0 mg, 0.0009 % yield) after recrystallyzation of the fraction H44 in MeOH. The isolation of compound MMS-3 was summarized as shown in **Scheme 8**.

Table 35. Combined fractions from the fraction H4

Fraction Code	Number of Eluates	Weight (mg)
H41	1-10	223.6
H42	11-16	44.9
H43	17-21	79.8
H44	22-25	20.2

3.4.3.3 Isolation of Compound MMS-4

Fraction H5 (0.41 g) was subjected to a Sephadex LH-20 column eluting with MeOH. Twenty 15-ml fractions were collected and combined into 4 main fractions (H51-H54, **Table 36**).

Table 36. Combined fractions from the fraction H5

Fraction Code	Number of Eluates	Weight (g)
H51	1-9	0.32
H52	10-14	0.04
H53	15-17	0.01
H54	18-20	0.04

Fraction H51 (0.32 g) was further fractionated by silica gel column chromatography (40 g, 2.4 x 20 cm) using CH_2Cl_2-acetone (4:1) as the eluting solvent, to yield 40 fractions (50 ml each). These fractions were combined according to their TLC patterns (solvent system: CH_2Cl_2-acetone = 4:1) into 7 fractions (H511-H517, **Table 37**). Fraction H511 was recrystallized in MeOH and gave compound MMS-4 (42 mg, 0.0021 % yield) as pale yellow needles.

Table 37. Combined fractions from the fraction H51

Fraction Code	Number of Eluates	Weight (mg)
H511	1-8	51.7
H512	9-13	46.1
H513	14-17	39.3
H514	18-25	84.7
H515	26-30	17.6
H516	31-32	3.9
H517	33-40	60.4

3.5 Extraction and Isolation of Compounds with Advanced Glycation End-product (AGE) Inhibitory Activity from the Leaves of *Uvaria rufa*

3.5.1 Extraction

Dried leaves of *U. rufa* (290 g) were ground then macerated with hexane (5 x 1.5 L), EtOAc (5 x 1.5 L) and MeOH (5 x 1.5 L), successively. Each filtrate was pooled and evaporated to dryness under reduced pressure at temperature not exceeding 40 ºC to yield the hexane extract (8.10 g, 2.79 % based on dried weight of leaves), EtOAc extract (9.61 g, 3.31 % of dried weight) and MeOH extract (29.94 g, 10.32 % of dried weight).

3.5.2 Isolation of Bioactive Compounds (URL6-URL10) from the EtOAc Extract of *U. rufa* Leaves

The isolation of bioactive compounds from the EtOAc extract was done through bioassay-guided fractionation. The extract (2.5 g) was subjected to reversed-phase MPLC column (pre-packed column: Licroprep RP-18, 30 x 250 mm, flow rate 5 ml/min, detected at 254 nm) with gradient mixture of MeOH and water (0:1 to 4:1) as the eluent. The eluates were collected and combined based on their HPLC chromatograms (analytical column: Cosmosil C18 ARII, 4.6 x 15 nm, flow rate 1 ml/min, mobile phase: 15 % MeCN in water) into 11 fractions. These fractions were tested for their inhibitory activity against AGE formation, as shown in **Table 38**.

Table 38. Combined fractions from the EtOAc extract of *U. rufa* leaves and their percentage
inhibition of AGE formation

Fraction Code	Weight (g)	% inhibition
I1	0.11	18.56
I2	0.14	5.99
I3	0.02	58.57
I4	0.84	61.65
I5	0.47	32.84
I6	0.05	31.28
I7	0.13	46.79
I8	0.09	53.13
I9	0.23	57.79
I10	0.01	54.90
I11	0.30	53.88

The most active fraction, fraction I4 (0.84 g), was further purified by semi-preparative HPLC using an ODS column (Cosmosil C18-AR II, 20×250 mm, flow rate 2 ml/min, detected at 254 nm) with gradient mixture of MeCN-water (1:9 to 4:1) as the eluent. All collected fractions were examined by analytical HPLC (analytical column: Cosmosil C18 ARII, 4.6×15 nm, flow rate 1 ml/min, mobile phase = 15 % MeCN in water). Eight fractions were afforded and their AGE inhibitory activity was confirmed. The results were displayed in **Table 38**. Five flavonol glycosides (URL-6 - URL-10) were obtained from fraction I41, I42, I44, I45 and I47, respectively, after removal of the solvent to dryness. The isolation of these compounds was summarized in **Scheme 9**.

Table 39. Combined fractions from the fraction I4 and their % inhibition of AGE formation

Fraction Code	Weight (mg)	% inhibition
I41	94.3	41.34
I42	155.4	33.19
I43	48.9	13.38
I44	184.6	55.16
I45	134.9	8.45
I46	107.2	16.38
I47	74.1	6.42
I48	37.8	61.51

Hexane extract of *Uvaria rufa* leaves
(7 g)

Quick CC
Hexane-Acetone (99:1 to 0:1)

A1	A2	A3	A4	A5
(2.74 g)	(0.91 g)	(1.14 g)	(0.77 g)	(0.68 g)

URL-1
(188 mg)

Scheme 1. Isolation of compound URL-1 from the hexane extract of *Uvaria rufa* leaves

EtOAc extract of *Uvaria rufa* leaves
(7 g)

Quick CC
Hexane-Acetone (9:1 to 0:1)

B1	B2	B3	B4	B5	B6	B7
(1.86 g)	(0.71 g)	(2.28 g)	(0.62 g)	(0.55 g)	(0.47 g)	(0.38 g)

Silica gel CC
Hexane-EtOAc (20:1)

B31	B32	B33	B34	B35	B36
(0.51 g)	(0.33 g)	(0.28 g)	(0.79 g)	(0.23 g)	(0.11 g)

Sephadex LH-20
CHCl$_3$-MeOH (2:1)

B341	B342	B343	B344	B345
(432.6 mg)	(205.0 mg)	(86.0 mg)	(48.1 mg)	(16.4 mg)

URL-1
(35 mg)

Silica gel CC
Cyclohexane-Acetone (5:1 to 0:1)

B41	B42	B43	B44	B45
(311.0 mg)	(77.4 mg)	(16.0 mg)	(25.8 mg)	(174.0 mg)

URL-2
(11 mg)

Silica gel CC
Cyclohexane-EtOAc (3:1)

B441	B442	B443	B444
(8.8 mg)	(10.6 mg)	(4.0 mg)	(2.1 mg)

URL-3
(6.4 mg)

URL-4
(4.0 mg)

URL-5
(1.9 mg)

Scheme 2. Isolation of compounds URL-1 - URL-5 from the EtOAc extract of *Uvaria rufa* leaves

Hexane extract of *Uvaria rufa* stems
(6 g)

Quick CC
Hexane-Acetone (99:1 to 0:1)

C1	C2	C3	C4	C5
(2.15 g)	(2.07 g)	(1.10 g)	(0.38 g)	(0.14 g)

Silica gel CC
Hexane-EtOAc (9:1)

Sephadex LH-20
CHCl3-MeOH (2:1)

C21	C22	C23	C24	C25	C31	C32	C33	C34
(1.02 g)	(0.56 g)	(0.30 g)	(0.01 g)	(0.06 g)	(460.3 mg)	(518.0 mg)	(61.0 mg)	(58.0 mg)

URS-1   **URS-2**   **URS-2**
(22 mg)   (5 mg)   (45 mg)

Scheme 3. Isolation of compounds URS-1 and URS-2 from the hexane extract of *Uvaria rufa* stems

EtOAc extract of *Uvaria rufa* stems
(9 g)

Quick CC
Hexane-Acetone (9:1 to 0:1)

D1	D2	D3	D4	D5	D6	D7	D8
(2.97 g)	(1.14 g)	(0.07 g)	(0.08 g)	(1.77 g)	(0.27 g)	(0.18 g)	(2.36 g)

Sephadex LH-20
CHCl3-MeOH (2:1)

Silica gel CC
CHCl3-Acetone (19:1 to 9:1)

D31	D32	D33	D51	D52	D53	D54	D55	D56
(31.4 mg)	(30.0 mg)	(7.7 mg)	(805.8 mg)	(13.4 mg)	(311.8 mg)	(15.0 mg)	(18.9 mg)	(557.2 mg)

URS-4
(27 mg)

URS-5
(12 mg)

URS-7
(14.4 mg)

Silica gel CC
Hexane-EtOAc (19:1 to 0:1)

Sephadex LH-20
MeOH

D11	D12	D13	D14	D15	D16	D17	D541	D542	D543
(0.83 g)	(0.55 g)	(0.36 g)	(0.90 g)	(0.13 g)	(0.04 g)	(0.13 g)	(2.6 mg)	(2.0 mg)	(10.2 mg)

URS-6
(10 mg)

Silica gel CC
Hexane-Acetone (20:1)

D141	D142	D143	D144
(412.1 mg)	(38.9 mg)	(17.0 mg)	(402.6 mg)

URS-3
(17 mg)

Silica gel CC
CHCl3-MeOH (9:1 to 8:2)

D81	D82	D83	D84	D85	D86	D87
(1.19 g)	(0.02 g)	(0.12 g)	(0.49 g)	(0.46 g)	(0.01 g)	(0.05 g)

URS-8
(16 mg)

Scheme 4. Isolation of compounds URS-3 - URS-8 from the EtOAc extract of *Uvaria rufa* stems

Hexane extract of *Mitrephora maingayi* leaves
(5.7 g)

Quick CC
Hexane-Acetone (99:1 to 0:1)

E1	E2	E3	E4	E5	E6	E7
(0.98 g)	(0.12 g)	(1.62 g)	(0.44 g)	(2.23 g)	(0.15 g)	(0.09 g)

MML-2
(118 mg)

Silica gel CC
Hexane-EtOAc (9:1)

E21	E22	E23	E24
(46.2 mg)	(21.0 mg)	(18.1 mg)	(33.3 mg)

Sephadex LH-20
CHCl3-MeOH (2:1)

E221	E222	E223
(10.5 mg)	(8.0 mg)	(1.3 mg)

MML-1
(8 mg)

Scheme 5. Isolation of compounds MML-1 and MML-2 from the hexane extract of
Mitrephora maingayi leaves

CHCl3 extract of *Mitrephora maingayi* leaves
(10 g)

Quick CC
Hexane-Acetone (9:1 to 0:1)

F1	F2	F3	F4	F5
(3.16 g)	(1.25 g)	(1.89 g)	(3.27 g)	(0.26 g)

Sephadex LH-20
CHCl3-MeOH (2:1)

Silica gel CC
CH2Cl2-Acetone (19:1 to 0:1)

F21	F22	F23	F41	F42	F43	F44	F45
(1.10 g)	(0.13 g)	(0.02 g)	(0.44 g)	(0.01 g)	(0.12 g)	(1.98 g)	(0.69 g)

MML-2
(13.0 mg)

MML-5
(8.1 mg)

Sephadex LH-20
CHCl3-MeOH (2:1)

Sephadex LH-20
CHCl3-MeOH (2:1)

F411	F412	F413	F414	F415	F431	F432	F433
(210.6 mg)	(87.1 mg)	(24.0 mg)	(25.6 mg)	(86.9 mg)	(96.3 mg)	(7.7 mg)	(14.9 mg)

MML-3   **MML-4**
(18.5 mg)   (13.6 mg)

MML-6
(7.7 mg)

Scheme 6. Isolation of compounds MML-2 - MML-6 from the CHCl3 extract of *Mitrephora maingayi* leaves

Hexane extract of *Mitrephora maingayi* stems
(10 g)

Quick CC
Hexane-Acetone (99:1 to 0:1)

G1
(3.22 g)

G2
(2.76 g)

G3
(0.45 g)

G4
(3.49 g)

Sephadex LH-20
CHCl$_3$-MeOH (2:1)

Silica gel CC
Cyclohexane-EtOAc (9:1)

G31
(222.7 mg)

G32
(8.2 mg)

G33
(15.1 mg)

G34
(199.8 mg)

G41
(1.04 g)

G42
(0.09 g)

G43
(0.92 g)

G44
(0.68 g)

G45
(0.41 g)

G46
(0.29 g)

MML-2
(7.9 mg)

Sephadex LH-20
CHCl$_3$-MeOH (2:1)

G421
(55.6 mg)

G422
(19.3 mg)

G423
(9.7 mg)

G424
(4.9 mg)

MMS-1
(8 mg)

Scheme 7. Isolation of compounds MML-2 and MMS-1 from the hexane extract of

Mitrephora maingayi stems

CHCl3 extract of *Mitrephora maingayi* stems
(20 g)

Quick CC
CHCl3-MeOH (99:1 to 0:1)

H1	H2	H3	H4	H5	H6
(5.77 g)	(3.09 g)	(1.66 g)	(0.37 g)	(0.41 g)	(8.50 g)

Silica gel CC
Hexane-Acetone (2:1)

Sephadex LH-20
MeOH

H31	H32	H33	H34	H35	H41	H42	H43	H44
(0.44 g)	(0.05 g)	(0.21 g)	(0.83 g)	(0.11 g)	(223.6 mg)	(44.9 mg)	(79.8 mg)	(20.2 mg)

MMS-3
(18.0 mg)

Sephadex LH-20
MeOH

H321	H322	H323
(20.3 mg)	(25.0 mg)	(4.4 mg)

Sephadex LH-20
MeOH

MMS-2
(21.0 mg)

H51	H52	H53	H54
(0.32 g)	(0.04 g)	(0.01 g)	(0.04 g)

Silica gel CC
CH2Cl2-Acetone (4:1)

H511	H512	H513	H514	H515	H516	H517
(51.7 mg)	(46.1 mg)	(39.3 mg)	(84.7 mg)	(17.6 mg)	(3.9 mg)	(60.4 mg)

MMS-4
(42.0 mg)

Scheme 8. Isolation of compounds MMS-2 - MMS-4 from the CHCl3 extract of *Mitrephora maingayi* stems

EtOAc extract of *Uvaria rufa* leaves
(2.5 g)

reversed phase MPLC
MeOH-water (0:1 to 8:2)

I1	I2	I3	I4	I5	I6	I7	I8	I9	I10	I11
(0.11 g)	(0.14 g)	(0.02 g)	(0.84 g)	(0.47 g)	(0.05 g)	(0.13 g)	(0.09 g)	(0.23 g)	(0.01 g)	(0.30 g)

semi-preperative HPLC
MeCN-water (1:9 to 8:2)

I41	I42	I43	I44	I45	I46	I47	I48
(94.3 mg)	(155.4 mg)	(48.9 mg)	(184.6 mg)	(134.9 mg)	(107.2 mg)	(74.1 mg)	(37.8 mg)

URL-6
(94.3 mg)

URL-7
(155.4 mg)

URL-8
(184.6 mg)

URL-9
(134.9 mg)

URL-10
(74.1 mg)
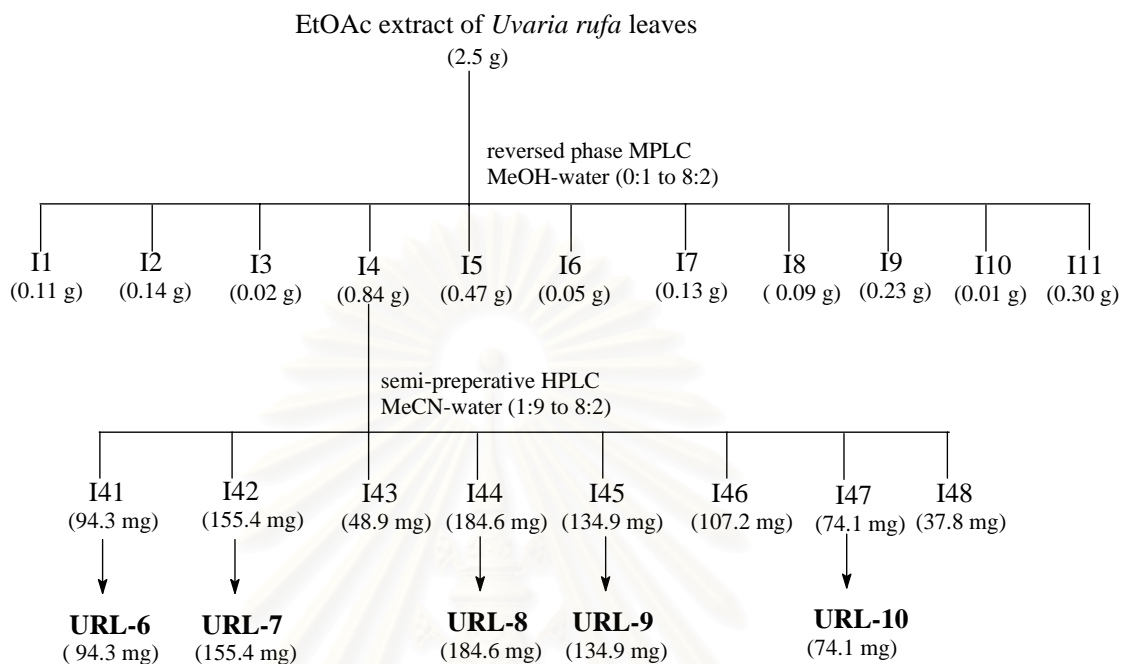
Scheme 9. Isolation of the anti-AGE inhibitory compounds from the EtOAc extract of
  Uvaria rufa leaves
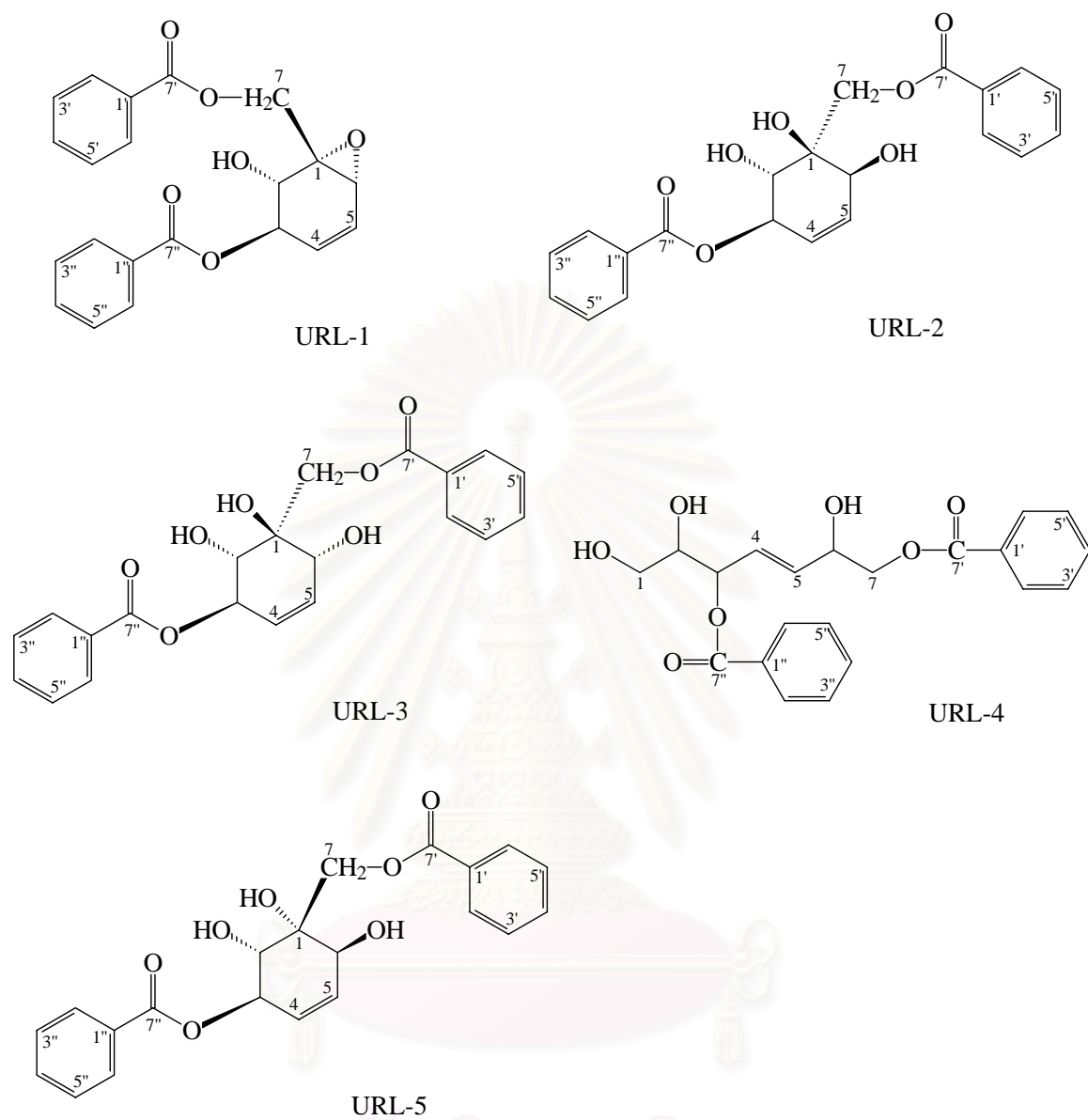
Figure 6. Chemical structures of compounds isolated from *Uvaria rufa* leaves
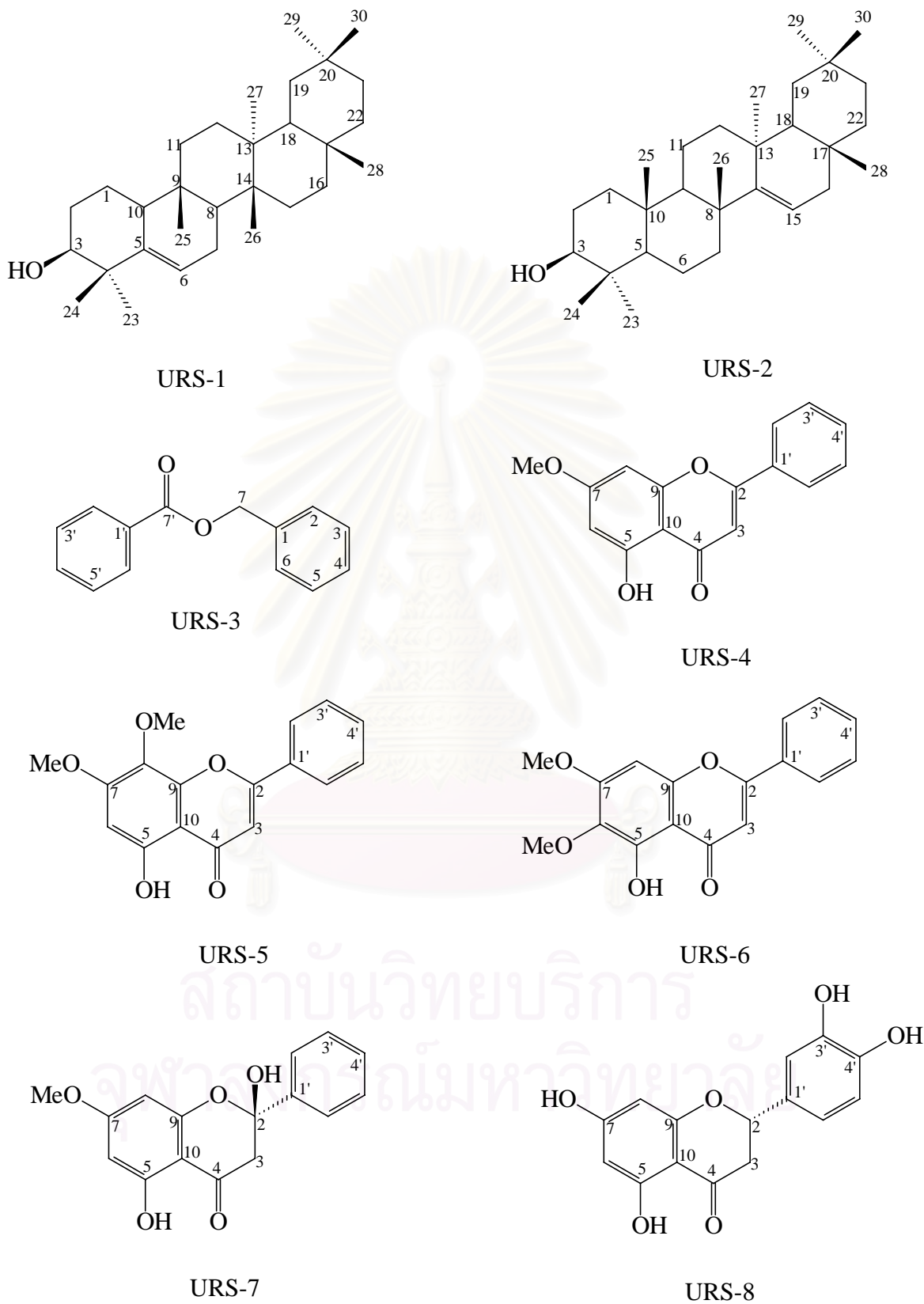
Figure 7. Chemical structures of compounds isolated from *Uvaria rufa* stems

MML-1

MML-2

MML-3

MML-4

MML-5

MML-6
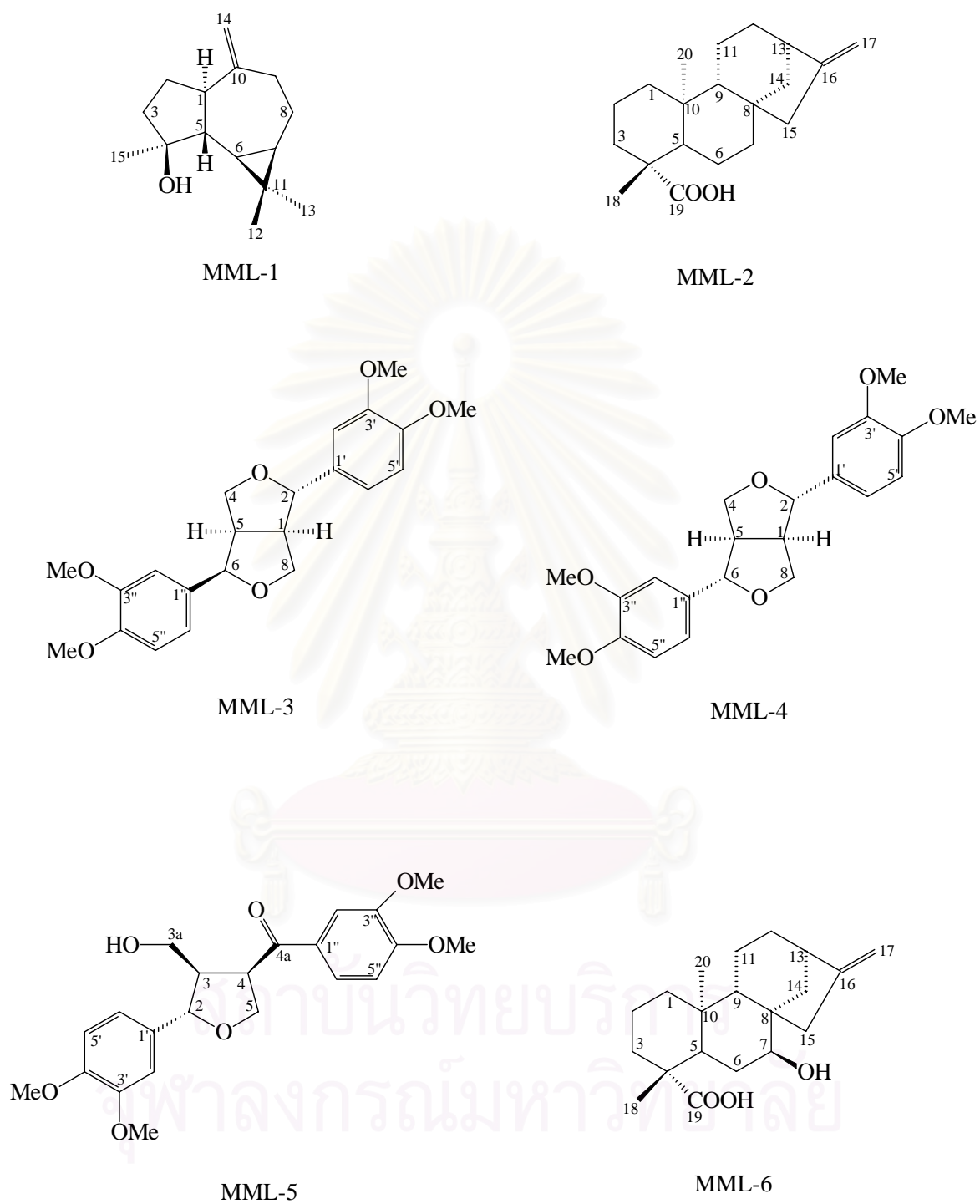
Figure 8. Chemical structures of compounds isolated from *Mitrephora maingayi* leaves

MML-2

MMS-1

MMS-2

MMS-3

MMS-4
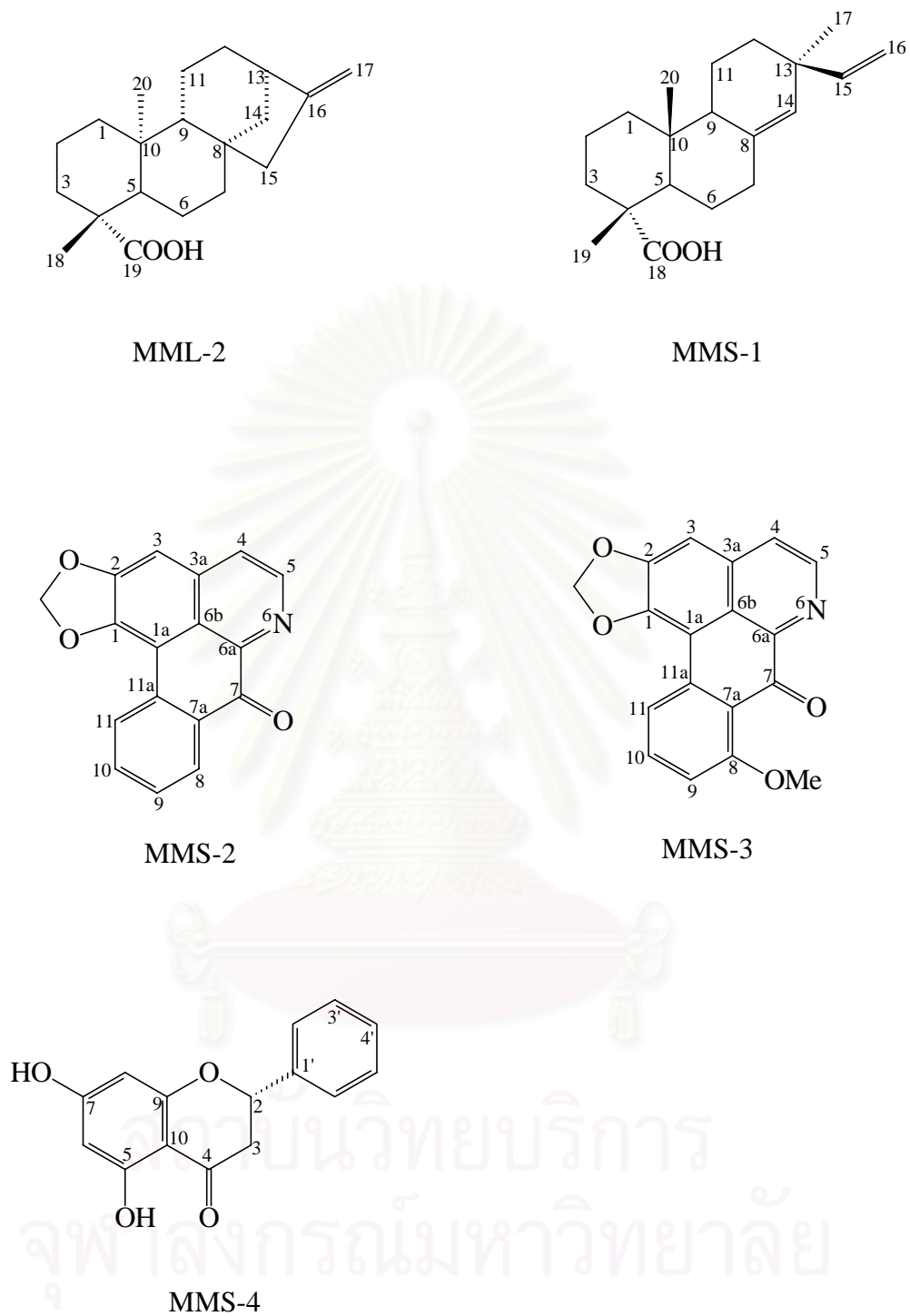
Figure 9. Chemical structures of compounds isolated from *Mitrephora maingayi* stems
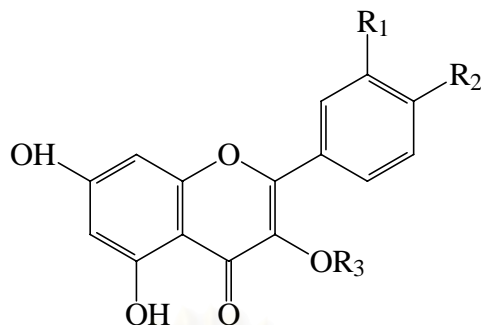
URL-6   : R$_1$ = OH,   R$_2$ = OH,   R$_3$ = rutinosyl

URL-7   : R$_1$ = OH,   R$_2$ = OH,   R$_3$ = β-D-glucopyranosyl

URL-8   : R$_1$ = H,   R$_2$ = OH,   R$_3$ = β-D-galactopyranosyl

URL-9   : R$_1$ = H,   R$_2$ = OH,   R$_3$ = β-D-glucopyranosyl

URL-10   : R$_1$ = OH,   R$_2$ = OH,   R$_3$ = β-D-glucopyranosyl-(6-acetate)

Figure 10. Chemical structures of compounds with AGE inhibitory activity isolated from EtOAc extract of *Uvaria rufa* leaves.

4. Physical and Spectral Data of Isolated Compounds

4.1 Compound URL-1

Compound URL-1 was obtained as white amorphous powder (188 mg, 0.075 % based on dried weight of leaves).

UV   : λ$_{max}$ nm (log ε), in CHCl$_3$; 243 (4.35), 276 (3.65); see **Figure 11**

IR   : ν$_{max}$ cm^{-1}, KBr; 3476, 1713, 1602, 1452, 1279, 1118, 1066, 905, 710, 687; see **Figure 12**

ESITOFMS   : *m/z*; 367 [M+H]$^+$; see **Figure 13**

Mp   : 148 – 150 ^{o}C

[α]$^{25}_D$: -36.5^o (*c* 0.17, CHCl$_3$)

^{1}H NMR   : δ ppm, 500 MHz, in CDCl$_3$; see **Figures 14a** and **14b**

^{13}C NMR   : δ ppm, 125 MHz, in CDCl$_3$; **Figure 15**

4.2 Compound URL-2

Compound URL-2 was obtained as white amorphous powder (11 mg, 0.0052 %

based on dried weight of leaves)

UV : λmax nm (log ε), in $CHCl_3$; 243 (3.96), 276 (3.31); see **Figure 18**

IR : v_{max} cm^{-1}, KBr; 3449, 1716, 1272, 1112, 712; see **Figure 19**

ESITOFMS : *m/z*; 385 [M+H]$^+$; see **Figure 20**

Mp : 206 – 207 ^{o}C

$[α]^{25}_D$: -676° (*c* 0.24, $CHCl_3$)

^{1}H NMR : δ ppm, 500 MHz, in DMSO-d_6; see **Figures 21a** and **21b**

^{13}C NMR : δ ppm, 125 MHz, in DMSO-d_6; see **Figure 22**

4.3 Compound URL-3

Compound URL-3 was obtained as white amorphous powder (6.4 mg, 0.0030 % based on dried weight of leaves)

UV : λmax nm (log ε), in $CHCl_3$; 243 (3.96), 276 (3.31); see **Figure 23**

IR : v_{max} cm^{-1}, KBr; 3464, 1722, 1275, 1116, 714; see **Figure 24**

^{1}H NMR : δ ppm, 500 MHz, in $CDCl_3$; see **Figures 25** and **26**

^{13}C NMR : δ ppm, 125 MHz, in $CDCl_3$; see **Figure 27**

4.4 Compound URL-4

Compound URL-4 was obtained as white amorphous powder, (4 mg, 0.0019 % based on dried weight of leaves).

ESITOFMS : *m/z*; 387 [M+H]$^+$; see **Figure 28**

Mp : 111 – 113 ^{o}C

$[α]^{25}_D$: -13.2^o (*c* 0.3, in MeOH)

^{1}H NMR : δ ppm, 500 MHz, in DMSO-d_6; see **Figures 29a - 29c**

^{13}C NMR : δ ppm, 125 MHz, in DMSO-d_6; see **Figure 30**

^{1}H–^{1}H COSY : in DMSO-d_6; see **Figure 31**

4.5 Compound URL-5

Compound URL-5 was obtained as white amorphous powder (1.9 mg, 0.0009 % based on dried weight of leaves)

UV : $λ_{max}$ nm (log ε), in $CHCl_3$; 243 (4.19), 276 (3.54); see **Figure 35**

IR   : ν_{max} cm^{-1}, KBr; 3462, 1679, 1281, 1119, 712; see **Figure 36**

ESIMS   : *m/z*; 364; see **Figure 37**

Mp   : 137 – 140 ^{o}C

$[\alpha]^{25}_{D}$: -113.2^{o} (*c* 0.25, CHCl$_3$)

^{1}H NMR   : δ ppm, 500 MHz, in CDCl$_3$; see **Figure 38**

^{13}C NMR   : δ ppm, 125 MHz, in CDCl$_3$; see **Figure 39**

4.6 Compound URL-6

Compound URL-6 was obtained as yellow amorphous powder (94.3 mg, 0.1250 % based on dried weight of leaves)

^{1}H NMR   : δ ppm, 300 MHz, in DMSO-*d$_6$*; see **Figure 131**

^{13}C NMR   : δ ppm, 75 MHz, in DMSO-*d$_6$*; see **Figure 132**

4.7 Compound URL-7

Compound URL-7 was obtained as yellow amorphous powder (155.4 mg, 0.2060 % based on dried weight of leaves)

^{1}H NMR   : δ ppm, 300 MHz, in DMSO-*d$_6$*; see **Figure 133**

^{13}C NMR   : δ ppm, 75 MHz, in DMSO-*d$_6$*; see **Figure 134**

4.8 Compound URL-8

Compound URL-8 was obtained as yellow amorphous powder (184.6 mg, 0.2447 % based on dried weight of leaves)

^{1}H NMR   : δ ppm, 300 MHz, in DMSO-*d$_6$*; see **Figure 135**

^{13}C NMR   : δ ppm, 75 MHz, in DMSO-*d$_6$*; see **Figure 136**

4.9 Compound URL-9

Compound URL-9 was obtained as yellow amorphous powder (134.9 mg, 0.1788 % based on dried weight of leaves)

^{1}H NMR   : δ ppm, 300 MHz, in DMSO-*d$_6$*; see **Figure 137**

^{13}C NMR   : δ ppm, 75 MHz, in DMSO-*d$_6$*; see **Figure 138**

4.10 Compound URL-10

Compound URL-10 was obtained as yellow amorphous powder (74.1 mg, 0.0982 % based on dried weight of leaves)

^{1}H NMR : δ ppm, 300 MHz, in DMSO-d_6; see **Figure 139**

^{13}C NMR : δ ppm, 75 MHz, in DMSO-d_6; see **Figure 140**

4.11 Compound URS-1

Compound URS-1 was obtained as white amorphous powder (22 mg, 0.0015 % based on dried weight of stems).

UV : λ_{max} nm (log ε), in MeOH; 244.5 (0.745), 229 (0.091); see **Figure 40**

IR : ν_{max} cm^{-1}, KBr; 3477, 2929, 1713, 1454, 1386, 1037; see **Figure 41**

ESITOFMS : m/z; 427.12 [M+H]$^+$; see **Figure 42**

Mp : 210-213 ^{o}C

$[\alpha]^{25}_D$: +63.3^o (c 0.71, in CHCl$_3$)

^{1}H NMR : δ ppm, 300 MHz, in CDCl$_3$; see **Figure 43**

^{13}C NMR : δ ppm, 75 MHz, in CDCl$_3$; see **Figure 44**

4.12 Compound URS-2

Compound URS-2 was obtained as white amorphous powder (45 mg, 0.0030 % based on dried weight of stems).

UV : λ_{max} nm (log ε), in MeOH; 244 (0.23), 234 (0.051); see **Figure 46**

IR : ν_{max} cm^{-1}, KBr; 3488, 2933, 1725, 1642, 1473, 1384, 1037, 1000, 816, 690; see **Figure 47**

ESITOFMS : m/z; 427 [M+H]$^+$; see **Figure 48**

Mp : 282 – 283 ^{o}C

$[\alpha]^{25}_D$: +0.72^o (c 0.97, in CHCl$_3$)

^{1}H NMR : δ ppm, 300 MHz, in CDCl$_3$; see **Figure 49**

^{13}C NMR : δ ppm, 75 MHz, in CDCl$_3$; see **Figure 50**

4.13 Compound URS-3

Compound URS-3 was obtained as colorless oil, (17 mg, 0.0012 % based on

dried weight of stems)

IR : ν_{max} cm^{-1}, KBr; 3400, 2921, 2851, 1732, 1639, 1571, 1463, 1378, 1260, 1074, 1029, 800; see **Figure 52**

ESITOFMS : m/z; 213 [M+H]$^{+}$; see **Figure 53**

^{1}H NMR : δ ppm, 300 MHz, in CDCl$_3$; see **Figure 54**

^{13}C NMR : δ ppm, 75 MHz, in CDCl$_3$; see **Figure 55**

4.14 Compound URS-4

Compound URS-4 was obtained as yellow amorphous powder, (27 mg, 0.0019 % based on dried weight of stems)

UV : λ_{max} nm (log ε), in MeOH; 269 (1.22), 233 (0.05); see **Figure 57**

IR : ν_{max} cm^{-1}, KBr; 3070, 3015, 2844, 2689, 1668, 1609, 1588, 1496, 1353, 1203, 1160, 1070, 905, 866, 850, 807, 770, 694, 645; see **Figure 58**

EITOFMS : m/z; 269 [M+H]$^{+}$; see **Figure 59**

Mp : 163-164 ^{o}C

$[\alpha]^{25}_{D}$: 0° (c 0.25, CHCl$_3$)

^{1}H NMR : δ ppm, 300 MHz, in CDCl$_3$; see **Figure 60**

^{13}C NMR : δ ppm, 75 MHz, in CDCl$_3$; see **Figure 61**

4.15 Compound URS-5

Compound URS-5 was obtained as pale yellow powder, (12 mg, 0.0008 % based on dried weight of stems)

UV : λ_{max} nm (log ε), in CHCl$_3$; 276 (1.49), 233 (0.05); see **Figure 63**

IR : ν_{max} cm^{-1}, KBr; 2923, 2852, 1650, 1610, 1511, 1451, 1377, 1340, 1274, 1124, 1034, 836, 800, 687; see **Figure 64**

ESITOFMS : m/z ; 299 [M+H]$^{+}$; see **Figure 65**

^{1}H NMR : δ ppm, 300 MHz, in CDCl$_3$; see **Figure 66**

^{13}C NMR : δ ppm, 75 MHz, in CDCl$_3$; see **Figure 67**

4.16 Compound URS-6

Compound URS-6 was obtained as yellow powder, (10 mg, 0.0007 % based on

dried weight of stems)

UV   : λ_{max} nm (log ε), in CHCl$_3$; 311 (1.57), 297 (1.29), 269 (2.49), 229 (0.16);

    see **Figure 69**

IR   : ν_{max} cm^{-1}, KBr; 3071, 2945, 2848, 1665, 1500, 1459, 1360, 1304, 1199,

    1130, 851, 809, 764, 680; see **Figure 70**

ESITOFMS : m/z; 299 [M+H]$^+$; see **Figure 71**

Mp   : 150 ^{o}C

^{1}H NMR   : δ ppm, 300 MHz, in CDCl$_3$; see **Figure 72**

^{13}C NMR   : δ ppm, 75 MHz, in CDCl$_3$; see **Figure 73**

4.17 Compound URS-7

Compound URS-7 was obtained as yellow powder, (14.4 mg, 0.0010 % based on dried weight of stems)

Mp   : 128 - 130 ^{o}C

$[\alpha]^{25}_D$: -43.6 ^{o} (c 0.012, CHCl$_3$)

^{1}H NMR   : δ ppm, 300 MHz, in CDCl$_3$; see **Figure 75**

^{13}C NMR   : δ ppm, 75 MHz, in CDCl$_3$; see **Figure 76**

4.18 Compound URS-8

Compound URS-8 was obtained as yellow plates (16 mg, 0.0011 % based on dried weight of stems)

UV   : λ_{max} nm (log ε), in MeOH; 273 (0.79), 259 (0.60), 241 (2.50); see **Figure 78**

IR   : ν_{max} cm^{-1}, KBr; 3357, 2928, 2853, 1734, 1600, 1517, 1497, 1456, 1422,

    1379, 1336, 1266, 1143, 1029, 963, 857, 813, 761; see **Figure 79**

ESITOFMS : m/z; 288 [M]$^+$; see **Figure 80**

Mp   : 267 ^{o}C

^{1}H NMR   : δ ppm, 300 MHz, in acetone-d_6; see **Figure 81**

^{13}C NMR   : δ ppm, 75 MHz, in acetone-d_6; see **Figure 82**

4.19 Compound MML-1

Compound MML-1 was obtained as colorless oil (8 mg, 0.0016 % based on

dried weight of leaves).

UV : λ_{max} nm (log ε), in CHCl$_3$; 225 (2.08); see **Figure 84**

IR : ν_{max} cm^{-1}, KBr; 3383, 2930, 2871, 1704, 1654, 1458, 1376, 917; see

Figure 85

ESIMS : m/z; 243 [M+Na]$^+$; see **Figure 86**

^{1}H NMR : δ ppm, 300 MHz, in CDCl$_3$; see **Figure 87**

^{13}C NMR : δ ppm, 75 MHz, in CDCl$_3$; see **Figure 88**

DEPT : in CDCl$_3$; see **Figure 89**

4.20 Compound MML-2

Compound MML-2 was obtained as colorless needles (430 mg, 0.086 % based on dried weight of leaves).

UV : λ_{max} nm (log ε), in MeOH; 221 (1.48); see **Figure 90**

IR : ν_{max} cm^{-1}, KBr; 3066, 2929, 2852, 1693, 1658, 1461, 1261, 1178, 872, 797;

see **Figure 91**

ESITOFMS : m/z; 303 [M+H]$^+$; see **Figure 92**

Mp : 179-180 ^{o}C

$[\alpha]^{25}_D$: -110° (c = 0.5, CDCl$_3$)

^{1}H NMR : δ ppm, 300 MHz, in CDCl$_3$; see **Figure 93**

^{13}C NMR : δ ppm, 75 MHz, in CDCl$_3$; see **Figure 94**

DEPT : in CDCl$_3$; see **Figure 95**

4.21 Compound MML-3

Compound MML-3 was obtained as colorless needles (18.5 mg, 0.0037 % based on dried weight of leaves).

UV : λ_{max} nm (log ε), in MeOH; 278 (0.83), 252 (0.32), 229 (1.92); see **Figure 96**

IR : ν_{max} cm^{-1}, KBr; 2957, 2839, 1590, 1518, 1469, 1257, 1138, 1025, 852, 764;

see **Figure 97**

ESITOFMS : m/z; 387 [M+H]$^+$; see **Figure 98**

Mp : 133-134 ^{o}C

^{1}H NMR : δ ppm, 500 MHz, in CDCl$_3$; see **Figures 99a** and **99b**

^{13}C NMR : δ ppm, 125 MHz, in CDCl$_3$; see **Figure 100**

4.22 Compound MML-4

Compound MML-4 was obtained as colorless needles (13.6 mg, 0.0027 % based on dried weight of leaves).

IR : ν$_{max}$ cm^{-1}, KBr; 3408, 3188, 1698, 1657, 1501, 1459, 1413, 1377, 1325, 1271, 1232, 1184, 1131, 1055, 1034, 845, 742, 683; see **Figure 101**

ESITOFMS : m/z; 387 [M+H]$^+$; see **Figure 102**

^{1}H NMR : δ ppm, 300 MHz, in CDCl$_3$; see **Figure 103**

^{13}C NMR : δ ppm, 75 MHz, in CDCl$_3$; see **Figure 104**

4.23 Compound MML-5

Compound MML-5 was obtained as colorless rod-shape crystals (8.1 mg, 0.0016 % based on dried weight of leaves).

UV : λ$_{max}$ nm (log ε), in MeOH; 277 (1.43), 253 (0.63), 244 (0.87), 229 (0.14); see **Figure 105**

IR : ν$_{max}$ cm^{-1}, KBr; 3522, 2937, 2839, 1668, 1594, 1516, 1464, 1420, 1264, 1161, 1024, 813, 765; see **Figure 106**

ESITOFMS : m/z; 403 [M+H]$^+$; see **Figure 107**

Mp : 149-150 ^{o}C

$[\alpha]^{25}_D$: +24.7° (c = 0.5, MeOH)

^{1}H NMR : δ ppm, 500 MHz, in CDCl$_3$; see **Figure 108**

^{13}C NMR : δ ppm, 125 MHz, in CDCl$_3$; see **Figure 109**

4.24 Compound MML-6

Compound MML-6 was obtained as white powder (7.7 mg, 0.0015 % based on dried weight of leaves).

Mp : 239 – 243 ^{o}C

^{1}H NMR : δ ppm, 500 MHz, in acetone-d_6; see **Figure 110**

^{13}C NMR : δ ppm, 75 MHz, in CDCl$_3$; see **Figure 111**

4.25 Compound MMS-1

Compound MMS-1 was obtained as colorless needles (8.0 mg, 0.0016 % based on dried weight of stems).

Mp	: 218 – 220 ^{o}C
^{1}H NMR	: δ ppm, 500 MHz, in CDCl$_3$; see **Figures 113a** and **113b**
^{13}C NMR	: δ ppm, 75 MHz, in CDCl$_3$; see **Figure 114**

4.26 Compound MMS-2

Compound MMS-2 was obtained as yellow needles (21.0 mg, 0.0010 % based on dried weight of stems).

UV	: λ$_{max}$ nm (log ε), in MeOH; 410.5 (1.88), 340 (0.56), 306 (1.38), 293 (1.14), 275 (2.50); see **Figure 117**
IR	: ν$_{max}$ cm^{-1}, KBr; 3288, 3074, 2927, 1653, 1577, 1423, 1310, 1262, 1227, 1052, 966, 785; see **Figure 118**
ESITOFMS	: *m/z*; 276 [M+H]$^{+}$; see **Figure 119**
^{1}H NMR	: δ ppm, 300 MHz, in CDCl$_3$; see **Figure 120**

4.27 Compound MMS-3

Compound MMS-3 was obtained as yellow powder (18.0 mg, 0.0009 % based on dried weight of stems).

UV	: λ$_{max}$ nm (log ε), in MeOH; 420 (0.20), 323 (0.06), 221 (0.74); see **Figure 121**
IR	: ν$_{max}$ cm^{-1}, KBr; 3406, 2924, 2853, 1737, 1628, 1580, 1474, 1412, 1261, 1044, 972, 875, 791; see **Figure 122**
ESITOFMS	: *m/z*; 306 [M+H]$^{+}$; see **Figure 123**
Mp	: 270-271°C
^{1}H NMR	: δ ppm, 300 MHz, in CDCl$_3$; see **Figure 124**

4.28 Compound MMS-4

Compound MMS-4 was obtained as pale yellow needles (42.0 mg, 0.0021 % based on dried weight of stems).

UV	: λ_{max} nm (log ε), in MeOH; 287 (1.89), 248 (0.09), 224 (1.74) see **Figure 125**
IR	: ν_{max} cm^{-1}, KBr; 3090, 2890, 2753, 2641, 1629, 1603, 1488, 1303, 1170, 1090, 829, 715; see **Figure 126**
ESITOFMS	: m/z; 257 [M+H]$^+$; see **Figure 127**
Mp	: 137-138°C
^{1}H NMR	: δ ppm, 300 MHz, in CDCl$_3$; see **Figure 128**
^{13}C NMR	: δ ppm, 75 MHz, in CDCl$_3$; see **Figure 129**

5. Evaluation of Biological Activities

5.1 Determination of Antimycobacterial Activity

Antimycobacterial activity was assessed against *Mycobacterium tuberculosis* H$_{37}$Ra using the Microplate Alamar Blue Assay (MABA) (Collins and Franzblau, 1997). The mycobacteria were grown in 100 ml of 7H9GC broth containing 0.005 % Tween 80. Culture was incubated in 500 ml plastic flask on a rotary shaker at 200 rpm and 37 °C until they reached an optical density of 0.4-0.5 at 550 nm. Bacteria were washed and suspended in 20 ml of phosphate-buffered saline and passed through a filter. The filtrates were aliquoted and stored at -80°C.

The susceptibility testing was performed in 96-well microplates. Samples were initially diluted with either dimethyl sulfoxide or distilled deionized water, then diluted by Middlebrook 7H9 media containing 0.2 % v/v glycerol and 1.0 g/L 7H9GC broth, and subsequent two-fold dilutions were performed in 0.1 ml of 7H9CG broth in microplates. Frozen inocula were diluted 100 times in 7H9GC broth and adding of 0.1 ml to the well resulted in final bacterial titers of about 5 x 10^4 CFU/ml. The wells containing sample only were used to determine whether the test samples themselves can reduce the dye or not. Additional control wells were consisted of bacteria only (B) and medium only (M). Plates were incubated at 37 °C. Starting at day 6 of the incubation, 20 µl of Alamar Blue solution and 12.5 µl of 20 % Tween 80 were added to one B well and one M well, and the plates were reincubated at 37 °C. The B wells were observed for a color change from blue to pink, at which time reagents were added to all remaining wells. Plates were then incubated at 37 °C, and results were recorded at 24 h after the addition of reagents. Visual MIC values were defined as the lowest concentration of sample that prevented a color change. Rifampicin,

isoniazid and kanamycin sulfate, which are standard drugs in the treatment of tuberculosis, were used as the reference compounds.

5.2 Determination of Antimalarial Activity

The parasite *Plasmodium falciparum* (K1, multi-drug resistant strain) was cultivated *in vitro* using the method of Trager and Jensen (Trager and Jensen, 1976) in RPMI 1640 medium containing 20 mM HEPES (N-2-hydroxyethylpiperazine-N′-2-ethanesulfonic acid), 32 mM $NaHCO_3$ and 10 % heat-inactivated human serum with 3 % erythrocytes and incubated at 37 ℃ in an incubator with 3 % CO_2. The cultures were diluted with fresh medium and erythrocytes every day according to cell growth. Quantitative assessment of antimalarial activity *in vitro* was determined by microculture radioisotope techniques based upon the method of Desjardins *et al.* (1979). Briefly, a mixture of 200 µl of 1.5 % erythrocytes with 1 % parasitemia at the early ring stage was pre-exposed to 25 µl of the medium containing a test sample dissolved in 1% DMSO (0.1 % final concentration) for 24 h, employing the incubation condition described above. Subsequently, 25 µl of $[^3H]$-hypoxanthine (Amersham, USA) in culture medium (0.5 µCi) were added to each well and the plates were incubated for an additional 24 h. Levels of incorporated labeled hypoxanthine indicating parasite growth were determined using the TopCount microplate scintillation counter (Packard, USA). The IC_{50} value represents the concentration which indicates 50 % reduction of parasite growth. The standard sample for positive control was dihydroartemisinin (DHA).

5.3 Determination of Cytotoxic Activity
5.3.1 Human Small Cell Lung Carcinoma (NCI-H187)

Cytotoxicity to NCI-H187 cells (human small cell lung carcinoma, ATCCCRL-5804) was determined by MTT assay (Plumb *et al.*, 1989). Briefly, cells were diluted to 10^5 cells/ml. Test compounds were diluted in distilled water and added to microplates in a total volume of 200 µl. Plates were incubated at 37 °C, 5 % CO_2 for 5 days. Then, 50 µl of 2 mg/ml MTT solution (3-[4,5-dimethylthiazol-2-yl]-2,5-diphenyltetrazolium bromine; thiazolyl blue) was added to each well of the plate. The plates were wrapped with aluminium foil and incubated for 4 h. After the incubation period, the microplates were spun

at 200 rpm for 5 min. MTT was then removed from the wells and the formazan crystals were dissolved in 200 µl of DMSO and 25 µl of Sorensen's glycine buffer. Absorbance was read in microplate reader at the wavelength of 510 nm. The reference substance was ellipticine. The activity was expressed as 50 % inhibitory concentration (IC_{50}), the concentration which inhibits cell growth by 50 % compared with untreated cells.

5.3.2 Human Epidermoid Carcinoma (KB) and Breast Cancer (BC)

Cytotoxicity to KB (human epidermoid carcinoma of cavity, ATTCC CCL-17) and BC (breast cancer) cell lines were determined by a colorimetric assay that measured cell growth from cellular protein content (Skehan *et al.*, 1990). Ellipticine and doxorubicin were used as positive control. DMSO was used as negative control. Briefly, cells at a logarithmic growth phase were harvested and diluted to 10^5 cells/ml with fresh medium and gently mixed. Extracts or test compounds were diluted in distilled water and put into microplates in a total volume of 200 µl. Plates were incubated at 37 ℃, 5 % CO_2 for 72 h. After the incubation period, cells were fixed by 50 % trichloroacetic acid. The plates were incubated at 4 ℃ for 30 min, washed with tap water and air-dried at room temperature. The plates were then stained with 0.05 % sulforhodamine B (SRB), dissolved in 1 % acetic acid for 30 min. After the staining period, SRB was removed with 1 % acetic acid. Plates were air-dried before the bound dye was solubilized with 10 mM Tris-base for 5 min on shaker. Absorbance was read in microplate reader at the wavelength of 510 nm. The criteria of cytotoxic potency of the compound testing in this system are as follows:

IC_{50} (µg/ml)	Activity
> 20	Inactive
> 10 – 20	Weakly active
5 – 10	Moderately active
< 5	Strongly active

5.3.3 Vero cell

Compounds were tested for their toxicity against Vero cells (African green monkey kidney fibroblast) in 96-well tissue culture plates. Vero cell suspension (190 µl)

containing 10^5 cells/ml and 10 µl of test compound solution were added to each well in triplicate. Ellipticine and 10% DMSO were used as positive and negative control, respectively. The cells were incubated at 37 °C for 72 h in 5% CO_2. After the incubation, the cytotoxicity was determined as in 5.3.2. If % cell viability $\geq$ 50% reported as $IC_{50} > 50$ µg/ml and if % cell viability <50% reported IC_{50} from two-fold serial dilution.

5.4 Determination of Anti-Herpes Simplex Activity

Anti-herpes simplex virus type 1 (HSV-1) activity of pure compounds was tested against HSV-1 strain ATCC VR 260, using colorimetric microplate assay as in 5.3.2. The growth of host cells (Vero cell line ATCC CCL-81) infected with the virus and treated with the extract was compared with control cells, which were infected with virus only. Acyclovir and DMSO were used as positive and negative control, respectively. The extracts were tested at non-cytotoxic concentrations (inhibition of cell growth < 50 %). The potency of activity criteria are as follows:

% Inhibition	Potency of Activity
25-35 %	weakly active
35-50 %	moderately active
> 50 %	active

Extracts that inhibited virus more than 50 % were further tested to determine the concentrations that inhibit viral activity by 50 % (IC_{50}).

5.5 Determination of Advanced Glycation End-Product (AGE) Formation Inhibitory Activity

Assay of this inhibitory activity employed the measurement of fluorescent material based on AGEs in order to detect the inhibitory effect of test samples on the Maillard reaction (Matsuura *et al.*, 2002a). The plant extract or pure compound was dissolved in DMSO. The reaction mixtures, containing 400 µg bovine serum albumin (BSA), 200 mM glucose and 10 µl of test sample solution or DMSO in a total volume of 500 µl of 50 mM phosphate buffer, pH 7.4, were incubated at 60 °C for 30 h. The blank sample, which contained no plant extract or pure compound, was kept at 4 °C until measurement. After

cooling, aliquots of 250 µl were transferred to 1.5 ml plastic tubes, then, 25 µl of trichloroacetic acid (TCA) was added to each tube and stirred. The supernatant was removed after centrifugation (15,000 rpm) at 4 $^{\circ}$C for 4 min and the AGE-BSA precipitate was dissolved with 1 ml of alkaline phosphate buffer saline (PBS). Using spectrofluorometer, these solutions were monitored by comparing their fluorescence spectra (ex. 360 nm) and the changes in fluorescence intensity (ex. 360 nm, em. 460 nm) based on AGEs. The % inhibition of test sample was calculated as:

$$[1 - (\Delta A \text{ sample/min} - \Delta A \text{ blank/min}) / (\Delta A \text{ control/min} - \Delta A \text{ blank/min})] \times 100$$

whereas ΔA sample/min represents a decrease of absorbance for 1 min with a test sample, ΔA blank/min with DMSO and water instead of a sample and a substrate, respectively, and ΔA control/min with DMSO in place of a sample.

CHAPTER IV

RESULTS AND DISCUSSION

The pulverized leaves and stems of *Uvaria rufa* Blume were separately extracted with organic solvents to afford hexane, EtOAc and MeOH extracts. Separation of the leaf extracts using several chromatographic techniques yielded 10 compounds (URL-1, URL-2, URL-3, URL-4, URL-5, URL-6, URL-7, URL-8, URL-9 and URL-10), whereas the stem extracts gave 8 compounds (URS-1, URS-2, URS-3, URS-4, URS-5, URS-6, URS-7 and URS-8).

The dried, ground leaves and stems of *Mitrephora maingayi* Hook F. & Thomson were successively macerated with hexane, $CHCl_3$ and MeOH, to give hexane, $CHCl_3$ and MeOH extracts of the leaves and stems, respectively. Six compounds (MML-1, MML-2, MML-3, MML-4, MML-5 and MML-6) were isolated from the leaf extracts. The extracts of its stems were chromatographed to yield another 4 compounds (MMS-1, MMS-2, MMS-3 and MMS-4).

The structures of these isolated compounds were identified and elucidated by interpretation of their UV, IR, MS and NMR spectral data, and confirmed by comparison with those reported in the literature.

## 1. Structure Determination of Compounds Isolated from *Uvaria rufa*

1.1 Identification of Compound URL-1

Compound URL-1 was obtained as colorless needle crystals, soluble in $CHCl_3$ and EtOAc. Its UV absorption maxima at 243 and 276 nm (**Figure 11**) were indicative of the presence of benzoyl group(s). Its IR spectrum (**Figure 12**) suggested the presence of hydroxy group (3476 cm^{-1}), ester carbonyl (1713 cm^{-1}), mono-substituted phenyl ring (1602, 1452, 710 and 687 cm^{-1}) and epoxide ring (1279, 1066 and 905 cm^{-1}). The molecular formula of compound URL-1, $C_{21}H_{18}O_6$, was determined by ESITOF mass spectrometry (**Figure 13**).

The ^{1}H-NMR spectrum (**Figures 14a** and **14b**) of compound URL-1 displayed signals of the ten protons of two mono-substituted phenyl rings at δ 7.42 (4H, *m*, H-3′, H-3″, H-5′ and H-5″), 7.56 (2H, *m*, H-4′ and H-4″), and 8.04 (4H, *m*, H-2′, H-2″, H-6′ and H-6″). Two olefinic proton signals at δ 5.88 (1H, *dt*, *J* = 9.8, 1.8 Hz, H-4) and 6.07 (1H, *ddd*, *J* =

9.8, 3.9, 2.8 Hz, H-5) with HMQC correlations (**Figure 16**) to ^{13}C-NMR signals (**Figure 15**) at δ 133.0 (C-4) and 124.7 (C-5), respectively, represent the double bond between positions 4 and 5 within the cyclohexene ring. A methine proton attached to a hydroxy-bearing position appeared as a doublet at δ 4.31 (*J* = 7.9 Hz, H-2), whereas the signals of H-3 and H-6 appeared at δ 5.66 (1H, *ddd*, *J* = 7.9, 2.8, 1.8 Hz) and δ 3.58 (1H, *dd*, *J* = 3.9, 1.8 Hz), respectively. Long-range HMBC correlations (**Figure 17**) between both methylene protons of position 7 (at δ 4.47 and δ 4.98) to carbonyl carbon signal of the attached benzoate (at δ 166.2) could also be observed.

The relative stereochemistry of compound URL-1 was established upon its large coupling constant between H-2 and H-3 (*J* = 7.9 Hz), indicating the *trans* pseudo-diaxial arrangement of these two protons. Based on the analysis of spectral data and comparison with reported values (Nkunya *et al*., 1987), compound URL-1 was identified as a cyclohexene epoxide named (-)-pipoxide.

URL-1
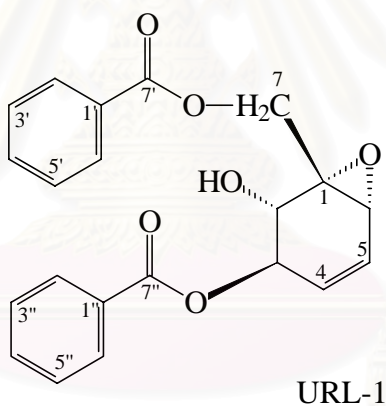
Cyclohexene epoxides have aroused widespread interest among natural products and synthetic chemists owing to their unusual structures, biogenesis and biological activities such as tumor inhibitory, antileukemic and antibiotic activities. Even though the compound pipoxide can be found scattered in a number of different plants, including *Croton macrostachys* (Kupchan, Hemingway and Smith, 1969), *Piper hookeri* (Singh, Dhar and Actal, 1970) and *Kaempferia sp.* (Pancharoen *et al*., 1989), the richest source of this compound is the *Uvaria* plants (Thebtaranonth, 1986). (-)-Pipoxide, isolated from the stem bark of *U. pandensis*, showed anti-malarial activity against *Plasmodium falciparum* parasites (IC$_{50}$ value of 12.5 µg/ml) (Nkunya *et al*., 1987).

Table 40. Comparison of the ^{1}H and ^{13}C NMR spectral data of (-)-pipoxide and compound

URL-1 (in CDCl$_3$, 500 MHz)

Position	(-)-Pipoxide†	URL-1	
	^{1}H	^{1}H	^{13}C
1	-	-	59.5
2	4.27 (1H, *m*)	4.31 (1H, *d*, *J* = 7.9 Hz)	71.0
3	5.64 (1H, *dt*, *J* < 2.0 Hz)	5.66 (1H, *ddd*, *J* = 7.9, 2.8, 1.8 Hz)	74.8
4	5.89 (1H, *dt*, *J* = 10.0 Hz)	5.88 (1H, *dt*, *J* = 9.8, 1.8 Hz)	133.0
5	6.06 (1H, *ddd*, *J* = 4.0 Hz)	6.07 (1H, *ddd*, *J* = 9.8, 3.9, 2.8 Hz)	124.7
6	3.56 (1H, *dd*, *J* = 2.0 Hz)	3.58 (1H, *dd*, *J* = 3.9, 1.8 Hz)	54.2
7	4.48 (1H, *d*, *J* = 12.0 Hz)	4.47 (1H, *d*, *J* = 12.1 Hz)	62.9
	5.02 (1H, *d*, *J* = 12.0 Hz)	4.98 (1H, *d*, *J* = 12.1 Hz)	
1′	-	-	129.4
2′,6′	7.3-8.1 (2H, *m*)	8.04 (2H, *m*)	129.8
3′,5′	7.3-8.1 (2H, *m*)	7.42 (2H, *m*)	128.5
4′	7.3-8.1 (2H, *m*)	7.56 (1H, *m*)	133.4
7′	-	-	166.2
1″	-	-	129.4
2″,6″	7.3-8.1 (2H, *m*)	8.04 (2H, *m*)	129.8
3″,5″	7.3-8.1 (2H, *m*)	7.42 (2H, *m*)	128.5
4″	7.3-8.1 (2H, *m*)	7.56 (1H, *m*)	133.4
7″	-	-	166.8

† Nkunya *et al*., 1987 (in CDCl$_3$, 90 MHz)

### 1.2 Identification of Compound URL-2

Compound URL-2 was obtained as white amorphous powder, soluble in acetone and MeOH. Its UV absorption maxima at 243 and 276 nm (**Figure 18**) were suggestive of the presence of benzoyl group(s). Its IR spectrum (**Figure 19**) indicated the presence of hydroxy group (3449 cm^{-1}), ester carbonyl (1716 cm^{-1}) and aromatic moieties (1272, 1112 and 712 cm^{-1}). Its molecular formula was determined to be C$_{21}$H$_{20}$O$_7$ from the [M+H]$^+$ peak at *m/z* 385 in the ESITOF mass spectrum (**Figure 20**).

The ^{1}H NMR spectrum of compound URL-2 (**Figure 21**) exhibited the signals of three oxygenated methine protons at δ 4.14 (1H, *dd*, *J* = 7.9, 6.6 Hz, H-2), 4.80 (1H, *dd*, *J* = 4.6, 0.8 Hz, H-6) and 5.67 (1H, *dtd*, *J* = 7.9, 2.1, 0.8 Hz, H-3), oxygenated methylene protons

at δ 4.51 (1H, *d*, *J* = 11.8 Hz, H-7a) and 4.59 (1H, *d*, *J* = 11.8 Hz, H-7b), together with those of *cis*-olefinic protons at δ 5.81 (1H, *dd*, *J* = 9.8, 2.1 Hz, H-4) and 5.98 (1H, *ddd*, *J* = 9.8, 4.6, 2.1 Hz, H-5). The large value of the coupling constant between H-2 and H-3 signals (7.9 Hz) indicated a *trans* pseudo-diaxial arrangement of these two protons, whereas the small value of $J_{3,6}$ (0.8 Hz) and large value of $J_{5,6}$ (4.6 Hz) indicate that H-6 is pseudoequatorial, and therefore the substituents at C-3 and C-6 are *cis*.

The ^{13}C NMR spectrum (**Figure 26**) showed the corresponding olefinic carbon signals at δ 128.0 (C-4) and 127.9 (C-5), three oxygenated methine carbons at δ 57.5 (C-6), 68.6 (C-2) and 73.9 (C-3), as well as an oxygenated methylene signal at δ 67.9 (C-7).

Based on the spectral data analysis and comparison with reported values, compound URL-2 was identified as the cyclohexene derivative 1-epizeylenol, previously isolated from *Uvaria zeylanica* and *U. purpurea* (Jolad *et al*., 1984). Slight revision in the NMR assignments of the compound was reported in this study.
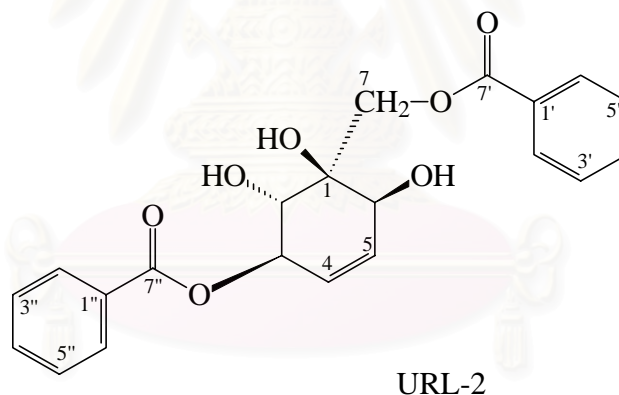
URL-2

Table 41. Comparison of the ^{1}H and ^{13}C NMR spectral data of 1-epizeylenol and compound
URL-2 (in DMSO-d_6, 500 MHz)

Position	1-Epizeylenol*		URL-2	
	^{1}H	^{13}C	^{1}H	^{13}C
1	-	75.5	-	74.9
2	4.98	69.5	4.14 (1H, *dd*, *J* = 7.9, 6.6 Hz)	68.6
3	6.60 (1H, *J* = 7.5 Hz)	74.6	5.67 (1H, *dtd*, *J* = 7.9, 2.1, 0.8 Hz)	73.9
4	6.09 (1H, *J* = 2.2 Hz)	128.1	5.81 (1H, *dd*, *J* = 9.8, 2.1 Hz)	128.0
5	6.02 (1H, *J* = 9.9, 1.8 Hz)	127.8	5.98 (1H, *ddd*, *J* = 9.8, 4.6, 2.1 Hz)	127.9
6	5.32 (1H, *J* = 4.2 Hz)	58.2	4.80 (1H, *dd*, *J* = 4.6, 0.8 Hz)	57.5
7	5.27 (1H, *J* = 12.0 Hz) 5.57 (1H, *J* = 12.0 Hz)	68.1	4.51 (1H, *d*, *J* = 11.8 Hz) 4.59 (1H, *d*, *J* = 11.8 Hz)	67.9
1′		130.1	-	129.8
2′, 6′		129.1	8.06 (2H, *m*)	129.4
3′, 5′		127.9	7.53 (2H, *m*)	128.7
4′		132.4	7.66 (1H, *m*)	133.4
7′		165.8	-	165.7
1″		130.1	-	129.7
2″, 6″		129.1	8.00 (2H, *m*)	129.4
3″, 5″		127.9	7.53 (2H, *m*)	128.7
4″		132.4	7.66 (1H, *m*)	133.4
7″		165.8	-	165.7
2-OH				
6-OH				

* Jolad *et al*., 1984 (in CDCl$_3$, 250 MHz for ^{1}H and 62.9 MHz for ^{13}C)

1.3 Identification of Compound URL-3

Compound URL-3 was obtained as white amorphous powder, soluble in CHCl$_3$
and EtOAc. Its UV absorption maxima at 243 and 276 nm (**Figure 23**) were suggestive of
the presence of benzoyl group(s). Its IR spectrum (**Figure 24**) indicated the presence of
hydroxy group (3464 cm^{-1}), ester carbonyl (1722 cm^{-1}) and aromatic moieties (1275, 1116
and 714 cm^{-1}).

The ^{1}H NMR spectrum of compound URL-3 (**Figures 25** and **26**) exhibited the
signals of three oxygenated methine protons at δ 4.21 (1H, *d*, *J* = 7.5 Hz, H-2), 4.61 (1H, *d*, *J*

= 2.0 Hz, H-6) and 5.90 (1H, *dd*, *J* = 10.0, 7.5 Hz, H-3), oxygenated methylene protons at δ 4.60 (1H, *d*, *J* = 12.1 Hz, H-7a) and 4.70 (1H, *d*, *J* = 12.1 Hz, H-7b), together with those of *cis*-olefinic protons at δ 5.67 (1H, *dt*, *J* = 10.0, 2.0 Hz, H-4) and 5.74 (1H, *dd*, *J* = 10.0 2.0 Hz, H-5).

The ^{13}C NMR spectrum (**Figure 27**) showed the corresponding olefinic carbon signals at δ 126.9 (C-4) and 132.2 (C-5), three oxygenated methine carbons at δ 67.4 (C-6), 69.8 (C-2) and 73.7 (C-3), as well as an oxygenated methylene signal at δ 56.9 (C-7).

Based on the spectral data analysis and comparison with reported values, compound URL-3 was identified as the cyclohexene derivative ellipeiopsol B, previously isolated from *Ellipeiopsis cherrevensis* (Kijjoa *et al*., 2002). Slight revision in the NMR assignments of the compound was reported in this study.

Table 42. Comparison of the ^{1}H and ^{13}C NMR spectral data of ellipeiopsol B and compound URL-3 (in CDCl$_3$, 500 MHz)

Position	Ellipeiopsol B*		URL-3	
	^{1}H	^{13}C	^{1}H	^{13}C
1	-	76.3	-	75.5
2	4.13 (1H, *d*, *J* = 7.5 Hz)	74.7	4.21 (1H, *d*, *J* = 7.5 Hz)	73.7
3	5.80-5.83 (1H, *m*)	74.0	5.90 (1H, *dd*, *J* = 10.0, 7.5 Hz)	69.8
4	5.66 (1H, *dt*, *J* = 10.3, 2.5 Hz)	124.9	5.67 (1H, *dt*, *J* = 10.0, 2.0 Hz)	126.9
5	5.81 (1H, *dd*, *J* = 10.3, 2.2 Hz)	132.2	5.74 (1H, *dd*, *J* = 10.0, 2.0 Hz)	132.2
6	4.46 (1H, *d*, *J* = 2.2 Hz)	72.7	4.61 (1H, *d*, *J* = 2.0 Hz)	67.4
7	4.67 (1H, *d*, *J* = 12.0 Hz)	63.4	4.60 (1H, *d*, *J* = 12.1 Hz)	56.9
	4.77 (1H, *d*, *J* = 12.0 Hz)		4.70 (1H, *d*, *J* = 12.1 Hz)	
1′	-	129.5	-	129.6
2′, 6′	8.00 (2H, *dt*, *J* = 8.0, 1.4 Hz)	129.8	7.92 (2H, *dt*, *J* = 7.0, 1.0 Hz)	129.5
3′, 5′	7.36 (2H, *td*, *J* = 8.0, 1.4 Hz)	128.4	7.36 (2H, *td*, *J* = 7.0, 1.0 Hz)	128.3
4′	7.49 (1H, *tt*, *J* = 8.0, 1.4 Hz)	133.2	7.49 (1H, *tt*, *J* = 7.0, 1.0 Hz)	133.2
7′	-	167.7	-	166.9
1″	-	129.5	-	129.6
2″, 6″	8.00 (2H, *dt*, *J* = 8.0, 1.4 Hz)	129.7	7.92 (2H, *dt*, *J* = 7.0, 1.0 Hz)	129.4
3″, 5″	7.36 (2H, *td*, *J* = 8.0, 1.4 Hz)	128.3	7.36 (2H, *td*, *J* = 7.0, 1.0 Hz)	128.3
4″	7.49 (1H, *tt*, *J* = 8.0, 1.4 Hz)	133.1	7.49 (1H, *tt*, *J* = 7.0, 1.0 Hz)	133.1
7″	-	166.6	-	166.8

* Kijjoa *et al*., 2002 (in CDCl$_3$, 300 MHz)

URL-3
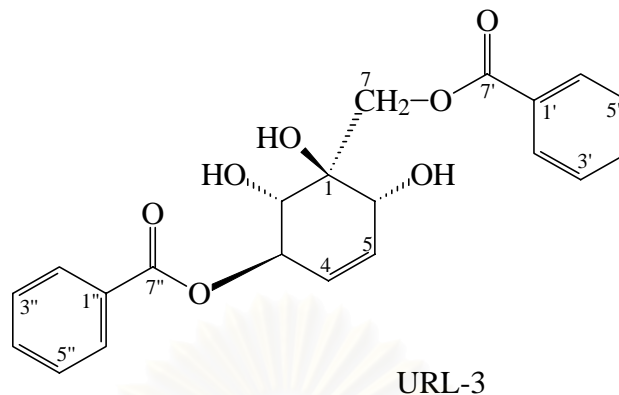
1.4 Identification of Compound URL-4

Compound URL-4 was obtained as white amorphous powder, soluble in acetone and MeOH. The presence of benzoyl group(s) within the molecule could be deduced from its UV absorption maxima at 228, 272 and 278 nm (**Figure 27**). The molecular formula of compound URL-4, $C_{21}H_{22}O_7$, was determined by ESITOF mass spectrometry (**Figure 28**).

The presence of 10 aromatic proton signals at δ 7.42–8.04 in the ^{1}H NMR spectrum (**Figures 29a** - **29c**), together with the signals for 10 carbons at δ 165.6, 164.8, 133.3, 133.2, 130.0, 129.7, 129.3, 129.2, 128.7 and 128.6 in ^{13}C NMR spectrum (**Figure 30**), indicated the presence of two benzoyl moieties in the molecule. The signals for the two coupling olefinic protons at δ 5.95 (1H, *ddd*, *J* = 15.8, 7.0, 1.2 Hz) and 5.83 (1H, *ddd*, *J* = 15.8, 5.5, 0.9 Hz) represent a double bond in the molecular structure. The large coupling constant between these two protons (15.8 Hz) indicate the *trans* geometry of the double bond.

In the ^{1}H–^{1}H COSY spectrum (**Figure 31**), correlation between the resonances at δ 5.95 (1H, *ddd*, *J* = 15.8, 7.0, 1.2 Hz, H-4) and 5.52 (1H, *dd*, *J* = 7.0, 4.3 Hz, H-3) and between those signals at δ 5.83 (1H, *ddd*, *J* = 15.8, 5.5, 0.9 Hz, H-5) and 4.36 (1H, *m*, H-6) could clearly be observed. These proton signals were assigned, through the analysis of the HMQC spectrum, as being connected with the carbon signals at δ 126.0, 75.4, 133.9 and 68.3, respectively (**Figures 32-33**). The H-3 signal was further correlated to the hydroxy-bearing H-2 signal at δ 3.75 (*ddd*, *J* = 11.0, 5.4, 4.3 Hz), which in turn cross-linked to the methylenehydroxy H-1 signal at δ 3.41 (*ddd, J* = 9.8, 5.8, 4.3 Hz), while H-6 was similarly connected to the H-7 doublet at δ 4.15 (2H, *d, J* = 5.2 Hz).

The HMBC correlation of the proton signal at δ 4.15 (2H, *d*, *J* = 5.2 Hz, H$_2$-7) with the carbonyl resonance at δ 165.6 (C-7′) suggested that a benzoyloxy group was attached to the position 7, while the correlation of the H-3 signal at δ 5.52 to another carbonyl carbon signal at δ 164.8 (C-7″) indicated the attachment of the second benzoyloxy group at position 3 (**Figures 34a** and **34b**).

From the above analysis and upon comparison with previously reported data (Chayunkiat, Wiriyachitra and Taylor, 1984), compound URL-4 was identified as a seco-cyclohexene derivative previously named (*E*)-3,7-bisbenzoyloxyhept-4-en-1,2,6-triol (Chayunkiat *et al*., 1984) or microcarpin B (Lu *et al*., 1995).
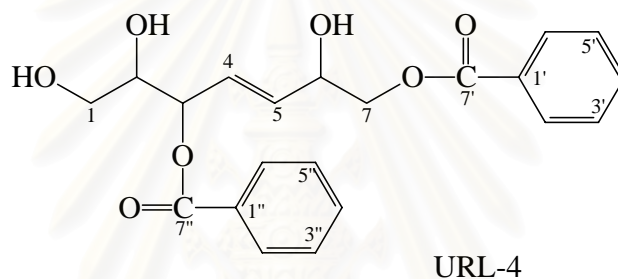
URL-4

Table 43. Comparison of the ^{1}H and ^{13}C NMR spectral data of microcarpin B and compound URL-4 (in DMSO-d_6, 500 MHz)

Position	Microcarpin B		URL-4	
	^{1}H†	^{13}C†	^{1}H	^{13}C
1	3.64 (1H, *m*) and 3.74 (1H, *m*)	61.2	3.41 (2H, *ddd*, *J* = 9.8, 5.8, 4.3 Hz)	62.2
2	3.88 (1H, *br s*)	71.7	3.75 (1H, *ddd*, *J* = 11.0, 5.4, 4.3 Hz)	72.7
3	5.54 (1H, *dd*, *J* = 6.5, 6.0 Hz)	73.7	5.52 (1H, *dd*, *J* = 7.0, 4.3 Hz)	75.4
4	6.07 (1H, *dd*, *J* = 15.5, 6.5 Hz)	125.4	5.95 (1H, *ddd*, *J* = 15.8, 7.0, 1.2 Hz)	126.0
5	6.01 (1H, *dd*, *J* = 15.5, 5.0 Hz)	132.7	5.83 (1H, *ddd*, *J* = 15.8, 5.5, 0.9 Hz)	133.9
6	4.56 (1H, *br s*)	67.5	4.36 (1H, *m*)	68.3
7	4.34 (1H, *dd*, *J* = 11.0, 6.0 Hz) 4.42 (1H, *dd*, *J* = 11.3, 4.0 Hz)	66.6	4.15 (2H, *d*, *J* = 5.2 Hz)	67.8
1′	-	128.6	-	129.7
2′,6′	8.01 (2H, *d*)	126.9	7.92 (2H, *dd*)	129.2
3′,5′	7.41 (2H, *m*)	128.0	7.42 (2H, *t*)	128.6
4′	7.60 (1H, *m*)	131.5	7.60 (1H, *t*)	133.2
7′	-	163.6	-	165.6
1″	-	128.9	-	130.0
2″,6″	8.01 (2H, *d*)	126.9	7.97 (2H, *dd*)	129.3
3″,5″	7.41 (2H, *m*)	128.0	7.51 (2H, *t*)	128.7
4″	7.60 (1H, *m*)	131.5	7.65 (1H, *t*)	133.3
7″	-	164.5	-	164.8
1-OH	2.3 (1H, *br s*)	-	4.65 (1H, *t*, *J* = 5.8 Hz)	-
2-OH	2.8 (1H, *br s*)	-	5.08 (1H, *d*, *J* = 5.4 Hz)	-
6-OH	2.9 (1H, *br s*)	-	5.35 (1H, *d*, *J* = 5.2 Hz)	-

† Chayunkiat *et al*., 1984 (in CDCl$_3$, 400 MHz for ^{1}H and CDCl$_3$ + DMSO-d_6, 100 MHz for ^{13}C)

1.5 Identification of Compound URL-5

Compound URL-5 was obtained as white amorphous powder, soluble in acetone and MeOH. Its UV absorption maxima at 243 and 276 nm (**Figure 35**) were suggestive of the presence of benzoyl group. Its IR spectrum (**Figure 36**) indicated the presence of hydroxy group (3462 cm^{-1}), ester carbonyl (1679 cm^{-1}) and aromatic moieties (1281, 1119 and 712 cm^{-1}). Its molecular formula was determined to be $C_{21}H_{20}O_7$ from the [M+H]$^+$ peak

at *m/z* 385 in the ESI mass spectrum (**Figure 37**).

The ^{1}H NMR spectrum of compound URL-5 (**Figure 38**) exhibited the resonances of three oxygenated methine protons at δ 4.22 (*d*, *J* = 6.0 Hz, H-2), 4.32 (*d*, *J* = 4.0 Hz, H-6) and 5.69 (*m*, H-3), a pair of geminal oxygenated methylene protons at δ 4.72 (1H, *d*, *J* = 12.0 Hz, H-7a) and 4.86 (1H, *d*, *J* = 12.0 Hz, H-7b), together with two *cis*-olefinic protons at δ 5.84 (*ddd*, *J* = 10.3, 2.5, 0.5 Hz, H-4) and 5.98 (*ddd*, *J* = 10.3, 4.0, 2.0 Hz, H-5). The ^{13}C NMR spectrum (**Figure 39**) showed the corresponding olefinic carbon signals at δ 126.8 (C-4) and 129.7 (C-5), three oxygenated methine carbons at δ 68.6 (C-6), 70.8 (C-2) and 74.2 (C-3), as well as an oxygenated methylene signal at δ 66.7 (C-7).

Based on the spectral data analysis and comparison with reported values (Jolad *et al*., 1981; Pan and Yu, 1995), compound URL-5 was identified as the cyclohexene derivative zeylenol.

Zeylenol has been found in annonaceous plants, all of which are from the genus *Uvaria* i.e. *Uvaria zeylanica* (Jolad *et al*., 1981), *U. grandiflora* (Pan and Yu, 1995) and *U. kweichowensis* (Xu *et al*., 2005). Moreover, it can be found in *Piper cubeb* (Taneja *et al*., 1991) and *Kaempferia angustifolia* (Pancharoen *et al*., 1989). Bioactivity evaluation of zeylenol showed antitumor activity against A549 bronchogenic carcinoma cell with IC$_{50}$ value of 28 μg/ml, determined by MTT assay (Xu *et al*., 2005).
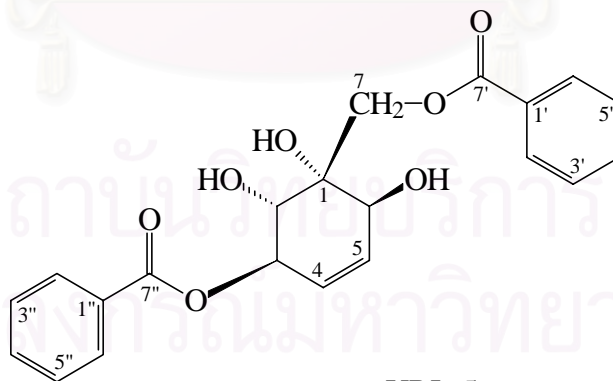
URL-5

Table 44. Comparison of the ^{1}H and ^{13}C NMR spectral data of zeylenol and compound URL-5 (in CDCl$_3$, 500 MHz)

Position	Zeylenol			URL-5	
	^{1}H†	^{13}C‡		^{1}H	^{13}C
1	-	76.0		-	75.9
2	4.32 (1H, *d*, *J* = 6.1 Hz)	68.7		4.22 (1H, *d*, *J* = 6.0 Hz)	70.8
3	5.70 (1H, *dddd*, *J* = 6.1, 2.6, 1.6, 1.1 Hz)	74.4		5.69 (1H, *m*)	74.2
4	5.88 (1H, *ddd*, *J* = 10.1, 2.6, 0.7 Hz)	127.0		5.84 (1H, *ddd*, *J* = 10.3, 2.5, 0.5 Hz)	126.8
5	5.99 (1H, *ddd*, *J* = 10.1, 4.0, 1.6 Hz)	129.5		5.98 (1H, *ddd*, *J* = 10.3, 4.0, 2.0 Hz)	129.7
6	4.32 (1H, *ddd*, *J* = 4.0, 1.1, 0.7 Hz)	70.9		4.32 (1H, *d*, *J* = 4.0 Hz)	68.6
7	4.75 (1H, *J* = 12.3 Hz) 4.89 (1H, *J* = 12.3 Hz)	66.8		4.72 (1H, *J* = 12.0 Hz) 4.86 (1H, *J* = 12.0 Hz)	66.7
1′	-	128.5		-	129.2
2′, 6′	7.3-8.1 (2H, *m*)	129.9		7.98 (2H, *dd*, *J* = 8.0, 1.5 Hz)	129.8
3′, 5′	7.3-8.1 (2H, *m*)	128.5		7.36 (2H, *m*)	128.4
4′	7.3-8.1 (1H, *m*)	133.5		7.51 (1H, *m*)	133.4
7′	-	165.0		-	167.8
1″	-	128.5		-	129.4
2″, 6″	7.3-8.1 (2H, *m*)	129.9		7.94 (2H, *dd*, *J* = 8.5, 1.5 Hz)	129.8
3″, 5″	7.3-8.1 (2H, *m*)	128.5		7.36 (2H, *m*)	128.4
4″	7.3-8.1 (1H, *m*)	133.5		7.51 (1H, *m*)	133.5
7″	-	165.0		-	167.1

† Pan and Yu, 1995 (in CDCl3, 500 MHz)

‡ Jolad *et al*., 1981 (in CDCl3, 65 MHz)

1.6 Identification of Compound URS-1

Compound URS-1 was obtained as white amorphous powder. Its molecular formula was determined by EITOFMS (**Figure 42**) as C$_{30}$H$_{50}$O, from its [M+H]$^{+}$ ion peak at *m/z* 427.. The IR absorption band (**Figure 41**) at 3477 cm^{-1} was suggestive of the presence of hydroxy group(s) in its structure.

The ^{13}C NMR and DEPT spectrum (**Figures 44** and **45**) displayed thirty carbon

signals, corresponding to eight methyl (δ 34.6, 32.5, 32.1, 29.1, 25.6, 19.8, 18.5, 16.3), ten methylene (δ 39.0, 36.1, 35.2, 34.7, 33.2, 32.2, 30.5, 27.9, 23.8, 18.4), five methine (δ 121.9, 76.3, 49.8, 47.5, 43.2) and seven quaternary carbons (δ 141.5, 40.9, 39.4, 37.9, 34.9, 30.2, 28.4).

The ^{1}H NMR spectrum of compound URS-1(**Figure 43**) showed signals for eight singlet methyls at δ 0.83, 0.93, 0.97, 0.98, 1.02, 1.07, 1.12 and 1.14, one methine proton geminal to a secondary hydroxy as broad singlet at δ 3.44, and a trisubstituted double bond as a doublet-like multiplet at δ 5.61 (1H, J = 4.5 Hz). On the basis of its spectral analysis and compariron with the literature values (Gonzalez, Ferro and Ravelo, 1987; Matsunaga, Tanaka and Akagi, 1988), compound URS-1 was found to be glut-5(6)-en-3β-ol, previously isolated from a number of plants, including *Uvaria narum* (Parmar *et al.*, 1995) and *Maytenus horrida* (Gonzalez *et al.*, 1987).
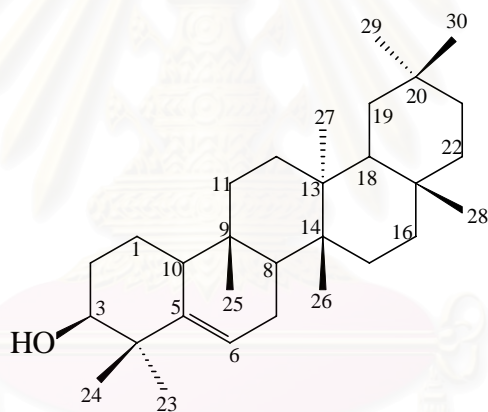
URS-1

Table 45. Comparison of the ^{13}C NMR spectral data of glut-5(6)-en-3β-ol and compound
URS-1 (in CDCl$_3$, 300 MHz)

Position	Glut-5(6)-en-3β-ol *	URS-1
1	18.3	18.4
2	27.9	27.9
3	76.4	76.3
4	40.9	40.9
5	141.8	141.5
6	122.1	121.9
7	23.7	23.8
8	47.6	47.5
9	34.9	34.9
10	49.8	49.8
11	33.2	33.2
12	30.5	30.5
13	38.0	37.9
14	39.4	39.4
15	34.7	34.7
16	35.2	36.1
17	30.2	30.2
18	43.2	43.2
19	35.2	35.2
20	28.3	28.4
21	32.2	32.2
22	39.1	39.0
23	29.0	29.1
24	25.5	25.6
25	16.3	16.3
26	18.5	18.5
27	19.7	19.8
28	32.5	32.5
29	32.1	32.1
30	34.6	34.6

* Gonzalez *et al*., 1987 (in CDCl$_3$, 50 MHz)

1.7 Identification of Compound URS-2

Compound URS-2 was obtained as white amorphous powder. Its molecular formula was determined by ESITOF MS (**Figure 48**) as C$_{30}$H$_{50}$O, from its [M+H]$^+$ ion peak at *m/z* 427. The UV absorption showed maxima (**Figure 46**) at 244 and 234 nm, and the IR

absorption band (**Figure 47**) at 3488 cm^{-1} was suggestive of the presence of hydroxy group in its structure.

The ^{13}C NMR and DEPT spectrum of compound URS-2 (**Figures 50** and **51**) displayed thirty carbon signals, corresponding to eight methyl (δ 33.5, 30.0, 30.0, 28.1, 26.0, 21.4, 15.6, 15.6), ten methylene (δ 41.4, 37.8, 36.8, 35.9, 35.2, 33.8, 33.2, 27.3, 18.9, 17.6), five methine (δ 116.8, 79.1, 55.6, 49.4, 48.8) and seven quaternary carbons (δ 157.9, 39.1, 38.6, 38.1, 37.8, 37.7, 28.9).

The ^{1}H NMR spectrum (**Figure 49**) showed the signal of the trisubstituted double bond between positions 14 and 15 as a broad doublet at δ 5.51 (1H, *d*, *J* = 5.4 Hz), the hydroxy-substituted H-3 at δ 3.17 (1H, *m*) and eight methyl singlets at δ 0.78, 0.80, 0.89, 0.89, 0.91, 0.93, 0.96 and 1.07. Based upon these data and comparison with reported values in the literature (Corbett *et al.*, 1972; Sakurai, Yaguchi and Inoue, 1987), compound URS-2 was identified as the taraxerane-type triterpenoid taraxerol.

Taraxerol is widely distributed among several plant species e.g. *Taraxacum officinales*, *Rhododendron* spp., *Euphobia* spp., and could also be isolated from the lichen *Pertusaria ophthalmiza* (Hesse, 1988). This triterpenoid showed marked anti-inflammatory activity against 12-*O*-tetradecanoylphorbol-13-acetate (TPA)-induced ear oedema in mice (Akihisa *et al.*, 1996).
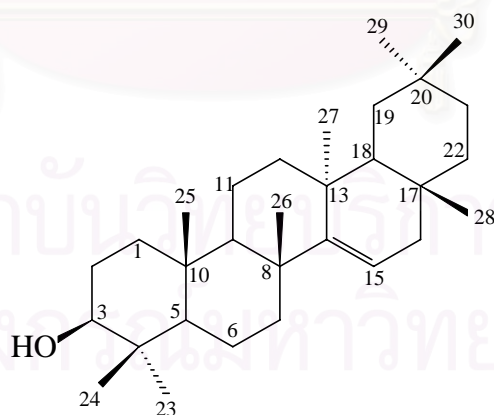
URS-2

Table 46. Comparison of the ^{13}C NMR spectral data of taraxerol and compound URS-2 (in

CDCl$_3$, 300 MHz)

Position	Taraxerol *	URS-2
1	38.1	37.8
2	27.3	27.3
3	79.2	79.1
4	39.1	39.1
5	55.7	55.6
6	19.0	18.9
7	35.3	35.2
8	38.9	38.9
9	48.9	48.8
10	37.9	37.7
11	17.7	17.6
12	35.9	35.9
13	37.9	38.1
14	158.1	157.9
15	117.0	116.8
16	36.9	36.8
17	38.1	37.8
18	49.4	49.4
19	41.4	41.4
20	29.0	28.9
21	33.9	33.8
22	33.2	33.2
23	28.1	28.1
24	15.6	15.6
25	30.1	30.0
26	15.6	15.6
27	26.0	26.0
28	30.1	30.0
29	33.5	33.5
30	21.5	21.4

* Sakurai *et al.*, 1987 (in CDCl$_3$, 25 MHz)

1.8 Identification of Compound URS-3

Compound URS-3 was obtained as colorless oil. Its molecular formula was determined by ESITOFMS (**Figure 53**) as $C_{14}H_{12}O_2$, from its [M+H]$^+$ ion peak at *m/z* 213. The IR spectrum was presented in **Figure 52**.

The ^{1}H NMR spectrum (**Figure 54**) showed the resonances of an methylenehydroxy group at δ 5.36 (2H, *s*) and two mono-substituted aromatic rings at δ 7.36-7.43 (7H, *m*), 7.53 (1H, *d*, *J* = 6.9 Hz) and 8.07 (2H, *br d*, *J* = 6.9 Hz), whereas the ^{13}C NMR and DEPT spectrum of this compound (**Figure 55** and **56**) displayed twelve carbon signals, corresponding to one ester carbonyl at δ 166.2, one methylenehydroxy at δ 66.7, and ten aromatic carbon at δ 135.9, 132.9, 129.6, 128.5, 128.2, 128.1 and 128.0. Compared with the previously reported spectral data (Rosenberg and Brinker, 2003), compound URS-3 was identified as benzyl benzoate.

URS-3
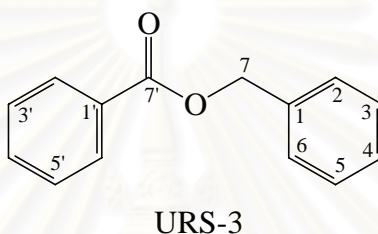
Benzyl benzoate is an ester which is widely distributed in the plant kingdom. This aromatic ester was reported to be acaricide and pediculicide agent. It was used in perfumery as fixative, in food flavoring and as a component in insect repellent formulation (Berrens, 1992).

1.9 Identification of Compound URS-4

Compound URS-4 was obtained as yellow amorphous powder, soluble in CHCl$_3$, EtOAc and acetone. The TOF mass spectrum (**Figure 59**) exhibited [M+H]$^+$ ion peak at *m/z* 269 and the molecular formula C$_{16}$H$_{12}$O$_4$. The UV maxima at 269 and 233 nm (**Figure 57**), coupled with the singlet at δ 6.65 in the ^{1}H NMR spectrum, indicated a flavone. The IR spectrum (**Figure 58**) exhibited absorption bands for hydroxy and conjugated carbonyl functionalities at 3422 and 1659 cm^{-1}, respectively.

In the ^{1}H NMR spectrum, the resonances at δ 7.88 (2H, *d*, *J* = 7.5 Hz, H-2′ and H-6′) and δ 7.51 (3H, *m*, H-3′, H-4′ and H-5′) (**Figure 60**) indicated that the B-ring of the flavone was unsubstituted, characteristic of flavonoids found in plants of the family Annonaceae. The remaining two aromatic broad singlet signals at δ 6.48 (1H, *s*) and 6.36 (1H, *s*) implied that A-ring had two substituents, one of which was the 5-hydroxy substitution as represented by the most downfield singlet at δ 12.69.

Sixteen carbon signals could be seen in the ^{13}C NMR spectrum (**Figure 61**). DEPT experiment was utilized to classify these signals into those of one methoxy carbon at δ 55.9, eight methine carbons at δ 92.7, 98.1, 105.8, 126.2 (2C), 129.0 (2C), 131.7, six quaternary carbons at δ 105.7, 131.7, 157.6, 162.0, 163.8, 165.4, and one carbonyl carbon at δ 182.2 (**Figure 62**).

Identification of compound URS-4 as the flavone tectochrysin was then carried out by comparison of its NMR data with the reported data (Lojanapiwatna *et al*., 1981).

Tectochrysin was found to exhibit considerable antimutagenic property against olfloxacin-induced bleaching of *Euglena gracilis* (Krizkova *et al*., 1998), as well as potent and specific inhibitory activity against breast cancer resistant protein ABCG2 (Ahmed-Belkacem *et al*., 2005).

Table 47. Comparison of the ^{1}H and ^{13}C NMR spectruml data of tectochrysin and compound URS-4 (in CDCl$_3$, 300 MHz)

Position	Tectochrysin *		URS-4	
	^{1}H	^{13}C	^{1}H	^{13}C
2	-	163.3	-	163.8
3	6.66 (1H, *s*)	105.2	6.65 (1H, *s*)	105.8
4	-	181.5	-	182.2
5	-	157.2	-	162.0
6	6.38 (1H, *d*, *J* = 2.0 Hz)	97.8	6.36 (1H, *s*)	98.1
7	-	165.2	-	165.4
8	6.54 (1H, *d*, *J* = 2.0 Hz)	92.6	6.48 (1H, *s*)	92.7
9	-	157.2	-	157.6
10	-	105.2	-	105.7
1′	-	130.6	-	131.2
2′, 6′	7.84-8.01 (2H, *m*)	126.0	7.88 (2H, *d*, *J* = 7.5 Hz)	126.2
3′, 5′	7.44-7.66 (2H, *m*)	129.0	7.51 (2H, *m*)	129.0
4′	7.44-7.66 (1H, *m*)	130.6	7.51 (1H, *m*)	131.7
7-OMe	3.90 (3H, *s*)	55.7	3.86 (3H, *s*)	55.9
5-OH	12.69 (1H, *br s*)	-	12.69 (1H, *br s*)	-

* Lojanapiwatna *et al*., 1981 (in DMSO-d_6)
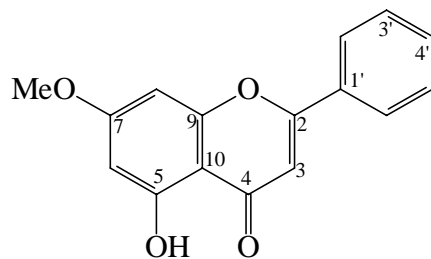
URS-4

1.10 Identification of Compound URS-5

Compound URS-5 was obtained as pale yellow powder, soluble in $CHCl_3$, EtOAc and acetone. The TOF mass spectrum (**Figure 65**) exhibited [M+H]$^+$ ion peak at *m/z* 299, suggesting the molecular formula $C_{17}H_{14}O_5$. The UV spectrum displayed absorption maxima at 276 and 233 nm (**Figure 63**). The IR spectrum was shown in **Figure 64**.

The ^{1}H NMR spectrum (**Figure 66**) exhibited aromatic signals of the unsubstituted B-ring of the flavonoid skeleton at δ 7.93 (2H, *d*, *J* = 5.1 Hz, H-2′ and H-6′) and δ 7.54 (3H, *m*, H-3′, H-4′ and H-5′), as well as an aromatic A-ring signals as a singlet at δ 6.42 (H-6) and H-3 as another singlet at δ 6.66. The signals of two methoxy groups appeared at δ 3.94 (6H, *s*) and the hydrogen-bonded hydroxy proton at position 5 appeared as a broad singlet at δ 12.54.

Seventeen carbon signals were visible in the ^{13}C NMR spectrum (**Figure 67**). DEPT experiment helped in classifying these signals into those of two methoxy group at δ 56.4 and 61.7, seven methine carbons at δ 95.8, 105.3, 126.2 (2C), 129.0 (2C), 131.8, seven quaternary carbons at δ 104.9, 129.0, 131.3, 157.4 (2C), 158.6, 163.7 and one carbonyl carbon at δ 182.5 (**Figure 68**).

Comparison of these spectral data of compound URS-5 with previously reported data (Lojanapiwatna *et al*., 1981) led to the identification of this flavonoid as 7-*O*-methylwogonine.
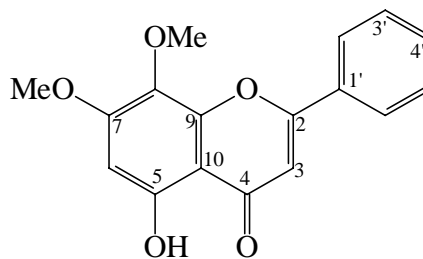
URS-5

Table 48. Comparison of the ^{1}H and ^{13}C NMR spectral data of 7-O-methylwogonine and compound URS-5 (in CDCl$_3$, 300 MHz)

Position	7-O-Methylwogonine *		URS-5	
	^{1}H	^{13}C	^{1}H	^{13}C
2	-	163.2	-	163.7
3	6.58 (1H, s)	105.1	6.66 (1H, s)	105.3
4	-	182.4	-	182.5
5	-	157.4	-	157.4
6	6.35 (1H, s)	95.7	6.42 (1H, s)	95.8
7	-	158.6	-	158.6
8	-	128.9	-	129.0
9	-	157.4	-	157.4
10	-	104.7	-	104.9
1′	-	131.2	-	131.3
2′,6′	7.82-8.0 (2H, m)	126.1	7.93 (2H, d, J = 5.1 Hz)	126.2
3′,5′	7.42-7.60 (2H, m)	128.9	7.54 (2H, m)	129.0
4′	7.42-7.60 (1H, m)	131.7	7.54 (1H, m)	131.8
7-OMe, 8-OMe	3.90 (6H, s)	56.2, 61.6	3.94 (6H, s)	56.4, 61.7
5-OH	12.53 (1H, s)	-	12.69 (1H, s)	-

* Lojanapiwatna *et al*., 1981

1.11 Identification of Compound URS-6

Compound URS-6 was obtained as yellow amorphous powder, soluble in CHCl$_3$, EtOAc and acetone. The TOF mass spectrum (**Figure 71**) exhibited [M+H]$^+$ ion peak at *m/z* 299, suggesting the molecular formula C$_{17}$H$_{14}$O$_5$. The UV spectrum showed absorption maxima at 311, 297, 269 and 229 nm (**Figure 69**). The IR spectrum (**Figure 70**) exhibited absorption bands for hydroxy and conjugated carbonyl functionalities at 2945 and 1665 cm^{-1}, respectively.

The ^{1}H NMR spectrum (**Figure 72**) displayed aromatic signals of unsubstituted B-ring at δ 7.88 (2H, *d*, *J* = 6.6 Hz, H-2′ and H-6′) and δ 7.52 (3H, *m*, H-3′, H-4′ and H-5′), an aromatic A-ring signals at δ 6.67 (1H, *s*, H-8) and H-3 at δ 6.56 (1H, *s*). Two methoxyl signals appeared as singlets at δ 3.96 (3H, *s*) and δ 3.91 (3H, *s*). The most downfield signal was that of the hydrogen-bonded 5-OH at δ 12.66 (1H, *s*).

Seventeen carbon signals could be observed in the ^{13}C NMR spectrum (**Figure 73**), and DEPT experiment was employed to classify these signals into those of two methoxyl carbons at δ 56.4 and 60.9, seven methine carbons at δ 90.6, 105.6, 126.2 (2C), 129.0 (2C) and 131.7, and eight quaternary carbons at δ 106.3, 131.2, 132.7, 152.9, 153.2, 158.7, 163.8 and 182.5 (**Figure 74**).

By comparison of its NMR data with the reported data (Lojanapiwatna *et al*., 1981; Stierle, Stierle and Larsen, 1988), compound URS-6 was identified as 6,7-*O,O*-dimethylbaicalein (6,7-dimethoxy-5-hydroxyflavone).

Table 49. Comparison of the ^{1}H and ^{13}C NMR spectral data of 6,7-*O,O*-dimethylbaicalein and compound URS-6 (in CDCl$_3$, 300 MHz)

Position	6,7-*O,O*-dimethylbaicalein		URS-6	
	[1]H†	[13]C‡	[1]H	[13]C
2	-	163.9	-	163.8
3	6. 55 (1H, *s*)	105.5	6.56 (1H, *s*)	105.6
4	-	182.7	-	182.5
5	-	158.9	-	158.7
6	-	132.7	-	132.7
7	-	153.3	-	153.2
8	6.64 (1H, *s*)	90.6	6.67 (1H, *s*)	90.6
9	-	153.0	-	152.9
10	-	106.2	-	106.3
1′	-	131.2	-	131.2
2′,6′	7.81-7.97 (2H, *m*)	126.2	7.88 (2H, *d*, *J* = 6.6 Hz)	126.2
3′,5′	7.47-7.65 (2H, *m*)	129.0	7.52 (2H, *m*)	129.0
4′	7.47-7.65 (1H, *m*)	131.8	7.52 (1H, *m*)	131.7
OMe	3.94 (3H, *s*)	56.3	3.96 (3H, *s*)	56.4
OMe	3.94 (3H, *s*)	60.8	3.91 (3H, *s*)	60.9
5-OH	12.69 (1H, *s*)	-	12.66 (1H, *s*)	-

† Lojanapiwatna *et al*., 1981 (in CDCl$_3$, 60 MHz)

‡ Stierle *et al*., 1988 (in CDCl$_3$, 62.5 MHz)
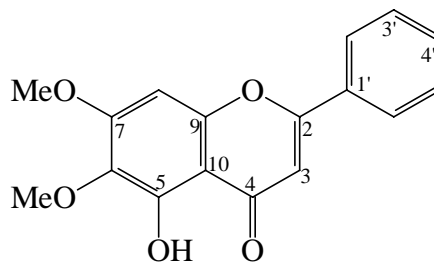
URS-6

1.12 Identification of Compound URS-7

Compound URS-7 was obtained as pale yellow powder, soluble in CHCl$_3$, acetone and MeOH.

The ^{1}H NMR spectrum (**Figure 75**) showed a downfield singlet at δ 11.90 (1H, *s*, 5-OH), and monosubstituted aromatic proton signals at δ 7.66 (2H, *d*, *J* = 6.6 Hz, H-2′ and H-6′) and 7.43 (3H, *m*, H-3′, H-4′ and H-5′), suggesting a 5-hydroxyflavanone with an unsubstituted B-ring. The spectrum also displayed two singlet integrated for two protons at δ 6.09 (H-6 and H-8) and 3.03 (H$_2$-3) and a methoxy singlet at δ 3.81.

The absence of the H-2 doublet of doublets, normally couples with the H$_2$-3 protons in flavanones, in the region of δ 5.20-5.30 suggested the substitution with a hydroxy group at this position, as represented by a hydroxy singlet at δ 3.24 and a doubly oxygenated *sp^3* carbon signal at δ 101.6 (C-2) in the ^{13}C NMR spectrum (**Figure 76**).

The ^{13}C NMR spectrum and DEPT experiment of compound URS-7 displayed sixteen carbon signals, corresponding to one keto carbonyl at δ 193.9, one methoxy carbon at δ 55.8, one methylene carbon at δ 48.4, seven methine carbons at δ 95.2, 95.4, 124.8 (2C), 128.6 (2C) and 129.2, and six quaternary carbons at δ 101.6, 102.6, 141.7, 159.2, 163.7 and 167.7 (**Figures 76** and **77**). These spectral data are in agreement with the previously reported data of an unusual flavanone (Chantrapromma *et al.*, 1989; Fleischer *et al.*, 1997), and, therefore, compound URS-7 was identified as 2,5-dihydroxy-7-methoxyflavanone.

Prior to this study, the compound 2,5-dihydroxy-7-methoxyflavanone has been isolated from *Populus nigra* (Chadenson, Hauteville and Chopin, 1972) of the Salicaceae family and two annonaceous plants: *Uvaria rufa* (Chantrapromma *et al.*, 1989) and

Friesodielsia enghiana (Fleischer *et al.*, 1997). Although flavanones are widespread in nature, the occurrence of the stable hemiacetals with hydroxy substitution at position C-2, as in this compound, is quite rare.
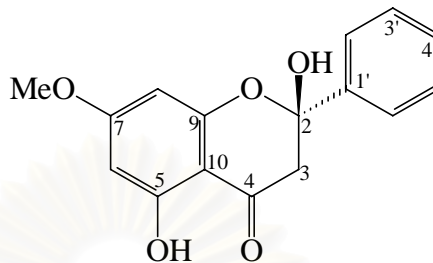
URS-7

Table 50. Comparison of the ^{1}H and ^{13}C NMR spectral data of 2,5-dihydroxy-7-methoxyflavanone and compound URS-7 (in CDCl$_3$, 300 MHz)

Position	2,5-Dihydroxy-7-methoxyflavanone		URS-7	
	^{1}H†	^{13}C‡	^{1}H	^{13}C
2	-	101.9	-	101.6
3$_{eq}$	2.77 (1H, *d*, *J* = 17.0 Hz)	49.2	3.03 (2H, *s*)	48.4
3$_{ax}$	2.56 (1H, *dd*, *J* = 17.0, 2.6 Hz)			
4	-	195.1	-	193.9
5	-	163.5	-	163.7
6	6.13 (1H, *d*, *J* = 2.0 Hz)	94.9	6.09 (1H, *s*)	95.4
7	-	167.6	-	167.7
8	6.19 (1H, *d*, *J* = 2.0 Hz)	94.5	6.09 (1H, *s*)	95.2
9	-	160.1	-	159.2
10	-	101.9	-	102.6
1′	-	142.6	-	141.7
2′, 6′		128.2	7.66 (2H, *d*, *J* = 6.6 Hz)	128.6
3′, 5′		125.4	7.43 (2H, *m*)	124.8
4′		128.6	7.43 (1H, *m*)	129.2
7-OMe	3.13 (1H, *s*)	55.4	3.81 (1H, *s*)	55.8
2-OH	2.84 (1H, *d*, *J* = 2.6 Hz)	-	3.24 (1H, *s*)	-
5-OH	12.56 (1H, *s*)	-	11.90 (1H, *s*)	-

† Fleischer *et al*., 1997 (in C$_6$D$_6$, 400 MHz)

‡ Chantrapromma *et al*., 1989 (in CDCl$_3$ + DMSO-d_6, 20.1 MHz)

1.13 Identification of Compound URS-8

Compound URS-8 was obtained as yellow plates, soluble in MeOH. The TOF mass spectrum (**Figure 80**) exhibited [M]$^{+}$ peak at *m/z* 288, suggesting the molecular formula of $C_{15}H_{11}O_6$. The UV spectrum displayed absorption maxima at 273, 259 and 241 nm (**Figure 78**). The IR spectrum (**Figure 79**) exhibited absorption bands for hydroxy group(s) at 3352 cm^{-1} and conjugated carbonyl functionalities at 1639 cm^{-1}.

The flavanone nucleus was determined from the ^{1}H NMR spectrum (**Figure 81**), in which the signals due to H-2 and H$_2$-3 could be observed as an ABX system at δ 5.38 (1H, *d*, *J* = 11.7 Hz), 2.71 (1H, *d*, *J* = 16.8 Hz) and δ 3.15 (1H, *d*, *J* = 16.8 Hz). In the aromatic region, the *meta*-coupled A-ring protons at positions 6 and 8 appeared as a broad singlet at δ 5.94, whereas the rest of the signals represented the 3′,4′-disubstituted B-ring. The chelated hydroxyl signal at δ 12.16 (1H, *s*, 5-OH) was also presented.

The ^{13}C NMR and DEPT experiments of this compound helped differentiating fifteen carbon signals into those of one carbonyl carbon at δ 196.6, one methylene carbon at δ 43.4, six methine carbon at δ 79.7, 95.5, 96.4, 114.3, 115.6 and 118.8, and seven quaternary at δ 103.3, 131.1, 145.6, 146.0, 163.8, 164.8 and 166.9 (**Figures 82** and **83**). Comparison with literature values (Gao *et al.*, 2005) led to the identification of compound URS-8 as the flavanone eriodictyol.
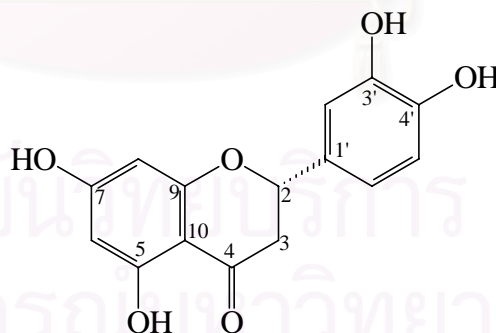
URS-8

Table 51. Comparison of the ^{1}H and ^{13}C NMR spectral data of eriodictyol and compound URS-8 (in acetone-d_6, 300 MHz)

Position	Eriodictyol *		URS-8	
	^{1}H	^{13}C	^{1}H	^{13}C
2	5.40 (1H, *dd*, *J* = 3.0, 12.5 Hz)	80.1	5.38 (1H, *d*, *J* = 11.7 Hz)	79.7
3	3.12 (1H, *dd*, *J* = 12.0, 16.5 Hz)	43.7	3.15 (1H, *d*, *J* = 16.8 Hz)	43.4
	2.68 (1H, *dd*, *J* = 3.0, 16.5 Hz)		2.71 (1H, *d*, *J* = 16.8 Hz)	
4	-	197.4	-	196.6
5	-	165.4	-	164.8
6	5.93 (1H, *br s*)	95.9	5.94 (1H, *br s*)	96.4
7	-	167.4	-	166.9
8	5.94 (1H, *br s*)	96.9	5.94 (1H, *br s*)	95.5
9	-	164.5	-	163.8
10	-	103.3	-	103.3
1′	-	131.7	-	131.1
2′	6.86 (1H, *s*)	114.8	6.86 (1H,*br s*)	114.3
3′	-	146.1	-	145.6
4′	-	146.5	-	146.0
5′	7.02 (1H, *d*, *J* = 7.5 Hz)	119.4	7.02 (1H, *br s*)	118.8
6′	6.86 (1H, *d*, *J* = 7.0 Hz)	116.1	6.86 (1H, *br s*)	115.6
5-OH	-	-	12.16 (1H, *br s*)	-

* Gao *et al*., 2005 (in DMSO-d_6, 500 MHz)

2. Structure Determination of Compounds Isolated from *Mitrephora maingayi*

2.1 Identification of Compound MML-1

Compound MML-1, a colorless oil, exhibited an [M+Na]$^+$ peak at *m/z* 243 in the ESI mass spectrum (**Figure 86**), indicating the molecular formula $C_{15}H_{24}O$ of a sesquiterpene alcohol. The IR spectrum of compound MML-1 (**Figure 85**) showed the absorption peaks of hydroxy function and double bond at 3383 and 1458 cm^{-1}, respectively, while its UV spectrum exhibited absorption maxima at 225 nm (**Figure 84**).

The ^{1}H NMR spectrum (**Figure 87**) exhibited three methyl singlets at δ 1.01, 1.03 and 1.26. The spectrum also showed two exomethylene broad singlets at δ 4.65 (2H, *d, J* = 7.8 Hz, H$_2$-14) and two most upfield signals methine protons of a cyclopropane ring at δ 0.45 (1H, *t, J* = 10.2 Hz, H-6) and 0.69 (1H, *dd, J* = 10.2, 6.9 Hz, H-7).

The ^{13}C-NMR spectrum (**Figure 88**) exhibited 15 carbon peaks classified into those of three methyl (δ 16.3, 26.1 and 27.4), five methylene (δ 24.8, 26.6, 38.8, 41.7 and

106.2), four methine (δ 27.4, 29.9, 53.4 and 54.3), and three quaternary carbons (δ 20.2, 80.9 and 153.4) by the DEPT experiment (**Figure 89**).

Therefore, compound MML-1 was identified as spathulenol, an aromadendrane sesquiterpenoid, by comparison of its spectroscopic data with those previously published (Iwabuchi, Yoshikura and Kamisako, 1989).

Spathulenol is a common sesquiterpene found widely in plants. Examples of annonaceous plants reported as having spathulenol as a constituent are *Xylopia aromatica* (Fournier *et al*., 1994), *Monanthotaxis diclina*, *Unonopsis guatterioides* (Fournier *et al*., 1999) and *Guatteria* sp. (Maia *et al*., 2005).

Spathulenol, isolated from *Xylopia brasiliensis,* was reported to exhibit antifungal activity (Moreira *et al*., 2003).

Table 52. Comparison of the ^{1}H and ^{13}C NMR spectral data of spathulenol and compound MML-1 (in CDCl$_3$, 300 MHz)

Position	Spathulenol *		MML-1	
	^{1}H	^{13}C	^{1}H	^{13}C
1		54.5	2.17 (1H, *m*)	54.3
2a		26.8	1.47 (1H, *m*)	26.6
2b		26.8	1.79 (1H, *m*)	
3a		41.8	1.61 (1H, *m*)	41.7
3b			1.73 (1H, *m*)	
4	-	80.9	-	80.9
5		53.4	1.29 (1H, *m*)	53.4
6	0.47 (1H, *dd*, *J* = 11.5, 9.5 Hz)	30.0	0.45 (1H, *t*, *J* = 10.2 Hz)	29.9
7	0.71 (1H, *ddd*, *J* = 11.4, 9.4, 5.9 Hz)	27.7	0.69 (1H, *dd*, *J* = 10.2, 6.9 Hz)	26.7
8a		24.9	0.94 (1H, *m*)	24.8
8b			2.02 (1H, *m*)	
9a	2.42 (1H, *m*)	39.0	2.10 (1H, *m*)	38.8
9b	2.42 (1H, *m*)		2.40 (1H, *m*)	
10	-	153.5	-	153.4
11	-	20.3	-	20.2
12	1.04 (3H, *s*)	28.7	1.01 (3H, *s*)	27.4
13	1.06 (3H, *s*)	16.4	1.03 (3H, *s*)	16.3
14	4.67, 4.69 (2H, *br s*)	106.3	4.65 (2H, *d*, *J* = 7.8 Hz)	106.2
15	1.28 (3H, *s*)	26.1	1.26 (3H, *s*)	26.1

* Iwabuchi *et al*., 1989 (in CDCl$_3$, 400 MHz)

MML-1
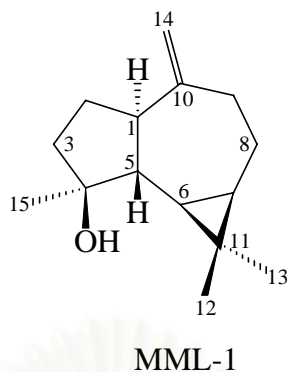
2.2 Identification of Compound MML-2

Compound MML-2 was obtained as colorless needles, soluble in CHCl$_3$ and EtOAc. Its UV spectrum displayed maxima at 221 nm (**Figure 90**). Its IR spectrum (**Figure 91**) showed the absorption bands at 2930 and 1693 cm^{-1}, typical of a carboxylic acid moiety, and also at 1658 cm^{-1} for an exocyclic double bond. The molecular formula of compound MML-2, C$_{20}$H$_{30}$O$_2$, was determined by ESITOF mass spectrometry (**Figure 92**) and corresponded to a diterpenoid structure.

The ^{1}H-NMR spectrum (**Figure 93**) of compound MML-2 displayed signals of the exomethylene H$_2$-17 as two broad singlets at δ 4.72 and 4.77, as well as two tertiary methyl protons at δ 0.93 and 1.22.

The ^{13}C-NMR and DEPT spectrum (**Figures 94** and **95**) presented 20 carbon signals of a kaurane-type diterpene acid, corresponding to two methyl carbons at δ 15.7 and 29.1, ten methylene carbons at δ 18.6, 19.2, 21.9, 33.2, 37.9, 39.8, 40.8, 41.3, 49.0 and 102.9, three methine carbons at δ 43.9, 55.1 and 57.1, four quaternary carbons at δ 39.8, 43.8, 44.3 and 155.7, and one carboxylic carbonyl at δ 184.3.

Based on the spectral data analysis and comparison with published values (Hasan, Healey and Waterman, 1982; Lu *et al*., 1995), compound MML-2 was identified as the kaurane-type diterpenoid *ent*-kaur-16-en-19-oic acid, trivially named kaurenoic acid.

Kaurenoic acid has been isolated from a number of different plants, some of which belonging to the family Annonaceae. Several bioactivities of this compound were reported. The diterpenoid, obtained from the hexane extract of *Montanoa tomentosa* leaves, was shown to have antispasmodic activity, through the *in vitro* inhibition of the rat uterine contraction (Lozoya *et al*., 1983), whereas this compound, isolated from another source

(*Viguiera robusta*), inhibited the *in vitro* contractility of rat carotid artery elicited by phenylephrine at the concentration of 20.0 µg/ml (Tirapelli *et al.*, 2002).

Kaurenoic acid, isolated from *Croton oblongifolius,* was identified as an inhibitor of the enzyme Na^+, K^+-ATPase which is essential in the active transport of sodium and potassium ions across the cell membrane (Ngamrojnavanich *et al*., 2003). Activity-guided fractionation of the stem bark of *Annona senegalensis* reported kaurenoic acid to be selectively cytotoxic against MCF-7 breast cancer cells (Fatope and Audu, 1998). This compound was also reported to exhibit *in vitro* trypanocidal activity against *Trypanosoma cruzi* (de Costa, Albuquerque and Vichnewski, 1996).

Table 53. Comparison of the ^{13}C NMR spectral data of kaurenoic acid and compound MML-2 (in $CDCl_3$, 75 MHz)

Position	Kaurenoic acid *	MML-2
1	41.3	41.3
2	19.1	19.2
3	39.7	39.8
4	43.7	43.8
5	55.1	55.1
6	21.8	21.9
7	40.7	40.8
8	44.2	44.3
9	57.1	57.1
10	39.7	39.8
11	18.4	18.6
12	33.1	33.2
13	43.9	43.9
14	37.8	37.9
15	49.0	49.0
16	155.9	155.7
17	103.0	102.9
18	29.0	29.1
19	183.8	184.3
20	15.6	15.7

* Lu *et al*., 1995 (in $CDCl_3$, 100 MHz)
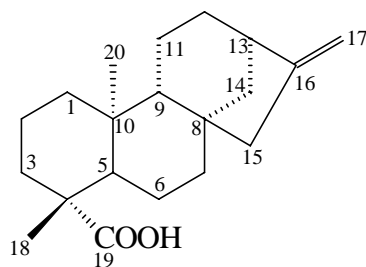
MML-2

2.3 Identification of Compound MML-3

Compound MML-3 was obtained as colorless needles, having the molecular formula $C_{22}H_{26}O_6$, as determined from the $[M+H]^+$ peak at *m/z* 387 (**Figure 98**). The UV absorption maxima (**Figure 96**) at 278, 252 and 229 nm and the IR bands at 1518 and 1469 cm^{-1} (**Figure 97**) indicated the presence of aromatic ring(s) in the molecule.

The ^{1}H NMR spectrum (**Figures 99a** and **99b**) exhibited two different proton systems of the bicyclic lignan skeleton: the aliphatic bicyclic and the two aromatic rings. Each group displayed COSY correlations within its own system. The first system consists of a methine proton appearing at δ 4.43 (*d, J* = 7.2 Hz, H-2) and methylene protons at δ 3.83 (1H, m, H-8α) and 4.12 (1H, *dd, J* = 9.5, 0.9 Hz, H-8β), both coupled to the methine signal at δ 2.90 (*ddd, J* = 15.3, 7.2, 1.1 Hz, H-1). The latter signal also coupled to another methine multiplet at δ 3.32, which in turn coupled to two multiplets of the H-4 methylene at δ 3.83 and 3.30, and a methine signal at δ 4.85 (*d, J* = 5.5 Hz). Aromatic proton signals of two symmetric 1,3,4-trisubstituted benzene rings resonated at δ 6.81-6.92 (6H, *m*, H-2′, H-5′, H-6′, H-2″, H-5″ and H-6″), and four methoxy singlets at δ 3.85, 3.86, 3.88 and 3.89. These are indicative of a lignan with 2,6-diaryl-3,7-dioxabicyclo-[3,3,0]-octane structure.

The ^{13}C-NMR spectrum (**Figure 100**) presented 22 carbon signals corresponding to four methoxy carbons at δ 55.9, two methylene carbons at δ 69.7 and 71.0, four aliphatic methine carbons at δ 50.1, 54.4, 82.0 and 87.6, six aromatic methine carbons at δ 108.9, 109.1, 111.0 (2C), 117.7 and 118.4, and six quaternary carbons at δ 130.9, 133.6, 148.0, 148.7, 148.8 and 149.2. Based on the analysis of these spectroscopic data and comparison with reported values (Pelter and Ward, 1976; Ahmed *et al*., 2002), compound MML-3 was identified as a bicyclic lignan, namely, (+)-epieudesmin.

(+)-Epieudesmin obtained from the heartwood of *Gmelina arborea* displayed antifungal activity against *Trametes versicolor* and *Fomitopsis palustris* (Kawamura**,** Ohara and Nishida**,** 2004), whereas the same compound, isolated from *Hernandia peltata* and *H. nymphaeifolia*, showed antineoplastic activity against murine P388 lymphocytic leukemia cell line and several human cancer cell lines (Pettit *et al*., 2004).

Table 54. Comparison of the ^{1}H and ^{13}C NMR spectral data of (+)-epieudesmin and compound MML-3 (in CDCl$_3$, 500 MHz)

Position	(+)-Epieudesmin		MML-3	
	[1]H†	**[13]C†**	**[1]H**	**[13]C**
1	2.93 (1H, *m*)	54.4	2.90 (1H, *ddd*, *J* = 15.3, 7.2, 1.1 Hz)	54.4
2	4.46 (1H, *d*, *J* = 7.0 Hz)	87.5	4.43 (1H, *d*, *J* = 7.2 Hz)	87.6
4	3.86 (1H, *m*)	69.6	3.83 (1H, *m*)	69.7
	3.33 (1H, *m*)		3.30 (1H, *m*)	
5	3.36 (1H, *m*)	50.1	3.32 (1H, *m*)	50.1
6	4.89 (1H, *d*, *J* = 5.6 Hz)	82.0	4.85 (1H, *d*, *J* = 5.5 Hz)	82.0
8	3.86 (1H, *m*)	70.9	3.83 (1H, *m*)	71.0
	4.14 (1H, *dd*, *J* = 9.5, 0.9 Hz)		4.12 (1H, *dd*, *J* = 9.5, 0.9 Hz)	
1′	-	133.5	-	133.6
2′	6.85-6.98 (1H, *m*)	109.0	6.81-6.92 (1H, *m*)	109.1
3′	-	148.5	-	149.2
4′	-	149.0	-	148.7
5′	6.85-6.98 (1H, *m*)	110.9	6.81-6.92 (1H, *m*)	111.0
6′	6.85-6.98 (1H, *m*)	118.3	6.81-6.92 (1H, *m*)	117.7
1″	-	130.8	-	130.9
2″	6.85-6.98 (1H, *m*)	108.9	6.81-6.92 (1H, *m*)	108.9
3″	-	147.8	-	148.8
4″	-	148.7	-	148.0
5″	6.85-6.98 (1H, *m*)	110.9	6.81-6.92 (1H, *m*)	111.0
6″	6.85-6.98 (1H, *m*)	117.6	6.81-6.92 (1H, *m*)	118.4
4 x OMe	3.89-3.92 (12H, *s*)	55.8	3.89 (3H, *s*), 3.88 (3H, *s*), 3.86 (3H, *s*), 3.85 (3H, *s*)	55.9

† Ahmed *et al*., 2002 (in CDCl$_3$, 500 MHz)

‡ Pelter and Ward, 1976 (in CDCl$_3$, 65 MHz)

MML-3
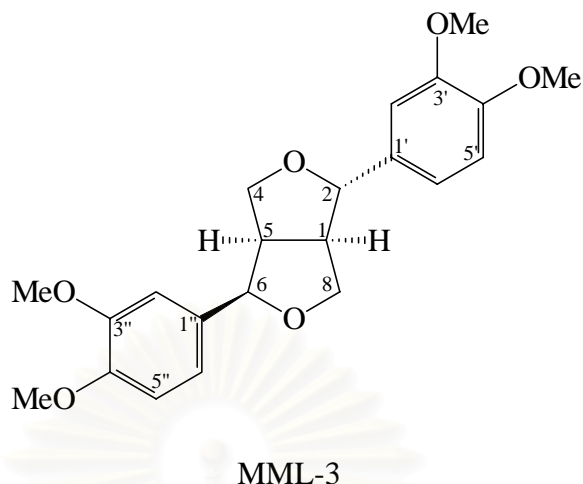
2.4 Identification of Compound MML-4

Compound MML-4 was obtained as colorless needles. Its molecular formula, $C_{22}H_{26}O_6$ was determined from the $[M+H]^+$ peak at m/z 387 (**Figure 102**). The IR bands at 1501 and 1459 cm^{-1} (**Figure 101**) indicated the presence of aromatic ring(s) in the molecule. The presence of only eleven carbon signals in its ^{13}C NMR spectrum suggests that the molecule is composed of two symmetrical portions.

The ^1H NMR spectrum (**Figure 103**) exhibited one methylene signal at δ 4.24 (4H, *dd*, $J = 8.4$, 6.3 Hz, H$_2$-4 and H$_2$-8), two methine signals at δ 4.74 (2H, *d*, $J = 3.6$ Hz, H-2 and H-6) and 3.10 (2H, *br s*, H-1 and H-5). These signals represent the bicyclic substructure at the center of the lignan molecule. Three aromatic proton signals at δ 6.89 (2H, *s*), 6.84 (2H, *d, J* = 4.2 Hz) and 6.82 (2H, *d, J* = 8.1 Hz), and two methoxy signals at δ 3.88 (6H, *s*) and 3.85 (6H, *s*), represent two symmetrical 1,3,4-trisubstituted aromatic rings.

Eleven carbon signals (**Figure 104**)could be classified into those of four methoxy carbons at δ 56.0, two methylene carbons at δ 71.7, ten methine carbons at δ 54.2 (2C), 85.8 (2C), 109.2 (2C), 111.0 (2C) and 118.1 (2C), and six quaternary carbons at δ 133.4 (2C), 148.5 (2C) and 149.1 (2C). Comparison with reported values (Pelter and Ward, 1976; Suginome *et al*., 1995) helped identify compound MML-4 as (±)-eudesmin. This bicyclic lignan was shown to inhibit the production of tumor necrosis factor-alpha and T-cell proliferation (Cho *et al*., 1999).

Table 55. Comparison of the ^{1}H and ^{13}C NMR spectral data of (±)-eudesmin and compound MML-4 (in CDCl$_3$, 300 MHz)

Position	(±)-Eudesmin			MML-4	
	^{1}H†	^{13}C‡		^{1}H	^{13}C
1	3.12 (1H, *ddd*, *J* = 7.3, 4.4, 3.9 Hz)	54.3		3.10 (1H, *br s*)	54.2
2	4.76 (1H, *d*, *J* = 4.4 Hz)	85.8		4.74 (1H, *d*, *J* = 3.6 Hz)	85.8
4	4.26 (2H, *dd*, *J* = 9.5, 7.3 Hz)	71.7		4.24 (2H, *dd*, *J* = 8.4, 6.3 Hz)	71.7
5	3.12 (1H, *ddd*, *J* = 7.3, 4.4, 3.9 Hz)	54.3		3.10 (1H, *br s*)	54.2
6	4.76 (1H, *d*, *J* = 4.4 Hz)	85.8		4.74 (1H, *d*, *J* = 3.6 Hz)	85.8
8	4.26 (2H, *dd*, *J* = 9.5, 7.3 Hz)	71.7		4.24 (1H, *dd*, *J* = 8.4, 6.3 Hz)	71.7
1′,1″	-	134.0		-	133.4
2′, 2″	6.91 (2H, *d*, *J* = 2.0 Hz)	109.7		6.89 (2H, *s*)	109.2
3′, 3″	-	148.9		-	148.5
4′, 4″	-	149.5		-	149.1
5′, 5″	6.84 (2H, *d*, *J* = 8.3 Hz)	111.4		6.82 (2H, *d*, *J* = 8.1 Hz)	111.0
6′, 6″	6.88 (1H, *dd*, *J* = 8.3, 2.0 Hz)	118.4		6.84 (2H, *d*, *J* = 8.1 Hz)	118.1
2 x OMe	3.90 (6H, *s*)	55.9		3.88 (6H, *s*)	56.0
2 x OMe	3.88 (6H, *s*)	55.6		3.85 (6H, *s*)	56.0

† Suginome *et al.*, 1995 (in CDCl$_3$, 270 MHz)

‡ Pelter and Ward, 1976 (in CDCl$_3$, 65 MHz)
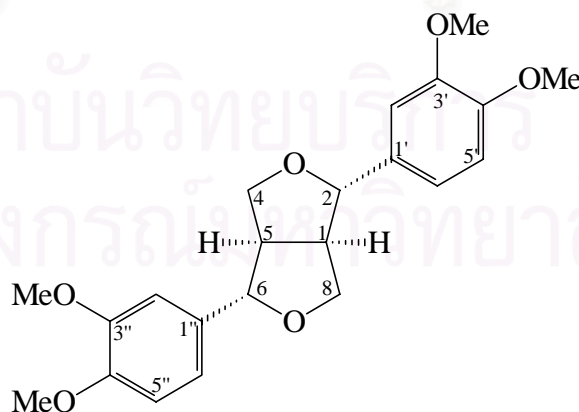
MML-4

2.5 Identification of Compound MML-5

Compound MML-5 was obtained as colorless rod-shaped crystals, soluble in CHCl$_3$ and EtOAc. The UV absorption maxima at 277, 253, 244 and 229 nm (**Figure 105**) and IR absorptions at 3522 and 1668 cm^{-1} (**Figure 106**) suggested the presence of hydroxy group and carbonyl group conjugated with an aromatic ring in the furanoid lignan skeleton (Banerji *et al*., 1984). The CI mass spectrum exhibited a [M+H]$^+$ peak at *m/z* 403.

The ^{1}H NMR spectrum of compound MML-5 (**Figure 25**) displayed four methoxy groups at δ 3.86, 3.90, 3.93 and 3.95 (each 3H, *s*), two nonequivalent methylene protons at δ 3.67 (1H, *dd*, *J* = 10.7, 5.5 Hz, Ha-3a), 3.77 (1H, *dd*, *J* = 10.7, 4.3 Hz, Hb-3a), and six aromatic protons as two ABX systems, one at δ 7.02 (1H, *d*, *J* = 2.1 Hz, H-2′), 6.82 (1H, *d*, *J* = 8.4 Hz, H-5′), 6.93 (1H, *dd*, *J* = 8.4, 2.1 Hz, H-6′) and the other at δ 7.56 (1H, *d*, *J* = 1.8 Hz, H-2″), 6.91 (1H, *d*, *J* = 8.2 Hz, H-5″), 7.59 (1H, *dd*, *J* = 8.2, 1.8 Hz, H-6″), indicating the presence of two 1,3,4-trisubstituted benzene rings. The spectrum also showed the signals of the methylene protons at position 5 of the central furanoid ring at δ 4.30 (1H, *t*, *J* = 11.3 Hz) and 4.16 (1H, *m*), and the remaining three methine proton at δ 4.68 (1H, *d*, *J* = 9.2 Hz, H-2), 4.18 (1H, *m*, H-4) and 2.91 (1H, *m*, H-3).

The ^{13}C NMR and DEPT spectra (**Figures 26** and **27**) suggested that the molecular structure of this lignan consisted of 22 carbons: four methoxy (δ 55.9, 55.9, 56.0, 56.1), two methylene (δ 61.5, 70.9), nine methine (δ 49.7, 52.2, 83.8, 109.6, 110.1, 110.6, 110.9, 119.3, 123.2), and six quaternary carbons (δ 129.8, 133.0, 149.0, 149.3, 149.3, 153.7), as well as one carbonyl signal at δ 197.9.

From these data, the structure of compound MML-5 could be proposed as a 2,3,4-trisubstituted tetrahydrofuran-type lignan having two veratryl moieties. The carbonyl group could be located at C-4a, according to the HMBC correlations between the proton signals of H-4, H-5, H-2″ and H-6″ to the carbonyl signal at δ 197.9. Moreover, the signals of H-3, H-3a, H-4, H-5, H-2′ and H-6′ were correlated to the signal of C-2 at δ 83.8. The structure of compound MML-5 could therefore be assigned as tetrahydro-2-(3,4-dimethoxyphenyl)-4-(3,4-dimethoxybenzoyl)-3-hydroxymethylfuran. The *trans* orientation of substituents at C-2 and C-3 was assigned according to the chemical shift of H-2 at about 4.6-4.7 (Jung *et al*., 1998). The NOESY correlations between H-2 and H-3a, and H-3 and H-4, but none between H-2 and H-3, led to the assignment of *trans* and *cis* orientations for H-

2/H-3 and H-3/H-4, respectively.

Therefore, compound MML-5 was identified as magnone A, previously isolated from the flower buds of *Magnolia fargesii* (Jung *et al*., 1998). The lignan was shown to have antagonistic activity against platelet-activating factor (PAF) in the PAF receptor binding assay.

Table 56. Comparison of the ^{1}H and ^{13}C NMR spectral data of magnone A and compound
MML-5 (in CDCl$_3$, 500 MHz)

Position	Magnone A *			MML-5	
	^{1}H	^{13}C		^{1}H	^{13}C
2	4.63 (1H, *d*, *J* = 9.1 Hz)	83.8		4.68 (1H, *d*, *J* = 9.2 Hz)	83.8
3	2.85 (1H, *m*)	52.1		2.91 (1H, *m*)	52.2
3a	3.63 (1H, *dd*, *J* = 10.9, 5.6 Hz)	61.4		3.67 (1H, *dd*, *J* = 10.7, 5.5 Hz)	61.5
	3.72 (1H, *dd*, *J* = 10.7, 4.4 Hz)			3.77 (1H, *dd*, *J* = 10.7, 4.3 Hz)	
4	4.13 (1H, *m*)	49.7		4.18 (1H, *m*)	49.7
4a	-	198.0		-	197.9
5	4.13 (1H, *m*)	70.8		4.16 (1H, *m*)	70.9
	4.25 (1H, *dd*, *J* = 11.2, 10.7 Hz)			4.30 (1H, *t*, *J* = 11.3 Hz)	
1′	-	132.9		-	133.0
2′	6.96 (1H, *d*, *J* = 1.9 Hz)	109.5		7.02 (1H, *d*, *J* = 2.1 Hz)	109.6
3′	-	148.9		-	149.0
4′	-	149.2		-	149.3
5′	6.76 (1H, *d*, *J* = 8.3 Hz)	110.8		6.82 (1H, *d*, *J* = 8.4 Hz)	110.9
6′	6.88 (1H, *dd*, *J* = 8.3, 1.9 Hz)	119.3		6.93 (1H, *dd*, *J* = 8.4, 2.1 Hz)	119.3
1″	-	129.7		-	129.8
2″	7.51 (1H, *d*, *J* = 2.0 Hz)	110.6		7.56 (1H, *d*, *J* = 1.8 Hz)	110.6
3″	-	149.2		-	149.3
4″	-	153.6		-	153.7
5″	6.86 (1H, *d*, *J* = 8.3 Hz)	110.1		6.91 (1H, *d*, *J* = 8.2 Hz)	110.1
6″	7.54 (1H, *dd*, *J* = 8.3, 2.0 Hz)	123.2		7.59 (1H, *dd*, *J* = 8.2, 1.8 Hz)	123.2
OMe	3.81 (3H, *s*)	55.9		3.86 (3H, *s*)	55.9
	3.85 (3H, *s*)	56.0		3.90 (3H, *s*)	56.0
	3.88 (3H, *s*)	56.1		3.93 (3H, *s*)	56.1
	3.89 (3H, *s*)			3.95 (3H, *s*)	

* Jung *et al*., 1998 (in CDCl$_3$, 400 MHz)
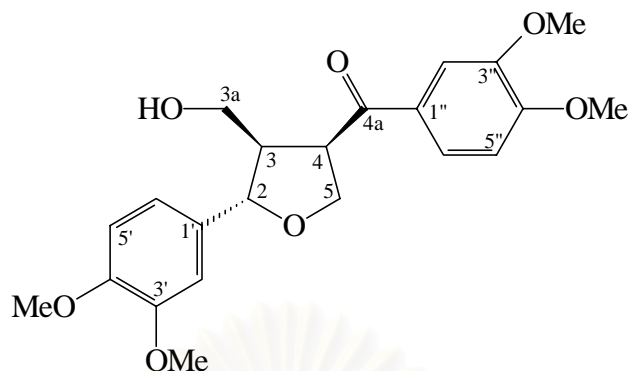
MML-5

2.6 Identification of Compound MML-6

Compound MML-6 was obtained as white powder, soluble in CHCl₃ and EtOAc. The ^{1}H-NMR spectrum (**Figure 110**) of compound MML-6 was very similar to that of kaurenoic acid (compound MML-2), suggesting its nature as kaurane-type diterpenoid. The spectrum displayed signals of two tertiary methyl singlets at δ 0.97 and 1.14, the exomethylene protons as two broad singlets at δ 4.77 and 4.72, and an extra hydroxymethine proton at δ 3.52 (1H, *m*), indicating the presence of a secondary hydroxy group within the molecule.

The ^{13}C-NMR and DEPT spectra (**Figure 111** and **Figure 112**) presented 20 carbon signals, corresponding to two methyl groups at δ 15.7 and 28.8, nine methylenes at δ 18.1, 19.2, 29.1, 33.6, 38.8, 39.4, 40.5, 45.4, and 103.6, four methines at δ 43.8, 49.2, 47.3 and 77.1, four non-protonated carbons at δ 37.9, 43.3, 48.3 and 154.6, and one carbonyl at δ 182.4. These signals are also similar to those of kaurenoic acid, except for the lack of one methylene carbon and the presence of an extra methine carbon at δ 77.1.

Comparison of the ^{1}H and ^{13}C NMR spectra of this terpenoid with those of kaurenoic acid indicated the presence of one hydroxy group at C-7. This was confirmed by the downfield shift of C-6 and C-7 carbon signals, whereas those of C-5 and C-9 were shifted upfield by about 6-9 ppm. The H-7 methine proton appeared at δ 3.52 as a singlet-like multiplet with $W_{1/2}$ of about 6 Hz, in agreement with the presence of an axial hydroxyl in a rigid cyclohexane system (Mitra *et al.*, 1980). Therefore, compound MML-6 was identified as 7β-hydroxy-*ent*-kaurene-19-oic acid, trivially named didymooblongin. This diterpenoid

has been shown to be an intermediate in the metabolic transformation of (-)-*ent*-16-kaurene to gibberellin GA_3. Its occurrence in plant species was reported for the first time from *Didymocarpus oblonga* (Mitra *et al.*, 1980), a plant in the family Gesneriaceae. Later, it has been reported as a constituent of two annonaceous plants, *Xylopia aetiopica* (Hasan, Healey and Waterman, 1982a) and *X. acutiflora* (Hasan, Healey and Waterman, 1982b), and *Solidago missouriensis* of the family Compositae (Le Quesne *et al.*, 1985).

Table 57. Comparison of the ^{1}H and ^{13}C NMR spectral data of didymooblongin and compound MML-6 (in acetone-d_6, 500 MHz)

Position	Didymooblongin		MML-6	
	^{1}H†	^{13}C‡	^{1}H	^{13}C
1		40.9		40.5
2		19.7		19.2
3		38.5		37.9
4		43.7		43.3
5		49.5		49.2
6		30.4		29.1
7	3.55 (1H, *t*, *J* = 6.0 Hz)	76.2	3.52 (1H, *m*, $W_{1/2}$ = 6.0 Hz)	77.1
8		48.9		48.3
9		47.4		47.3
10		39.5		39.4
11		18.5		18.1
12		34.0		33.6
13	2.60 (1H, *m*)	44.3	2.62 (1H, *m*)	43.8
14		39.1		38.8
15		46.6	2.31 (1H, *m*)	45.4
16		156.2		154.6
17	4.75 (2H, *br s*)	103.6	4.77 (1H, *br s*), 4.72 (1H, *br s*)	103.6
18	1.15 (3H, *s*)	28.6	1.14 (3H, *s*)	28.8
19		178.2	-	182.4
20	1.00 (3H, *s*)	15.7	0.97 (3H, *s*)	15.7

† Hasan *et al*., 1987 (in acetone-d_6, 90 MHz)

‡ Hutchison, Lewer and MacMillan, 1984 (in pyridine-d_5)
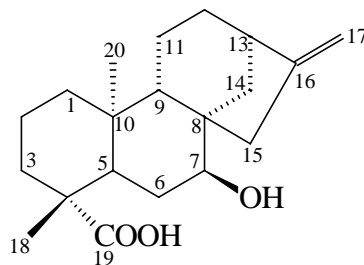
MML-6

2.7 Identification of Compound MMS-1

Compound MMS-1 was obtained as colorless needles, soluble in CHCl₃ and EtOAc. The ^{1}H-NMR spectrum (**Figures 113a** and **113b**) of compound MMS-1 displayed signals of three tertiary methyl groups at δ 0.75 (3H, *s*), 0.97 (3H, *s*) and 1.18 (3H, *s*), the vinyl protons at δ 5.70 (1H, *dd*, *J* = 17.2, 10.4 Hz, H-15), 4.89 (1H, *dd*, *J* = 17.2, 2.0 Hz, H-16a) and 4.93 (1H, *dd*, *J* = 10.4, 2.0 Hz, H-16b), as well as one methine proton at δ 5.12 (1H, *d*, *J* = 1.4 Hz, H-14).

The ^{13}C-NMR and DEPT spectra (**Figures 114** and **115**) presented 20 carbon signals of a pimarane-type diterpene acid, corresponding to three methyls at δ 15.1, 16.9 and 29.5, eight methylenes at δ 18.2, 19.1, 24.9, 35.4, 35.7, 37.1, 38.2 and 112.7, four methines at δ 48.8, 51.5, 128.2 and 147.1, four quaternary carbons at δ 37.8, 38.7, 47.3 and 137.8, and one carbonyl at δ 185.1. Assignments of the ^{13}C-NMR data were made by comparison with those of related diterpenes in the pimarane series.

The ^{1}H-^{13}C HMBC experiment (500 MHz, in CDCl₃) (**Figures 116a** - **116d**) was performed in order to confirm the position of the substituents. Correlations could be observed between the signals of 17-methyl protons at δ 0.92 and C-12 (δ 35.7), C-13 (δ 38.7), C-14 (δ 128.2) and C-15 (δ 147.1). The H-15 methine proton at δ 5.65 showed correlations to C-12, C-13, C-14, C-16 (δ 112.7) and C-17 (δ 29.5), whereas the H-14 methine proton at δ 5.08 exhibited correlations to the signals of C-7 (δ 35.4), C-9 (δ 51.5), C-12, C-13, C-14, C-16 and C-17. The methyl signal at δ 0.75 displayed correlations to C-1 (δ 38.2), C-5 (δ 48.8) and C-9, confirming its position to be at C-20, whereas another methyl signal at δ 1.14 was assigned to position 19 due to its two- and three-bond correlations to C-3 (δ 37.1), C-4 (δ 47.3) and C-5.

The spectral data of compound MMS-1 were then compared with literature (Darling and Turro, 1998) and the diterpene was identified as 8(14),15-pimaradien-18-oic acid, trivially named pimaric acid.

Pimaric acid was commonly found as a constituent of several species in the family Pinaceae. The compound, isolated from *Pinus oocarpa*, was tested *in vitro* against epimastigotes of *Trypanosoma cruzi*, the causative agent of Chagas disease, and found to be as active as nifurtimox, a drug effective in the treatment of acute trypanosomiasis (Rubioa *et al*., 2005).

Table 58. Comparison of the ^{1}H and ^{13}C NMR spectral data of pimaric acid and compound MMS-1 (in CDCl$_3$, 500 MHz)

Position	Pimaric acid		MMS-1	
	[1]H†	[13]C‡	[1]H	[13]C
1		38.6		38.2
2		18.5		18.2
3		37.5		37.1
4		47.6		47.3
5		49.1	1.91 (1H, *dd*, *J* = 12.3, 2.4 Hz)	48.8
6		25.5		24.9
7		35.8		35.4
8		138.5		137.8
9		51.9		51.5
10		38.1		37.8
11		19.5		19.1
12		36.0		35.7
13		39.0		38.7
14	5.15 (1H, *s*)	128.2	5.12 (1H, *d*, *J* = 1.4 Hz)	128.2
15		147.8	5.70 (1H, *dd*, *J* = 17.2, 10.4 Hz)	147.1
16		113.2	4.89 (1H, *dd*, *J* = 17.2, 2.0 Hz) 4.93 (1H, *dd*, *J* = 10.4, 2.0 Hz)	112.7
17	1.00 (3H, *s*)	29.9	0.97 (3H, *s*)	29.5
18		185.7	-	185.1
19	1.21 (3H, *s*)	17.6	1.18 (3H, *s*)	16.9
20	0.79 (3H, *s*)	15.4	0.75 (3H, *s*)	15.1

† Wenkert *et al*., 1965 (60 MHz, in CDCl$_3$)

‡ Darling and Turro, 1998 (15 MHz, in CDCl$_3$)
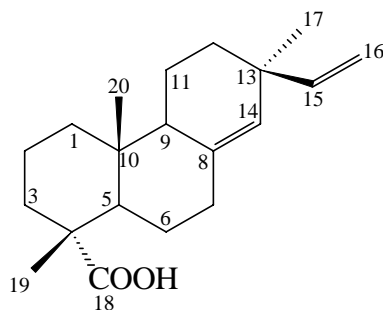
MMS-1

2.8 Identification of Compound MMS-2

Compound MMS-2, which gave yellow fluorescence under UV light at 366 nm, was obtained as yellow needles. Its UV spectrum (**Figure 117**) showed characteristics of a phenanthrene chromophore at λ_{max} 410, 340, 306, 293 and 275 nm. The molecular formula was determined as $C_{17}H_9NO_3$ by mass spectrometry (**Figure 119**), observing [M+H]$^+$ at *m/z* 276. The compound was positive to Dragendorff's spray reagent, confirming its nature as an alkaloid. The IR spectrum (**Figure 118**) revealed the presence of a conjugated carbonyl band at 1653 cm^{-1}.

The ^{1}H NMR spectrum (**Figure 120**) showed the presence of one methylenedioxy signal at δ 6.35 (2H, *s*) and seven aromatic protons at δ 7.17 (1H, *s*, H-3), 7.58 (1H, *t*, *J* = 7.8 Hz, H-9), 7.70 (1H, *m*, H-10), 7.75 (1H, *d*, *J* = 5.1 Hz, H-4), 8.56 (1H, *d*, *J* = 7.8 Hz, H-8), 8.62 (1H, *d*, *J* = 8.1 Hz, H-11) and 8.86 (1H, *d*, *J* = 5.1 Hz, H-5). The doublets at δ 7.75 and 8.86 were assigned to H-4 and H-5 of ring B, respectively, according to their pyridine ring coupling constant of about 5-6 Hz, while the other four proton signals at δ 7.58, 7.70, 8.56 and 8.62 were assigned to aromatic protons on ring D based on their multiplicities. The singlet proton at δ 7.17 was assigned to H-3, and the methylenedioxy group was assigned to C-1 and C-2.

Compound MMS-2 was identified as liriodenine by comparison of its spectral data to those of the same alkaloid reported from *Fissistigma glaucescens* (Wu *et al.,* 1987).
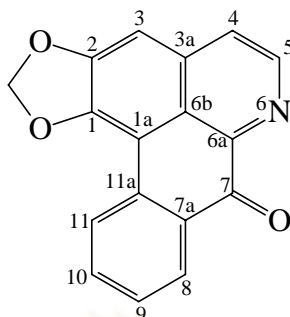
MMS-2

Liriodenine is a common oxoaporphine alkaloid. It has been isolated from many plant families including the Annonaceae, Araceae, Lauraceae, Magnoliaceae, Menispermaceae, Monimiaceae, Papaveraceae, Rhamnaceae and Ranunculaceae (Shamma and Guinaudeau, 1985; 1986). It was also known as spermatheridine when this aporphine alkaloid was isolated from Tasmanian sassafras (Bick and Douglas, 1966).

Liriodenine, isolated from *Thalictrum sessile* (Wu *et al*., 1988) and *Annona montana* (Wu *et al*., 1993) exhibited cytotoxicity against the KB, A-549, HCT-8, P-388, and L-1210 mammalian cell lines with ED_{50} values of 1.00, 0.72, 0.70, 0.57, and 2.33 µg/ml, respectively. The alkaloid was also demonstrated to inhibit adenosine 5´-diphosphate- and collagen-induced platelet aggregation, but showed weak inhibition of arachidonic acid-induced platelet aggregation (Chen *et al*., 1996; 1997).

Liriodenine also displayed antimicrobial activities against Gram-positive bacteria, acid-fast bacteria, and several fungi such as *Trichophyton mentagrophytes* and *Syncephalestrum racemosum*, as well as against various pathogenic plant microorganisms (Hufford *et al*., 1975; 1980).

Liriodenine demonstrated *in vitro* antiviral activity against *herpes simplex* virus type 1 (HSV-1) with an IC_{50} of 48.0 µM, while the effective concentration required to inhibit the cytopathic effect by 50% (ED_{50}) was 7.0 µM (Montanha *et al*., 1995).

Recently, liriodenine, isolated from the aerial part of *Pseuduvaria setosa* was shown to possess antituberculosis activity against *Mycobacterium tuberculosis* at minimum inhibitory concentration (MIC) of 12.5 µg/ml, and antimalarial activity against *Plasmodium falciparum* with the 50% inhibitory concentration (IC_{50}) of 2.8 µg/ml.

Moreover, this alkaloid was strongly cytotoxic to both epidermoid carcinoma (KB) and breast cancer (BC) cell lines (Wirasathien *et al*., 2006).

Table 59. Comparison of the ^{1}H spectral data of liriodenine and compound MMS-2 (in CDCl$_3$, 300 MHz)

Position	Liriodenine*	MMS-2
3	7.16 (1H, *s*)	7.17 (1H, *s*)
4	7.74 (1H, *d*, *J* = 5.19 Hz)	7.75 (1H, *d*, *J* = 5.1 Hz)
5	8.87 (1H, *d*, *J* = 5.19 Hz)	8.86 (1H, *d*, *J* = 5.1 Hz)
8	8.57 (1H, *dd*, *J* = 7.93, 1.22 Hz)	8.56 (1H, *d*, *J* = 7.8 Hz)
9	7.57 (1H, *dt*, *J* = 7.93, 1.22 Hz)	7.58 (1H, *t*, *J* = 7.8 Hz)
10	7.72 (1H, *dt*, *J* = 7.94, 1.22 Hz)	7.70 (1H, *m*)
11	8.60 (1H, *d*, *J* = 7.94 Hz)	8.62 (1H, *d*, *J* = 8.1 Hz)
-OCH$_2$O-	6.36 (2H, *s*)	6.35 (2H, *s*)

* Wu *et al*., 1987

2.9 Identification of Compound MMS-3

Compound MMS-3 was obtained as yellow powder. Its UV spectrum (**Figure 121**) showed characteristics of a phenanthrene chromophore at λ$_{max}$ 420, 323 and 221 nm. The molecular formula was determined as C$_{18}$H$_{11}$NO$_4$ by EISTOF mass spectrometry (**Figure 123**), observing [M+H]$^+$ at *m/z* 306. The IR spectrum (**Figure 122**) of this compound revealed the presence of a carbonyl group as an absorption band at 1737 cm^{-1}. The compound was positive to Dragendorff's spray reagent and gave orange fluorescence under UV light at 366 nm.

The ^{1}H-NMR spectrum (**Figure 124**) of compound MMS-3 was rather similar to that of liriodenine (compound MMS-2), except for one methoxy proton signal at δ 4.03 (3H, *s*) and different coupling pattern for the aromatic protons on ring D. The rest of the proton signals were those of one methylenedioxy signal at δ 6.32 (2H, *s*) and six aromatic protons at δ 7.07 (1H, *d*, *J* = 8.4 Hz, H-9), 7.14 (1H, *s*, H-3), 7.62 (1H, *t*, *J* = 8.1 Hz, H-10), 7.67 (1H, *d*, *J* = 4.7 Hz, H-4), 8.27 (1H, *d*, *J* = 7.8 Hz, H-11) and 8.81 (1H, *d*, *J* = 4.8 Hz, H-5).

Through comparison with previously reported spectral data of other oxoaporphines, compound MMS-3 was identified as the aporphine alkaloid oxostephanine (Watanabe *et al*., 1975). Oxostephanine has been reported as a constituent of various

annonaceous species, and also from *Stephania japonica* (Menispermaceae) (Watanabe *et al.*, 1975). This compound showed potent anti-herpes activity (Montanha *et al.*, 1995), antituberculosis activity against *Mycobacterium tuberculosis* and significant cytotoxicity to both epidermoid carcinoma (KB) and breast cancer (BC) cell lines (Wirasathien *et al.*, 2006).

Table 60. Comparison of the ^{1}H NMR spectral data of oxostephanine and compound MMS-3 (in CDCl$_3$, 300 MHz)

Position	Oxostephanine*	MMS-3
3	7.60 (1H, *s*)	7.14 (1H, *s*)
4	8.45 (1H, *d*, *J* = 6.0 Hz)	7.67 (1H, *d*, *J* = 4.7 Hz)
5	8.76 (1H, *d*, *J* = 6.0 Hz)	8.81 (1H, *d*, *J* = 4.8 Hz)
9	7.42 (1H, *dd*, *J* = 8.5, 1.2 Hz)	7.07 (1H, *d*, *J* = 8.4 Hz)
10	8.08 (1H, *t*, *J* = 8.5 Hz)	7.62 (1H, *t*, *J* = 8.1 Hz)
11	8.59 (1H, *dd*, *J* = 8.5, 1.2 Hz)	8.27 (1H, *d*, *J* = 7.8 Hz)
-OCH$_2$O-	6.67 (2H, *s*)	6.32 (2H, *s*)
8-OMe	4.22 (3H, *s*)	4.03 (3H, *s*)

*Watanabe *et al.*, 1975 (in CF$_3$COOH)
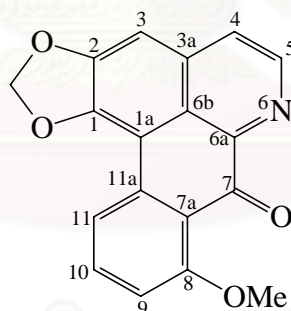
MMS-3

2.10 Identification of Compound MMS-4

Compound MMS-4 was obtained as pale yellow needles. The ESITOF mass spectrum (**Figure 127**) exhibited [M+H]$^+$ peak at *m/z* 257, suggesting the molecular formula of C$_{15}$H$_{12}$O$_4$. The UV spectrum displayed absorption maxima at 287, 248 and 224 nm (**Figure 125**). The IR spectrum (**Figure 126**) exhibited absorption bands for hydroxy group(s) at 3352 cm^{-1} and conjugated carbonyl functionalities at 1639 cm^{-1}.

The flavanone nucleus of compound MMS-4 was determined from the ^{1}H NMR

spectrum (**Figure 128**), in which the signals due to H-2 and H-3 could be observed as an ABX system at δ 5.40 (1H, *d*, *J* = 12.8 Hz, H-2), 2.80 (1H, *d*, *J* = 17.1 Hz, H-3a) and δ 3.07 (1H, *dd*, *J* = 17.1, 12.8 Hz, H-3b). In the aromatic region, the *meta*-coupled A-ring protons at positions 6 and 8 appeared as a broad singlet at δ 6.03. The chelated hydroxyl signal appeared as the most deshielded signal at δ 12.01 (1H, *s*, 5-OH).

The ^{13}C NMR and DEPT experiments of this compound helped differentiating fifteen carbon signals into those of one carbonyl carbon at δ 195.5, one methylene carbon at δ 43.4, eight methine carbons at δ 79.2, 95.5, 96.7, 126.0 (2C), and 128.8 (3C), and six quaternary carbons at δ 103.2, 138.1, 163.0, 164.2, 164.4 and 195.5 (**Figures 129** and **130**). Comparison with literature values (Bick, Brown and Hillis, 1972; Wagner, Chari and Sonnenbichler, 1976) led to the identification of compound MMS-4 as the flavanone pinocembrin.
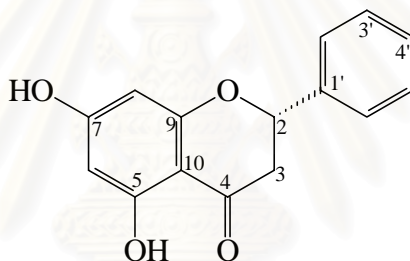
MMS-4

Pinocembrin showed antimicrobial activity against *Staphylococcus aureus*, *Bacillus subtilis* and *Mycobacterium smegmatis* at 50, 25, 25 μg/ml (Hufford and Lasswell, 1978). This flavonoid, isolated from the leaves of *Piper lanceaefolium*, was demonstrated to display activity against *Candida albicans* (Lopez, Ming and Towers, 2002)

Pinocembrin, obtained from *Helichrysum italicum,* exhibited anti-inflammatory activity in the sheep red blood cell-induced delayed-type hypersensitivity reaction (Sara *et al.*, 2003). The compound, isolated as a constituent of the ethanol extract of *Boesenbergia pandurata* rhizome exhibited mild anti-HIV-1 protease activity (Tewtrakul *et al.*, 2003).

Table 61. Comparison of the ^{1}H and ^{13}C NMR spectral data of pinocembrin and compound

MMS-4 (in CDCl$_3$, 300 MHz)

Position	Pinocembrin			MMS-4	
	^{1}H†	^{13}C‡		^{1}H	^{13}C
2	5.90 (1H, *q*, *J* = 13.0, 3.0 Hz)	78.4		5.40 (1H, *d*, *J* = 12.8, Hz)	79.2
3	3.07 (1H, *q*, *J* = 17.0, 3.0 Hz)	42.2		2.80 (1H, *d*, *J* = 17.1 Hz)	43.4
	3.52 (1H, *q*, *J* = 17.0, 13.0 Hz)			3.07(1H, *dd*, *J* = 17.1, 12.8 Hz)	
4	-	195.8		-	195.5
5	-	163.6		-	164.2
6	6.28 (1H, *s*)	96.1		6.03 (1H, *s*)	96.7
7	-	166.6		-	164.4
8	6.28 (1H, *s*)	95.1		6.03 (1H, *s*)	95.5
9	-	162.7		-	163.0
10	-	101.9		-	103.2
1′	-	138.0		-	138.1
2′, 6′	7.80 (2H, *m*)	126.5		7.39 (2H, *m*)	126.0
3′, 4′, 5′	7.80 (3H, *m*)	128.5		7.39 (3H, *m*)	128.8
5-OH	12.48 (1H, *s*)	-		12.01 (1H, *s*)	-
7-OH	11.20 (1H, *m*)	-		-	-

† Bick *et al*., 1972 (100 MHz, in DMSO-*d$_6$*)

‡ Wagner *et al*., 1976 (66 MHz, in DMSO-*d$_6$*)

3. Structure Determination of Compounds with Advanced Glycation End-product (AGE) Formation Inhibitory Activity from the Leaves of *Uvaria rufa*

Bioassay-guided fractionation led to the isolation of five compounds (URL-6 - URL-10) from the most active EtOAc fraction of *Uvaria rufa* leaves. Spectral data of these compounds showed characteristics of flavonol glycoside (**Figures 131-140**). Upon comparison with reported values of other flavonol glycosides, compounds URL-6 - URL-10 were identified as quercetin 3-*O*-β-D-rutinoside (rutin), quercetin 3-*O*-β-D-glucopyranoside (isoquercitrin), kaempferol 3-*O*-β-D-galactoside, kaempferol 3-*O*-β-D-glucopyranoside (astragalin) and quercetin 3-*O*-β-D-glucopyranoside-6-acetate, respectively (**Tables 62-66**).
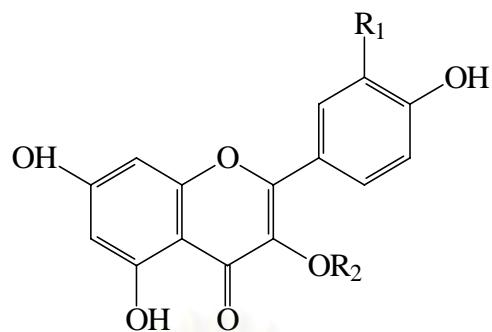
URL-6   : R$_1$ = OH, R$_2$ = rutinosyl

URL-7   : R$_1$ = OH, R$_2$ = β-D-glucopyranosyl

URL-8   : R$_1$ = H, R$_2$ = β-D-galactopyranosyl

URL-9   : R$_1$ = H, R$_2$ = β-D-glucopyranosyl

URL-10   : R$_1$ = OH, R$_2$ = β-D-glucopyranosyl-6-acetate

Table 62. Comparison of the ^{13}C NMR spectral data of rutin and compound URL-6 (in DMSO-d_6, 300 MHz)

Position	Rutin* ^{13}C	URL-6 ^{13}C	Position	Rutin* ^{13}C	URL-6 ^{13}C
2	156.4	156.8	rutinosyl		
3	133.6	133.6	1″	103.4	101.5
4	177.4	177.7	2″	75.3	74.4
5	161.2	161.5	3″	77.4	76.8
6	98.8	99.1	4″	71.1	70.4
7	164.0	164.4	5″	76.6	76.2
8	93.6	94.0	6″	68.7	67.3
9	156.6	157.0	1‴	102.0	101.1
10	105.2	104.3	2‴	71.5	70.7
1′	121.6	121.5	3‴	71.7	70.9
2′	115.3	115.6	4‴	73.2	72.2
3′	144.6	145.1	5‴	69.7	68.6
4′	148.3	148.8	6‴	18.6	18.6
5′	116.3	116.6			
6′	121.6	122.0			

* Markham and Ternai, 1976 (in DMSO-d_6, 90 MHz)

Table 63. Comparison of the ^{13}C NMR spectral data of isoquercitrin and compound URL-7 (in DMSO-d_6, 300 MHz)

Position	Isoquercitrin*	URL-7	Position	Isoquercitrin*	URL-7
	^{13}C	^{13}C		^{13}C	^{13}C
2	156.5	156.0	glucosyl		
3	133.7	133.2	1″	101.4	100.8
4	177.6	177.2	2″	74.3	74.1
5	161.3	161.0	3″	76.8	76.5
6	98.8	98.6	4″	70.3	70.0
7	164.2	164.0	5″	77.5	77.5
8	93.6	93.5	6″	61.3	61.0
9	156.5	156.1			
10	104.2	103.9			
1′	121.4	121.0			
2′	115.2	115.1			
3′	144.8	144.6			
4′	148.5	148.3			
5′	116.5	116.1			
6′	121.6	121.5			

* Markham *et al.*, 1978 (in DMSO-d_6, 90 MHz)

Table 64. Comparison of the ^{13}C NMR spectral data of kaempferol 3-*O*-β-D-galactoside and compound URL-8 (in DMSO-d_6, 300 MHz)

Position	Kaempferol 3-*O*-β-D-galactoside *	URL-8	Position	Kaempferol 3-*O*-β-D-galactoside *	URL-8
	^{13}C	^{13}C		^{13}C	^{13}C
2	156.4	156.5	galactosyl		
3	133.4	133.4	1″	101.9	101.8
4	177.5	177.6	2″	71.3	71.3
5	161.1	161.3	3″	73.1	73.2
6	98.8	98.8	4″	68.0	68.0
7	164.2	164.3	5″	75.7	75.9
8	93.8	93.8	6″	60.3	60.3
9	156.4	156.5			
10	104.0	104.0			
1′	120.9	121.0			
2′, 6′	131.0	131.0			
3′, 5′	115.1	115.1			
4′	159.9	160.0			

* Barbera *et al.*, 1986 (in DMSO-d_6, 90 MHz)

Table 65. Comparison of the ^{13}C NMR spectral data of astragalin and compound URL-9 (in DMSO-d_6, 300 MHz)

Position	Astragalin *	URL-9	Position	Astragalin*	URL-9
	^{13}C	^{13}C		^{13}C	^{13}C
2	156.4	156.2	glucosyl		
3	135.8	133.1	1″	104.7	100.8
4	179.8	177.2	2″	76.1	74.2
5	163.4	161.0	3″	78.5	76.4
6	100.8	98.7	4″	71.8	69.9
7	167.9	164.0	5″	78.8	77.5
8	95.5	93.6	6″	63.0	60.9
9	159.0	156.1			
10	105.7	103.9			
1′	123.2	120.8			
2′, 6′	132.7	130.7			
3′, 5′	116.5	115.0			
4′	162.0	159.8			

* *et al*., 2004 (in CD$_3$OD, 90 MHz)

Table 66. Comparison of the ^{13}C NMR spectral data of quercetin 3-*O*-β-D-glucopyranoside-6-acetate and compound URL-10 (in DMSO-d_6, 300 MHz)

Position	Quercetin 3-*O*-β-D-glucopyranoside-6-acetate*	URL-7	Position	Quercetin 3-*O*-β-D-glucopyranoside-6-acetate*	URL-7
	^{13}C	^{13}C		^{13}C	^{13}C
2	156.5	156.4	glucosyl		
3	133.2	133.1	1″	101.1	101.0
4	177.4	177.2	2″	74.0	74.1
5	156.5	161.1	3″	76.3	76.4
6	98.7	98.8	4″	69.8	69.6
7	164.2	164.1	5″	74.0	74.1
8	93.6	93.6	6″	62.8	62.9
9	161.2	156.3	O<u>C</u>OCH$_3$	169.7	169.8
10	103.9	103.9	OCO<u>C</u>H$_3$	20.9	20.4
1′	121.1	121.1			
2′	115.1	115.2			
3′	144.8	144.8			
4′	148.5	148.5			
5′	116.2	116.2			
6′	121.5	121.5			

* Takagi *et al*., 1981 (in DMSO-d_6, 90 MHz)

4. Bioactivities of Compounds Isolated from *Uvaria rufa* and *Mitrephora maingayi*

In the search for biologically active constituents of *Uvaria rufa* and *Mitrephora maingayi*, the hexane, EtOAc and MeOH extracts of the leaves and stems of *U. rufa*, as well as the hexane, CHCl$_3$ and MeOH extracts of the leaves and stems of *M. maingayi*, were subjected to *in vitro* screenings for their anticancer activity against three cancer cell lines (KB, BC and NCI-H187), antimalarial activity against *Plasmodium falciparum*, antituberculosis activity against *Mycobacterium tuberculosis* and anti-herpes simplex virus type 1. In addition, screening of the extracts of *U. rufa* leaves for potential inhibitors of advanced glycation end-product (AGE) formation was also performed.

4.1 Bioactive Compounds from *Uvaria rufa*

The hexane and EtOAc extracts of *U. rufa* leaves were strongly active against NCI-H187 cell lines (IC$_{50}$ = 1.03 and 3.98 µg/ml, respectively). They also exhibited antituberculosis activity against *Mycobacterium tuberculosis* (MIC = 50 and 12.5 µg/ml, respectively). In addition, the EtOAc extract was active against herpes simplex virus type 1 (HSV-1), with IC$_{50}$ value of 7.9 µg/ml.

Five compounds were isolated from the extracts of *U. rufa* leaves. (-)-Pipoxide, a cyclohexene derivative, was obtained from both the hexane and EtOAc extracts, whereas three other cyclohexene derivatives, namely 1-epizeylenol, ellipieopsol B and zeylenol, together with a seco-cyclohexene derivative, microcarpin B, were also isolated from the EtOAc extract.

The hexane and EtOAc extracts of the stems of *U. rufa* exhibited potent activities against NCI-H187 cell lines with IC$_{50}$ values of 0.09 and 1.81 µg/ml, respectively, whereas the EtOAc extract was weakly active against KB cell line with IC$_{50}$ value of 18.6 µg/ml. Both extracts also displayed inhibitory activity against *Mycobacterium tuberculosis* with MIC values of 25 and 50 µg/ml, respectively.

Isolation of the hexane extract of the stems afforded two pentacyclic triterpenoids: glut-5(6)-en-3β-ol and taraxerol. Benzyl benzoate, three flavones: tectochrysin, 7-*O*-methylwogonine and 6,7-*O*,*O*-dimethylbaicalein, and two flavanones: 2,5-dihydroxy-7-methoxyflavanone and eriodictyol, were isolated from the EtOAc extract.

All compounds were evaluated for their biological activities, the results of which are

summarized in **Table 67**.

4.1.1 Cytotoxic Activity

In this study, tectochrysin, previously found to exhibit considerable antimutagenic property against olfloxacin-induced bleaching of *Euglena gracilis* (Krizkova *et al*., 1998), as well as potent and specific inhibitory activity against breast cancer resistant protein ABCG2 (Ahmed-Belkacem *et al*., 2005), showed mild cytotoxictiy against NCI-H187 cell line, with IC_{50} of 20.0 µg/ml. Another flavonoid, 6,7-*O,O*-dimethylbaicalein, was cytotoxic to breast cancer cell line (BC) with IC_{50} of 15.07 µg/ml.

4.1.2 Antituberculosis Activity

Zeylenol, taraxerol, benzylbenzoate, 6,7-*O,O*-dimethylbaicalein and eriodictyol exhibited antituberculosis activity against *Mycobacterium tuberculosis* H37Ra with MIC values of 100, 200, 100, 25 and 200 µg/ml, respectively.

4.1.3 Anti HSV-1 Activity

Zeylenol, from the EtOAc extract of the leaves, displayed moderate anti HSV-1 activity, while 6,7-*O,O*-dimethylbaicalein was weakly active against the virus.

Table 67. Bioactivities of isolated compounds from *Uvaria rufa*

Compound	Anti HSV-1 IC$_{50}$ (µg/ml)	AntiTB MIC (µg/ml)	Antimalarial EC$_{50}$ (µg/ml)	Cytotoxicity IC$_{50}$ (µg/ml)			
				NCI-H187	KB	BC	Vero cell
Zeylenol (URL-5)	moderately active	100	inactive	inactive	inactive	inactive	>50
Glut-5(6)-ene-3β-ol (URS-1)	ND	inactive	inactive	inactive	inactive	inactive	ND
Taraxerol (URS-2)	ND	200	inactive	inactive	inactive	inactive	>50
Benzyl benzoate (URS-3)	ND	100	inactive	inactive	inactive	inactive	>50
Tectochrysin (URS-4)	ND	inactive	inactive	20.0	inactive	inactive	>50
7-*O*-Methylwogonine (URS-5)	inactive	inactive	inactive	inactive	inactive	inactive	>50
6,7-*O,O*-Dimethyl baicalein (URS-6)	weakly active	25	inactive	inactive	inactive	15.07	23.2
Eriodictyol (URS-8)	ND	200	inactive	inactive	inactive	inactive	>50
Rifampicin	-	0.0047	-	-	-	-	-
Kanamycin sulfate	-	2.5	-	-	-	-	-
Isoniazid	-	0.05	-	-	-	-	-
Ellipticine	-	-	-	0.35	0.38	0.32	-
Doxorubicin	-	-	-	-	0.17	0.18	-
Acyclovir	0.9-1.9	-	-	-	-	-	-
Dihydroartemisin	-	-	0.0043	-	-	-	-

ND = not determined

4.2 Bioactive Compounds from *Mitrephora maingayi*

The hexane and $CHCl_3$ extracts of *Mitrephora maingayi* leaves were active against *Mycobacterium tuberculosis* with MIC values of 50 and 200 µg/ml, respectively. In addition, the $CHCl_3$ extract displayed antimalarial activity with EC_{50} value of 6.0 µg/ml and showed weak cytotoxic activity against NCI-H187 cell line with IC_{50} value of 14.03 µg/ml.

Chemical investigation of the hexane extract of the leaves led to the isolation of a sesquiterpene, spathulenol, and a diterpene, kaurenoic acid, while the $CHCl_3$ extract afforded three lignans: (+)-epieudesmin, (±)-eudesmin and magnone A, together with two diterpenoids, kaurenoic acid and its hydroxyl derivative, didymooblongin.

Both hexane and $CHCl_3$ extracts of *M. maingayi* stems exhibited antituberculosis activity with MIC value of 100 µg/ml. The $CHCl_3$ extract also displayed moderate activity against NCI-H187 cell line with IC_{50} value of 8.1 µg/ml.

Four compounds were isolated from the extracts of the stems. Pimaric acid, which is a diterpene acid, was obtained from the hexane extract. Two oxoaporphine alkaloids, liriodenine and oxostephanine, together with a flavanone, pinocembrin, were afforded from the $CHCl_3$ extract.

The results of the bioactivity evaluation of these isolated compounds are presented in **Table 68**.

4.2.1 Cytotoxic activity

Kaurenoic acid, liriodenine and oxostephanine were shown to be cytotoxic. Kaurenoic acid was weakly active against BC cell line (IC_{50} = 13.39 µg/ml), whereas liriodenine and oxostephanine were strongly cytotoxic against KB (IC_{50} = 1.22 and 2.38 µg/ml, respectively) and BC cell lines (IC_{50} = 1.10 and 2.34 µg/ml, respectively).

4.2.2 Antituberculosis activity

Kaurenoic acid, (+)-epieudesmin, liriodenine, oxostephanine and pinocembrin exhibited inhibitory activity against *Mycobacterium tuberculosis* with MIC values of 100, 100, 12.5, 25 and 25 µg/ml, respectively.

4.2.3 Anti HSV-1 activity

The aporphine alkaloid oxostephanine showed weak activity against herpes simplex virus type 1.

Table 68. Bioactivities of isolated compounds from *Mitrephora maingayi*

Compound	Anti HSV-1 IC$_{50}$ (µg/ml)	AntiTB MIC (µg/ml)	Anti malarial EC$_{50}$ (µg/ml)	Cytotoxicity IC$_{50}$ (µg/ml)			
				NCI-H187	KB	BC	Vero cell
Kaurenoic acid (MML-2)	inactive	100	inactive	ND	inactive	13.39	>50
(±)-Eudesmin (MML-4)	ND	100	inactive	inactive	inactive	ND	ND
Liriodenine (MMS-2)	inactive	12.5	2.8	ND	1.22	1.10	2.0
Oxostephanine (MMS-3)	weakly active	25	inactive	ND	2.38	2.34	18.6
Pinocembrin (MMS-4)	inactive	25	ND	ND	ND	ND	>50
Rifampicin	-	0.0047	-	-	-	-	-
Kanamycin sulfate	-	2.5	-	-	-	-	-
Isoniazid	-	0.05	-	-	-	-	-
Ellipticine	-	-	-	0.35	0.38	0.32	-
Doxorubicin	-	-	-	-	0.17	0.18	-
Acyclovir	0.9-1.9	-	-	-	-	-	
Dihydroartemisin	-	-	0.0043	-	-	-	-

ND = not determined

4.3 Inhibition of AGE formation by compounds isolated from the EtOAc extract of *Uvaria rufa* leaves

In the preliminary screening for AGE inhibitors, the EtOAc extract of *Uvaria rufa* leaves showed inhibitory activity against AGE formation with 47.92 % inhibition. Accordingly, isolation of bioactive compounds from this plant extract was done through bioassay-guided fractionation.

Five flavonol glycosides, namely quercetin 3-*O*-β-D-rutinoside (rutin), quercetin

3-*O*-β-D-glucopyranoside (isoquercitrin), kaempferol 3-*O*-β-D-galactoside, kaempferol 3-*O*-β-D-glucopyranoside (astragalin) and quercetin 3-*O*-β-D-glucopyranoside-6-acetate, were isolated from the most active fraction. The % inhibition against AGE formation of these compounds, in comparison with quercetin as the positive control, are presented in **Table 69**.

Table 69. Inhibitory activity against AGE formation of the compounds isolated from the EtOAc extract of *Uvaria rufa* leaves.

Compounds	% inhibition
Quercetin 3-*O*-β-D-rutinoside (URL-6)	41.34
Quercetin 3-*O*-β-D-glucopyranoside (URL-7)	55.16
Kaempferol 3-*O*-β-D-galactoside (URL-8)	8.45
Kaempferol 3-*O*-β-D-glucopyranoside (URL-9)	16.38
Quercetin 3-*O*-β-D-glucopyranoside-6-acetate (URL-10)	61.51
Quercetin	63.38

It should be noted that the appearance of vicinal dihydroxy groups in the aglycone of these flavonoids might be a factor in their inhibitory activity against AGE formation. Three of these flavonoids which contain vicinal dihydroxy groups, i.e. quercetin 3-*O*-β-D-glucopyranoside-6-acetate, quercetin 3-*O*-β-D-glucopyranoside (isoquercitrin) and quercetin 3-*O*-β-D-rutinoside (rutin), were more potent than the other two flavonol glycosides, with the non-vicinal dihydroxy kaempferol as their aglycone.

Quercetin 3-*O*-β-D-glucopyranoside (isoquercitrin) and quercetin 3-*O*-β-D-glucopyranoside-6-acetate were then further evaluated for their ICs_{50}, compared with quercetin as the positive control (**Table 70**).

Table 70. Inhibitory activity of quercetin 3-*O*-β-D-glucopyranoside-6-acetate, isoquercitrin and quercetin against AGE formation

Compounds	IC$_{50}$ (µM)
Quercetin 3-*O*-β-D-glucopyranoside-6-acetate	6.85
Isoquercitrin	8.41
Quercetin	10.85

Quercetin has been reported as a protein glycation inhibitor (Morimitsu *et al.*, 1995; Ahmed, 2005), this flavonoid was thus selected as the positive reference for this study. However, both quercetin 3-*O*-β-D-glucopyranoside-6-acetate and isoquercitrin were shown to be more potent inhibitors of advanced glycation end-product formation, with smaller IC$_{50}$ values of 6.85 and 8.41 µM, respectively. The glycosidic nature of these two flavonol glycosides might therefore be important in enhancing the activity.

Isoquercitrin, as well as kaempferol 3-*O*-β-D-glucopyranoside (astragalin), isolated from the leaves of *Eucommia ulmoides*, have previously been shown to possess glycation inhibitory activity (Haraguchi *et al.*, 1997). The AGE inhibitory activity of other flavonol glycosides was investigated for the first time in this study.

CHAPTER V

CONCLUSION

The hexane and dichloromethane extracts of *Uvaria rufa* (family Annonaceae) exhibited strong cytotoxicity in preliminary screening. Investigation of the chemical constituents of this plant led to the isolation of eighteen compounds including cyclohexene derivatives, triterpenoids, flavonoids and an aromatic ester. From the leaves of this plant, five cyclohexene derivatives including (-)-pipoxide, 1-epizeylenol, ellipeiopsol B, zeylenol and microcarpin B, were isolated together with a series of flavonoid glycosides including rutin, isoquercitrin, kaempferol 3-*O*-β-D-glucopyranoside, astragalin and quercetin 3-*O*-β-D-glucopyranoside-6-acetate. From the stems, three flavones, tectochrysin, 7-*O*-methylwogonine, and 6,7-*O,O*-dimethylbaicalein, two flavanones, 2,5-dihydroxy-7-methoxyflavanone and eriodictyol, two triterpenoids, glut-5(6)-ene-3β-ol and taraxerol, and benzyl benzoate were isolated.

Among the isolated compounds, tectochrysin was demonstrated as mildly cytotoxic against human small cell lung carcinoma (NCI-H187) cell line with IC_{50} of 20.0 µg/ml, whereas 6,7-*O,O*-dimethylbaicalein was cytotoxic to breast cancer (BC) cell line with IC_{50} of 15.07 µg/ml.

Fractionation of *U. rufa* leaf extract according to its activity as inhibitor of advanced glycation end-product (AGE) formation led to the isolation of the series of five flavonoid glycosides, among which quercetin 3-*O*-β-D-glucopyranoside-6-acetate and isoquercitrin were shown to be more potent inhibitors of AGE formation than the positive control (quercetin), displaying smaller IC_{50} values of 6.85 and 8.41 µM, respectively.

Diverse types of compounds from this plant were active against the tuberculosis-causing *Mycobacterium tuberculosis* H37Ra. Zeylenol, taraxerol, benzyl benzoate, 6,7-*O,O*-dimethylbaicalein and eriodictyol exhibited antituberculosis activity against the mycobacterium with MIC values of 100, 200, 100, 25 and 200 µg/ml, respectively.

Only two compounds, zeylenol and 6,7-*O,O*-dimethylbaicalein, showed certain degrees of anti-herpes simplex activity. Zeylenol displayed moderate activity, while 6,7-*O,O*-dimethylbaicalein was weakly active against herpes simplex virus type 1.

Similar study on another annonaceous plant, *Mitrephora maingayi*, which exhibited moderate cytotoxic activity in the preliminary testing of its hexane and dichloromethane extracts, gave ten of its constituents including one sesquiterpenenoid (spathulenol), two diterpenoids (kaurenoic acid and didymooblongin) and three lignans [(+)-epieudesmin, (±)-eudesmin and magnone A] from the leaves, whereas a diterpene acid (pimaric acid), two oxoaporphine alkaloids (liriodenine and oxostephanine), and a flavanone (pinocembrin) were obtained from the extraction of its stems.

Kaurenoic acid, liriodenine and oxostephanine were shown to be cytotoxic. Kaurenoic acid was weakly active against BC cell line (IC_{50} = 13.39 µg/ml), while both oxoaporphine alkaloids, liriodenine and oxostephanine, were strongly cytotoxic against KB (IC_{50} = 1.22 and 2.38 µg/ml, respectively) and BC cell lines (IC_{50} = 1.10 and 2.34 µg/ml, respectively).

Similar to *U. rufa*, different types of compounds from *M. maingayi* showed antituberculosis activity. Kaurenoic acid, (+)-epieudesmin, liriodenine, oxostephanine and pinocembrin exhibited inhibitory activity against *Mycobacterium tuberculosis* with MIC values of 100, 100, 12.5, 25 and 25 µg/ml, respectively.

Only the aporphine alkaloid oxostephanine was weakly active against herpes simplex virus type 1.

REFERENCES

Thai

ปิยะ เฉลิมกลิ่น. 2544. <u>พรรณไม้วงศ์กระดังงา</u>. กรุงเทพมหานคร. สำนักพิมพ์บ้านและสวน. หน้า 17, 130, 332.

English

Achenbach, H. 1986. Investigations on west african medicinal plants. <u>Pure & Appl. Chem.</u> 58: 653-662.

Achenbach, H. and Hemrich, H. 1991. Alkaloids, flavonoids and phenylpropanoids of the West African plant *Oxymitra velutina*. <u>Phytochemistry</u> 30: 1265-1267.

Ahmed, A. A., Mahmoud, A. A., Ali, E. T., Tzakou, O., Couladis, M., Mabry, T. J., Gati, T. and Toth, G. 2002. Two highly oxygenated eudesmanes and 10 lignans from *Achillea holosericea*. <u>Phytochemistry</u> 59: 851-856.

Ahmed, N. 2005. Advanced glycation endproducts: role in pathology of diabetic complications. <u>Diabetes Res. Clin. Pract.</u> 67: 3-21.

Ahmed-Belkacem, A., Pozza, A., Munoz-Martınez, F., Bates, S. E., Castanys, S., Gamarro, F., Pietro, A. and M. Peŕez-Victoria, J. 2005. Flavonoid structure-activity studies identify 6-prenylchrysin and tectochrysin as potent and specific inhibitors of breast cancer resistance protein ABCG2. <u>Cancer Res</u> 65: 4852-4860.

Anam, E. M. 1994a. 2″″-Hydroxy-3″″-benzyluvarinol, 2″″″-hydroxy-5″″-benzylisouvarinol-A and 2‴-hydroxy-5″-benzylisouvarinol-B: three novel tetra-C-benzylated flavanones from the root extract of *Xylopia africana* (Benth.) oliver (Annonaceae). <u>Indian J. Chem.</u> 33B: 1009-1011.

Anam, E. M. 1994b. 7-*O*-Methylbenzylflavanones and 4′-*O*-methylbenzyldihydrochalcone from *Xylopia africana* (Benth.) oliver. <u>Indian J. Chem.</u> 33B: 870-873.

Aronson, D. 2003. Cross-linking of glycated collagen in the pathogenesis of arterial and myocardial stiffening of aging and diabetes. <u>J. Hypertension</u> 21: 3-12.

Banerji, A., Sarkar, M., Ghosal, T. and Pal, S. C. 1984. Sylvone, a new furanoid lignan of Piper sylvaticum. <u>Tetrahedron</u> 40: 5047-5052.

Barberá, O., Sanz, J. F., Sánchez-Parareda, J. and Marco, A. 1986. Further flavonol glycosides from *Anthyllis onobrychioides*. <u>Phytochemistry</u> 25: 2361-2365.

Batterham. T. J. and Highet, R. J. 1964. Nuclear magnetic resonance spectra of flavonoids. <u>Aust. J. Chem.</u> 14: 428-439.

Berrens, L. 1992. Benzyl benzoate: acaricide or anti-asthmatic. Ann. Allergy 69: 463-464.

Bick, I. R. C., Brown, R. B. and Hillis, W. E. 1972. Three flavanones from leaves of *Eucalyptus sieberi*. Aust. J. Chem. 25: 449-451.

Bohlmann, F., Kramp, W., Jakupovic, J., Robinson, H. and King, R. M. 1982. Diterpenes from *Baccharis* species. Phytochemistry 21: 399-403.

Cervantes-Laurean, D., Schramm, D. D., Jacobson, E. L., Halaweish, I., Bruckner, G. G. and Boissonneault, G. A. 2006. Inhibition of advanced glycation endproduct formation on collagen by rutin and its metabolites. J. Nutr. Biochem. 17: 531-40.

Chakrabarty, M. and Nath, A. C. 1992. A new clerodane-type butenolide diterpene from the bark of *Polyalthia longifolia*. J. Nat. Prod. 55: 256-258.

Chang, F. R., Wei, J. L., Hsieh, T. J., Cho, C. P. and Wu, Y. C. 2000. Chemical constituents from *Annona purpurea*. J. Nat. Prod. 31: 1457-1461.

Chang, F. R., Yang, P. Y., Lin, J. Y., Lee, K. H. and Wu, Y. C. 1998. Bioactive kaurane diterpenoids from *Annona glabra*. J. Nat. Prod. 61: 437-439.

Chantrapromma, K., Pakawatchai, C., Skelton, B. W., White, A. H. and Worapatamasri, S. 1989. 5-Hydroxy-7-methoxy-2-phenyl-4H-1-benzopyran-4-one (tectochrysin) and 2,5-dihydroxy-7-methoxy-2-phenyl-2,3-dihydro-4H-1-benzopyran-4-one: isolation from *Uvaria rufas* and x-ray structures. Aust. J. Chem. 42: 2289-2293.

Chaves, M. H., Roque, N. F. and Costa Ayres, M. C. 2004. Steroids and flavonoids of *Porcelia macrocarpa*. J. Braz. Chem. Soc. 15: 608-613.

Chayankiat, A., Wiriyachitra, P. and Taylor, W. 1984. A new compound from *Uvaria rufas*. J. Sci. Soc. Thailand 10: 239-245.

Chen, C. Y., Chang, F. R., Cho, C. P. and Wu, Y. C. 2000a. *Ent*-kaurane diterpenoids from *Annona glabra*. J. Nat. Prod. 63: 1000-1003.

Chen, C. Y., Chang, F. R., Shih, Y. C., Hsieh, T. J., Chia, Y. C., Tseng, H. Y., Chen, H. C., Chen, S. J., Hsu, M. C. and Wu, Y. C. 2000b. Cytotoxic constituents of *Polyalthia longifolia* var. *pendula*. J. Nat. Prod. 63: 1475-1478.

Chen, K. S., Wu, Y. C., Teng, C. M. Ko, F. N., Wu, T. S. 1997. Bioactive Alkaloids from *Illigera luzonensis*. J. Nat. Prod. 60: 645-647.

Chen, K.S., Ko, F. N., Teng, C. M. and Wu, Y.C. 1996. Antiplatelet and vasorelaxing actions of some aporphinoids. Planta Med. 62: 133-136.

Chi, V. V. 1997. Vietnamese Medical Plant Dictionary. Medicine Pub. Hanoi.

Cho, J. Y., Yoo, E. S., Baik, K. U., Park, M.H. 1999. Eudesmin inhibits tumor necrosis factor-alpha production and T cell proliferation. Arch Pharm Res. 22: 348-353.

Collins, L. A. and Franzblau, S. G. 1997. Microplates alamar blue assay versus BACTEC 460 system for high-throughput screening of the compounds against *Mycobacterium tuberculosis* and *Mycobacterium avium*. Antimicrob. Agents. Chemother. 41: 1004-1009.

Corbett, R. E. and Cumming, S. D. 1972. Lichens and fungi. Part X. 14α-taraxerane. J. C. S. Perkin I: 2827-2829.

Das, A. K., Mitra, S. R. and Adityachaudhury, N. 1979. Kaurenoid diterpenes of *Didymocarpus oblongga* Wall. Indian J. Chem. 18B: 550-552.

De Costa, F.B., Albuquerque, S. and Vichnewski, W. 1996. Diterpenes and synthetic derivaties from *Viguiera aspillioides* with trypanomicidal activity. Planta Med. 62: 557-559.

De Groot, J. 2004. The AGE of the matrix: chemistry, consequence and cure. Curr. Opin. Pharmacol. 4: 301-305.

Desjardins, R. E., Canfield, C. J. Haynes, J. D. and Chulay, J. D. 1979. Qauntitative assessment of antimalarial activity *in vitro* by a semiautomated micro dilution technique. Antimicrob. Agents Chemother. 16: 710-718.

Edelstein, D. and Brownlee, M. 1992. Mechanistic studies of advanced glycosylation end product inhibition by aminoguanidine. Diabetes. 41: 26-29.

Ekong, D. E. U., Olagbemi, E. O. amd Odutola, F. A. 1969. Further diterpenes from *Xylopia aethiopica*. Phytochemistry 8: 1053.

Ekpa, O. D. and Anam, E. M.1993. Uvarinol and novel iso-uvarinol: two *C*-benzylated flavanones from *Xylopia africana* (Annonaceae). Indian J. Chem. 32B: 1295-1297.

El-Sohly, H. N., Lasswell, Jr., W. L. and Hufford, C. D. 1979. Two new C- benzylated flavanones from *Uvaria chamae* and ^{13}C NMR analysis of flavonone methyl

Etse, J. T., Gray, A. I., Thomas, D. W. and Waterman, P. G. 1989. Terpenoid and alkaloid compounds from the seeds of *Monodora brevipes*. Phytochemistry 28: 2489-2492.

Fatope, M. O., Audu, O. T., Takeda, Y., Zeng, L., Shi, G., Shimada, H. and McLaughlin, J. L. 1996. Bioactive *ent*-kaurene diterpenenoids from *Annona senegalensis*. J. Nat. Prod. 59: 301-303.

Fleischer, T. C., Waigh, R. D. and Waterman, P. G. 1997. Bisabolene sesquiterpenes and flavanones from *Friesodielsia enghiana*. <u>Phytochemistry</u> 44: 315-318.

Fournier, G., Hadjiakhoondi, A., Charles, B., Fourniat, J., Leboeuf, M. and Cave, A. 1994. Chemical and biological studies of *Xylopia aromatica* stem bark and leaf oil. <u>Planta Med.</u> 60: 283-284.

Fournier, G., Hadjiakhoondi, A., Leboeuf, M., Cave, A. and Charles, B. 1999. Essential oil of Annonaceae: part II, essential oil of *Monanthotaxis diclina* (Sprague) Verdcourt and *Unonopsis guatterioides* R. E. Fries. <u>Flavor and Fragrance Journal</u> 12 : 95-98.

Franz, J. E. and Pearl, H. K. 1976. Uvaretin and isouvaretin, two novel cytotoxic *C*-benzylflavanones from *Uvaria chamae* L. <u>J. Org. Chem.</u> 41: 1297-1298.

Fu, M. X., Thorpe, S. R. and Baynes, J. W. 1994. Effects of aspirin on glycation, glycoxidation, and crosslinking of collagen. In: Labuza, T. P., Reineccius, G. A., Monnier, V. M., O'Brien, J. and Baynes, J., eds. Maillard reactions in chemistry, food and health. Cambridge: The Royal Society of Chemistry: 95-100.

Gao, F., Miski, M., Gage, D. A., Norris, J. A. and Mabry, T. J. 1985. Terpenoids from *Viguiera potosina*. <u>J. Nat. Prod.</u> 48: 489-490.

Gao, S., Fu, G. M., Fan, L. H., Yu, S. S. and Yu, D. Q. 2005. Flavonoids from *Lysidice rhodostegia* Hance <u>J. Integr. Plant Biol</u>. 47: 759-763.

Geahlen, R. L., Koonchanok, N., Jerry, M., McLaughlin, L. and Pratt, D. E. 1989. Inhibition of protein-tyrosine kinase activity by flavanoids and related Compounds. <u>J. Nat. Prod.</u> 52: 982-986.

Gonda, R., Takeda, T. and Akiyama, T. 2000. Studies on the constituents of *Anaxagorea luzonensis* A. Gray. <u>Chem. Pharm. Bull.</u> 48: 1219-1222.

Gonzalez, A. G., Ferro, E. A. and Ravelo, A.G. 1987. Triterpenes from *Maytenus horrida*. <u>Phytochemistry</u> 26: 2785-2788.

Gonzalez, A. G., Fraga, B. M., Hernandez, M.G. and Luis, J.G. 1973. New diterpenes from *Sideritis candicans*. <u>Phytochemistry</u> 12: 2721-2723.

Gugliucci, A. and Menini, T. 2002. The botanical extracts of *Achyrocline satureoides* and *Ilex paraguariensis* prevent methylglyoxal-induced inhibition of plasminogen and antithrombin. <u>Life Sciences</u> 72: 279-292.

Hans, J. J., Driver, R. W. and Burke, S. D. 2000. Direct transacylation of 2,2,2-trihaloethyl esters with amines and alcohols using phosphorus (III) reagents for reductive fragmentation and in situ activation. <u>J. Org. Chem.</u> 65: 2114-2121.

Hao, X. J., Yang, X. S., Zhang, Z., and Shang, L. J. 1995. Clerodane diterpenes from *Polyalthia longifolia*. Phytochemistry 39: 447-448.

Hao, X. Y., Shang, L. and Hao, X. J. 1993. Flavonoids from *Desmos chinensis*. Yunnan Zhiwu Yanjiu 15: 295-298.

Hara, N., Asaki, H., Fujimoto, Y., Gupta, Y. K., Singh, A. K. and Sahai, M. 1995. Clerodane and *ent*-halimane diterpenes from *Polyalthia longifolia*. Phytochemistry 38: 189-194.

Harrigan, G. G., Bolzani, V. S., Gunatilaka, A. A. L. and Kingston, D. G. I. 1994. Kaurane and trachylobane diterpenes from *Xylopia aethiopica*. Phytochemistry 36: 109-113.

Hasan, C. M., Healey, T. M. and Waterman, P. G. 1982a. 7β-Acetoxytrachyloban-18-oic acid from the stem bark of *Xylopia quintasii*. Phytochemistry 21: 177-179.

Hasan, C. M., Healey, T. M. and Waterman, P. G. 1985. Acutifloric acid: a diterpene dimer from the stem bark of *Xylopia acutiflora*. Phytochemistry 24: 192-194.

Hasan, C. M., Healey, T. M., and Waterman, P. G. 1982b. Kaurane and kaurene diterpenes from the stem bark of *Xylopia acutiflora*. Phytochemistry 21: 2134-2135.

Heywood, V. H. 1978. Flowering plants of the world. University Press, Oxford.

Hollands, R., Becher, D., Gaudemer, A., Polonsky, J. and Ricroch, N. 1968. Etude des constituants des fruits d'*Uvaria catocarpa* (Annonaceae) structure du senepoxyde et du seneol. Tetrahedron 24: 1633-1650.

Hoon, A. H., Lam, C. K. and Wah, M. J. 1995. Quantitative assessment of antimalarial activities from Malaysian *Plasmodium falciparum* isolates by modified *in vitro* microtechnique. Antimicrob. Agents Chemother. 39: 626–628.

Huang, L., Wall, M. E., Wani, M. C., Navarro, H., Santisuk, T., Reutrakul, V., Seo, E-K., Farnsworth, N. R. and Kinghorn, A. D. 1998. New compounds with DNA strand-scission activity from the combined leaf and stem of *Uvaria hamiltonii* J. Nat. Prod. 61: 446-450.

Hufford, C. D. and Lasswell, Jr. W. L. 1976. Uvaretin and isouvaretin. Two novel cytotoxic *C*-benzylflavanones from *Uvaria chamae* L. J. Org. Chem. 41:1297-1298.

Hufford, C. D. and Oguntimein, B. O. 1980. Dihydrochalcones from *Uvaria angolensis*. Phytochemistry 19: 2036–2038.

Hufford, C. D. and Oguntimein, B. O. 1982. New dihydrochalcones and flavanones from *Uvaria chamae*. J. Nat. Prod. 45: 337-342.

Hufford, C. D., and Lasswell Jr., W. L. 1978. Antimicrobial activities of constituents of *Uvaria chamae*. Lloydia 41: 156-160.

Hufford, C. D., and Lasswell Jr., W. L., Hirostu, K. and Clardy, J. 1979. Uvarinol: a novel cytotoxic tribenzylated flavanone from *Uvaria chamae*. J. Org. Chem. 44: 4709- 4710.

Hufford, C. D., Funderburk, M. J., Morgan, J. M. and Robertson, L. W. 1975. Two antimicrobial alkaloids from Heartwood of *Liriodendron tulipifera* L. J. Pharm. Sci. 64: 789-792.

Hufford, C. D., Oguntimein, B. O. and Baker J. K. 1981. New flavonoid and coumarin derivatives of *Uvaria afzelii*. J. Org. Chem. 46: 3073-3078.

Hufford, C. D., Sharma, A. S. and Oguntimein, B. O. 1980. Antibacterial and Antifungal Activity of liriodenine and related oxoaporphine alkaloids. J. Pharm. Sci. 69: 1180-1183.

Huong, D. T., Luong, D. V., Thao, T. T. and Sung, T. V. 2005. A new flavone and cytotoxic activity of flavonoid constituents isolated from *Miliusa balansae* (Annonaceae). Pharmazie 60: 627-629.

Hutchinson, J. 1964. The genera of flowering plants. vol I. University Press, Oxford.

Iwabuchi, H., Youshikura, M. and Kamisako, W. 1989. Studies on sesquiterpenoids of *Panax jinseng* C. A. Meyer.III. Chem. Pharm. Bull. 37: 509-510.

Jayasuriya, H., Herath, K. B., Ondeyka, J. G., Guan, Z., Borris, R. P., Tiwari, S., de Jong, W., Chavez, F., Moss, J., Stevenson, D. W., Beck, H. T., Slattery, M., Zamora, N., Schulman, M., Ali, A., Sharma, N., MacNual, K., Hayes, N., Menke, J. G. and Singh, S. B. 2005. Diterpenoid, steroid, and triterpenoid agonists of liver X receptors from diversified terrestrial plants and marine sources. 2005. J. Nat. Prod. 68: 1247-1252.

Jedsadayanmata, A. 2005. *In vitro* antiglycation activity of arbutin. Naresuan University Journal 13: 35-41.

Jolad, S. D., Hoffmann, J. J., Schram, K. H., and Cole, J. R. 1981. Structures of zeylenol and zeylena, constituents of. *Uvaria zeylanica*. (Annonaceae). J. Org. Chem. 46: 4267-4272.

Jolad, S.D., Hoffmann, J. J., Cole, J. R., Tempesta, M. S. and Bates, R. B. 1984. l-Epizeylenol from *Uvaria zeylanica* roots. Phytochemistry 23: 935-936.

Jongbunprasert, V., Bavovada, R., Theraratchailert, P., Rungserichai, R. and Likhitwitayawuid, K. 1999. Chemical constituents of *Fissistigma polyanthoides*. Science Asia 25: 31-33.

Joshi, B. S. and Gawad, D. H. 1974. Flavanones from the stem of *Unona lawii* Hook. f. & Thoms.: isolation of lawinal, desmethoxymatteucinol, desmethoxymatteucinol-7-methyl ether and a synthesis of lawinal. Indian J. Chem. 12: 1033-1037.

Joshi, B. S. and Gawad, D. H. 1976. Isolation and structure of some new flavones and dibenzoylmethanes from *Unona lawii* Hook. f. & Thoms. Indian J. Chem. 14B: 9-13.

Jung, J. H. and McLaughlin, J. L. 1990. ^{13}C-^{1}H NMR long-range coupling and deuterium isotope effects of flavanones. Phytochemistry 29: 1271-1275.

Jung, J. H., Pummangura, S., Chaichantipyuth, C., Patarapanich, C. and McLaughlin, J. L. 1990. Bioactive constituents of *Melodorum fruticosum*. Phytochemistry 29: 1667-1670.

Jung, K. Y., Oh, S. R., Park, S. H., Lee, I. S., Ahn, K. S., Lee, J. J. and Lee, H. K. 1998. Anti-complement activity of tiliroside from the flower buds of *Magnolia fargesii*. Biol. Pharm. Bull. 21: 1077-1078.

Kakeya, H., Imoto, M., Tabata, Y., Iwami, J., Matsumoto, H., Nakamura, K., Koyono, T., Tadano, K. I. and Umezawa, K. 1993. Isolation of a novel, substrate-competitive tyrosine kinase inhibitor, desmal, from the plant *Desmos chinensis*. FEBS Lett. 320: 169-172.

Khamis, S., Bibby, M.C., Brown, J. E., Cooper, P. A., Scowen, I. and Wright, C. W. 2004. Phytochemistry and preliminary biological evaluation of *Cyathostemma argenteum*, a malaysian plant used traditionally for the treatment of breast cancer. Phytother. Res. 18: 507-510.

Kiem, P. V., Minh, C. V., Huong, H. T., Lee, J. J., Lee, I. S. and Kim, Y. H. 2005. Phenolic constituents with inhibitory activity against NFAT transcription from *Desmos chinensis*. Arch. Pharm. Res. 28: 1345-1349.

Kijjoa, A., Bessa, J., Pinto, M. M. M., Anantachoke, C., Silva, A. M. S., Eaton, G. and Herz, W. 2002. Polyoxygenated cyclohexene derivatives from *Ellipeiopsis cherrevensis*. Phytochemistry 59: 543–549.

Kijjoa, A., Pinto, M. M. M., Pinho, P. M. M., Tantisewie, B. and Herz, W. 1990. Clerodane derivatives from *Polyalthia viridis*. Phytochemistry 29: 653-655.

Kijjoa, A., Pinto, M. M. M., Pinho, P. M. M., Tantisewie, B. and Herz, W. 1993. Clerodanes from *Polyalthia viridis*. Phytochemistry 34: 457-460.

Kim, H. Y. and Kim, K. 2003. Protein glycation inhibitory and antioxidative activities of some plant extracts *in vitro*. J. Agric. Food Chem. 51: 1586-1591.

Kim, H. Y., Moon, B. H., Lee, H. J. and Choi, D. H. 2004. Flavonol glycosides from the leaves of *Eucommia ulmoides* O. with glycation inhibitory activity. J. Ethnopharmacol. 93: 227-230.

Kodpinid, M., Thebtaranonth, C. and Thebtaranonth, Y. 1985. Benzyl benzoates and *O*-hydroxybenzyl flavanones from *Uvaria chamae*. Phytochemistry 24: 3071-3072.

Lasswell Jr., W. L. and Hufford, C. D. 1977. Cytotoxic *C*-benzylated flavonoids from *Uvaria chamae*. J. Org. Chem. 42: 1295-1302.

Le Quesne, P.W., Honkan, V., Onan, K. D., Morrow, P.A. and Tonkyn, D. 1985. Oxidized kaurene derivatives from leaves of *Solidago missouriensis* and *S. rigida*. Phytochemistry 24: 1785-1787.

Leboeuf, M., Cave, A., Bhaumik, P. K., Mukherjee, B. and Mukherjee, R. 1982. The phytochemistry of the Annonaceae. Phytochemistry 21: 2783-2813.

Lee, I., Ma, X., Chai, H., Madulid, D. A. Lamont, R. B., O'Neill, M. J., Besterman, J. M., Farnsworth, N. R., Soejarto, D. D. and Cordell, G. A. 1995. Novel cytotoxic labdane diterpenoids from *Neouvaria acuminatissima*. Tetrahedron 51: 21-28.

Lee, N. H., Xu, Y. J. and Goh, S. H. 1999. 5-Oxonoraporphines from *Mitrephora* cf. *maingayi*. J. Nat. Prod. 62: 1158-1159.

Li, C., Lee, D., Graf, T. N., Phifer, S. S., Nakanishi, Y., Burgess, J. P., Riswan, S., Setyowati, F. M., Saribi, A. M., Soejarto, D. D., Farnsworth, N. R., Falkinham III, J. O., Kroll, D. J., Kinghorn, A. D., Wani, M. C. and Oberlies, N. H. 2005. A hexacyclic *ent*-trachylobane diterpenoid possessing an oxetane ring from *Mitrephora glabra*. Org. Lett. 7: 5709-5712.

Li, W. L., Zheng, H. C., Bukuru, J. and de Kimpe, N. 2004. Natural medicines used in the traditional Chinese medical system for therapy of diabetes mellitus. J. Ethnopharmacol. 92: 1-21.

Loi, D. T. 2001. Glossary of Vietnamese Medical Plants. S & T Pub. Hanoi.

Lojanapiwatna, V., Prosuwansiri, K., Suwannatip, B. and Wiriyachitra, P. 1981. The flavonoids of *Uvaria rufas*. J. Sci. Soc. Thailand. 7: 83-86.

Lopez, A., Ming, D. S. and Towers, G.H. 2002. Antifungal activity of benzoic acid derivatives from *Piper lanceaefolium*. J. Nat. Prod. 65: 62-64.

Lozoya, X., Enrıquez, R. G., Bejar, E., Estrada A. V., Giron, H., Ponce-Monter, H. and Gallegos, A. J. 1983. Contraception 27:267.

Lu, T., Vargas, D., Franzblau, S. G. and Fischer, N. H. 1995. Diterpenes from *Solidago rugosa*. Phytochemistry 38: 451-456.

Lu, Y. P. Mu, Q., Zheng, H. L. and Li, C. M. 1995. Two new constituents from *Uvaria microcarpa*. Chin. Chem. Lett. 6: 775-778.

Ma, X., Lee, I., Chai, H., Zaw, K., Farnsworth, N.R., Soejarto, D.D., Cordell, G.A., Pezzuto, J.M. and Kinghorn, A.D. 1994. Cytotoxic clerodane diterpenes from *Polyalthia barnesii*. Phytochemistry 37: 1659-1662.

Mahato, S. B. and Kundu, A. P. 1994. ^{13}C NMR spectra of pentacyclic triterpenoids-a compilation and some salient features. Phytochemistry 37: 1517-1575.

Maia, J. G. S., Andrade, E. H. A., Silva, A. C. M., Oliveira, J., Carreira, L. M. M. and Araújo, J. S. 2005. Leaf volatile oils from four brazilian *Xylopia* species. Flavour and Fragrance Journal. 20: 474-477.

Markham, K. R. and Ternai, B. 1976. ^{13}C NMR of flavonoids—II : flavonoids other then flavone and flavonol aglycones. Tetrahedron 32: 2607-2612.

Markham, K. R., Ternai, B., Stanley, R., Geiger, H. and Mabry, T. J. 1978. Carbon-13 NMR studies of flavonoids—III : Naturally occurring flavonoid glycosides and their acylated derivatives Tetrahedron 34: 1389-1397.

Martins, D., Hamerski, L., Alvarenga, S. A. V. and Roque, N. F. 1999. Labdane dimers from *Xylopia aromatica*. Phytochemistry 51: 813-817.

Matsunaga, S., Tanaka, R. and Akagi, M. 1988. Triterpenoids from *Euphorbia maculate*. Phytochemistry 27: 535-537.

Matsuura, N., Aradate, T., Sasaki, C., Kojima, H., Ohara, M., Hasegaea, J. And Ubukata, M. 2002. Screening system for the Millard reaction inhibitor from natural product extracts. J.Health Sci. 48: 520-526.

Matsuura, N., Sasaki, C., Aradate, T., Ubukata, M., Kojima, H., Ohara, M. and Hasegawa, J. 2002. Plantagoside as Maillard reaction inhibitor - its inhibitory mechanism and application. Int. Congr. Ser. 1245: 411-412.

Metzner, J., Bekemeier, H., Paintz, M. and Schneidewind, E. 1979. On the antimicrobial activity of propolis and propolis constituents. Pharmazie 34: 97-102.

Mitra, S. R., Das, A. K., Kirtaniya, C. L. And Adityachaudhury, N. 1980. Didymooblongin, a new kaurenoid diterpene from *Didymocarpus oblonga* Wall. Indian J. Chem. 19B: 79-80.

Mizutani, K., Ikeda, K. and Yamori, Y. 2000. Resveratrol inhibits AGEs-induced proliferation and collagen synthesis activity in vascular smooth muscle cells from stroke-prone spontaneously hypertensive rats. Biochem. Biophys. Res. Commun. 274: 61-67.

Montanha, J. A., Amoros, M., Boustie, J. and Girre, L. 1995. Anti-herpes virus activity of aporphine alkaloids. Planta Med. 61, 419-424.

Moraes, M. P. L. and Roque, N. F. 1988. Diterpenes from the fruits of *Xylopia aromatica.* Phytochemistry 27: 3205-3208.

Moreira, I. C., Lago, J. H., Young, M. C. M. and Roque, N. F. 2003. Antifungal aromadendrane sesquiterpenoids from the leaves of *Xylopia brasiliensis*. J. Braz. Chem. Soc. 14: 828-831.

Morimitsu, Y., Yoshida, K., Esaki, S. and Hirota, A. 1995. Protein glycation inhibitors from thyme (*Thymus vulgaris*). Biosci. Biotechnol. Biochem. 59: 2018-2021.

Mu, Q., Tang, W., Li, C., Lu, Y., Sun, H., Lou, L., Hao, X, Xu, B. and Hu, C, Q. 2002. The absolute configuration of leiocarpin B. Heterocycles 57: 337-340.

Mu, Q., Tang, W., Li, C., Lu, Y., Sun, H., Zheng, H., Hao, X, Zheng, Q., Wu, N., Lou, L. and Xu, B. 1999. Four new styryllactones from *Goniothalamus leiocarpus.* Heterocycles 51: 2969-2976.

Nagasawa, T., Tabata, N., Ito, Y., Aiba, Y., Nishizawa, N. and Kitts, D. D. 2003. Dietary G-rutin suppresses glycation in tissue proteins of streptozotocin-induced diabetic rats. Mol. Cell. Biochem. 252: 141-147.

Nagasawa, T., Tabata, N., Ito, Y., Nishizawa, N., Aiba, Y. and Kitts, D. D. 2003. Inhibition of glycation reaction in tissue protein incubations by water soluble rutin derivative. Mol. Cell. Biochem. 249: 3-10.

Ngamrojnavanich, N. and Sirimongkon, S. 2003. Inhibition of Na^+, K^+-ATPase activity by(-)-*ent*-kaur-16-en-19-oic acid and its derivatives. Planta Med. 69: 555-556.

Ngouela, S., Nyasse, B. Tsamo, E., Brochier, M. C. and Martin, C. 1998. A trachylobane diterpenoid from *Xylopia aethiopica.* J. Nat. Prod. 61: 264-266.

Nkunya, M. H. H., Achenbach, H., Renner, C., Waibel, R. and Weenen, H. 1990. Schefflerin and isoschefflerin: Prenylated chalcones and other constituents of *Uvaria scheffleri.* Phytochemistry 29: 1261-1264.

Nkunya, M. H. H., Waibel, R. and Achenbach, H. 1993. Three flavonoids from the stem bark of the antimalarial *Uvaria dependens.* Phytochemistry 34: 853-856.

Nkunya, M. H. H., Weenen, H., Koyi, N. J., Thus, L. and Zwanenburg, B. 1987. Cyclohexene epoxides, (+)-pandoxide, (+)-β-senepoxide and (-)-pipoxide from *Uvaria pandensis*. Phytochemistry 26: 2563-2565.

Pan, X. P. and YU, D. Q. 1995. Two polyoxygenated cyclohexenes from *Uvaria grandiflora*. Phytochemistry 40: 1709-1711.

Pancharoen, O., Tuntiwachwattikul, P. and Taylor, W. C. 1989. Cyclohexane oxide derivatives from *Kaempferia angustifolia* and *Kaempferia* species. Phytochemistry 28: 1143-1148.

Panichpol, K. and Waterman, P. G. 1978. Novel flavonoids fron the stem of *Popowia cauliflora*. Phytochemistry 17: 1363-1367.

Pari, L. and Venkateswaran, S. 2003. Effect of an aqueous extract of *Phaseolus vulgaris* on the properties of tail tendon collagen of rats with streptozotocin-induced diabetes. Braz. J. Med. Biol. Res. 36: 861-870.

Parmar, V. S., Bisht, K. S., Malhotra, A., Jha, A., Errington, W., Howarth, O. W., Tyagi, O. D., Stein, P. C., Jensen, S., Boll, P. M. and Olsen, C. E. 1995. A benzoic acid ester from *Uvaria narum*. Phytochemistry 38: 951-955.

Parmar, V. S., Tyagi, O. D., Malhotra, A., Singh, S. K., Bisht, K. S. and Jain, R. 1994. Novel constituents of *Uvaria* species. Nat. Prod. Rep. 11: 219-224.

Pelter, A. and Ward, R. S. 1976. Revised structures for pluviatilol, methyl pluviatilol and xanthoxylol: general methods for the assignment of stereochemistry to 2,6-diaryl-3,7-dioxabicyclo[3.3.0]octane lignans. Tetrahedron 32: 2783-2788.

Pettit, G. R., Meng, Y., Gearing, R. P., Herald. D. L., Pettit, R. K. and Tackett, L. P. 2004. Antineoplastic Agents. 522. *Hernandia peltata* (Malaysia) and *Hernandia nymphaeifolia*. J. Nat. Prod. 67: 214 -220

Phadnis, A. P., Patwardhan, S. A., Dhaneshwar, N. N., Tavale, S. S. and Guru Row, T. N. 1988. Clerodane and diterpenoids from *Polyalthia longifolia*. Phytochemistry 27: 2899-2901.

Piacente, S., Aquino, R., de Tommasi, N., Pizza, C., De Ugaz, O. L., Orellana, H. C. and Mahmood, N. 1994. Constituents of *Werneria ciliolata* and their *in vitro* anti-HIV activity. Phytochemistry 36: 991-996.

Plantz, M. and Metzner, J. 1979. On the local anesthetic action of propolis and some of its constituents. Pharmazie 34: 839-841.

Plumb, J. A., Milroy, R. and Kaye, S. B. 1989. Effects of the pH dependence of 3-(4,5-dimethylthiazol-2-yl)-2,5-diphenyl-tetrazolium bromide-formazan absorption on chemosensitivity determined by a novel tetrazolium-based assay. <u>Cancer Res</u>. 49: 4435-4440.

Rahbar, S. and Figarola, J. L. 2003. Novel inhibitors of advanced glycation endproducts. <u>Arch. Biochem. Biophys.</u> 419: 63-79.

Rosenburg, M. G. and Brinker, U. H. 2003. Inter- and innermolecular reactions of chloro(phenyl)carbene. <u>J. Org. Chem.</u> 68: 4819-4832.

Rubio, J., Calderón, J. S., Flores, A., Castro, C. and Céspedes, C. L. 2005. Trypanocidal activity of oleoresin and terpenoids isolated from *Pinus oocarpa*. <u>Z. Naturforsch.</u> 60c: 711-716.

Sajithlal, G. B., Chithra, P. and Chandrakasan, G. 1998. Effects of curcumin on the advanced glycation and cross-linking of collagen in diabetic rats. <u>Biochemical Pharmacology</u> 56: 1607-1614.

Sakurai, N., Yaguchi, Y. and Inoue, T. 1987. Triterpenoids from *Myrica rubra.* <u>Phytochemistry</u> 26: 217-219.

Santos, D. and Salatino, M. 2000. Foliar flavonoids of Annonaceae from brazil: taxonomic significance. <u>Phytochemistry</u> 55: 567-573.

Shamma, M. and Guinaudeau, H. 1985. Aporphiniod Alkaloids. <u>Nat. Prod. Rep.</u> 2: 227-233.

Shamma, M. and Guinaudeau, H. 1986. Aporphiniod Alkaloids. <u>Nat. Prod. Rep.</u>3: 345-351.

Shang, L., Zhao, B., and Hao, X. 1994. The new flavonoid from *Fissistigma kwangsiense*. <u>Yunnan Zhiwa Yanjin</u> 16: 191-195.

Singh, J., Dhar, K. L. and Atal, C. K. 1970. Study on the genus *Piper*: structure of pipoxide. a new cyclohexene epoxide from *P. hookeri* Linn. <u>Tetrahedron</u> 26: 4403-4406.

Singh, R., Barden, A., Mori, T. and Beilin, L. 2001. Advanced glycation end-products: a review. <u>Diabetologia</u> 44: 129–146.

Sinz, A., Matusch, R., Santisuk, T., Chichana, S. and Reutrakul, V. 1998. Flavonol glycosides from *Dasymaschalon sootepense*. <u>Phytochemistry</u> 47: 1393-1396.

Skehan, P., Storeng, R., Scudiero, D., Monks, A., McMahon, J., Vistica, D., Warren, J.T., Bokesch, H., Kenney, S. and Boyd. M. R. 1990. New colorimetric cytotoxicity assay for anticancer-drug screening. <u>J. Natl. Cancer Inst.</u> 82: 1107-1112.

Stierle, D. B., Stierle, A. A. and Larsen, R. D. 1988. Terpenoid and flavone constituents of *Polemonium viscosum*. Phytochemistry 27: 571-522.

Stitt, A. W. 2003. The role of advanced glycation in the pathogenesis of diabetic retinopathy. Exp. Mol. Pathol. 75: 95-108.

Suarez, G., Rajaram, R., Oronsky, A. L. and Gawinowicz, M. A. 1989. Nonenzymatic glycation of bovine serum albumin by fructose (fructation). J. Biol. Chem. 264: 3674-3679.

Suginome, H., Orito, K., Yorita, K., Ishikawa, M.,. Shimoyama, N. and Sasaki, T. 1995. Photoinduced molecular transformations. 157. A new stereo- and regioselective synthesis of 2,6-diaryl-3,7-dioxabicyclo[3.3.0]octane. Lignans involving a β-scission of alkoxy1 radicals as the key step. New total syntheses of (±)-sesamin, (±)-eudesmin, and (±)-yangambin. J. Org. Chem. 60: 3052-3064.

Supudompol, B., Chaowasku, T., Kingfang, K., Burud, K., Wongseripipatana, S. and Likhitwitayawuid, K. 2004. A new pimarane from *Mitrephora tomentosa*. Nat. Prod. Res. 18: 387-390.

Suzuki, R., Okada, Y. and Okuyama, T. 2003. Two flavone *C*-glycosides from the style of *Zea mays* with glycation inhibitory activity. J. Nat. Prod. 66: 564-565.

Takagi, S., Yamaki, M., Masuda, M., Nishihama, Y., Kubota, M. and Lu, S. T. 1981. Yakugaku Zasshi 101: 482.

Takahashi, J. A., Vieira, H. S., Boaventura, M. A. D., Hanson, J. R., Hitchcock, P. B. and de Oliveira, A. B. 2001. Mono- and diterpenes from seeds of *Xylopia sericea*. Quim. Nova 24: 616-618.

Takhtajan, A. 1969. Flowering plants: origin and dispersal. Oliver & Boyd, Edinbergh.

Taneja, S. C., Koul, S. K., Pushpangadan, P., Dhar, K. L., Daniewski, W. M., Schilf , W. 1991. Oxygenated cyclohexanes from *Piper* species. Phytochemistry 30: 871-874.

Tang, S. Y., Whiteman, M., Peng, Z. F., Jenner, A., Yong, E. L. and Halliwell, B. 2004. Characterization of antioxidant and antiglycation properties and isolation of active ingredients from traditional Chinese medicine. Free Radic. Biol. Med. 36: 1575-1587.

Tewtrakul, S., Subhadhirasakul, S., Puripattanavong, J. and Panphadung, T. 2003. HIV-1 protease inhibitory substances from the rhizomes of *Boesenbergia pandurata* Holtt. Songklanakarin J. Sci. Technol. 25: 503-508.

Thebtaranonth, C. and Thebtaranonth, Y. 1986. Naturally occurring cyclohexene oxides. Acc. Chem. Res. 19: 84-90.

Thornalley, P. J. 2003. Use of aminoguanidine (Pimagedine) to prevent the formation of advanced glycation endproducts. Arch. Biochem. Biophys. 419: 31-40.

Tirapellib, C. R., Ambrosioc, S. R., Carlos R. Tirapelli, Sergio R., Da Costad, F. and De Oliveira, A. M. 2002. Inhibitory action of kaurenoic acid from *Viguiera robusta* (Asteraceae) on phenylephrine-induced rat carotid contraction. Fitoterapia 73:56-62.

Trager, W. and Jensen, J. B. 1976. Human malaria parasites in continuous culture. Science 193: 673-675.

Ulrich, P. and Cerami, A. 2001. Protein glycation, diabetes, and aging. Recent Progress in Hormone Research. 56: 1-21.

Vinson, J. A. and Howard III, T. B. 1996. Inhibition of protein glycation and advanced glycation end products by ascorbic acid and other vitamins and nutrients. Nat. Biochem. 7: 659-663.

Voziyan, P. A., Khalifah, R. G., Thibaudeau, C., Yildiz, A., Jacob, J. and Serianni, A. S. 2003. Modification of proteins in vitro by physiological levels of glucose. J. Biol. Chem. 278: 46616-46624.

Wagner, H., Chari, V. M. and Sonnenbicher, J. 1976. ^{13}C-NMR-spektren naturlich vorkommender flavonoide. Tetrahedron Lett. 21: 1799-1802.

Wang, S., Chen, R. Y., Yu, S. S. and Yu, D. O. 2003. Uvamalols D-G: novel polyoxygenated seco-cyclohexenes from the roots of *Uvaria macrophylla.* J. Asian Nat. Prod. Res. 5: 17-23.

Watanabe, Y., Matsui, M., Iibuchi, M. and Hiroe, S. 1975. Two oxoaporphine alkaloids of *Stephania japonica*. Phytochemistry 14: 2522-2523.

Waterman, P. G. and Pootakahm, K. 1979. Chemical studies on the Annonaceae: the alkaloids of the stem and fruit of *Monanthotaxis cauliflora.* Planta Med. 37: 247-252.

Waterman, P. G. and Pootakahm, K. 1979. Chemical studies on the Annonaceae. V. The flavonoids of the fruit of *Popovia cauliflora* Chipp. Planta Med. 35: 366-369.

Weenen, H., Nkunya, M. H. H. and Mgani, Q. A. 1991. Tanzanene, a spirobenzopyranyl sesquiterpene from *Uvaria tanzaniae* Verdc. J. Org. Chem. 56: 5865-5867.

Weenen, H., Nkunya, M. H. H., El-Fadl, A. A., Harkema, S. and Zwanenburg, B. 1990. Lucidene, a bis(benzopyranyl) sesquiterpene from *Uvaria lucida* ssp. *lucida*. J. Org. Chem. 55: 5107-5109.

Wijeratne, E. M. K., Gunatilaka, A. A. L., Kingston, D. G. I., Haltiwanger, R. C. and Eggleston, D.S. 1995. Artabotrine: a novel bioactive alkaloid from *Artabotrys zeylanicus*. Tetrahedron. 51: 7877-7882.

Williams, C. A., and Grayer, R. J. 2004. Anthocyanins and other flavonoids. Nat. Prod. Rep. 21: 539-573.

Wirasathien, L., Pengsuparp, T., Moriyasu, M., Kawanishi, K. and Suttisri, R. 2006. Cytotoxic *C*-benzylated chalcone and other constituents of *Ellipeiopsis cherrevensis*. Arch. Pharm. Res. 29: 497-502

Wu, C. H. and Yen, G. C. 2005. Inhibitory effect of naturally occurring flavonoids on the formation of advanced glycation endproducts. J. Agric. Food Chem. 53: 3167-3173.

Wu, J. H., Chang, X. H., Duh, C. Y. and Wang, S. K. 1993. Cytotoxic alkaloids of *Annona montana*. Phytochemistry 33: 497-500.

Wu, J. H., Liao, S. X. and Mao, S. L. 1997. Desmosflavanoe Ⅱ: A new flavanone from *Desmos cochinchinensis* Lour. J. Chin. Pharm. Sci. 6: 119-120.

Wu, J. H., Liao, S. X., Lan, C. Q., Yi, Y. H., and Su, Z. W. 1999. Isolation and identification of constituents from *Desmos dumosus*. SXVI International Botanical Congess. Abstract number: 5635.

Wu, J. H., Liao, S. X., Liang, H. Q. and Mao, S. L. 1994. Desmosflavone: a new flavone from *Desmos cochinchinensis* Lour. Chin. Chem. Lett. 5: 211-212.

Wu, J. H., Mao, S. L., Liao, S. X., Yi, Y. H., Lan, C.Q. and Su, Z. W. 2001. Desmosdumotin B: a new special flavone from *Desmos dumosus*. Chin. Chem. Lett. 12: 49-50.

Wu, J. H., Wang, X. H., Yi, Y. H. and Lee, K. H. 2003. Anti-AIDS agents 54. a potent anti-HIV chalcone and flavonoids from Genus *Desmos*. Bioorg. & Med. Chem. Lett. 13: 1813-1815.

Wu, Y. C., Hung, Y. C., Chang, F. R., Cosentino, M., Wang, H. K. and Lee, K. H. 1996. Identification of *ent*-16β, 17-dihydroxykauran-19-oic acid as an anti-HIV principle and isolation of the new diterpenoids annosquamosins A and B from *Annona squamosa*. J. Nat. Prod. 59: 635-637.

Wu, Y. C., Lu, S. T., Wu, T. S., Lee, K. H. 1987. Kuafumine, a new cytotoxic oxoaporphine alkaloid from *Fissistigma glaucescens*. Heterocycles. 26*:* 9-12.

Xu, Q. M., Zou, Z. M., Xu, L. Z. and Yang , S. L. 2005. New polyoxygenated cyclohexenes from *Uvaria kweichowensis* and their antitumour activities. Chem. Pharm. Bull. (Tokyo) 53: 826-828.

Yamaguchi, F., Ariga, T., Yoshimura, Y. and Nakazawa, H. 2000. Antioxidative and anti-glycation activity of garcinol from *Garcinia indica* fruit rind. J. Agric. Food Chem. 48: 180-185.

Yamaguchi, F., Ariga, T., Yoshimura, Y. and Nakazawa, H. 2000. Antioxidative and anti-glycation activity of garcinol from *Garcinia indica* fruit rind. J. Agric. Food Chem. 48: 180-185.

Yamasaki, K., Kohda, H., Kobayashi, T., Kasai, R. and Tanaka, O. 1976. Structure of stevia diterpene-glucosides: application of ^{13}C NMR. Tetrahedron Lett. 13: 1005-1008.

Yang, Y. L., Chang, F. R., Wu, C. C., Wang, W. Y. and Wu, Y. C. 2002. New *ent*-kaurane diterpenes with anti-platelet aggregation activity from *Annona squamosa*. J. Nat. Prod. 65: 1462-1467.

Yokozawa, T. and Nakagawa, T. 2004. Inhibitory effects of Luobuma tea and its components against glucose-mediated protein damage. Food Chem. Toxicol. 42: 975-981.

Yu, R., Li, B. G., Ye, Q. and Zhang, G. L. 2005. A novel alkaloid from *Mitrephora maingayi*. Nat. Prod. Res. 19: 359-362.

Zgoda, J. R., Freyer, A. J., Killmer, L. B. and Porter, J. R. 2001. Polyacetylene carboxylic acids from *Mitrephora celebica*. J. Nat. Prod. 64: 1348-1349.

Zgoda-Pols, J. R., Freyer, A. J., Killmer, L. B. and Porter, J. R. 2002. Antimicrobial diterpenes from the stem bark of *Mitrephora celebica*. Fitoterapia 73: 434-438.

Zhou, L. D., Yu, J. G., Guo, J., and Yang, S. L. 2001. A-ring formylated flavonoids and oxoaporphinoid alkaloid from *Dasymaschalon rostratum* Merr. Zhongguo Zhong Yao Za Zhi 26: 39-41.

APPENDIX
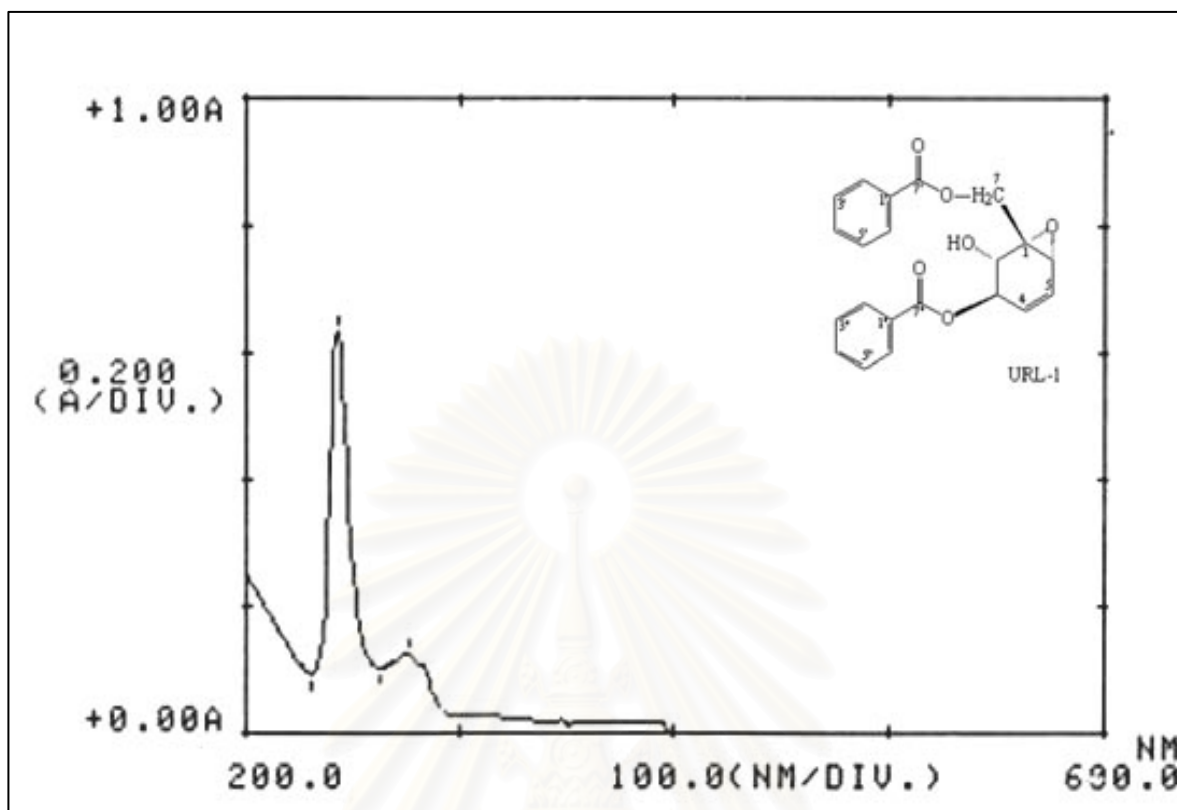
Figure 11. UV Spectrum of compound URL-1 (in CDCl$_3$)
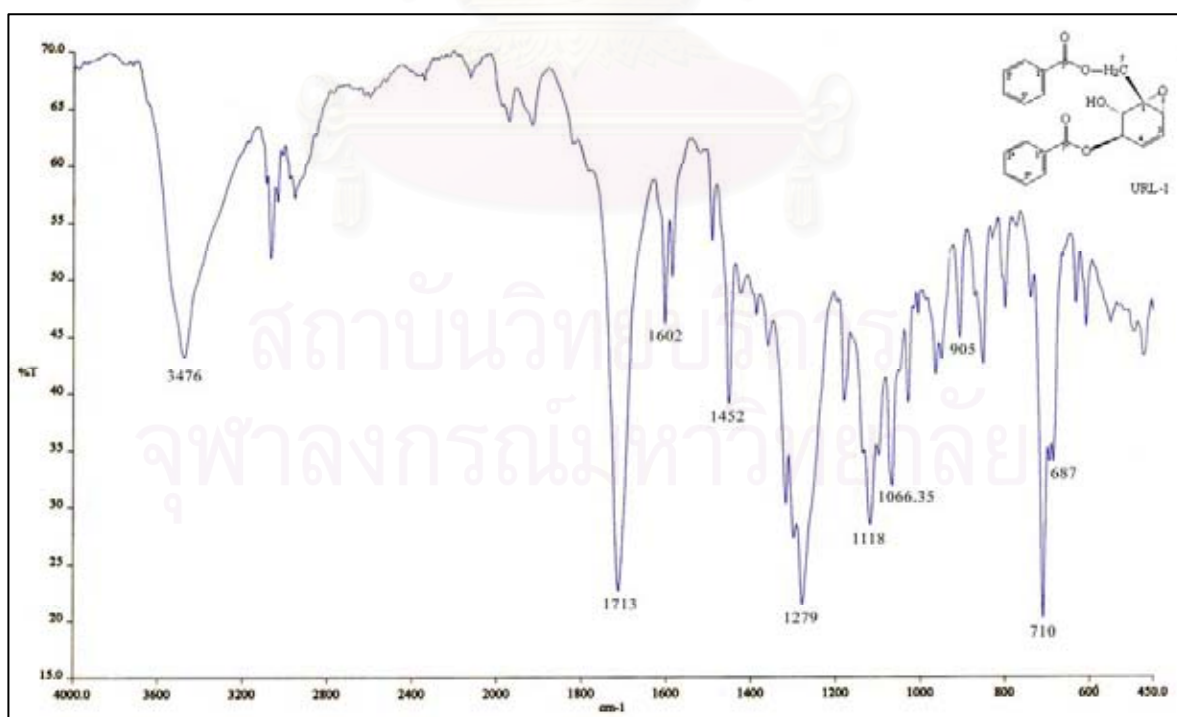
Figure 12. IR Spectrum of compound URL-1 (KBr disc)
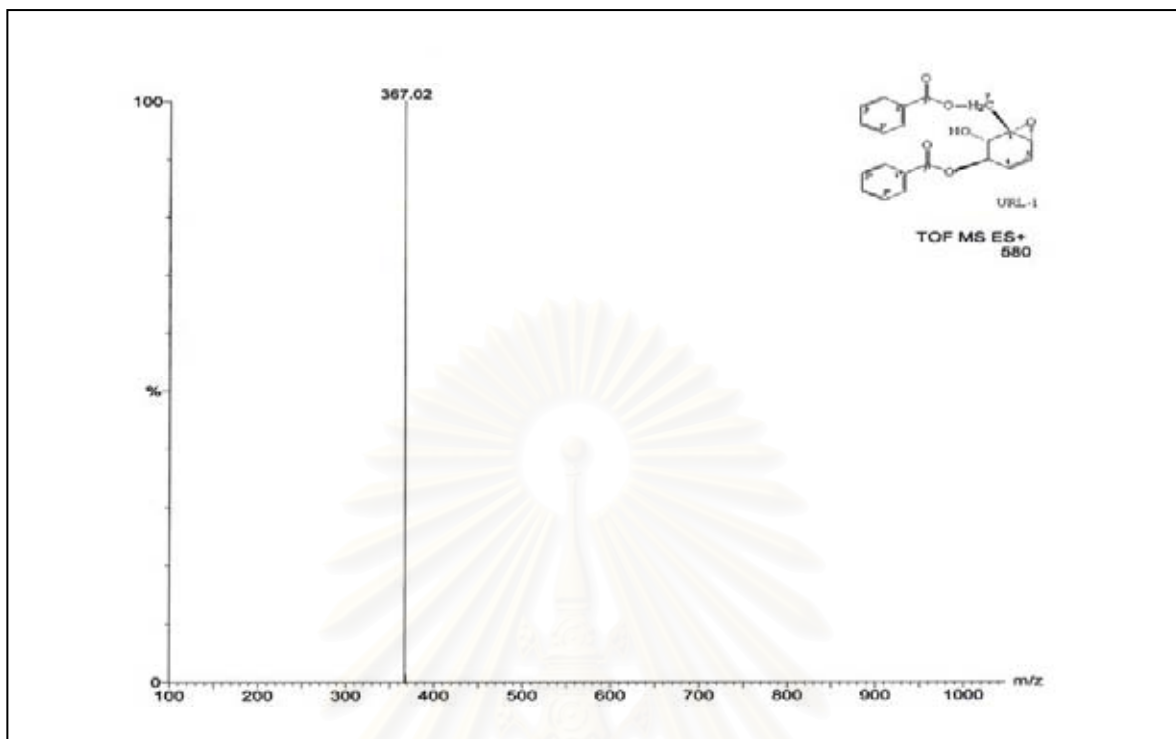
Figure 13. ESITOF Mass spectrum of compound URL-1
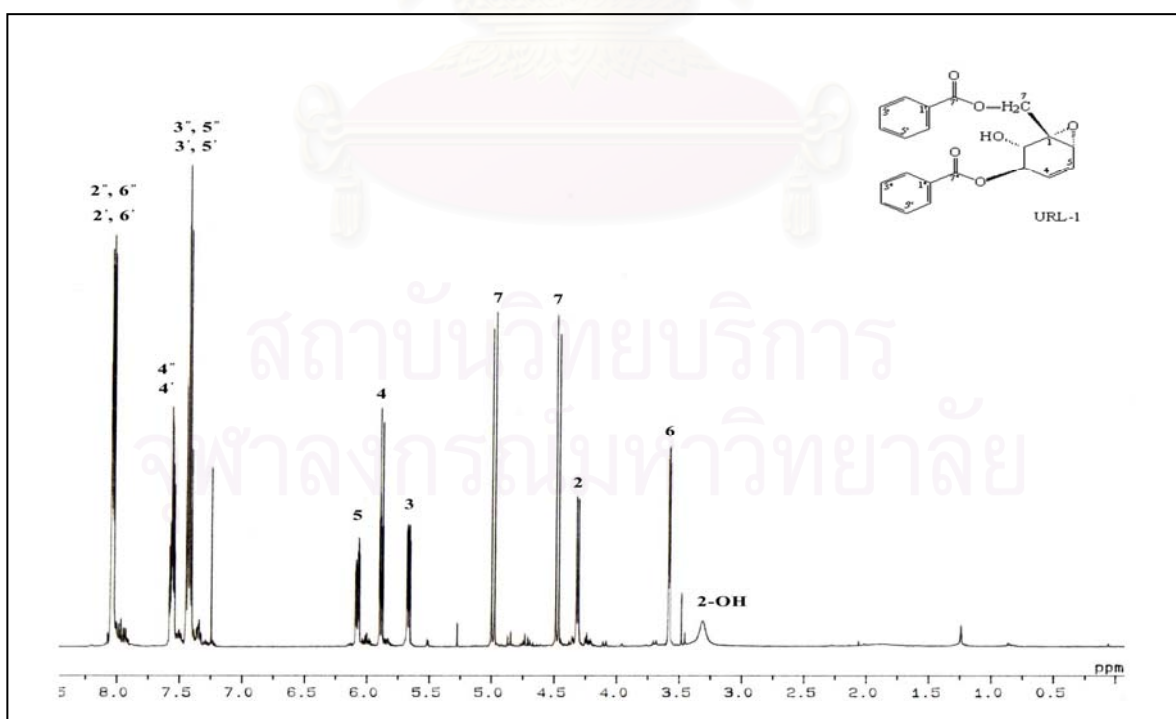
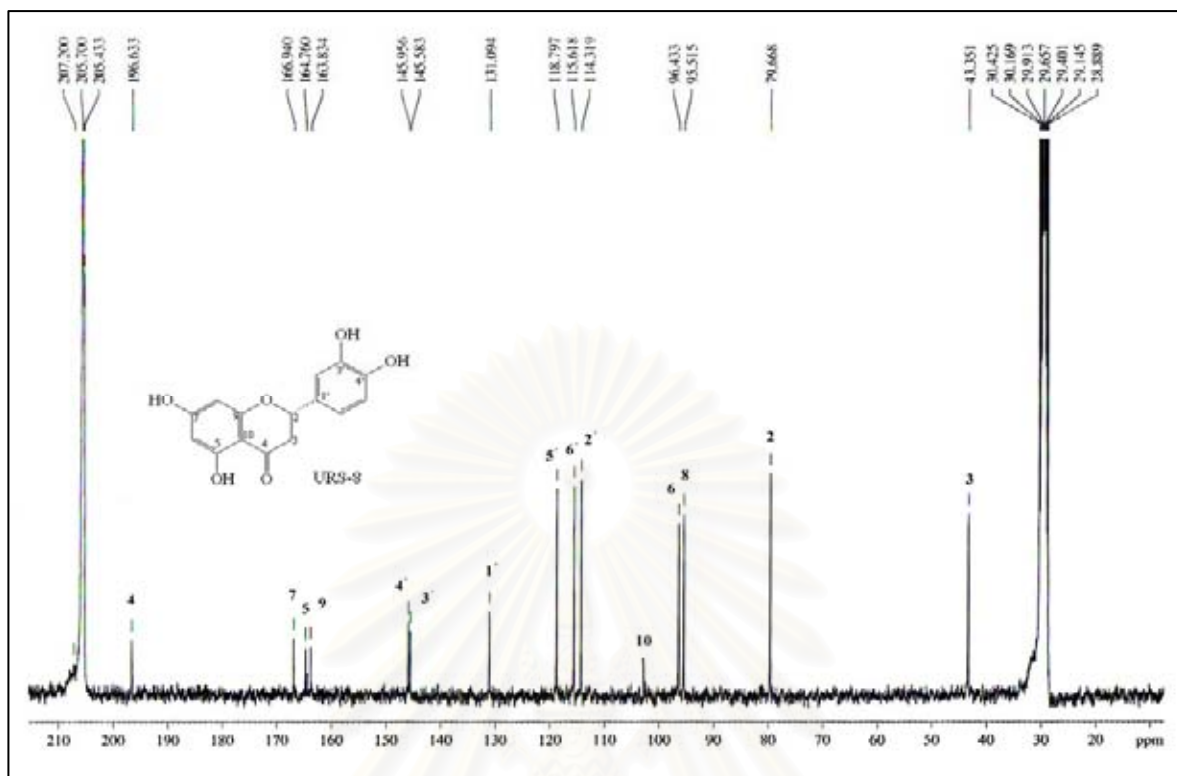**Figure 14a.** ^{1}H NMR (500 MHz) Spectrum of compound URL-1 (in CDCl$_3$)
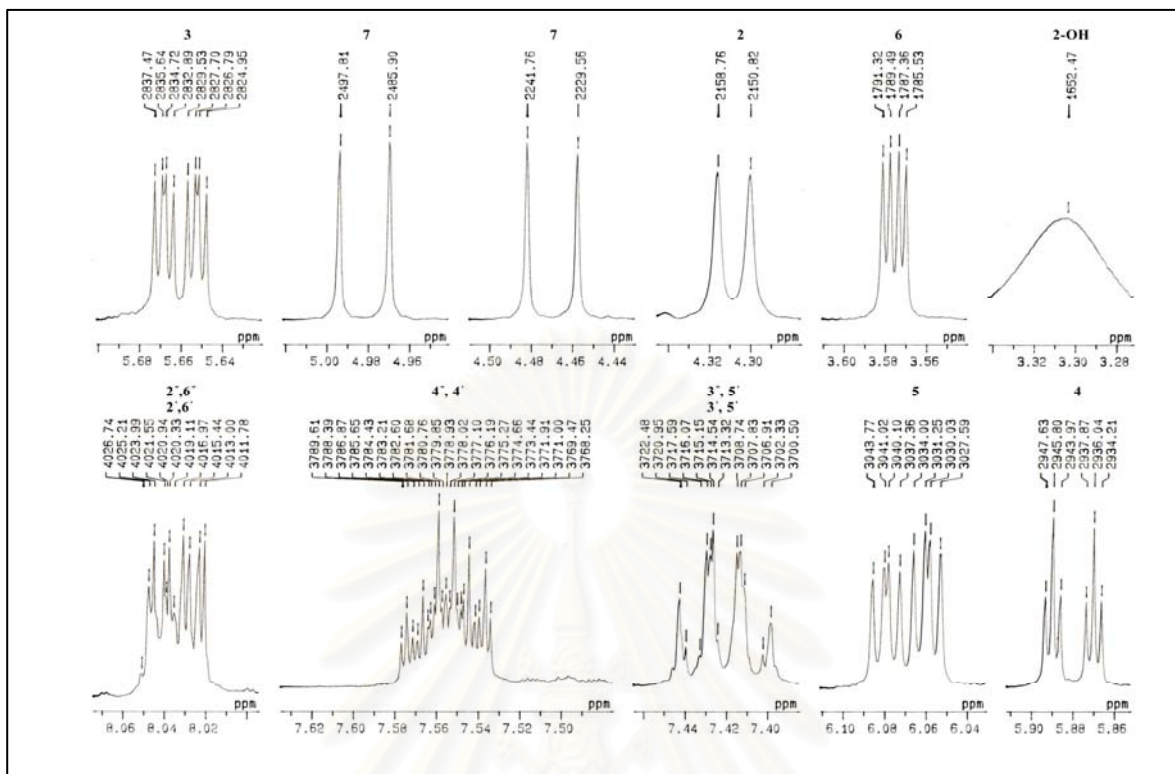
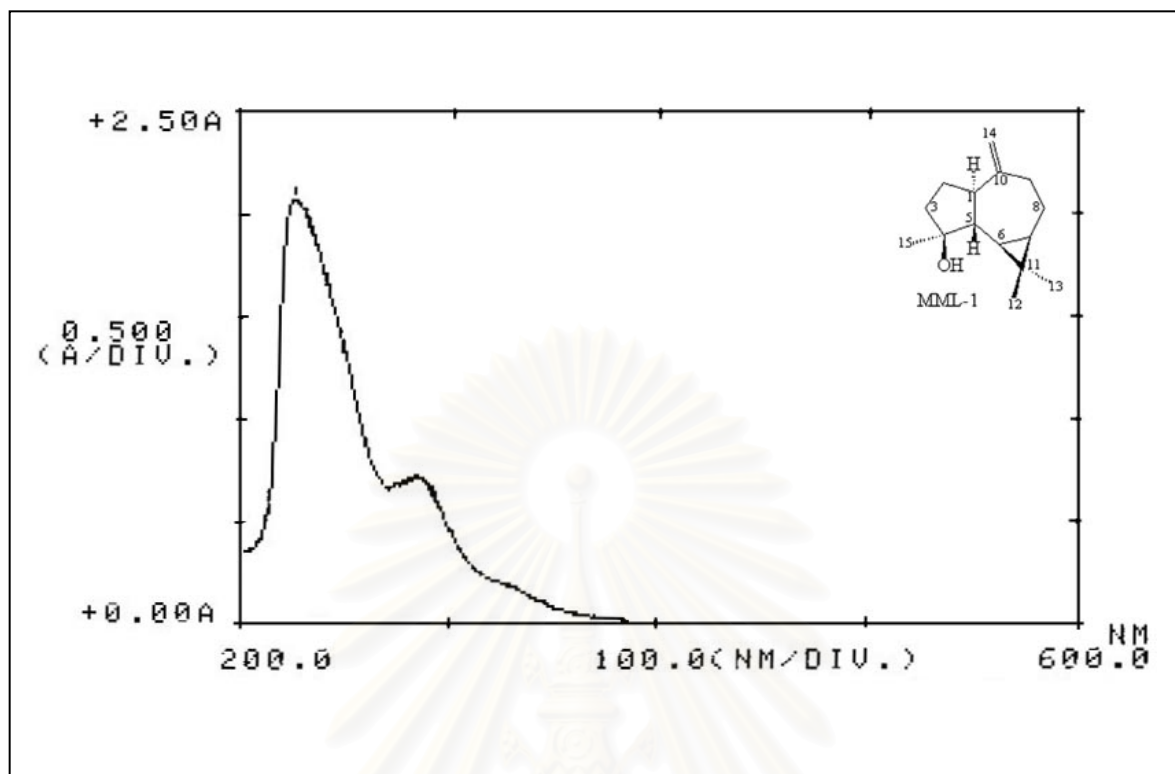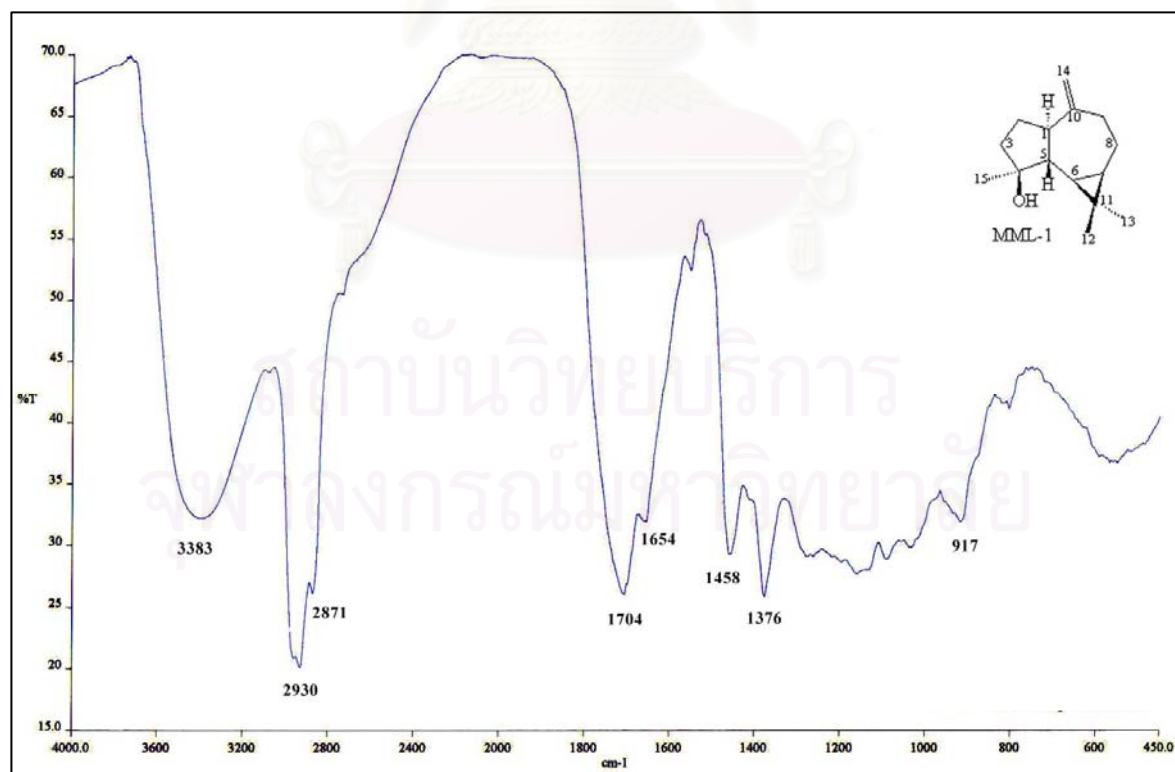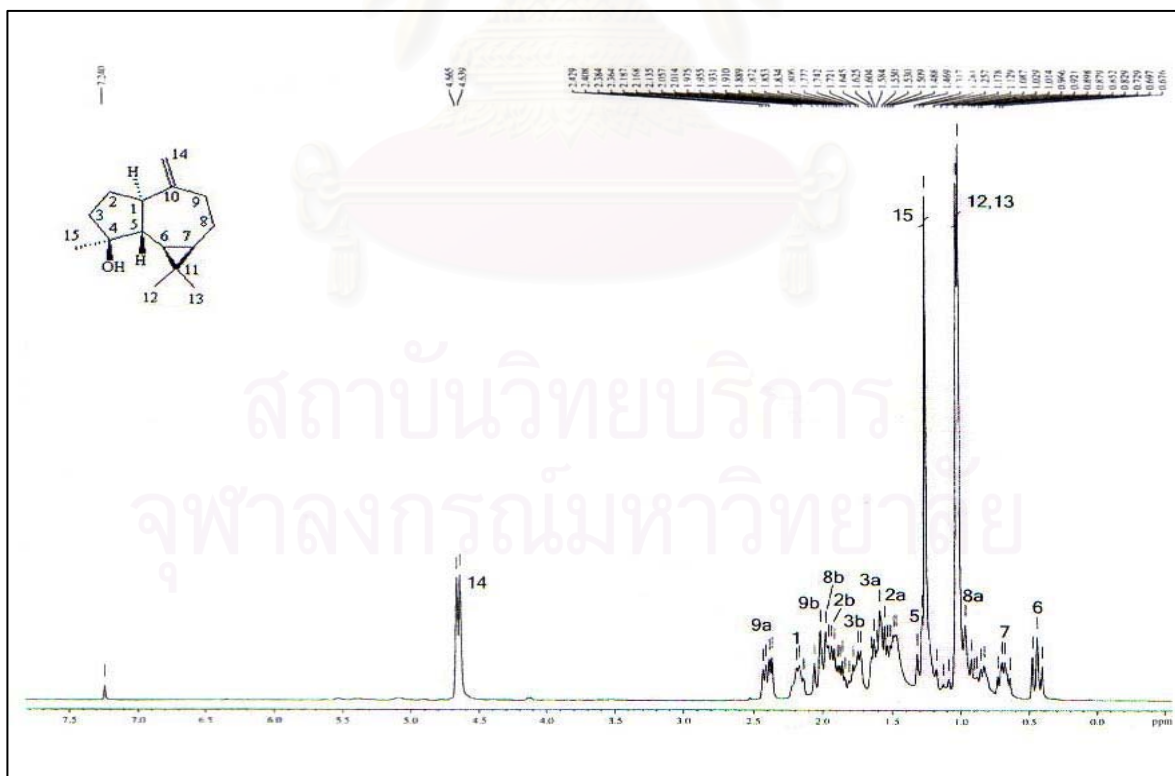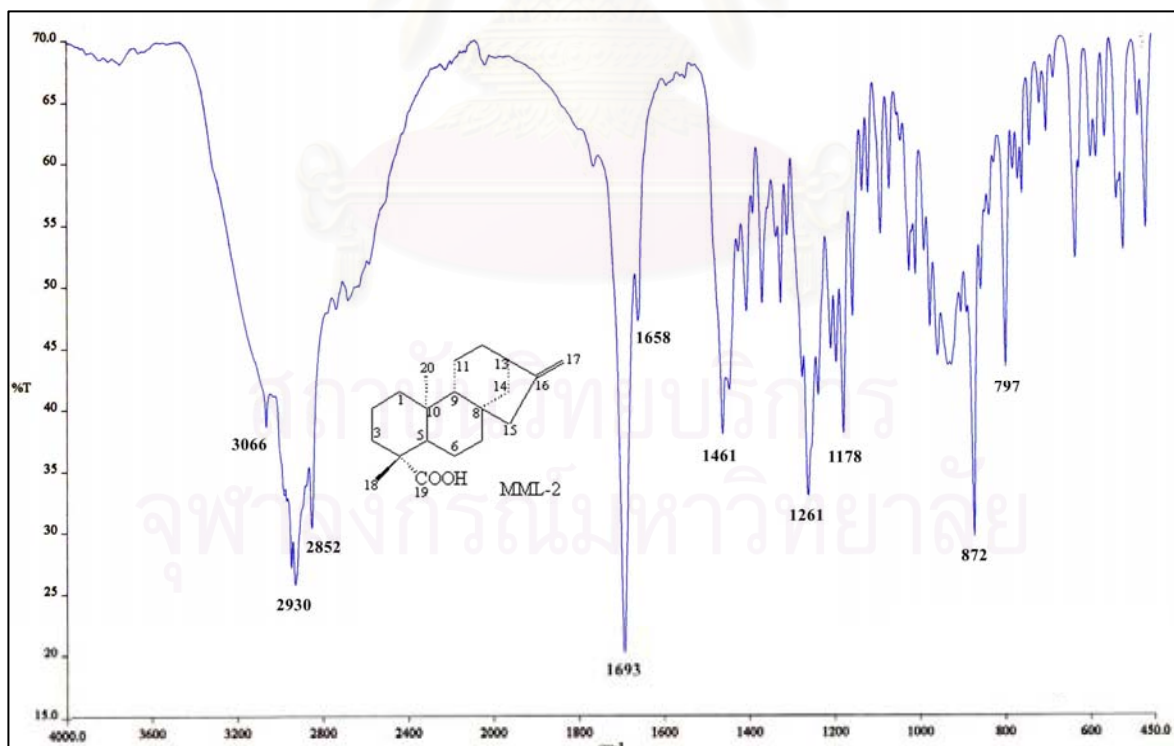**Figure 14b.** ^{1}H NMR (500 MHz) Spectrum of compound URL-1 (in CDCl$_3$, expansion)
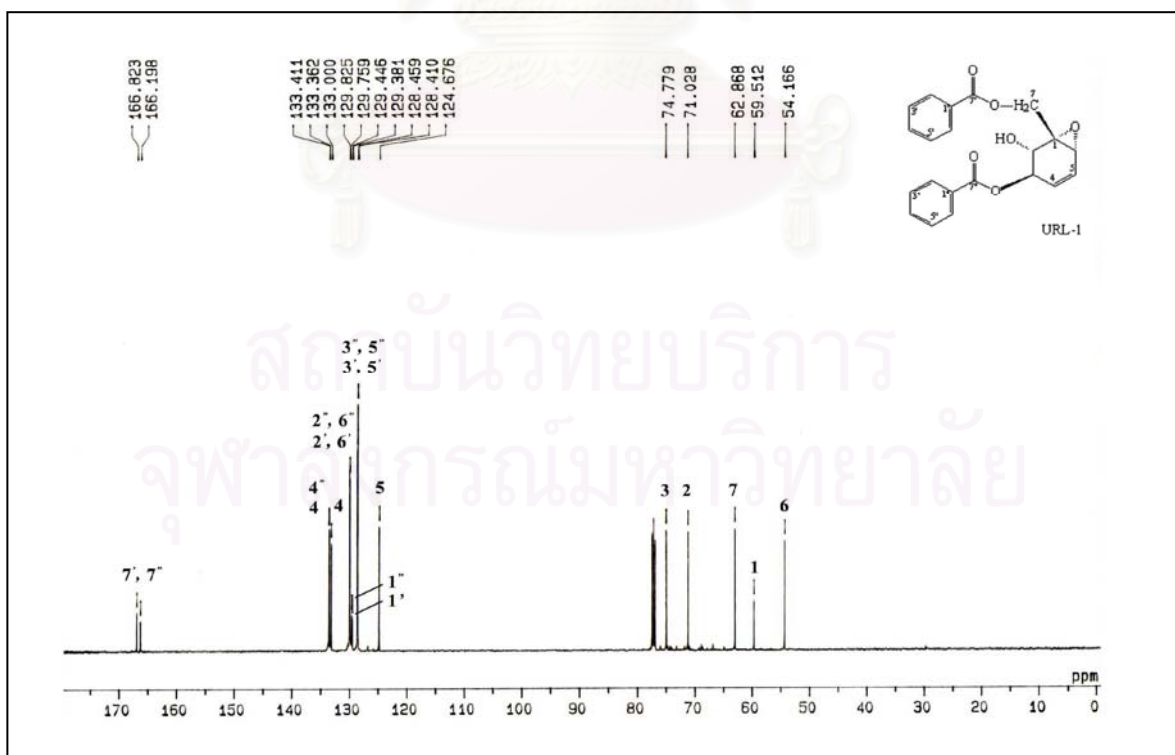
Figure 15. ^{13}C NMR (125 MHz) Spectrum of compound URL-1 (in CDCl$_3$)
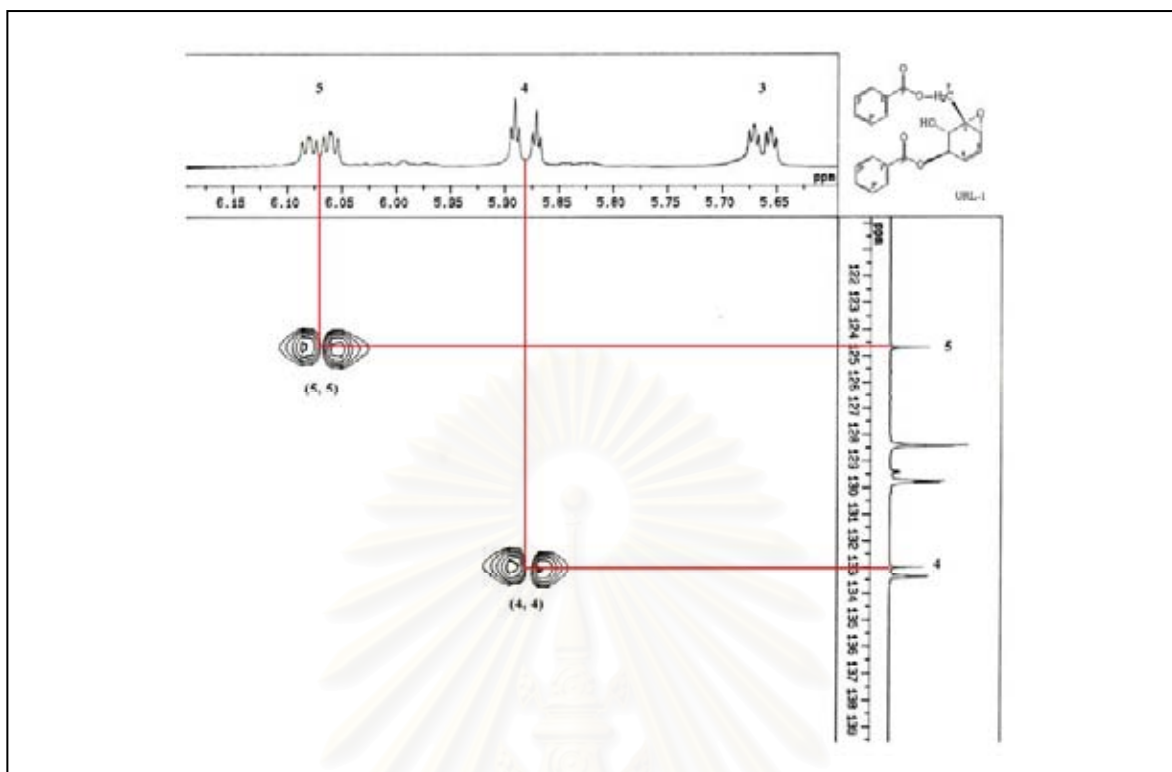
Figure 16. HMQC Spectrum of compound URL-1 (in CDCl₃)
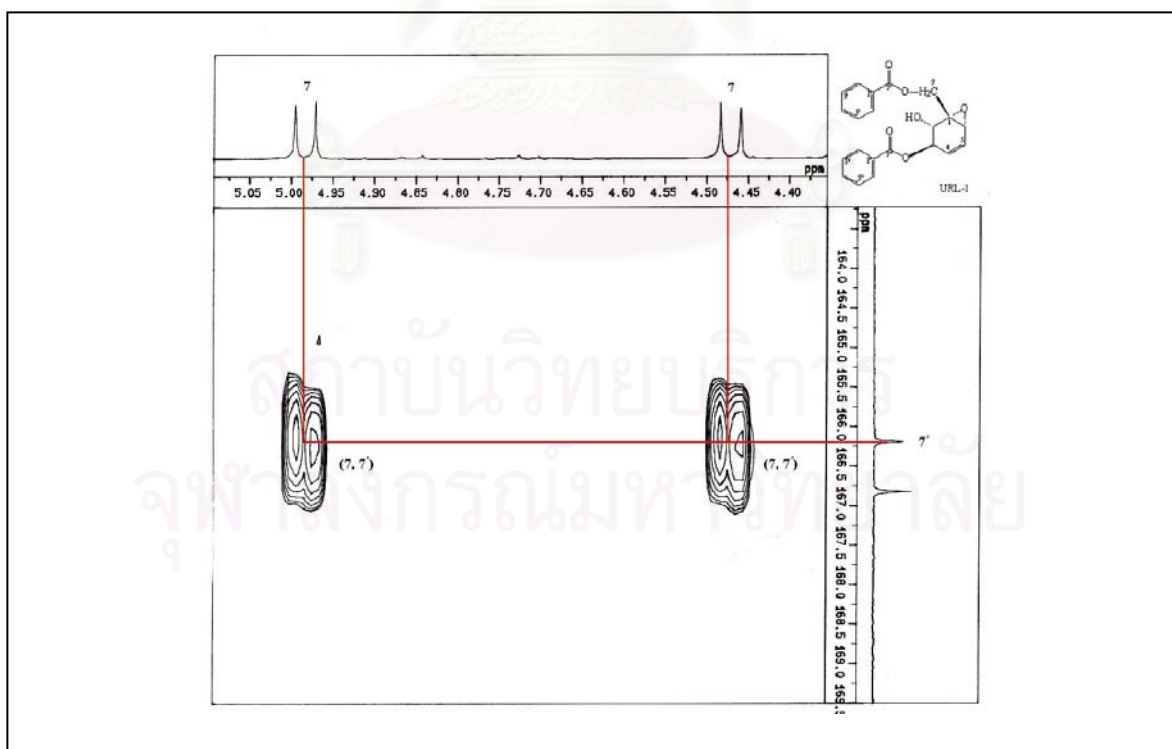
Figure 17. HMBC Spectrum of compound URL-1 (in CDCl₃)
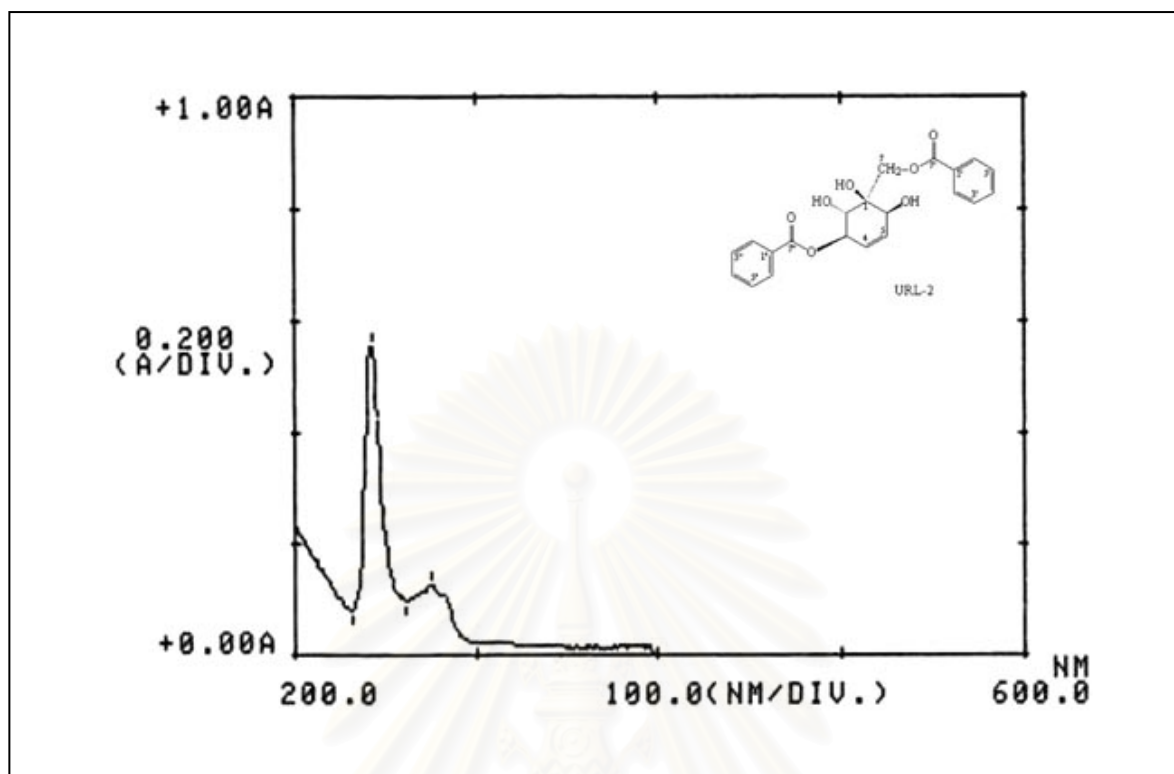
Figure 18. UV Spectrum of compound URL-2 (in CDCl$_3$)
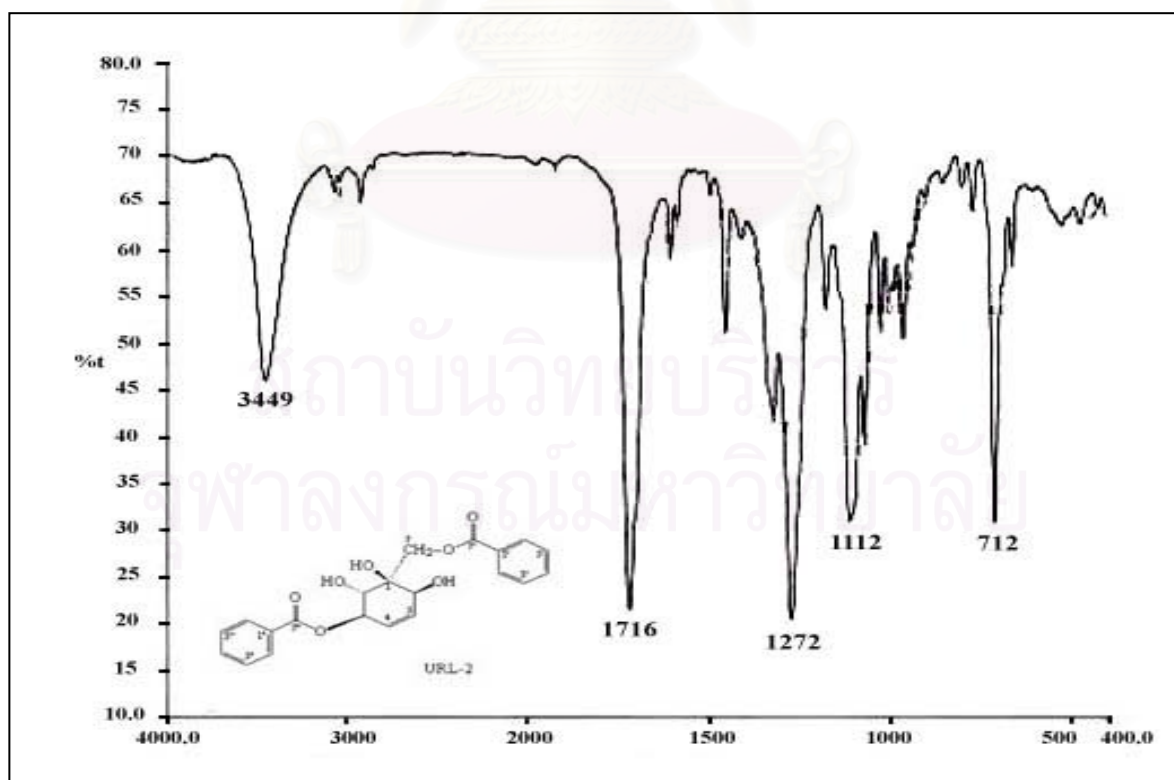
Figure 19. IR Spectrum of compound URL-2 (KBr disc)
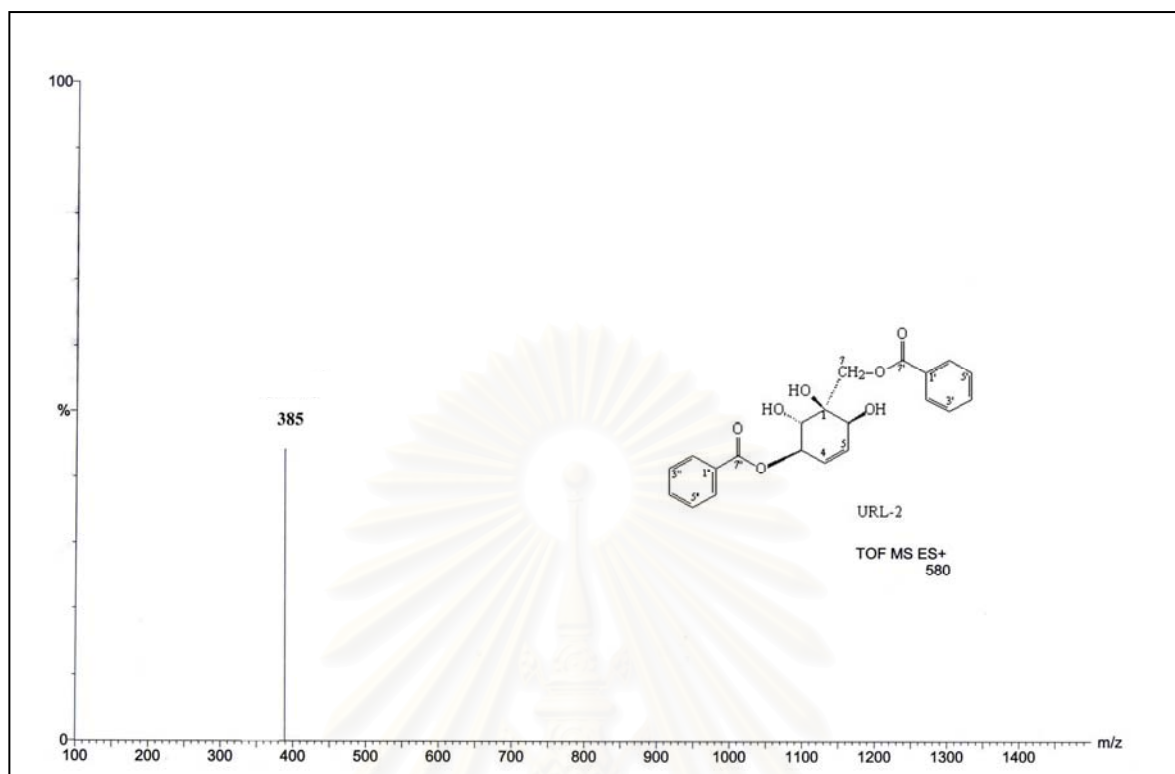
Figure 20. ESITOF Mass spectrum of compound URL-2
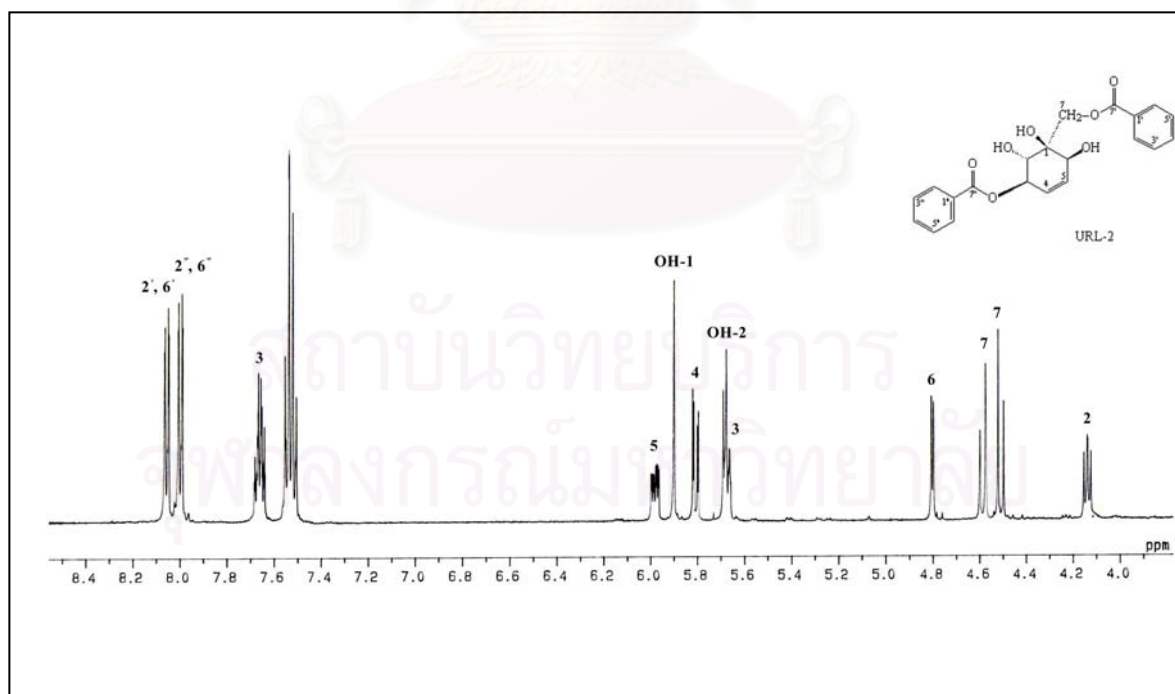
**Figure 21a.** ^{1}H NMR (500 MHz) Spectrum of compound URL-2 (in DMSO-d_6)
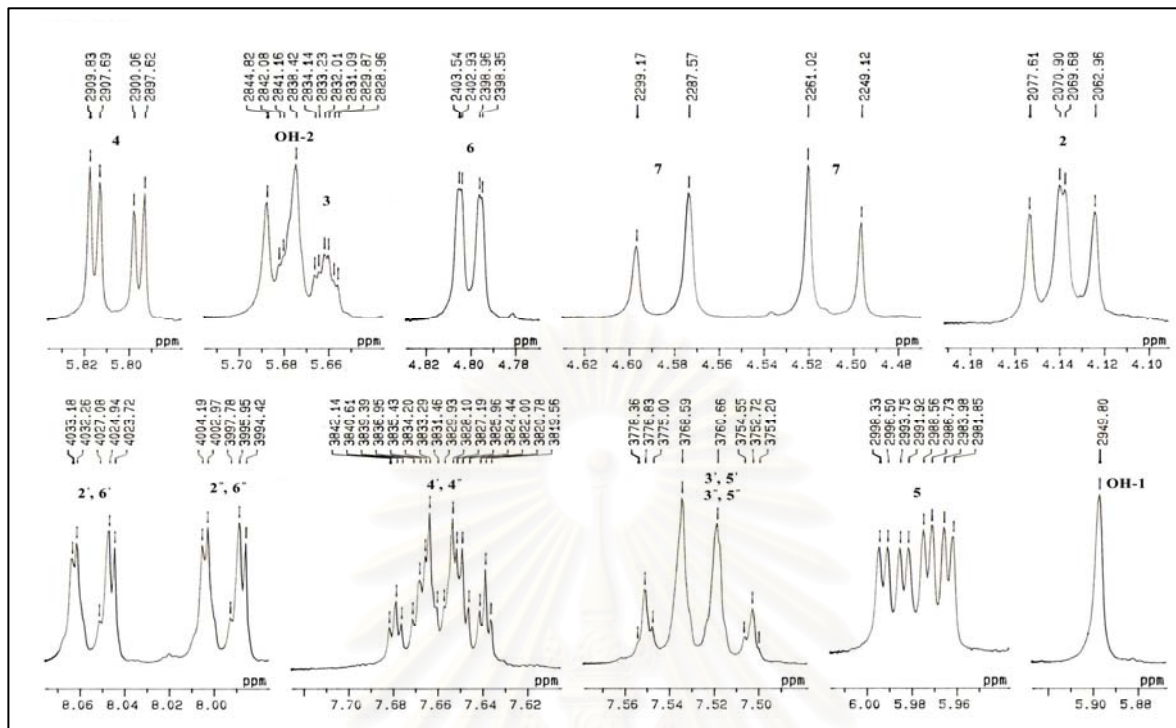
Figure 21b. ^{1}H NMR (500 MHz) Spectrum of compound URL-2 (in DMSO-d_6, expansion)
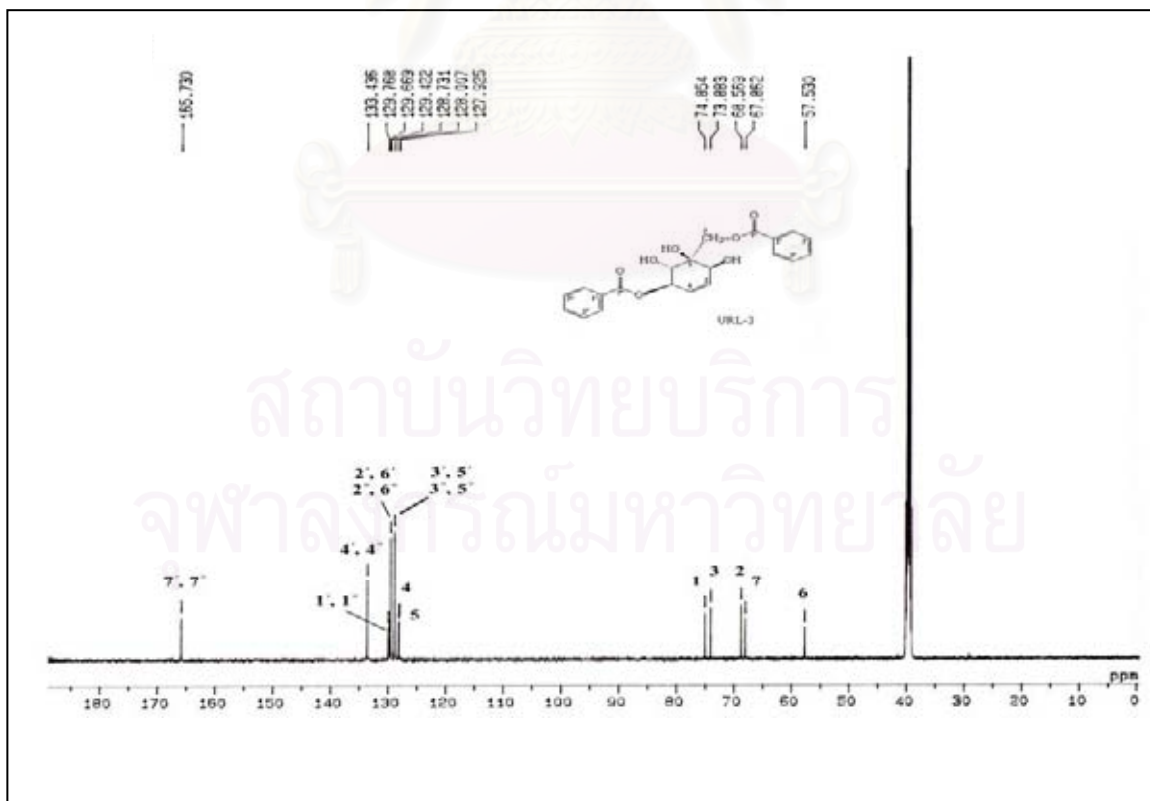
Figure 22. ^{13}C NMR (125 MHz) Spectrum of compound URL-2 (in DMSO-d_6)
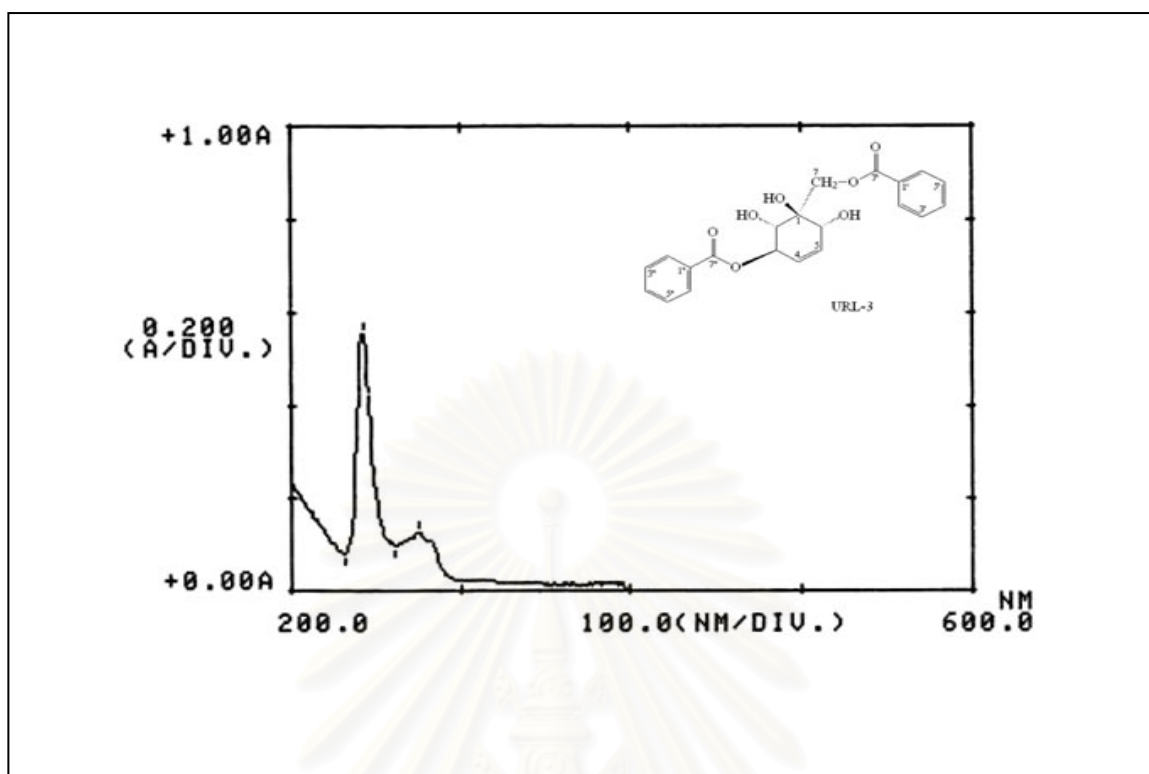
Figure 23. UV Spectrum of compound URL-3 (in CDCl$_3$)
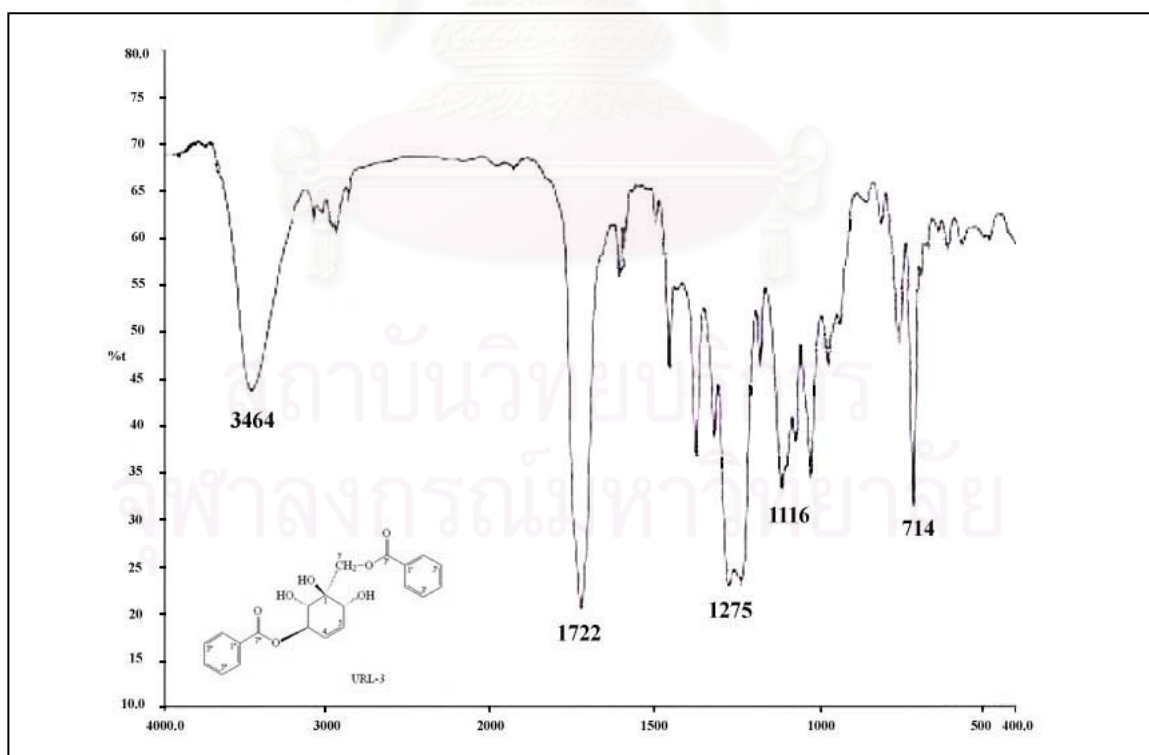
Figure 24. IR Spectrum of compound URL-3 (KBr disc)
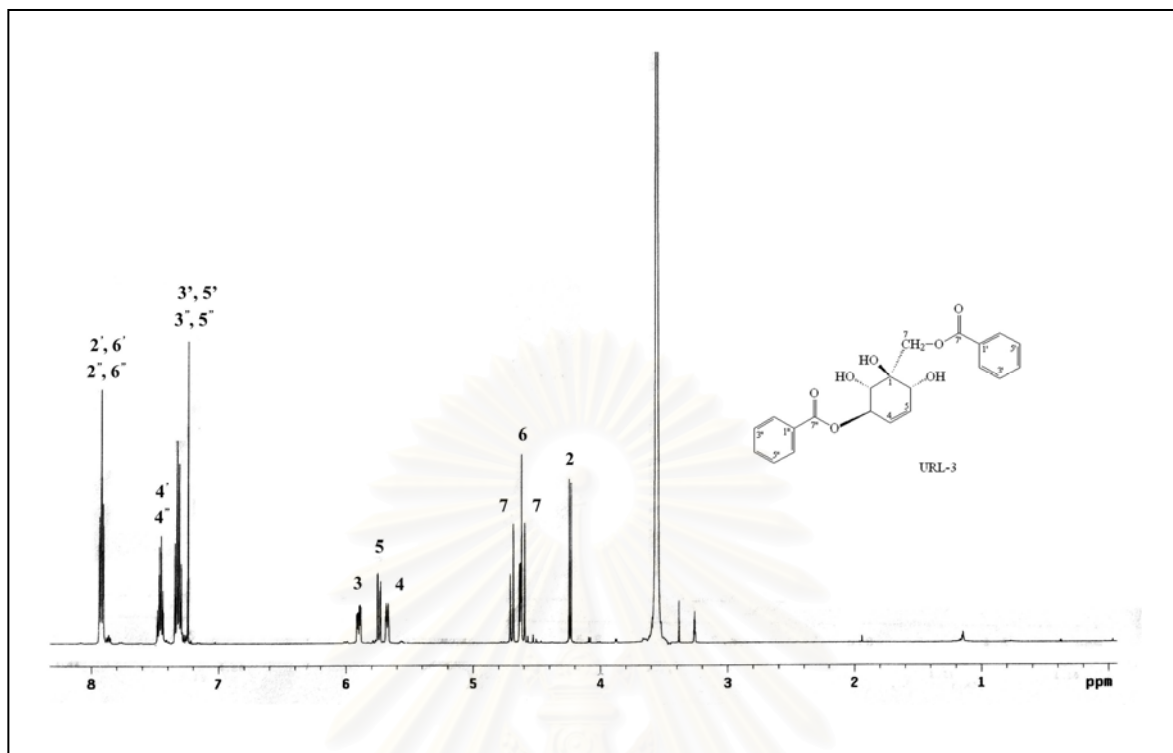
Figure 25. ^{1}H NMR (500 MHz) Spectrum of compound URL-3 (in CDCl$_3$)
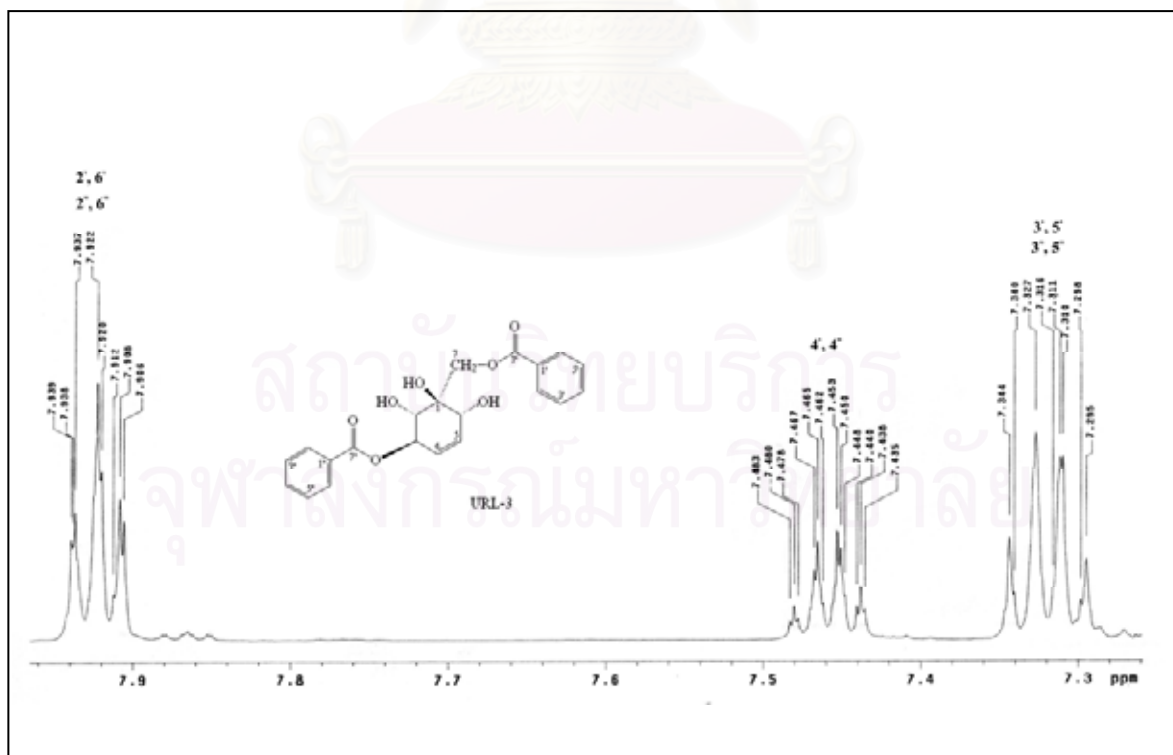
Figure 26. . ^{1}H NMR (500 MHz) Spectrum of compound URL-3 (in CDCl$_3$, expansion)

Figure 27. ^{13}C NMR (125 MHz) Spectrum of compound URL-3 (in CDCl$_3$)

Figure 28. ESITOF Mass spectrum of compound URL-4

Figure 29a. ^{1}H NMR (500 MHz) Spectrum of compound URL-4 (in DMSO-d_6)

Figure 29b. ^{1}H NMR (500 MHz) Spectrum of compound URL-4 (in DMSO-d_6, expansion)
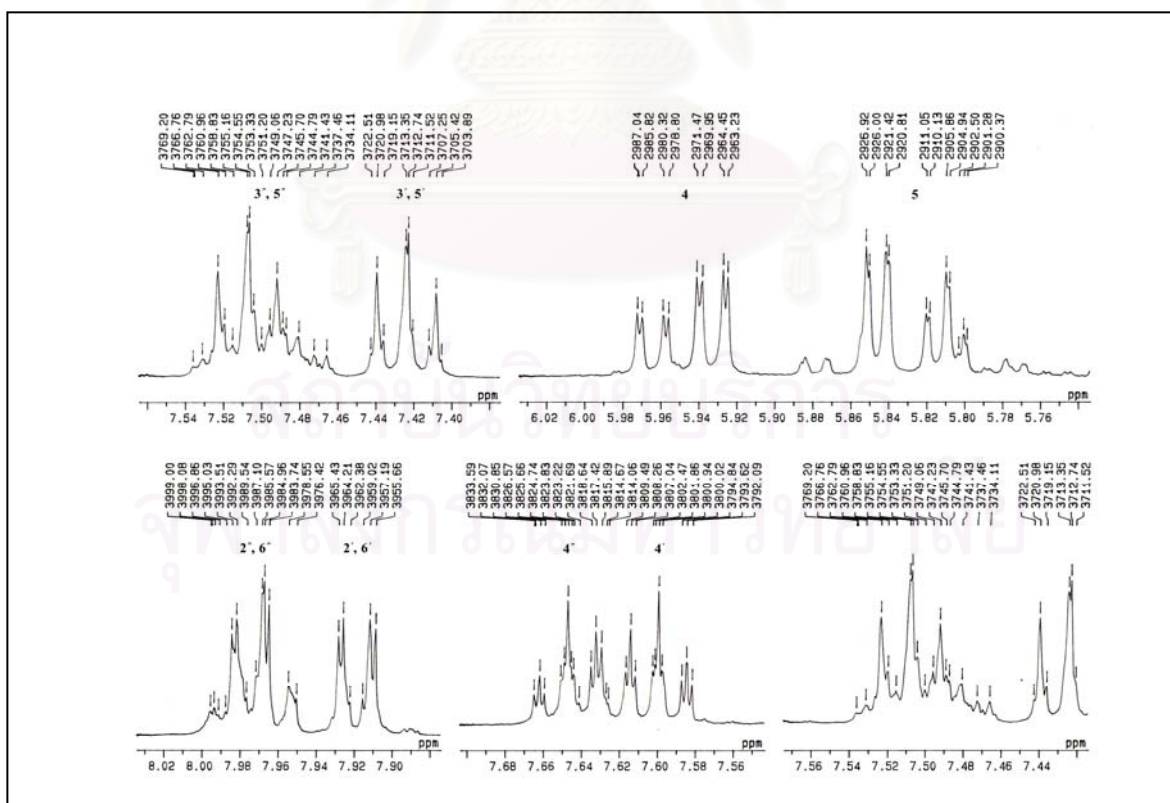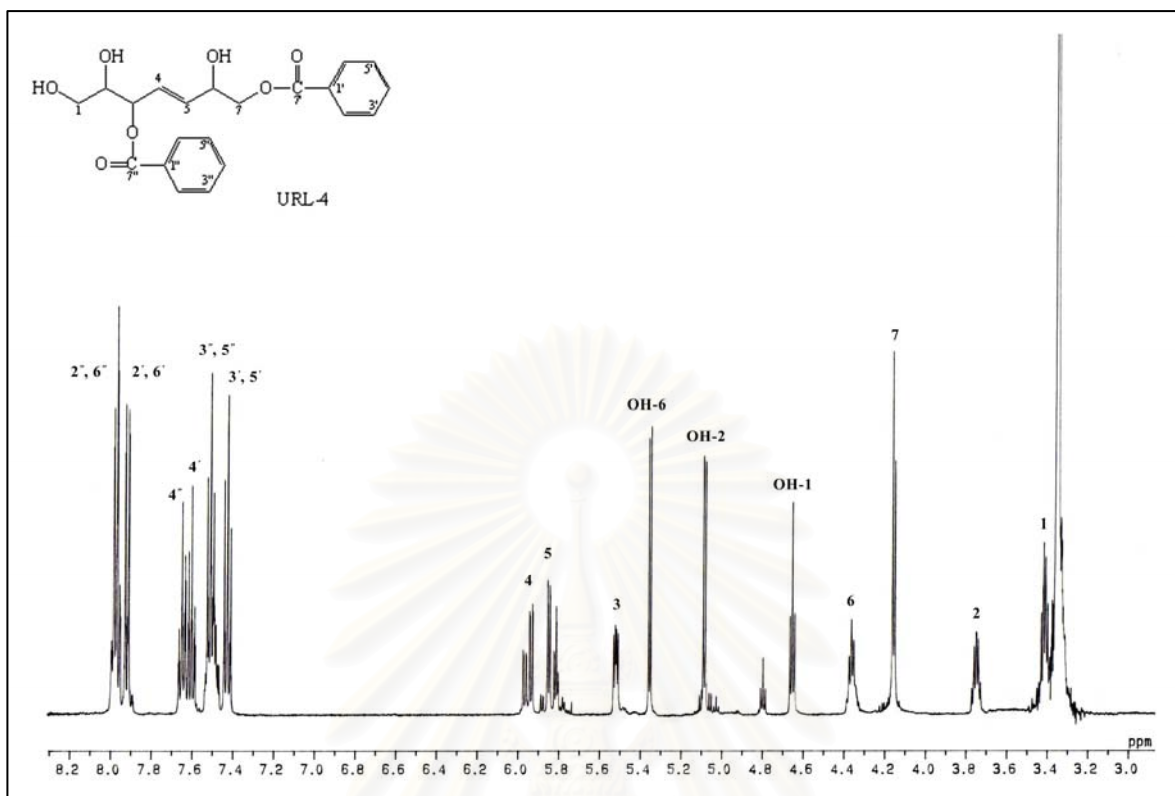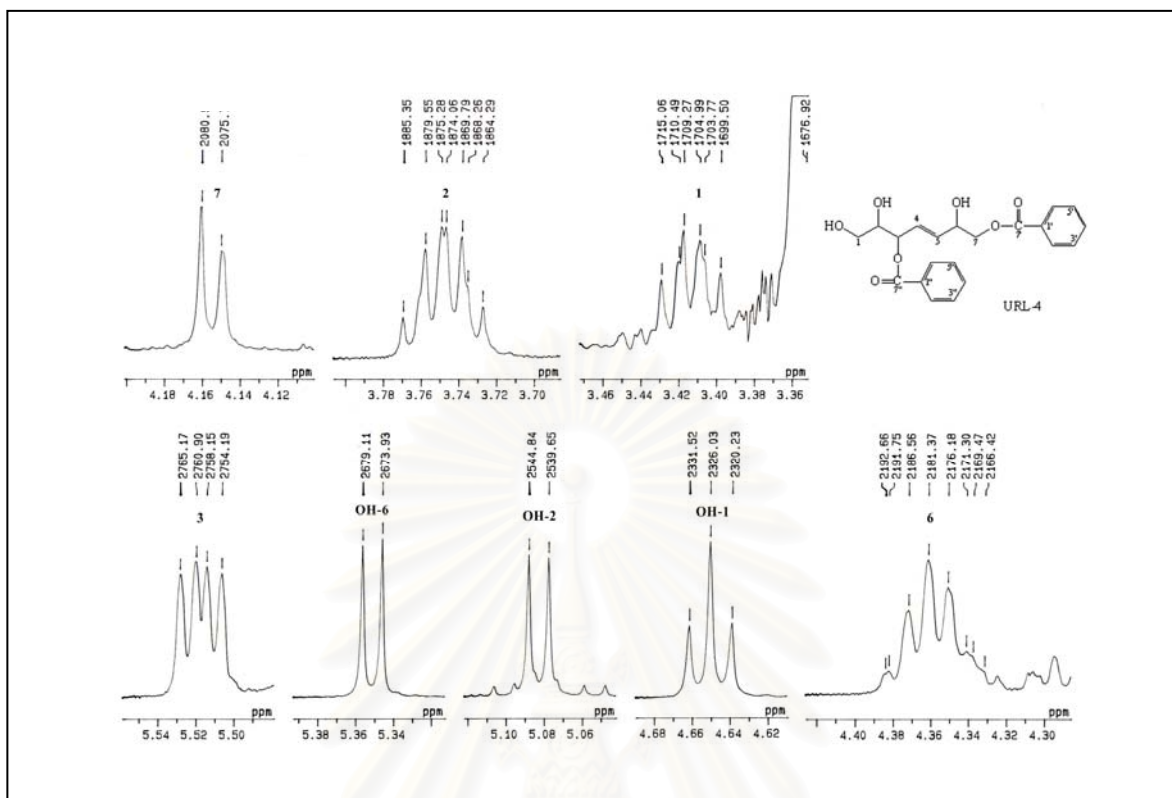
Figure 29c. ^{1}H NMR (500 MHz) Spectrum of compound URL-4 (in DMSO-d_6, expansion)
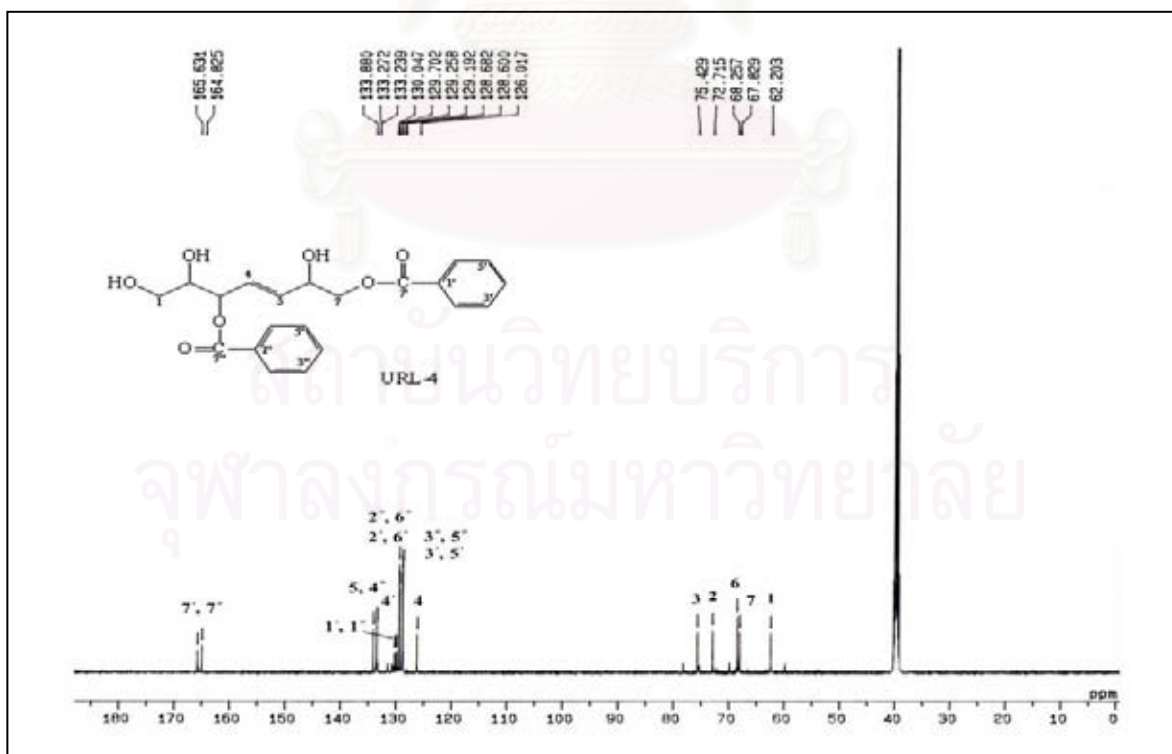
Figure 30. ^{13}C NMR (125 MHz) Spectrum of compound URL-4 (in DMSO-d_6)
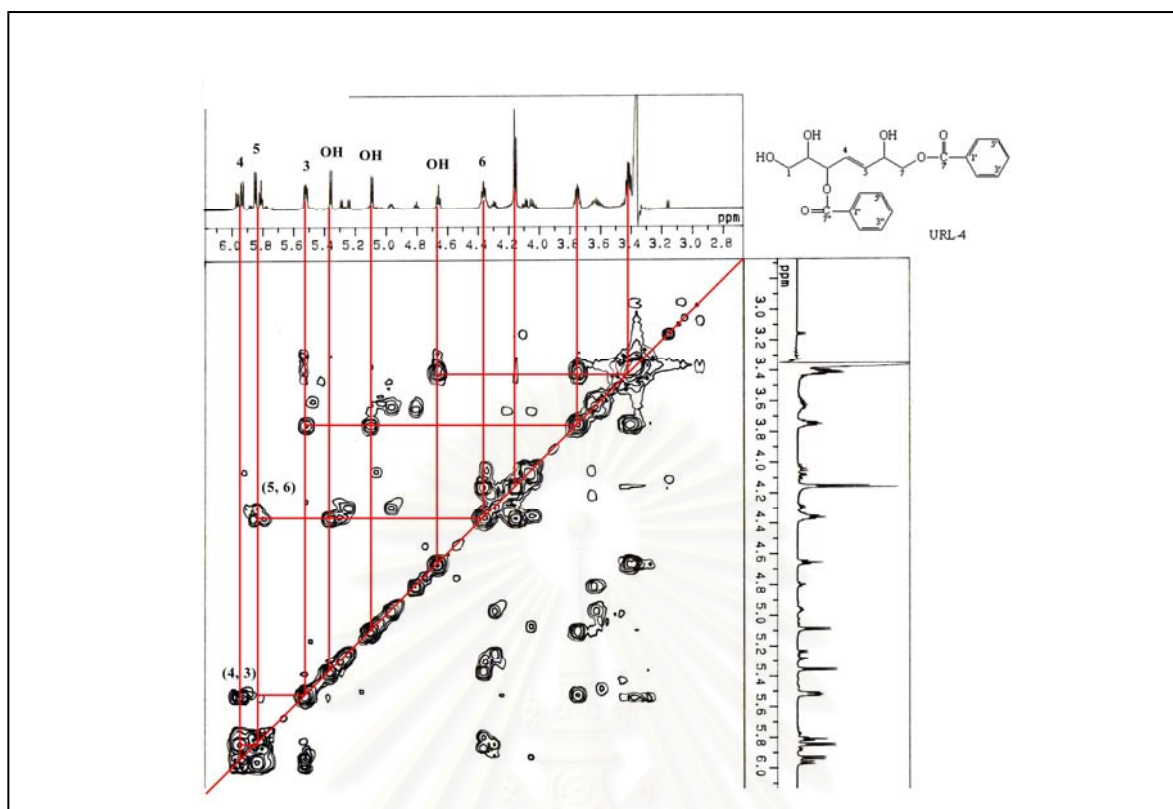
Figure 31. ^{1}H–^{1}H COSY Spectrum of compound URL-4 (in DMSO-d_6)
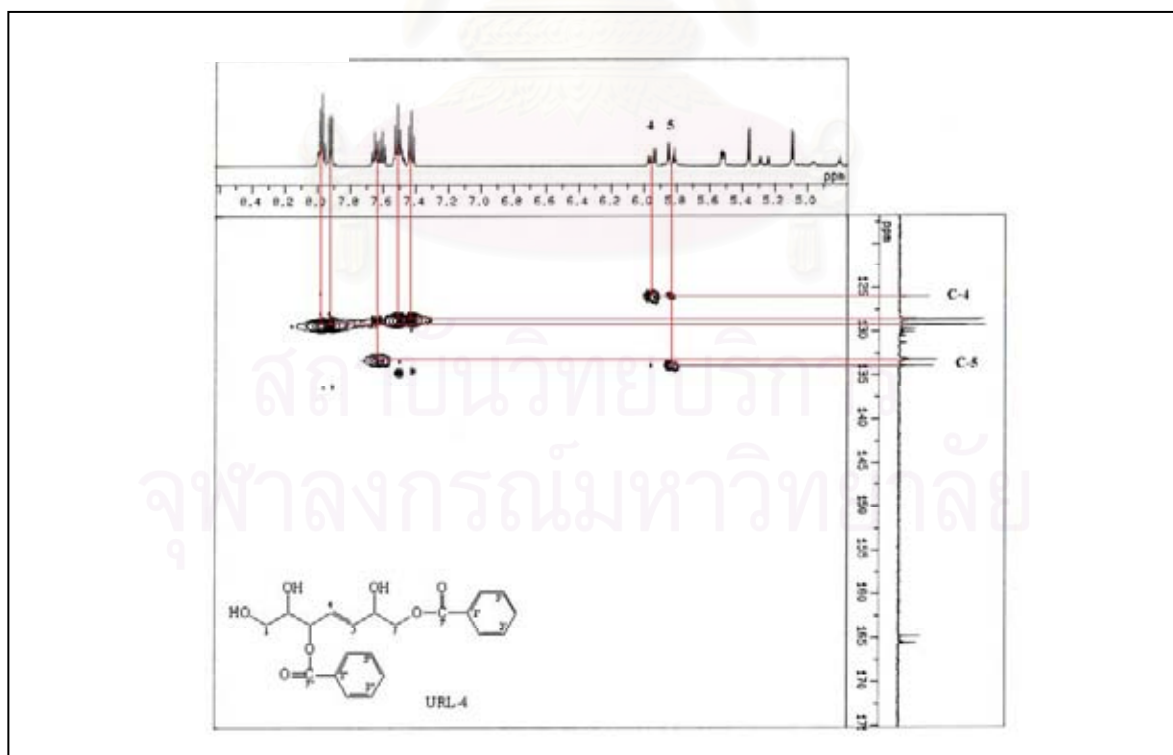
Figure 32. HMQC Spectrum of compound URL-4 (in DMSO-d_6)
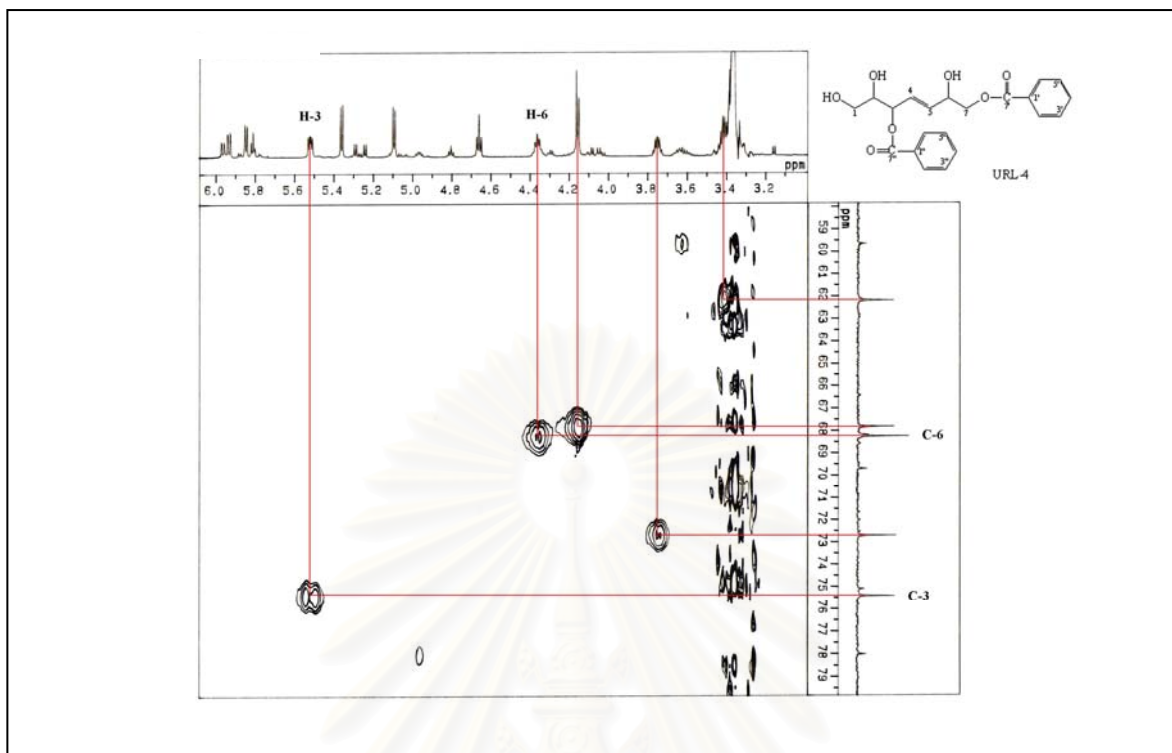
Figure 33. HMQC Spectrum of compound URL-4 (in DMSO-d_6, expansion)
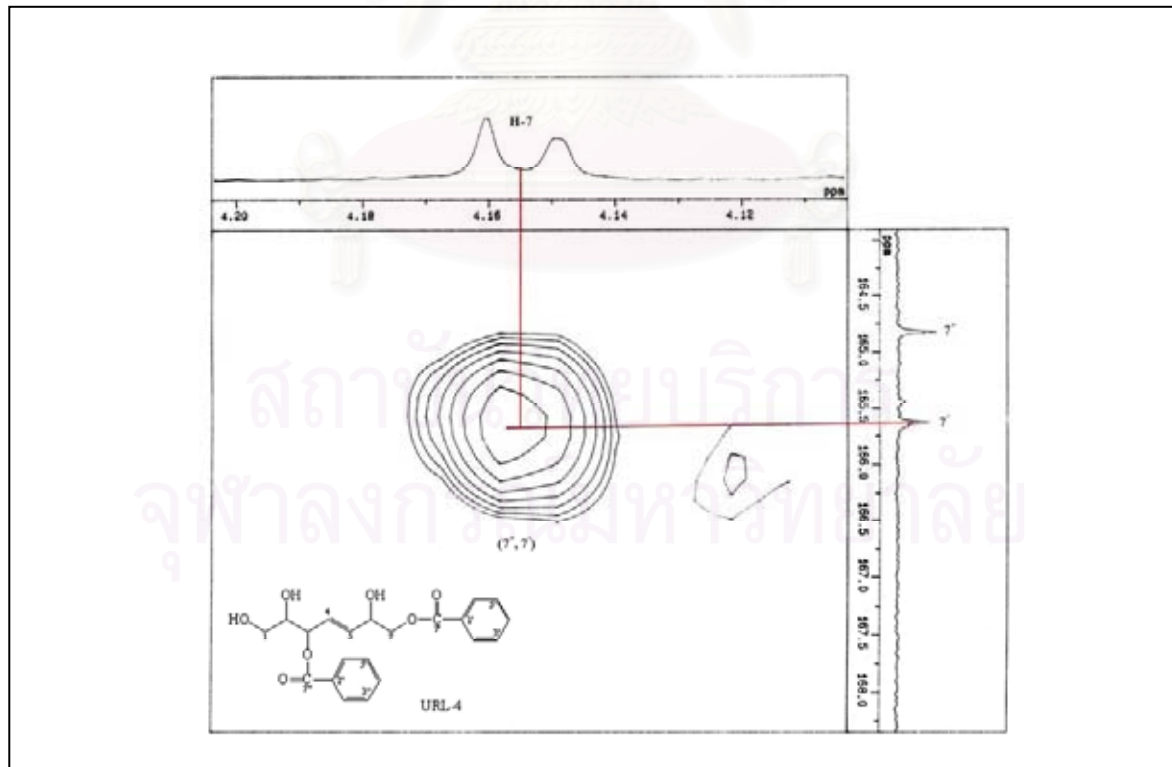
Figure 34a. HMBC Spectrum of compound URL-4 (in DMSO-d_6, expansion)
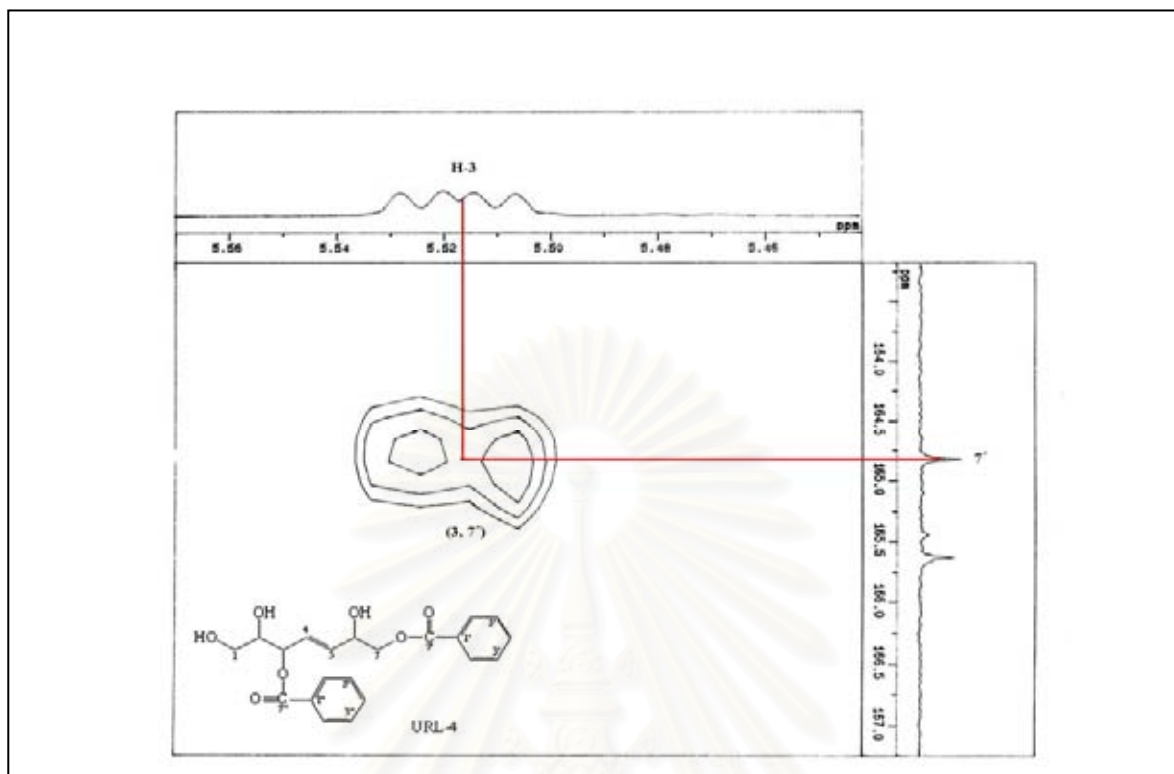
Figure 34b. HMBC Spectrum of compound URL-4 (in DMSO-d_6, expansion)
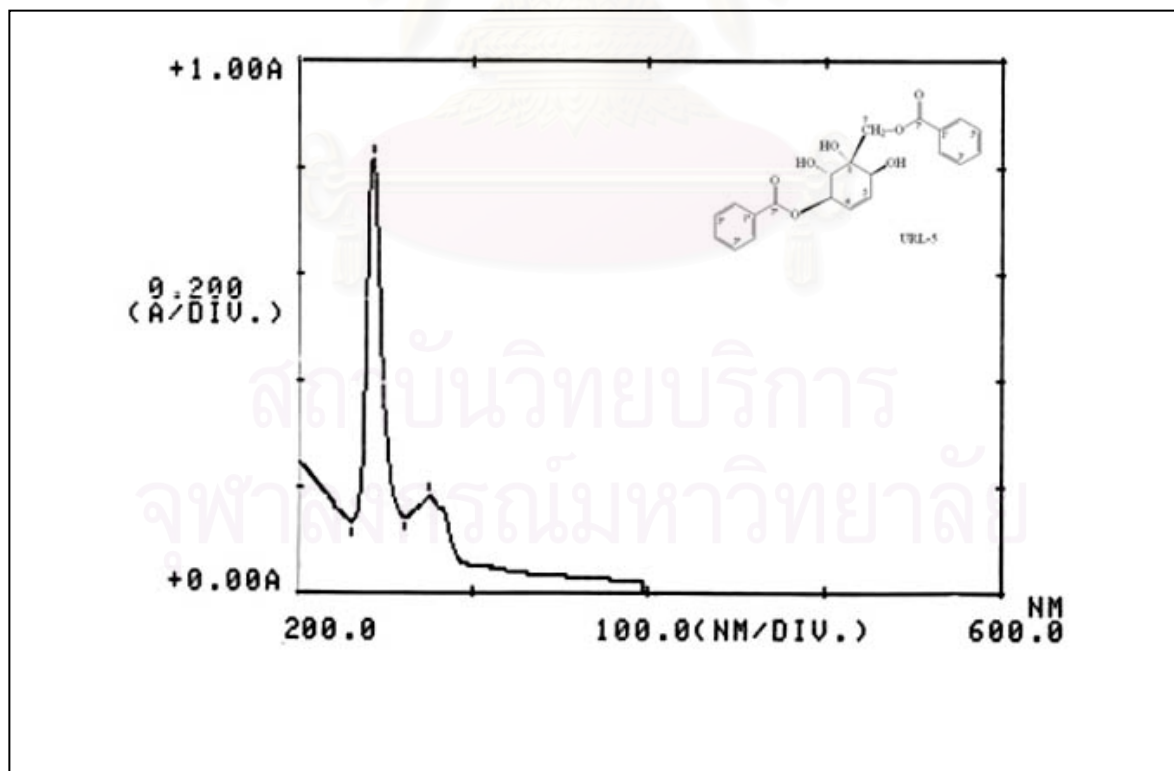
Figure 35. UV Spectrum of compound URL-5 (in CHCl$_3$)
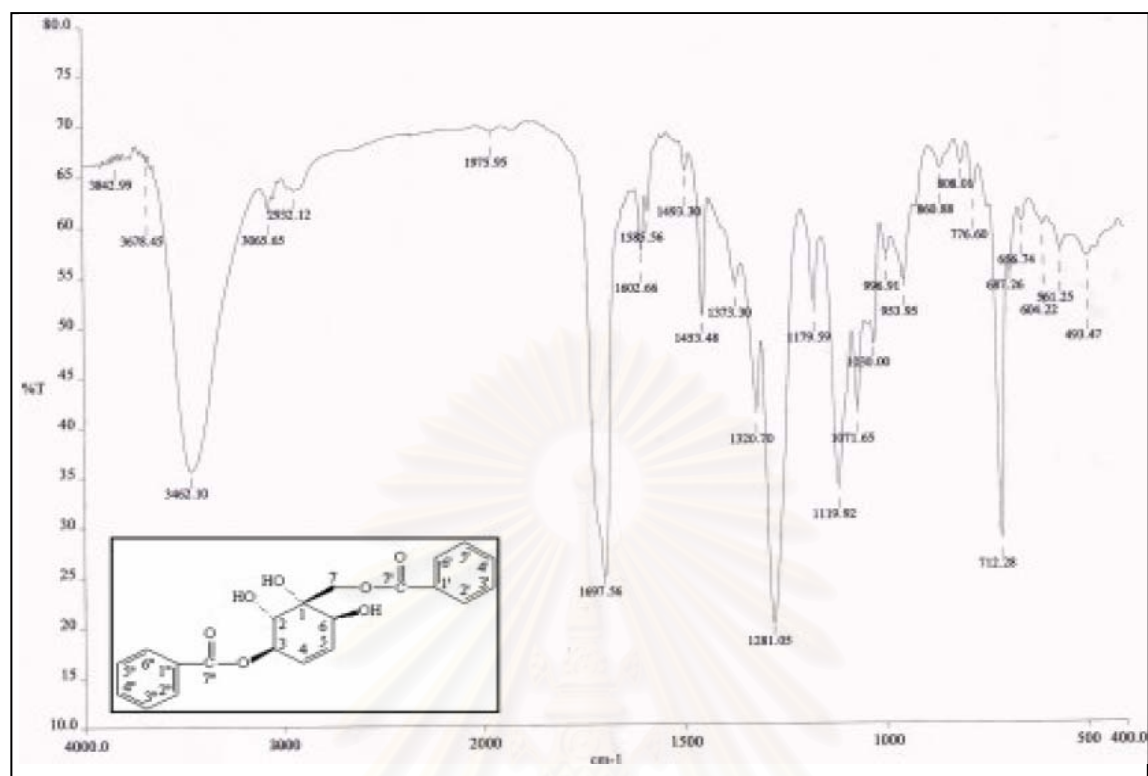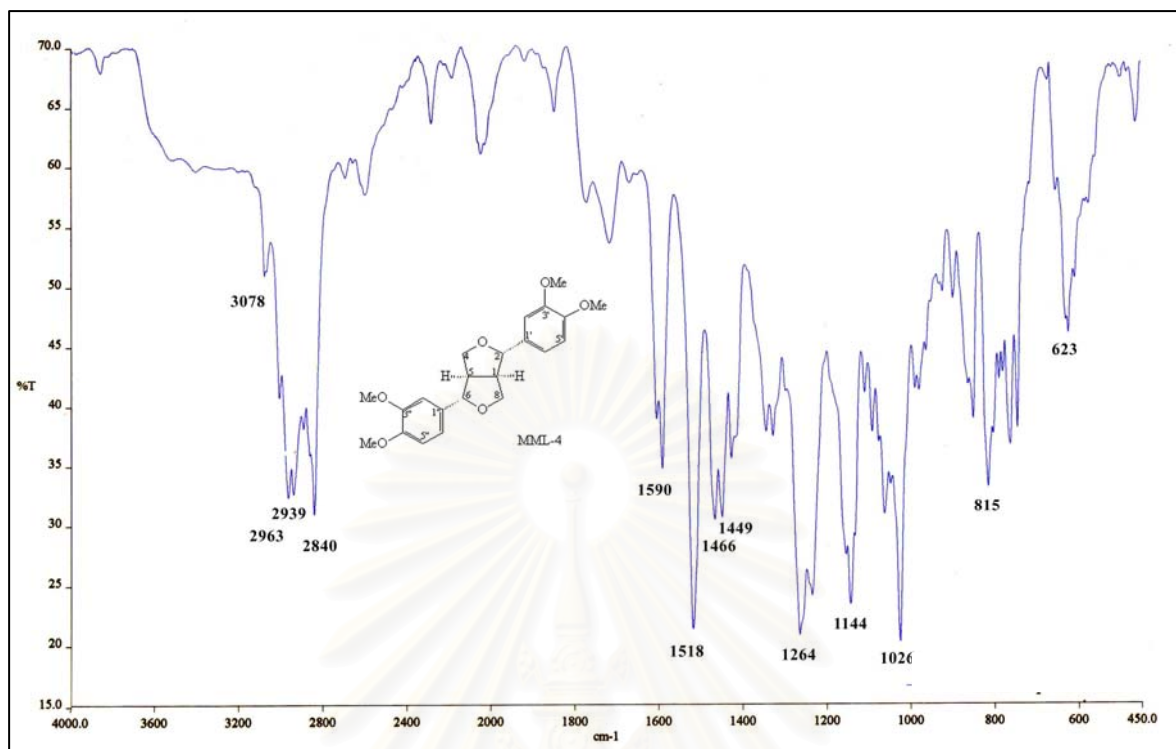
Figure 36. IR Spectrum of compound URL-5 (KBr disc)
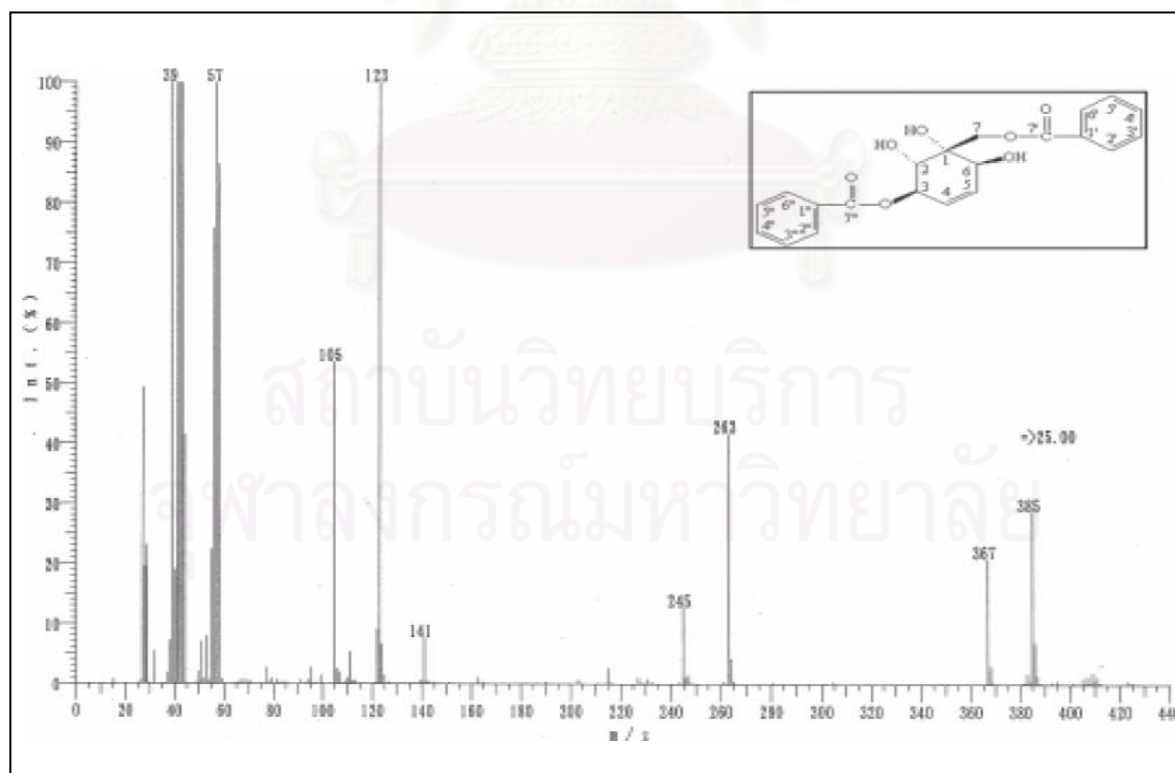
Figure 37. ESITOF Mass spectrum of compound URL-5

190
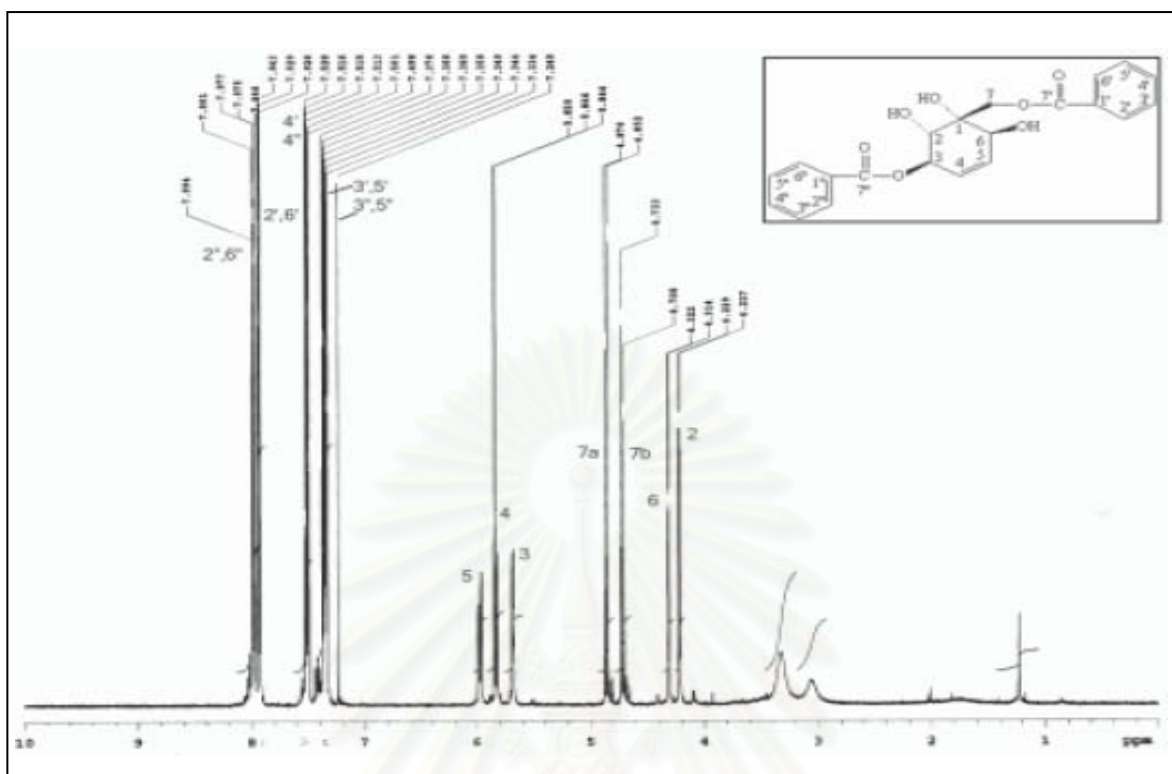
Figure 38. ^{1}H NMR (500 MHz) Spectrum of compound URL-5 (in CDCl$_3$)
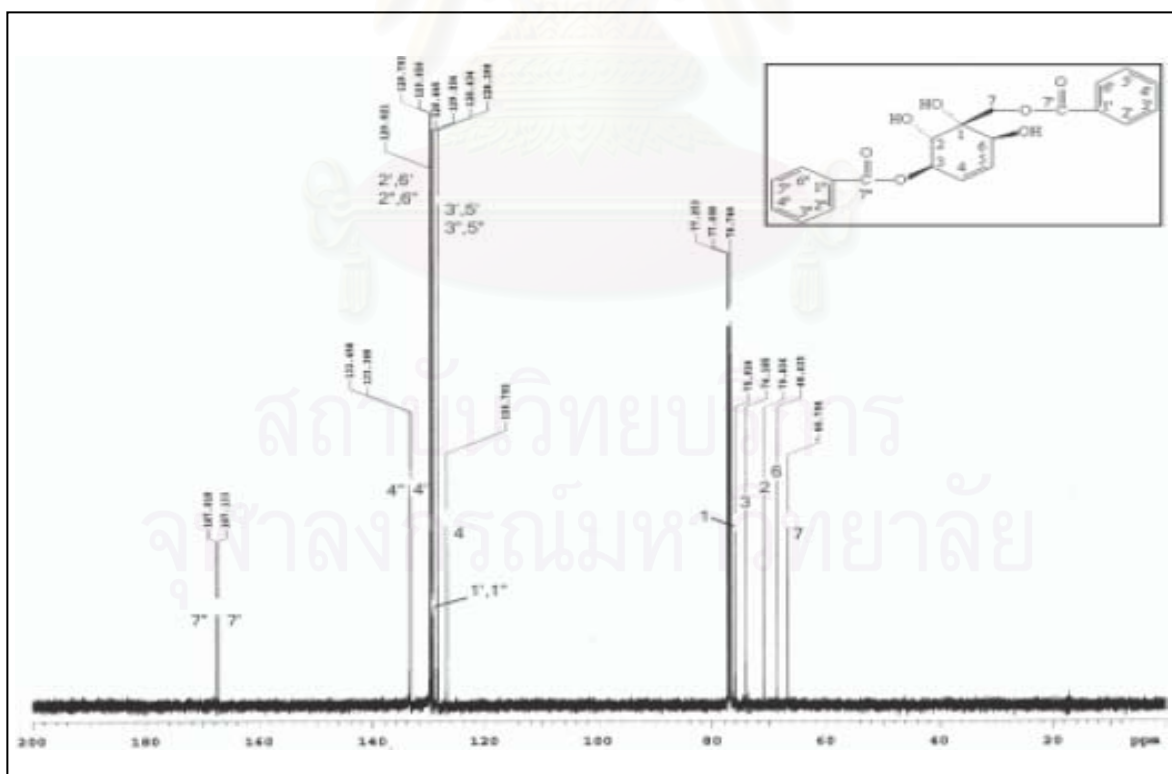
Figure 39. ^{13}C NMR (125 MHz) Spectrum of compound URL-5 (in CDCl$_3$)
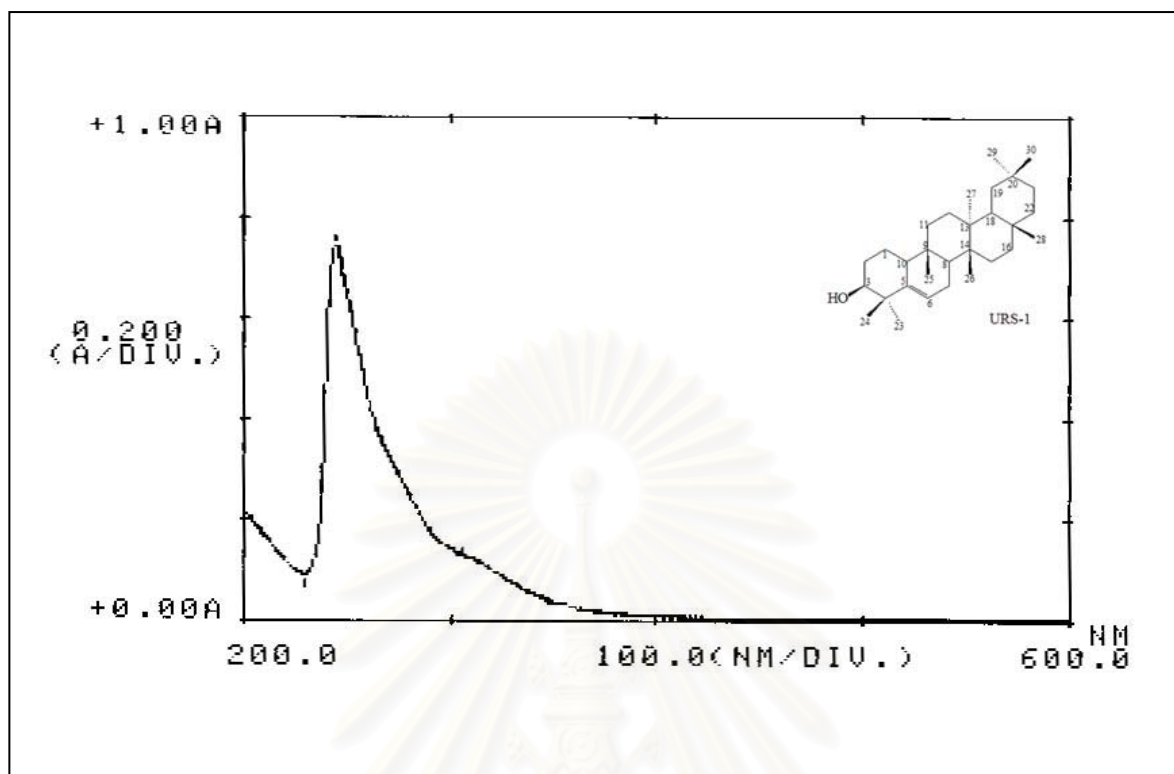
Figure 40. UV Spectrum of compound URS-1 (in MeOH)
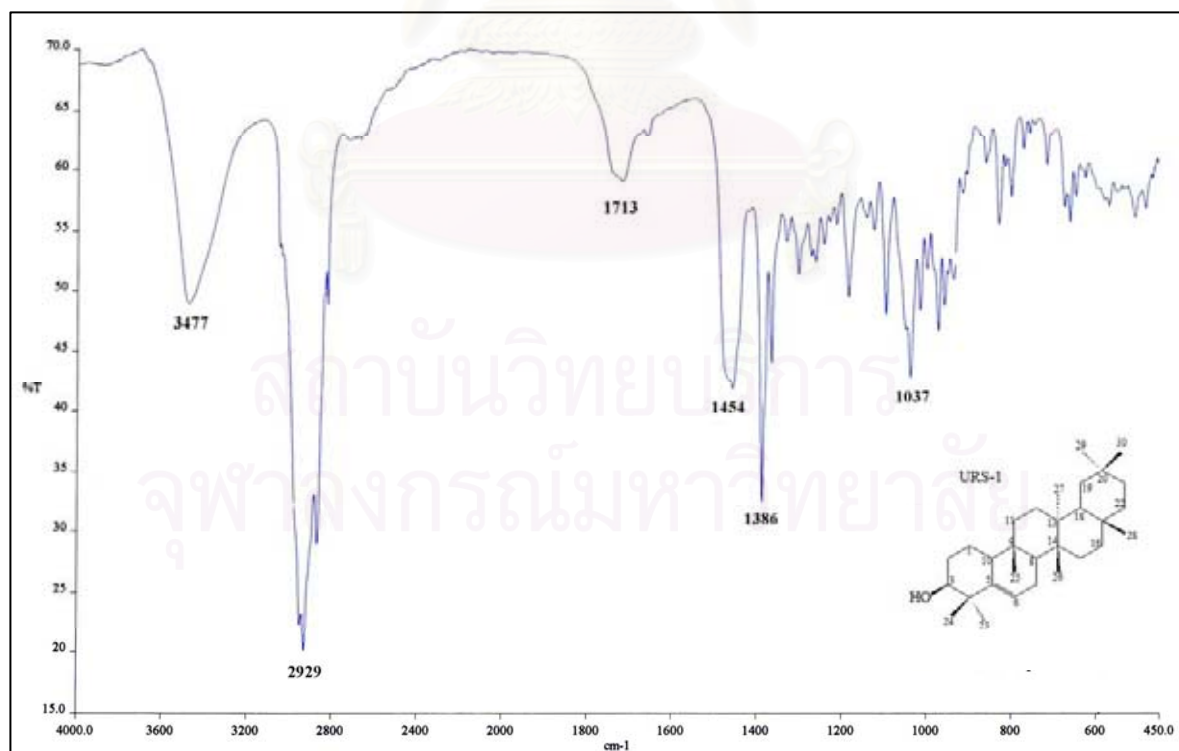
Figure 41. IR Spectrum of compound URS-1 (KBr disc)
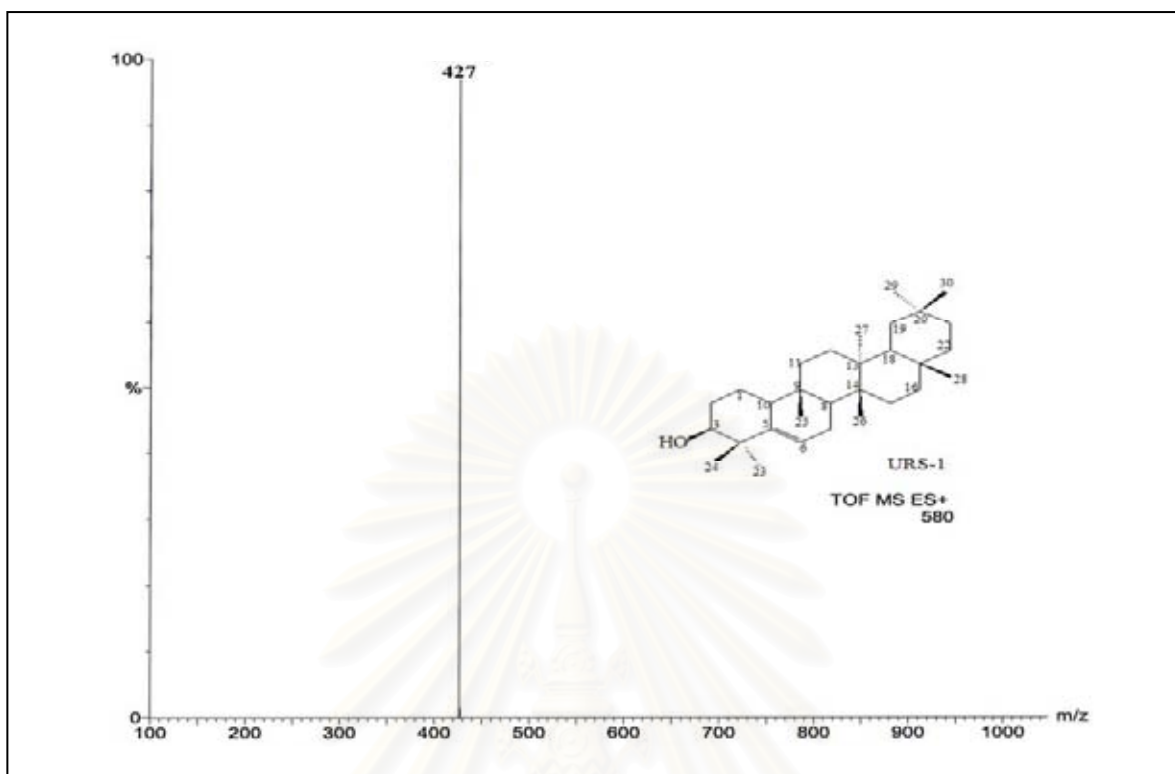
Figure 42. ESITOF Mass spectrum of compound URS-1
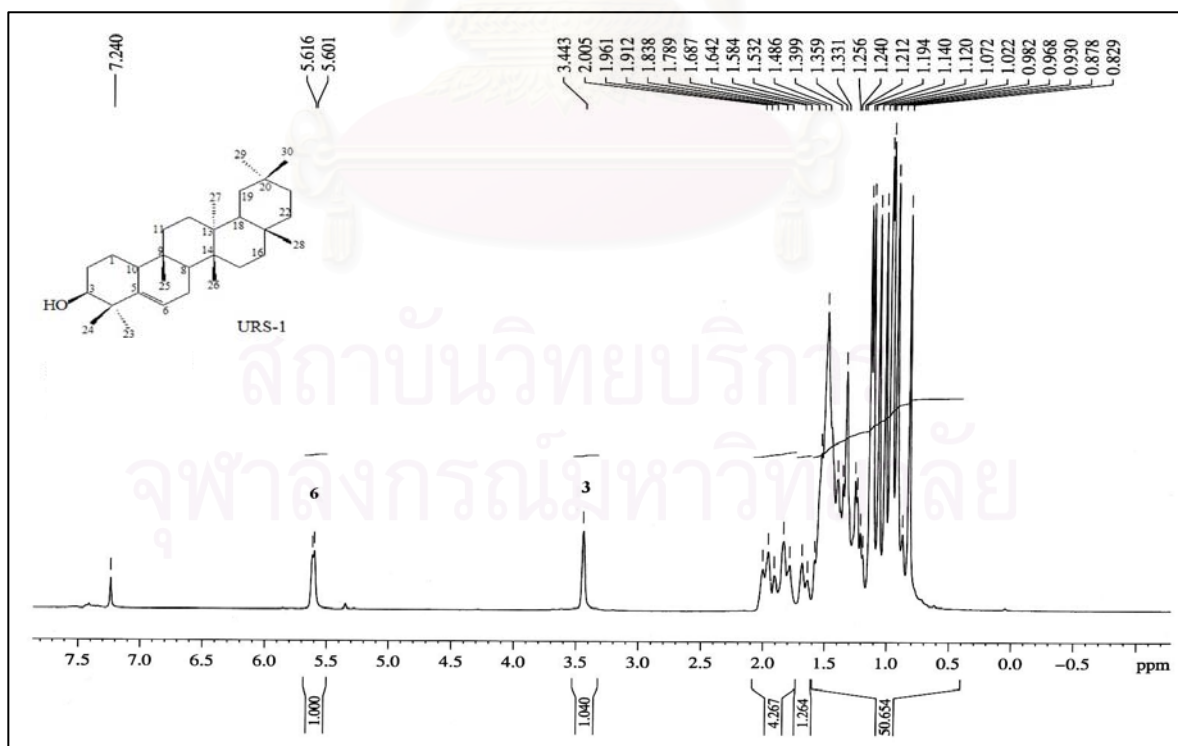
Figure 43. ^{1}H NMR (300 MHz) Spectrum of compound URS-1 (in CDCl$_3$)
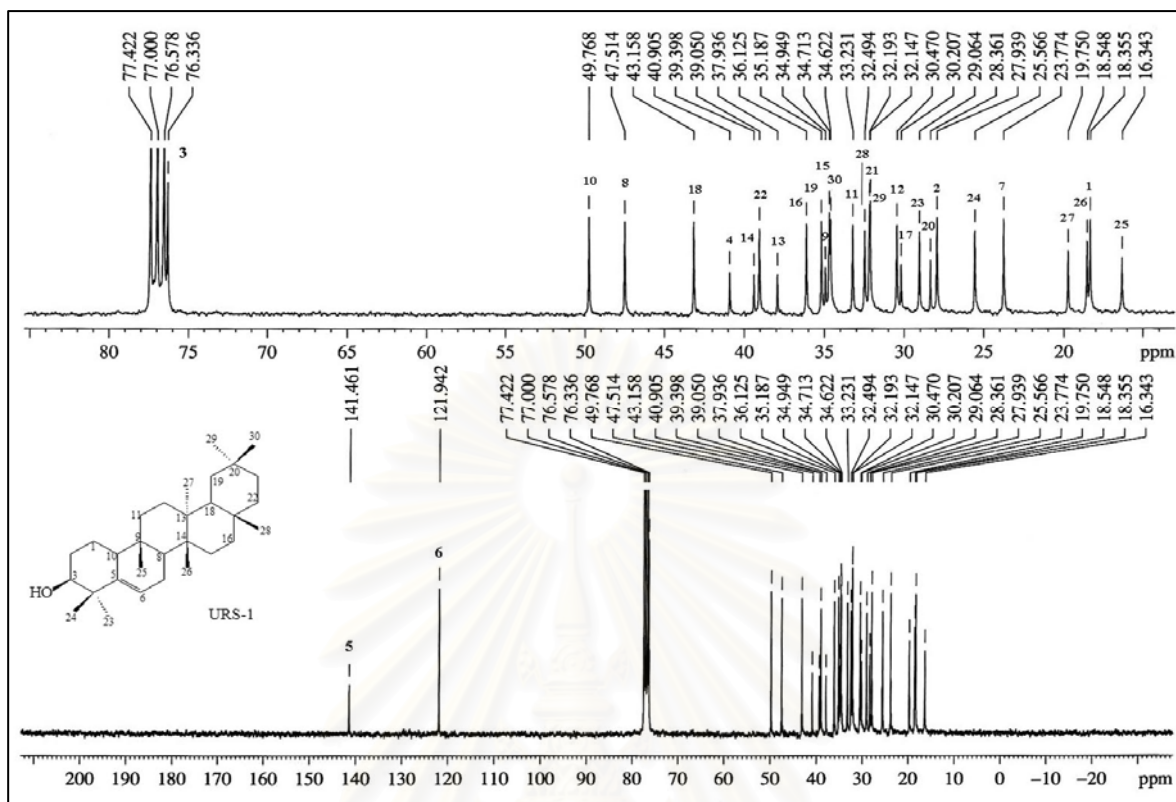
Figure 44. ^{13}C NMR (75 MHz) Spectrum of compound URS-1 (in CDCl$_3$)
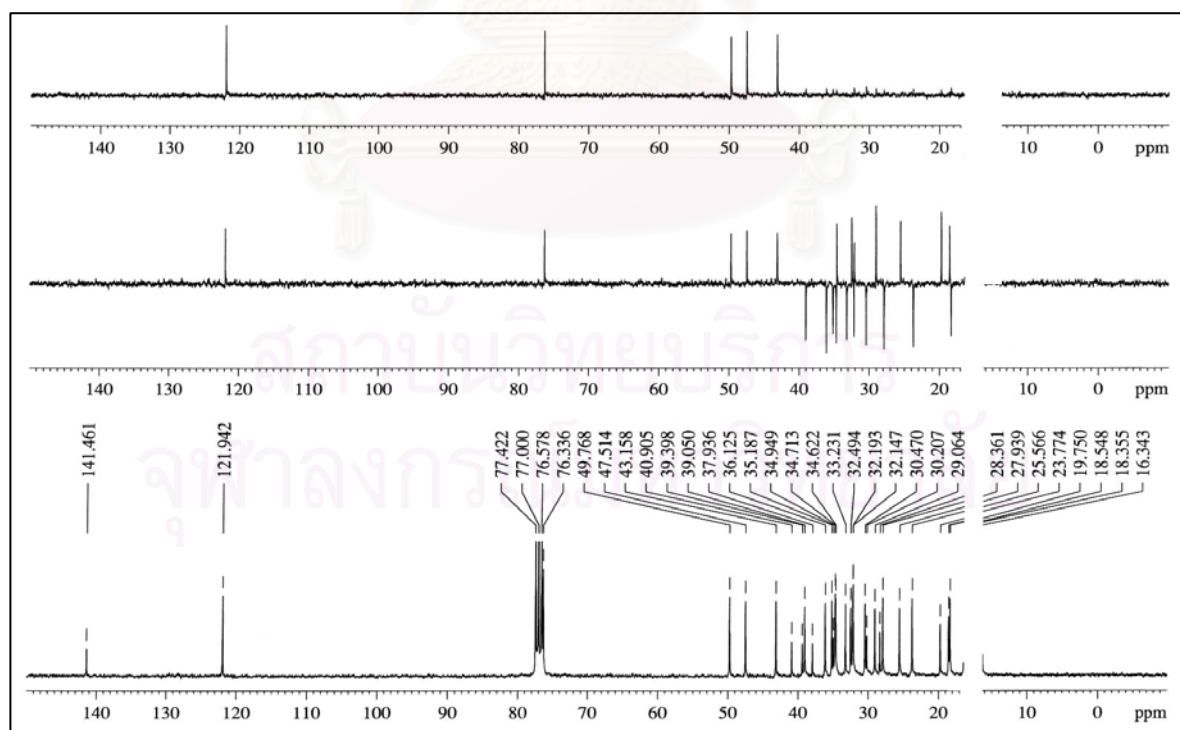
Figure 45. DEPT Spectra of compound URS-1 (in CDCl$_3$)
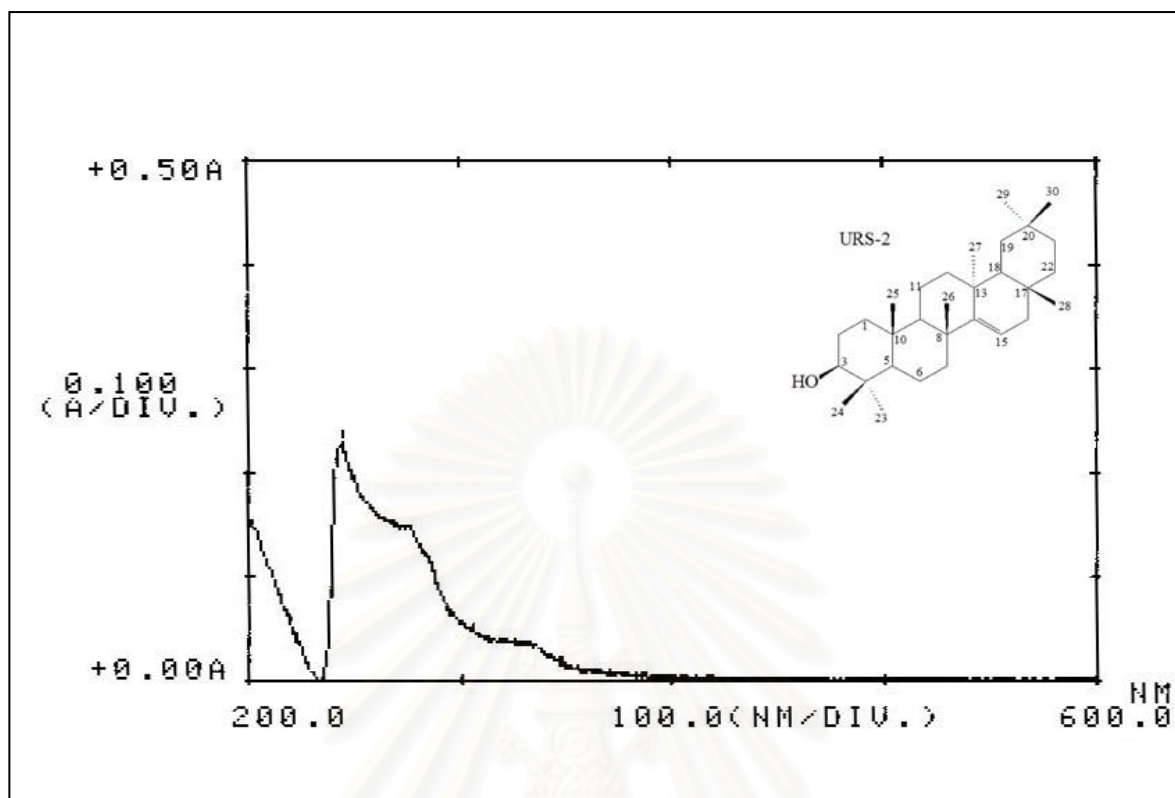
**Figure 46.** UV Spectrum of compound URS-2 (in MeOH)
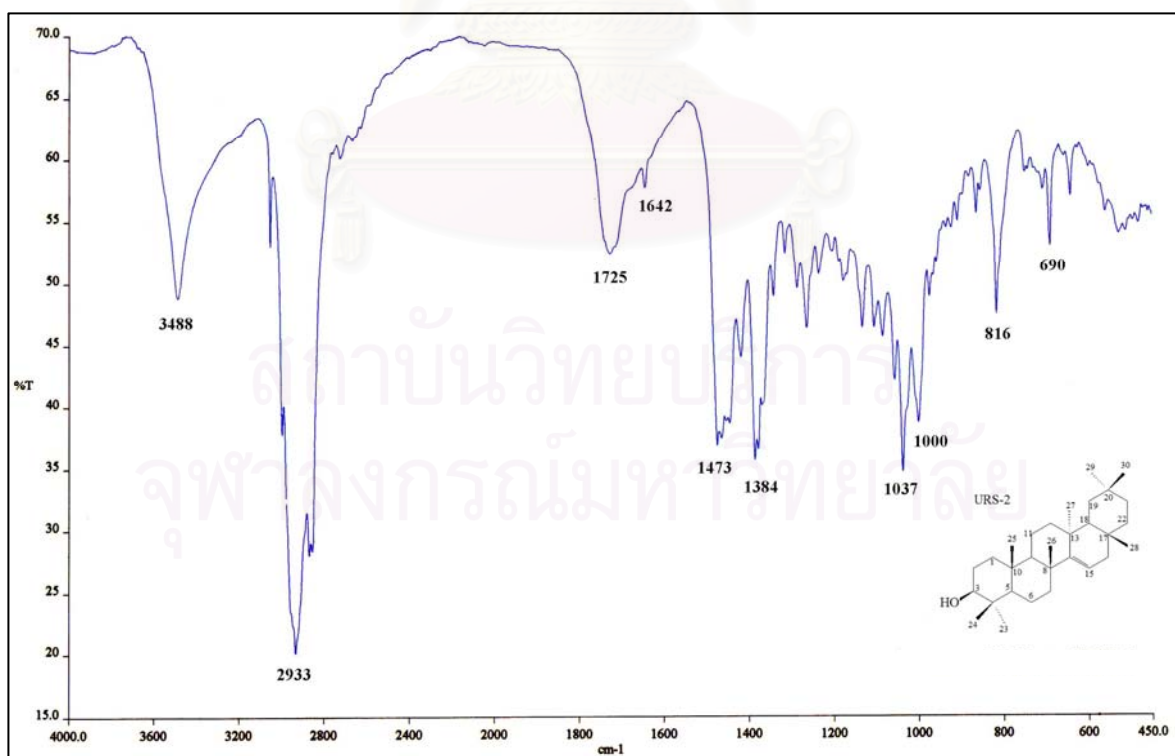
Figure 47. IR Spectrum of compound URS-2 (KBr disc)
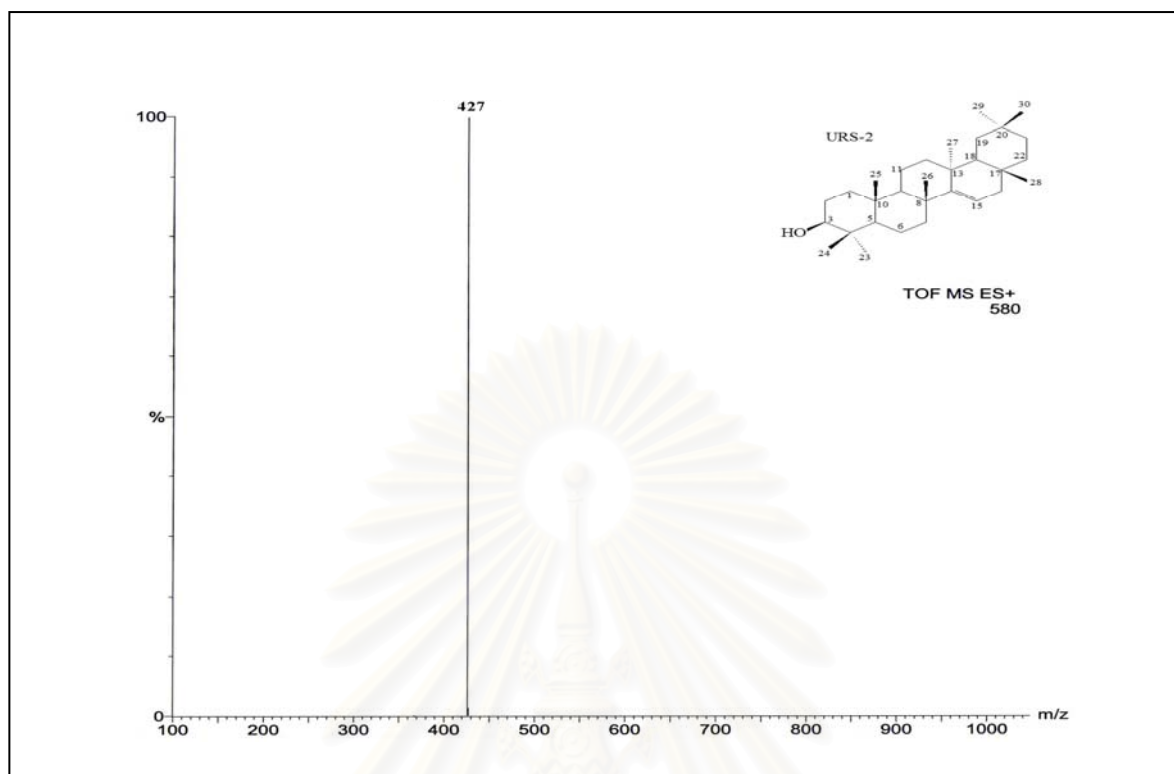
Figure 48. ESITOF Mass spectrum of compound URS-2
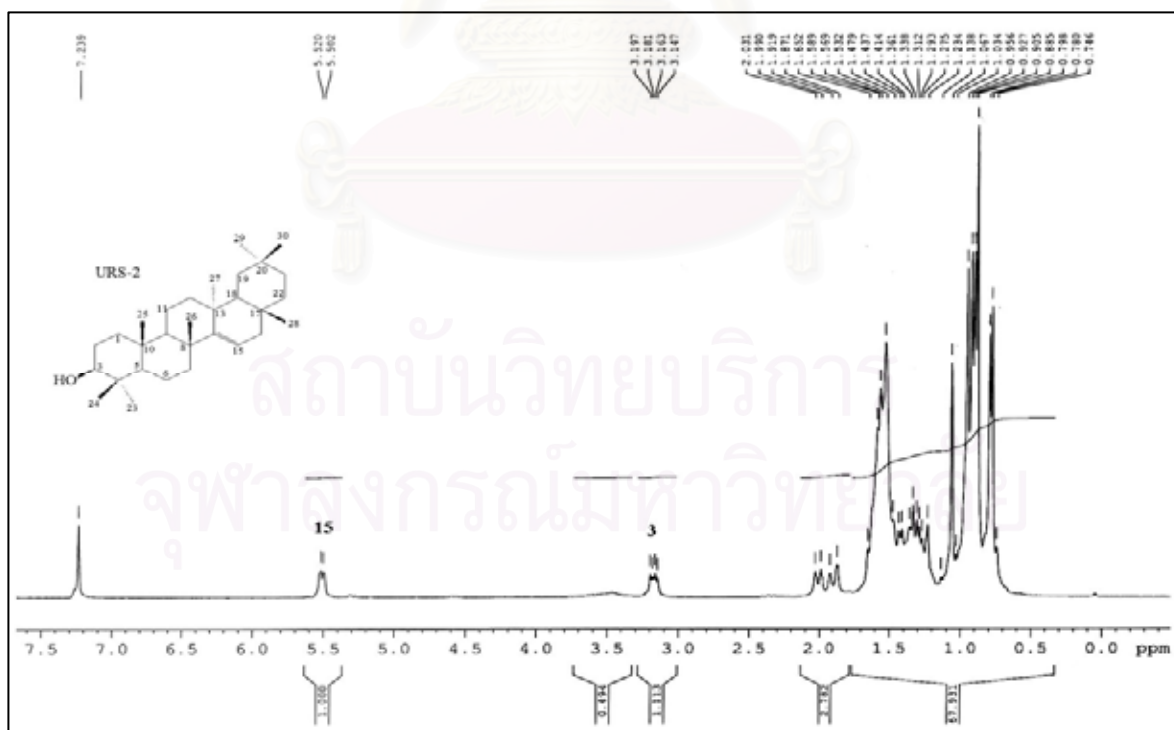
Figure 49. ^{1}H NMR (300 MHz) Spectrum of compound URS-2 (in CDCl₃)
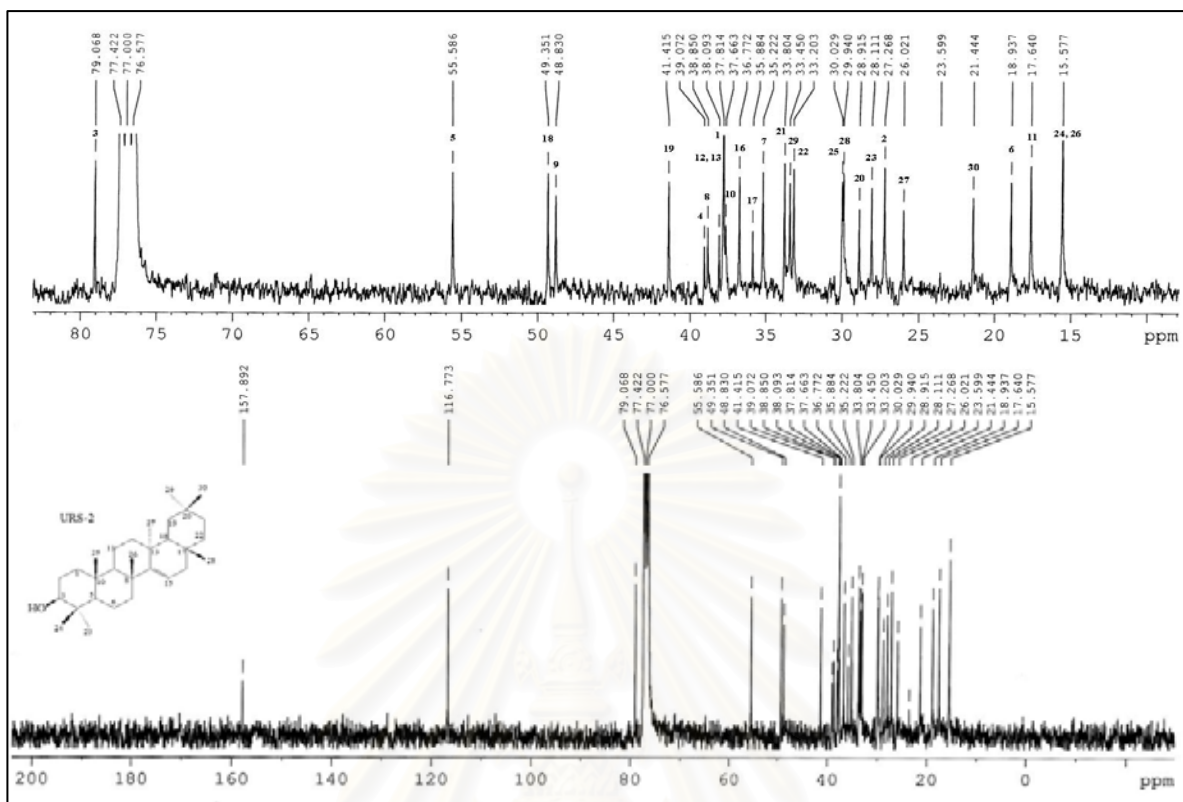
Figure 50. ^{13}C NMR (75 MHz) Spectrum of compound URS-2 (in CDCl$_3$)
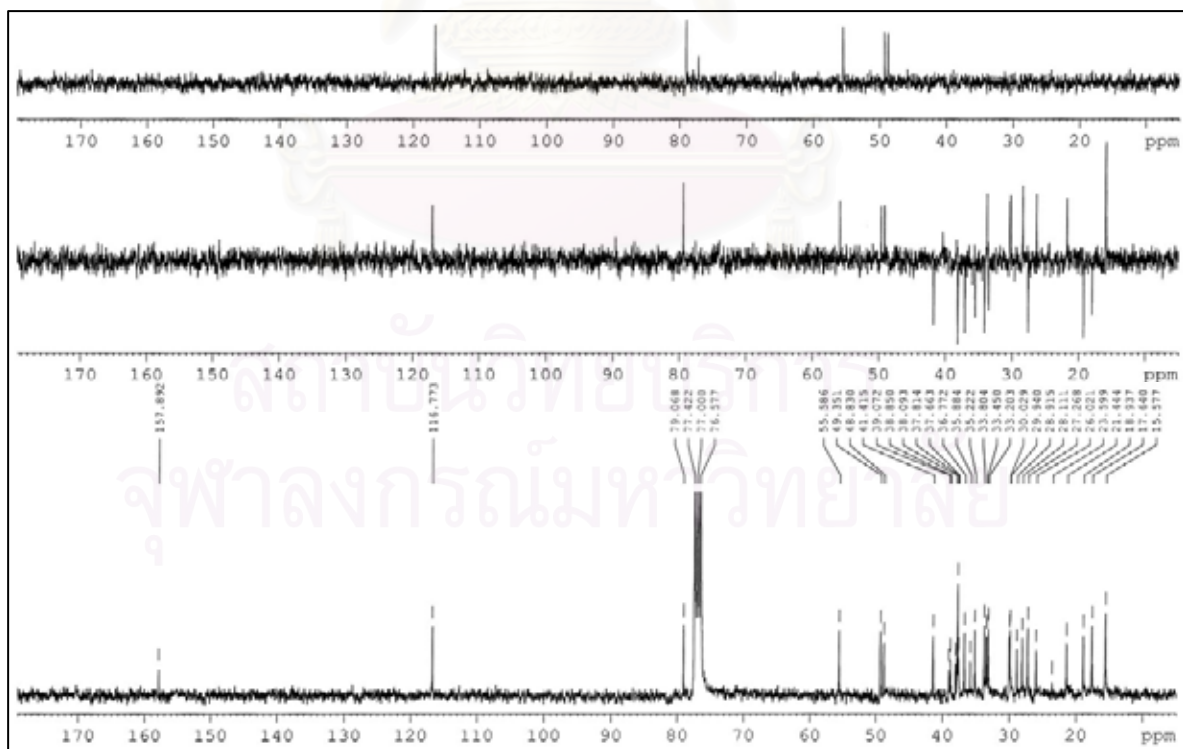
Figure 51. DEPT Spectra of compound URS-2 (in CDCl$_3$)
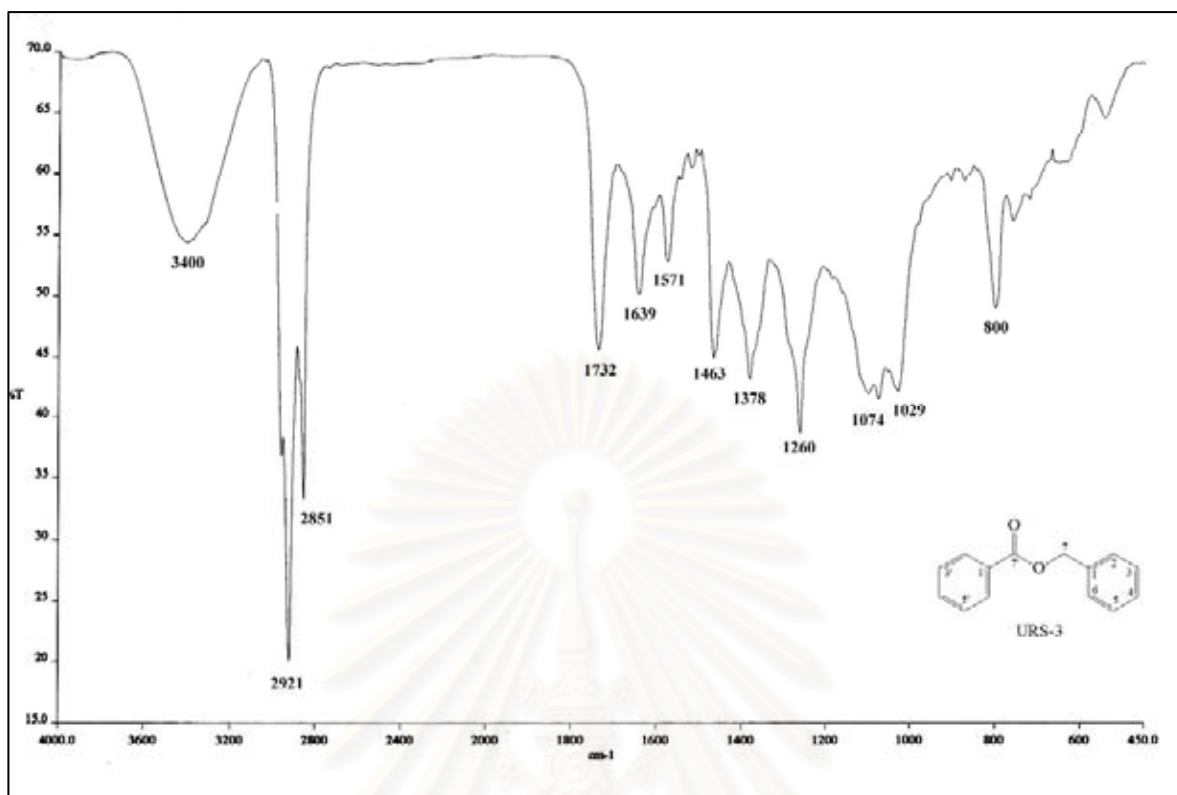
Figure 52. IR Spectrum of compound URS-3 (KBr disc)
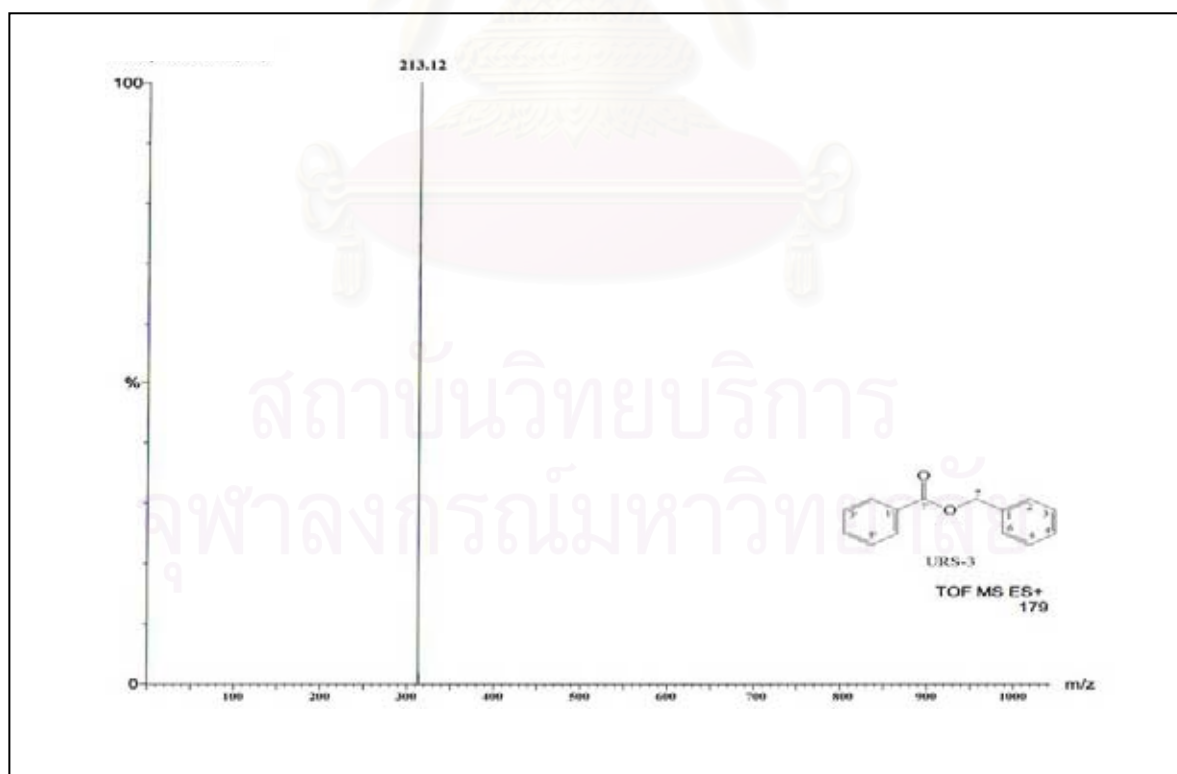
Figure 53. ESITOF Mass spectrum of compound URS-3
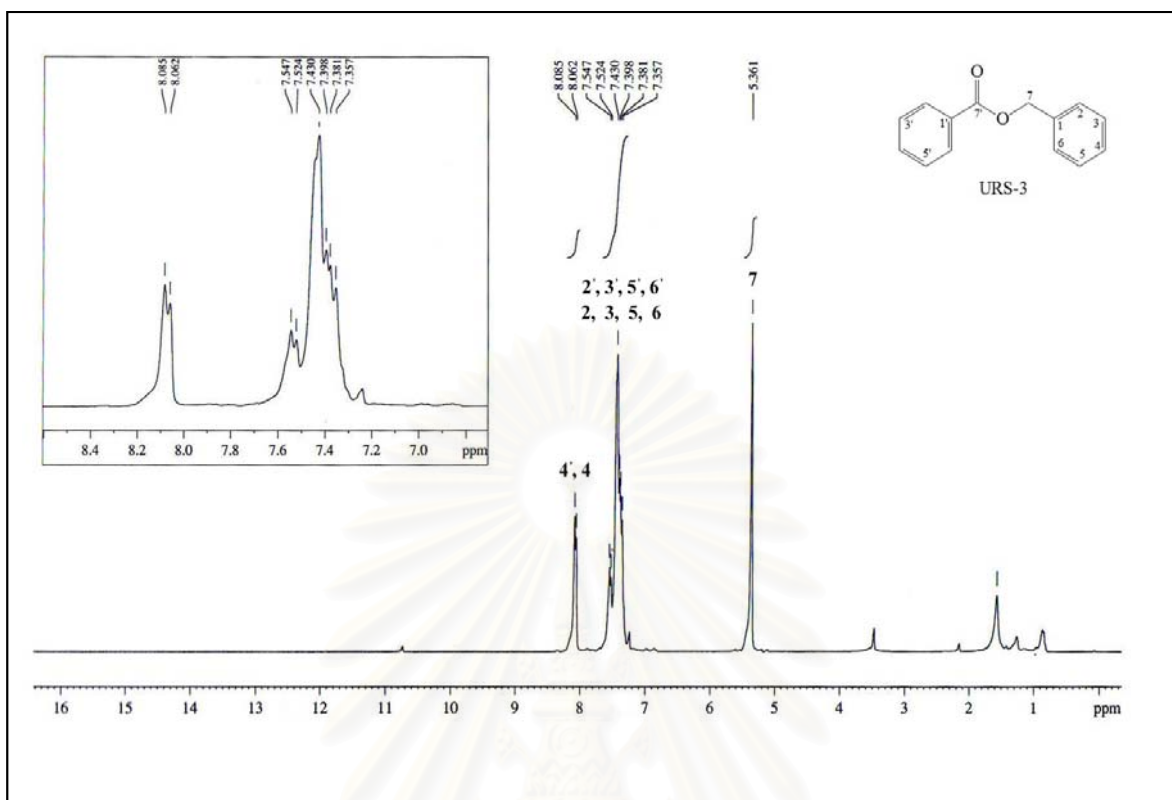
Figure 54. ^{1}H NMR (300 MHz) Spectrum of compound URS-3 (in CDCl$_3$)
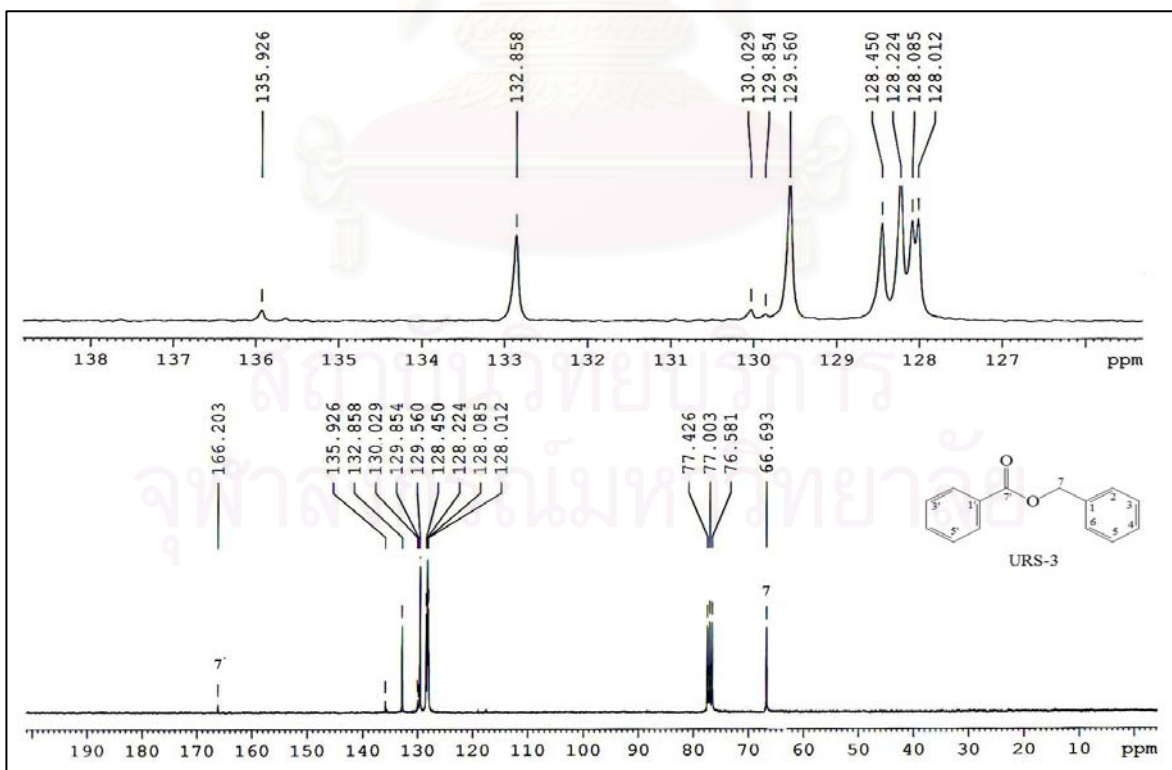
Figure 55. ^{13}C NMR (75 MHz) Spectrum of compound URS-3 (in CDCl$_3$)
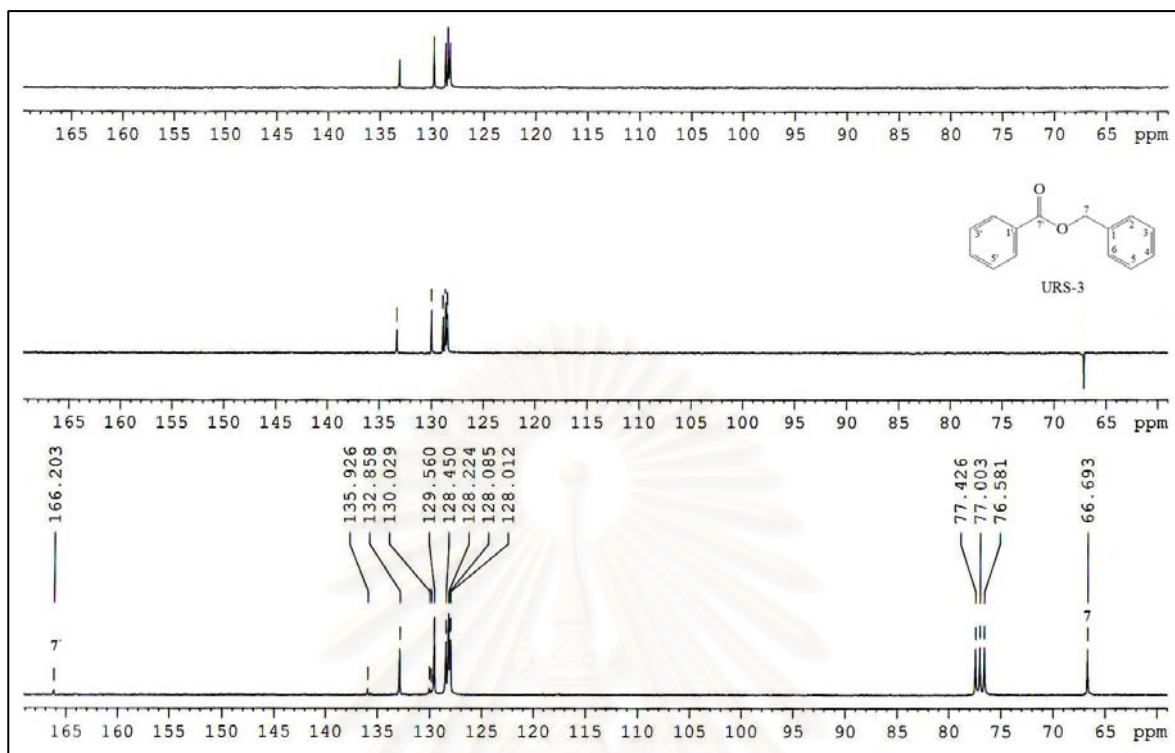
Figure 56. DEPT Spectra of compound URS-3 (in CDCl$_3$)
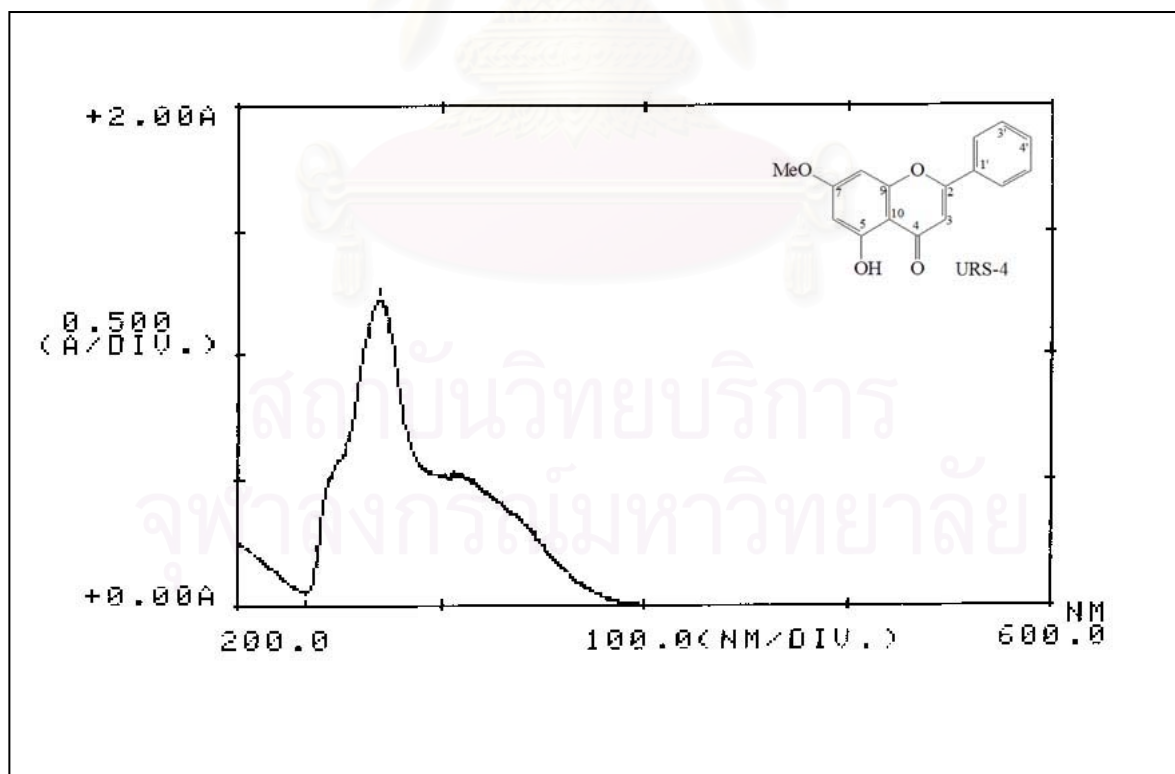
Figure 57. UV Spectrum of compound URS-4 (in MeOH)
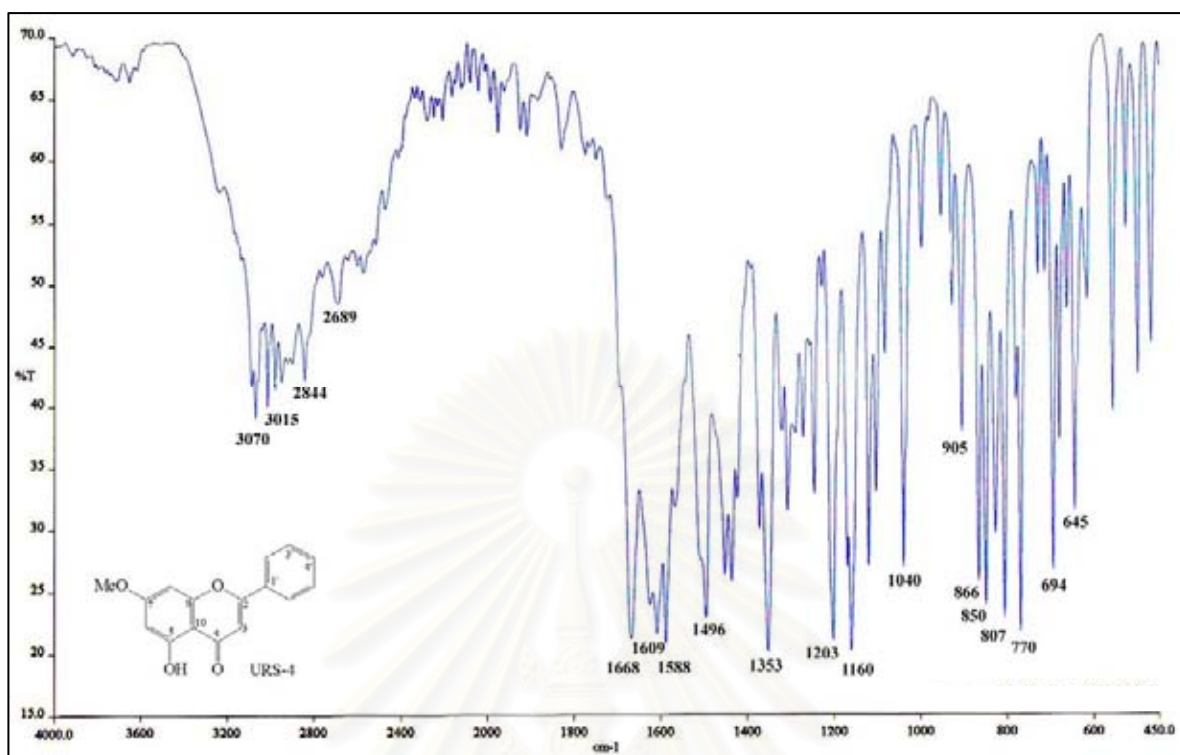
Figure 58. IR Spectrum of compound URS-4 (KBr disc)
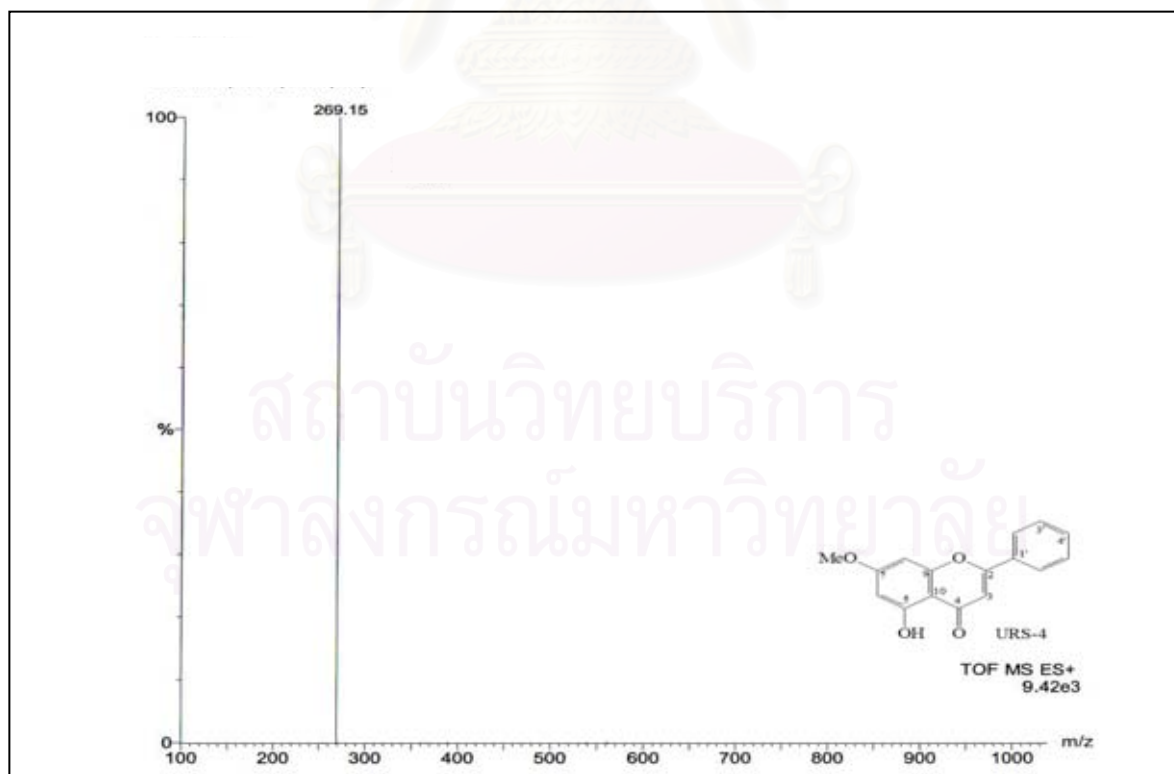
**Figure 59.** ESITOF Mass spectrum of compound URS-4
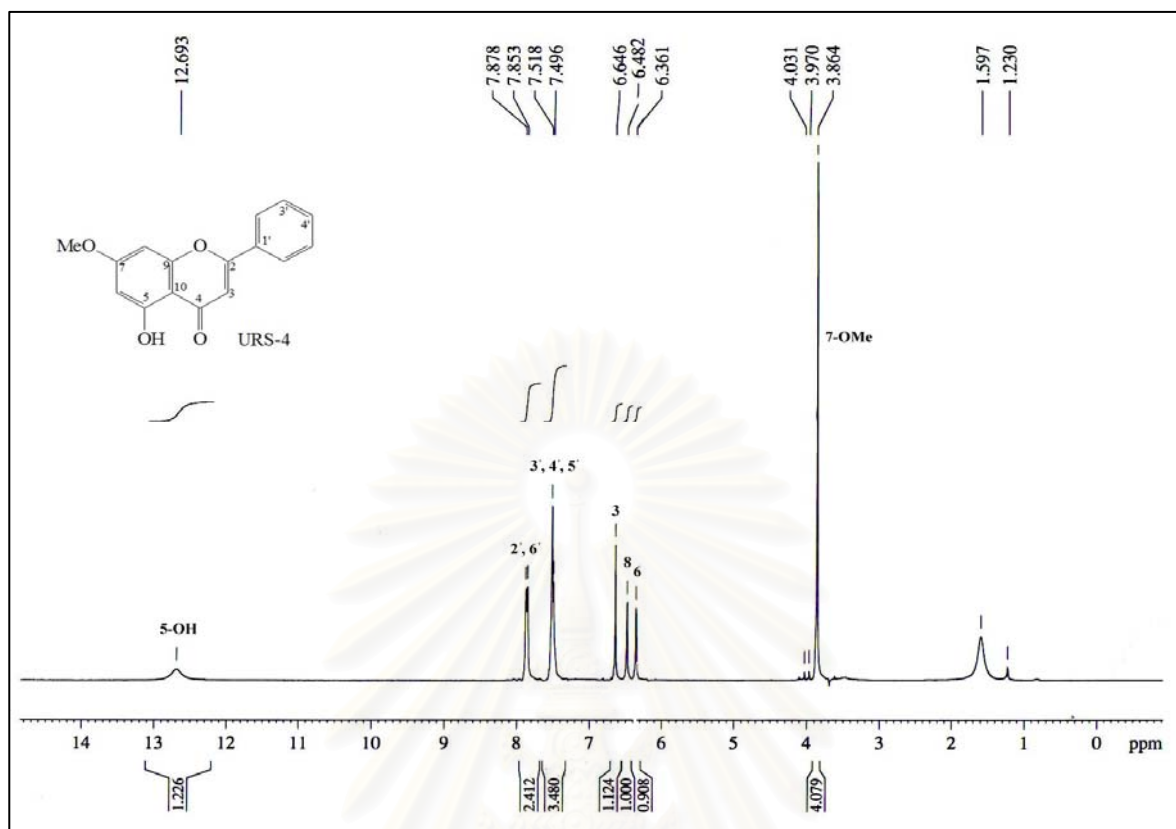
Figure 60. ¹H NMR (300 MHz) Spectrum of compound URS-4 (in CDCl₃)
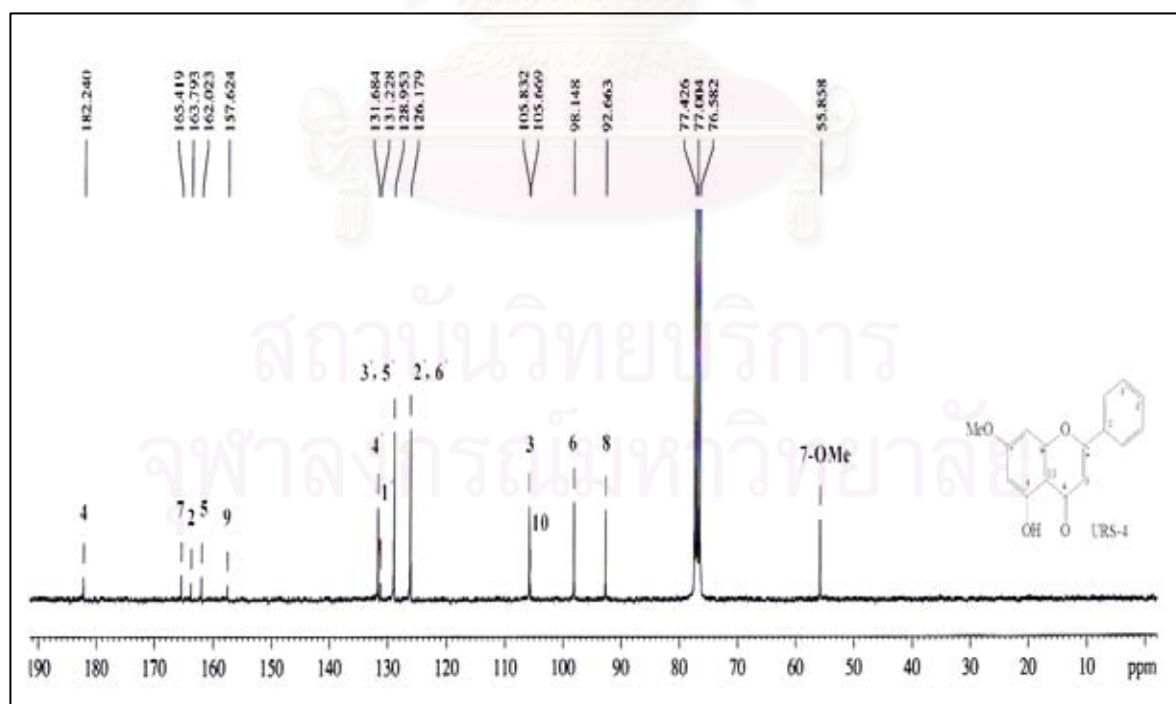
Figure 61. ¹³C NMR (75 MHz) Spectrum of compound URS-4 (in CDCl₃)
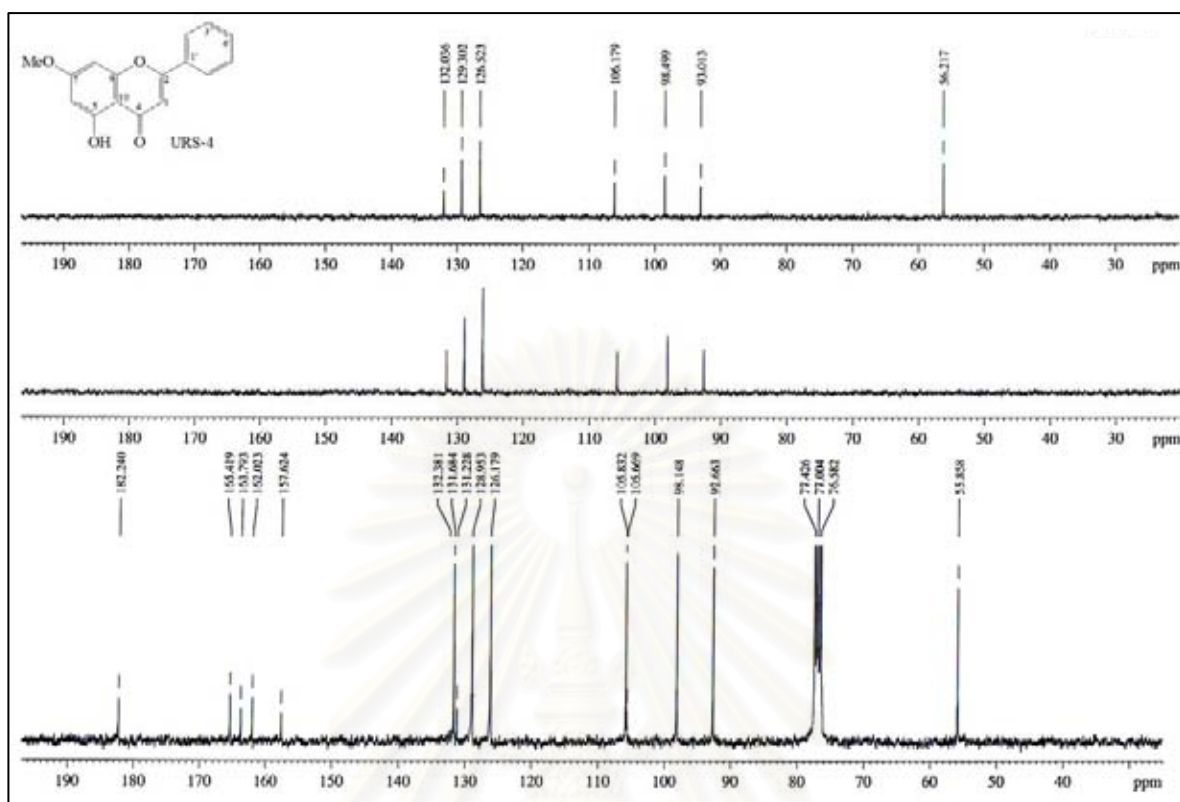
Figure 62. DEPT Spectra of compound URS-4 (in CDCl$_3$)
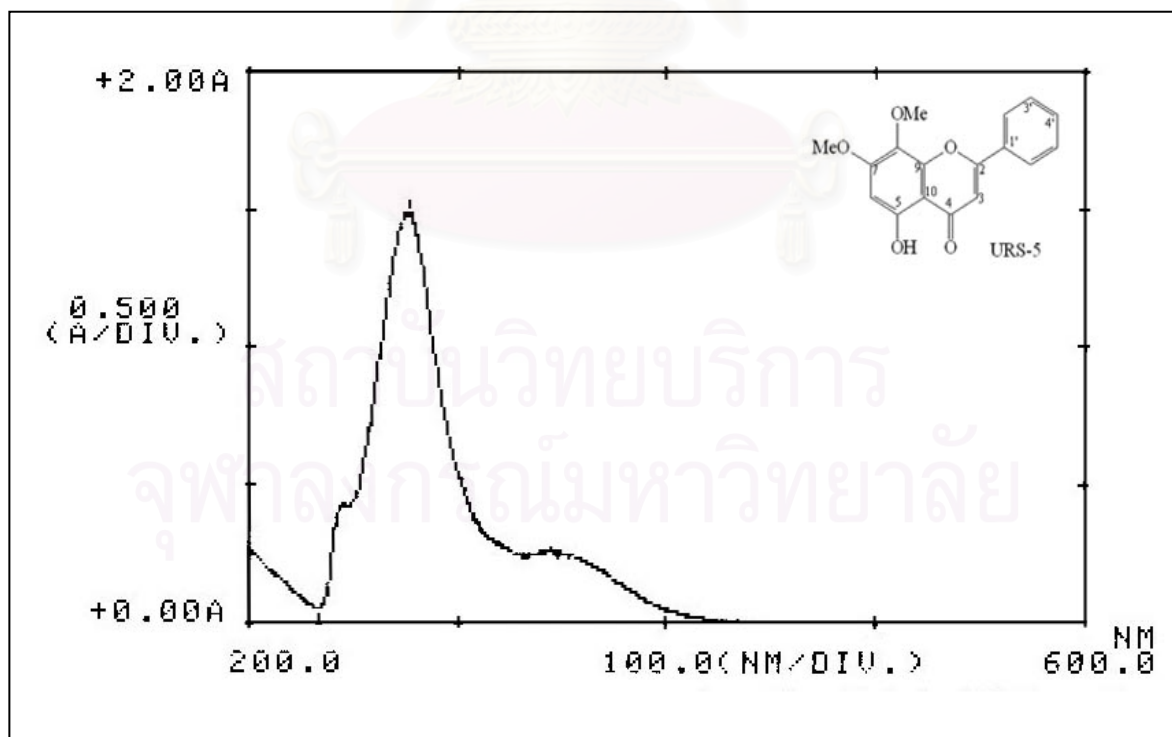
Figure 63. UV Spectrum of compound URS-5 (in MeOH)
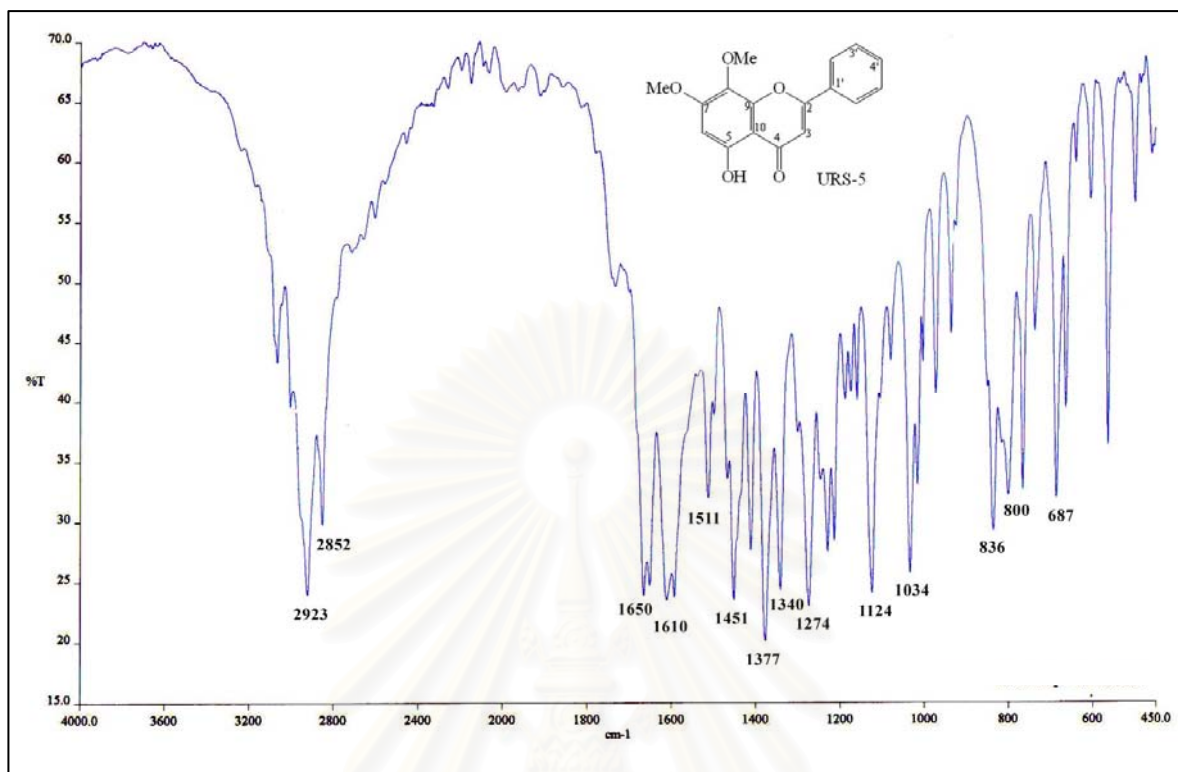
Figure 64. IR Spectrum of compound URS-5 (KBr disc)
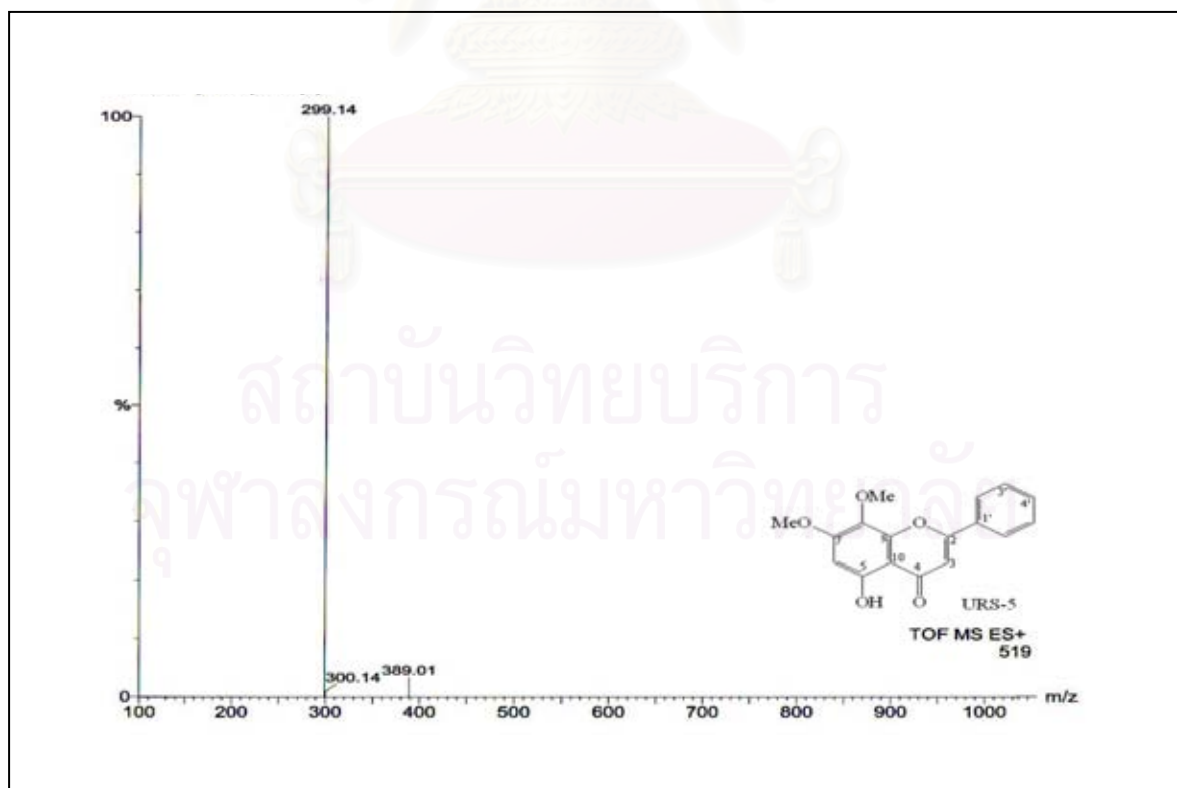
Figure 65. ESITOF Mass spectrum of compound URS-5

Figure 66. ^{1}H NMR (300 MHz) Spectrum of compound URS-5 (in CDCl$_3$)
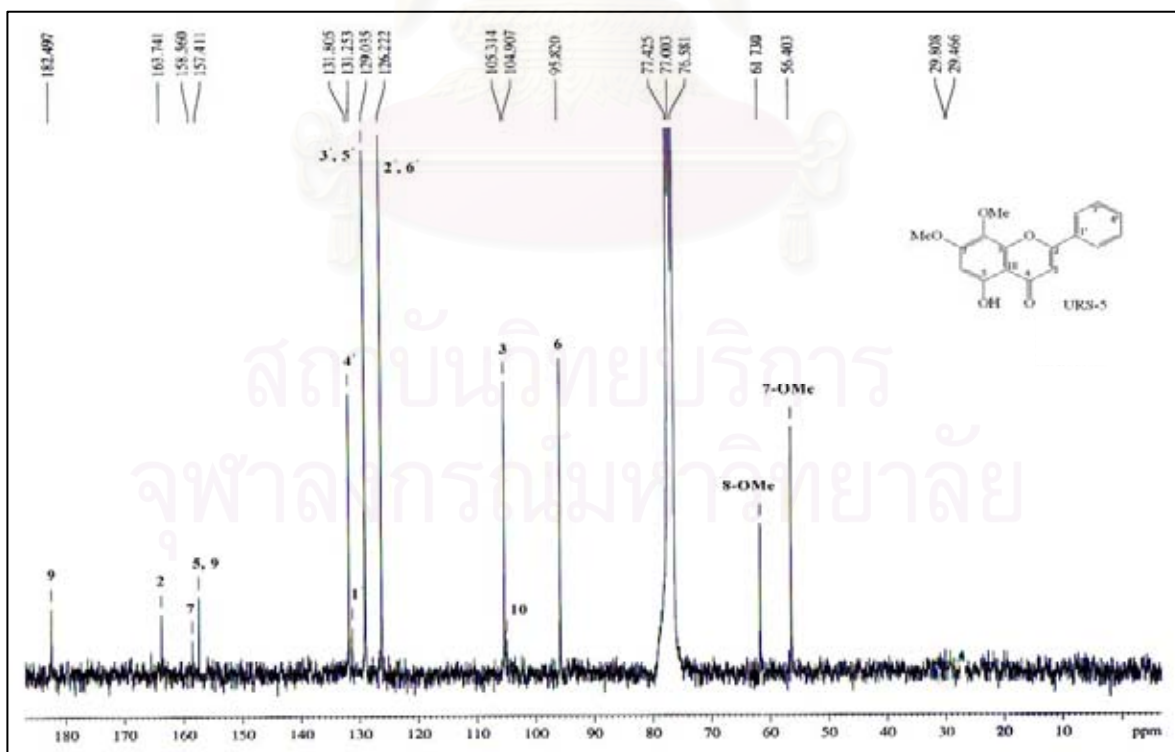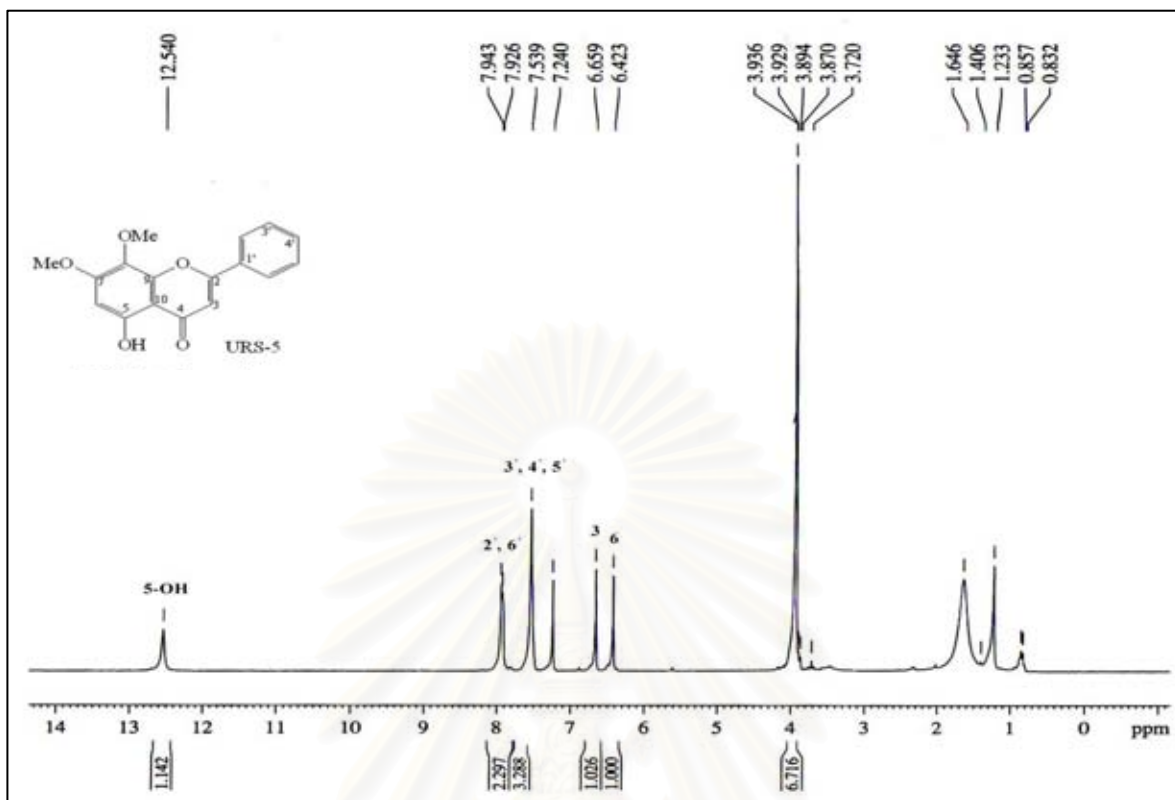
Figure 67. ^{13}C NMR (75 MHz) Spectrum of compound URS-5 (in CDCl$_3$)
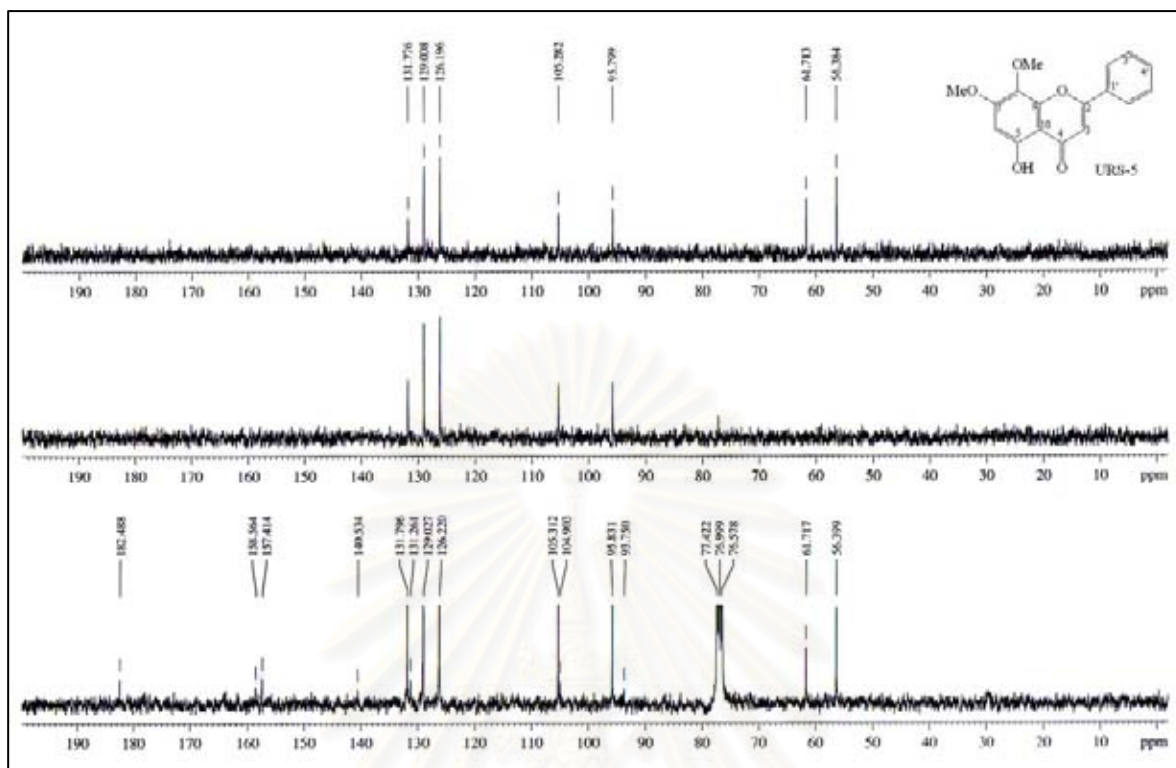
Figure 68. DEPT Spectra of compound URS-5 (in CDCl$_3$)
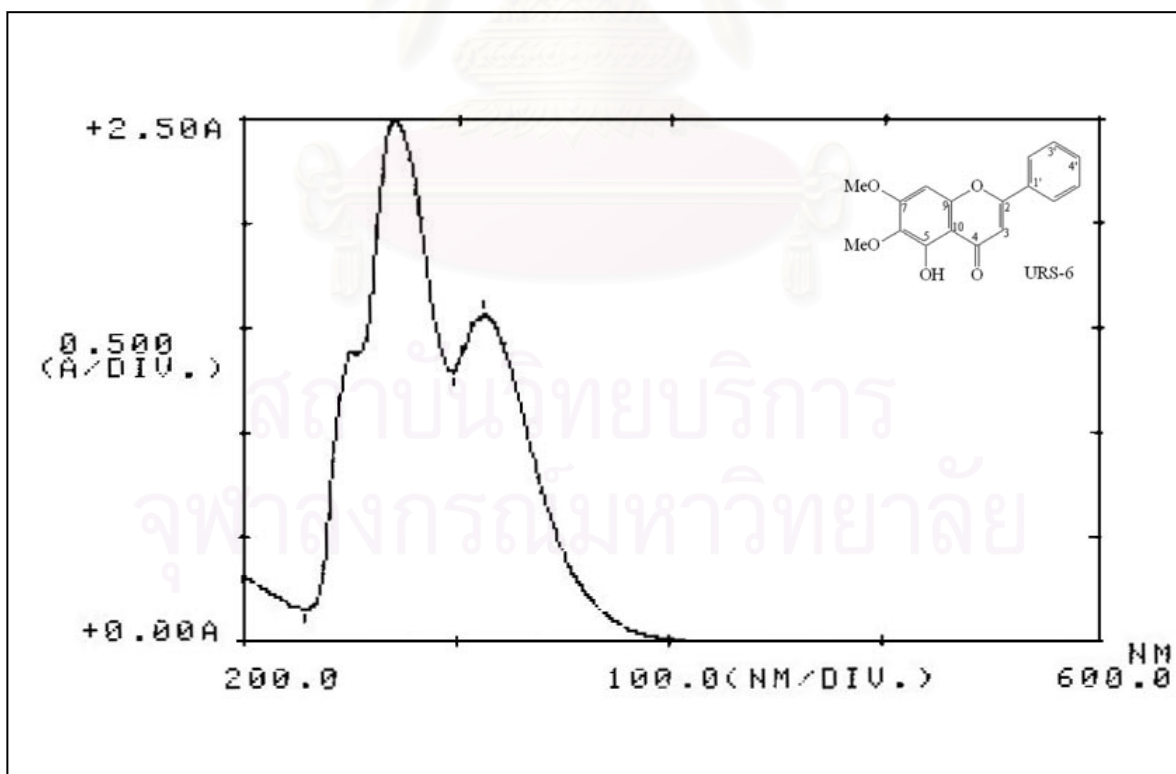
Figure 69. UV Spectrum of compound URS-6 (in CHCl$_3$)
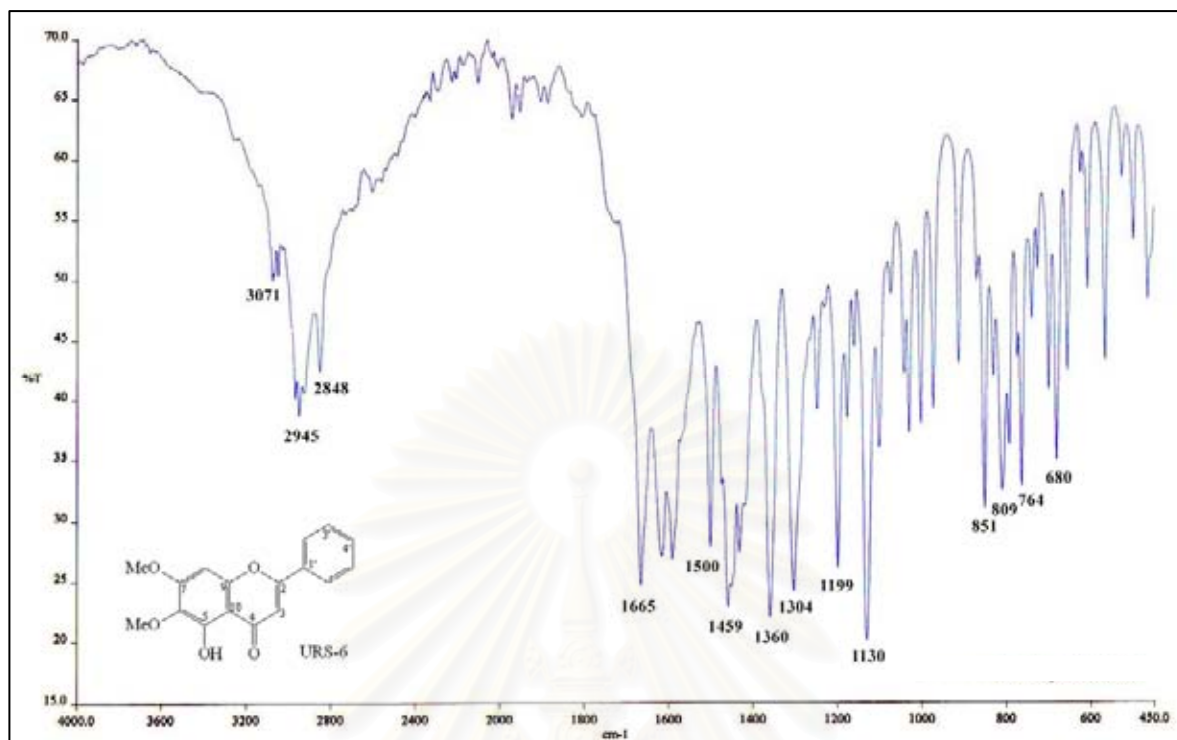
Figure 70. IR Spectrum of compound URS-6 (KBr disc)
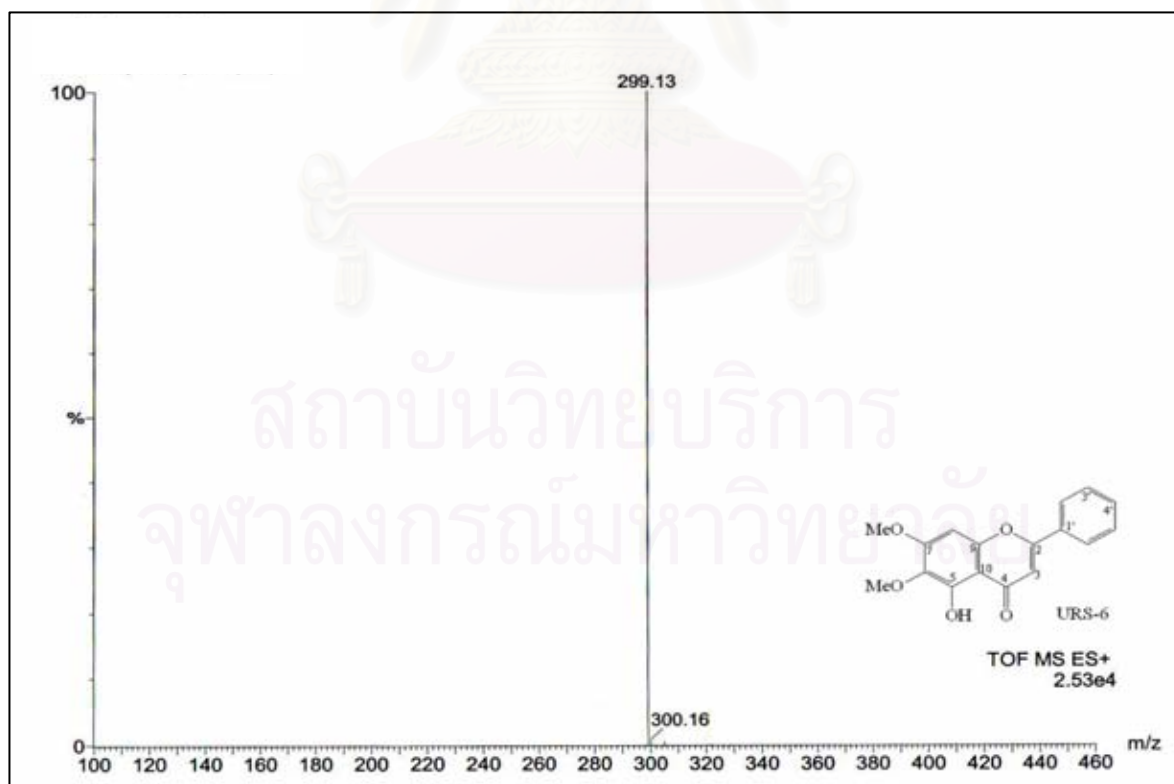
Figure 71. ESITOF Mass spectrum of compound URS-6

Figure 72. ^{1}H NMR (300 MHz) Spectrum of compound URS-6 (in CDCl$_3$)

Figure 73. ^{13}C NMR (75 MHz) Spectrum of compound URS-6 (in CDCl$_3$)
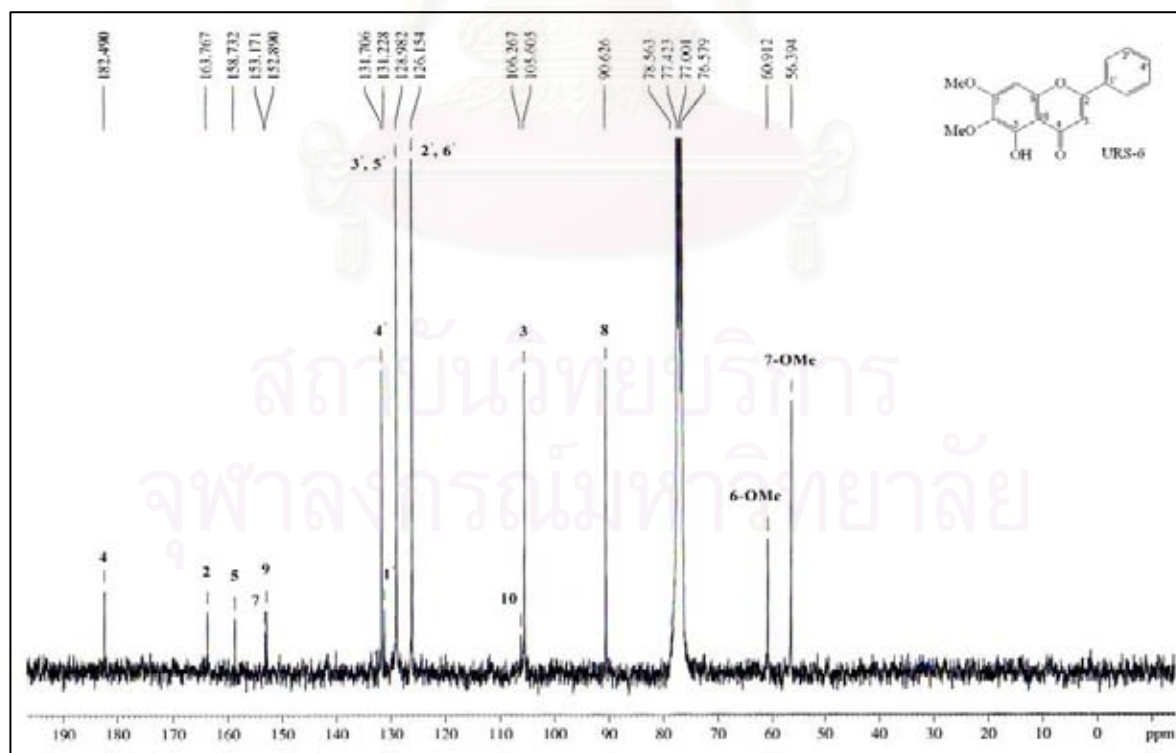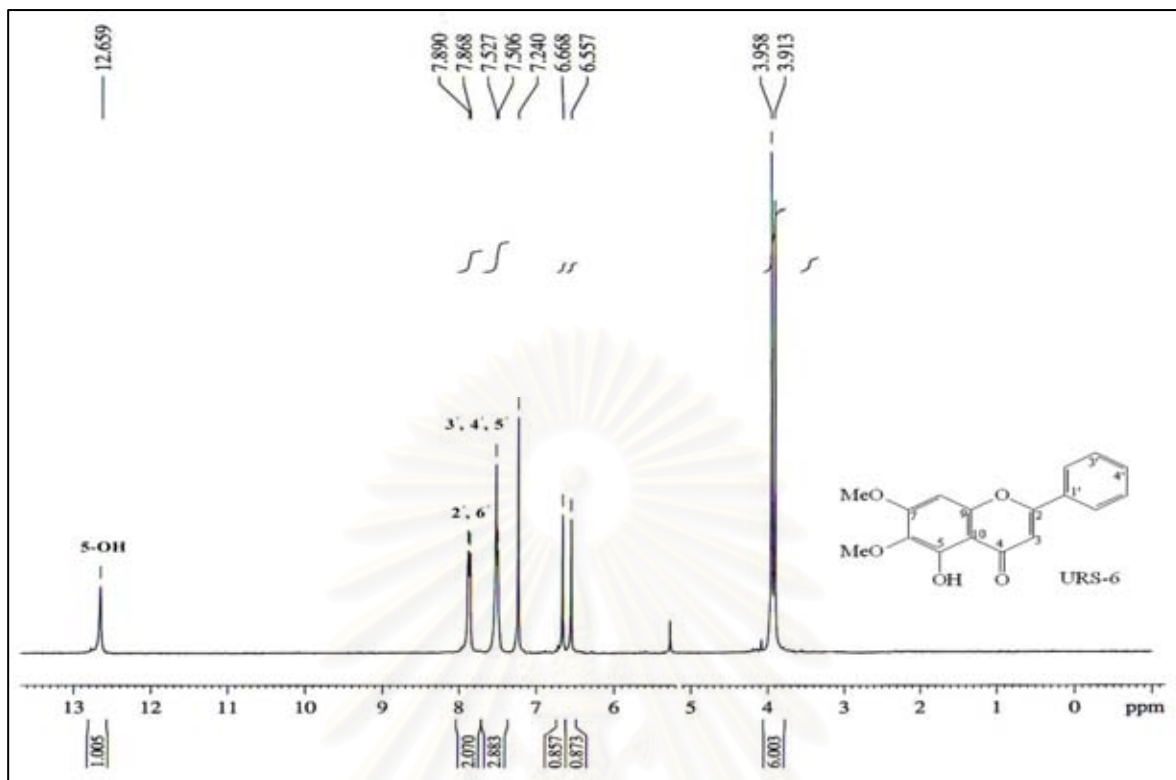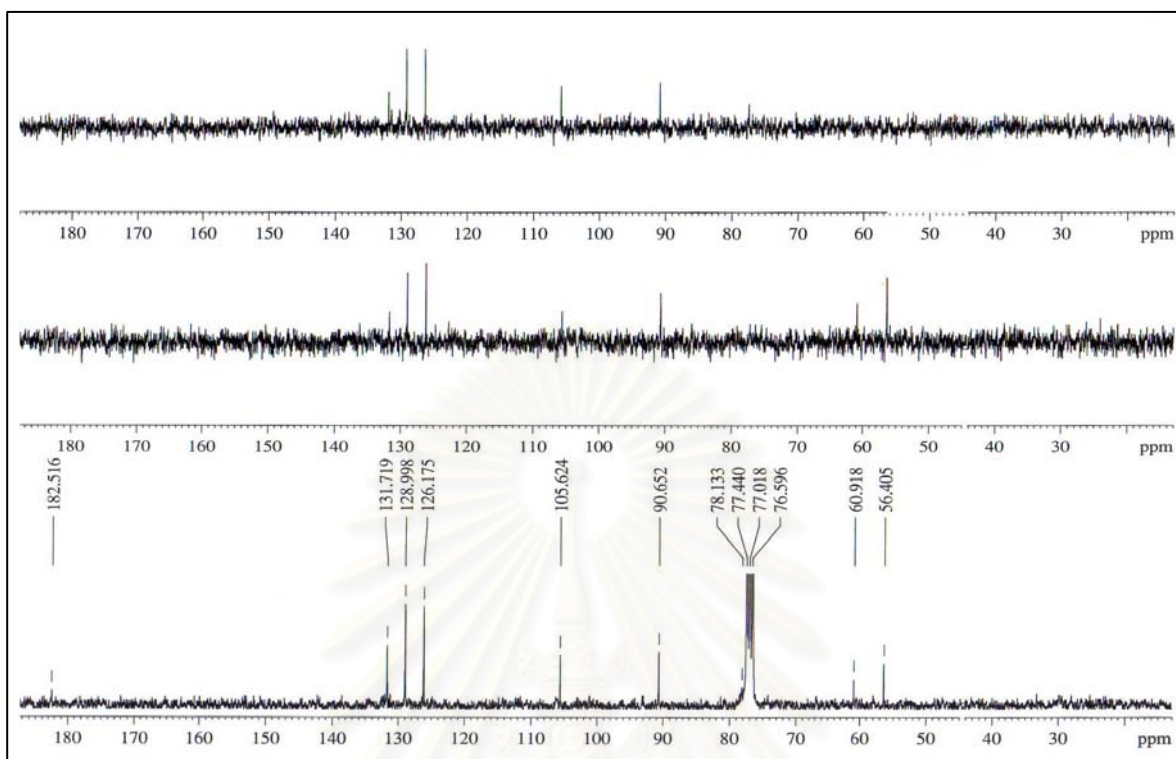
Figure 74. DEPT Spectra of compound URS-6 (in CDCl$_3$)
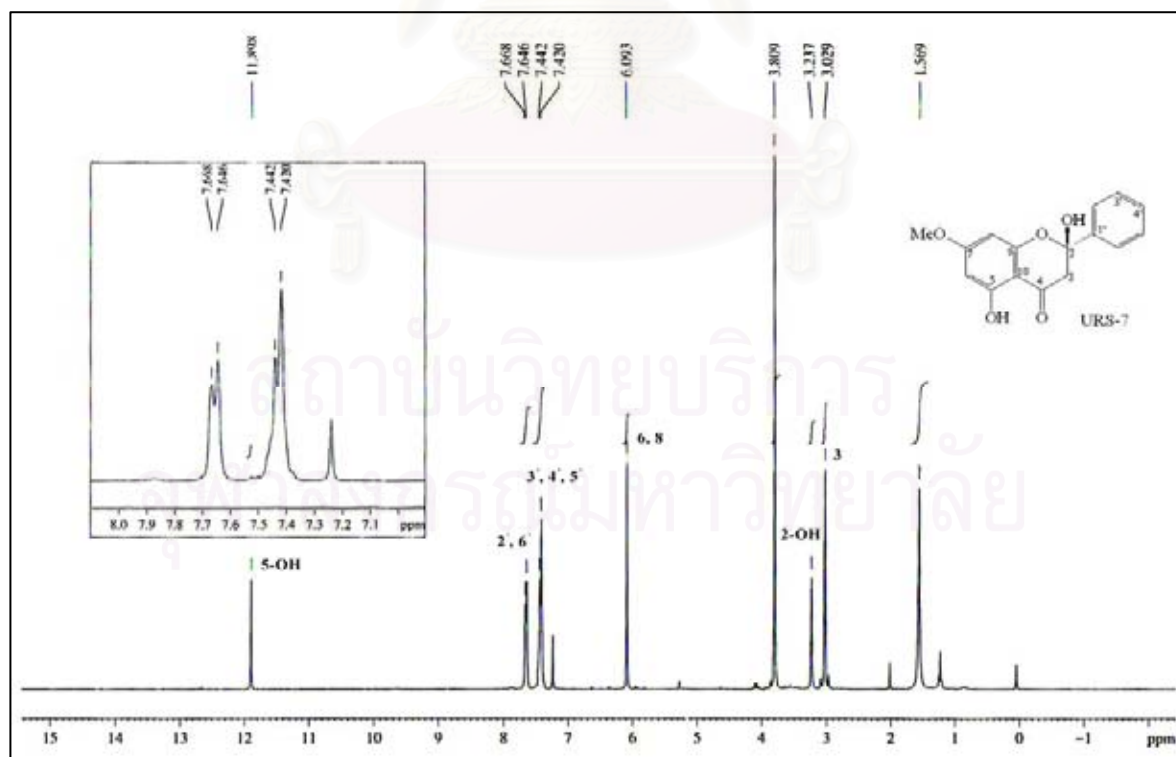
Figure 75. ^{1}H NMR (300 MHz) Spectrum of compound URS-7 (in CDCl$_3$)

209
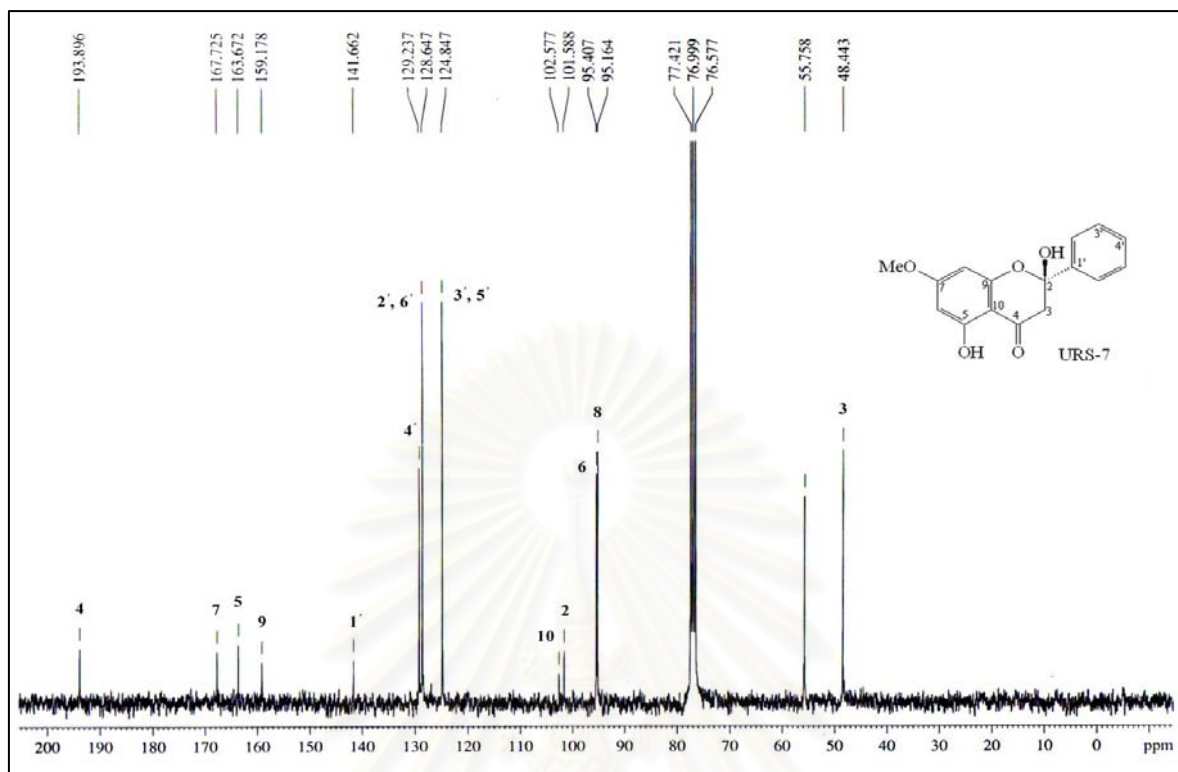
Figure 76. ^{13}C NMR (75 MHz) Spectrum of compound URS-7 (in CDCl$_3$)
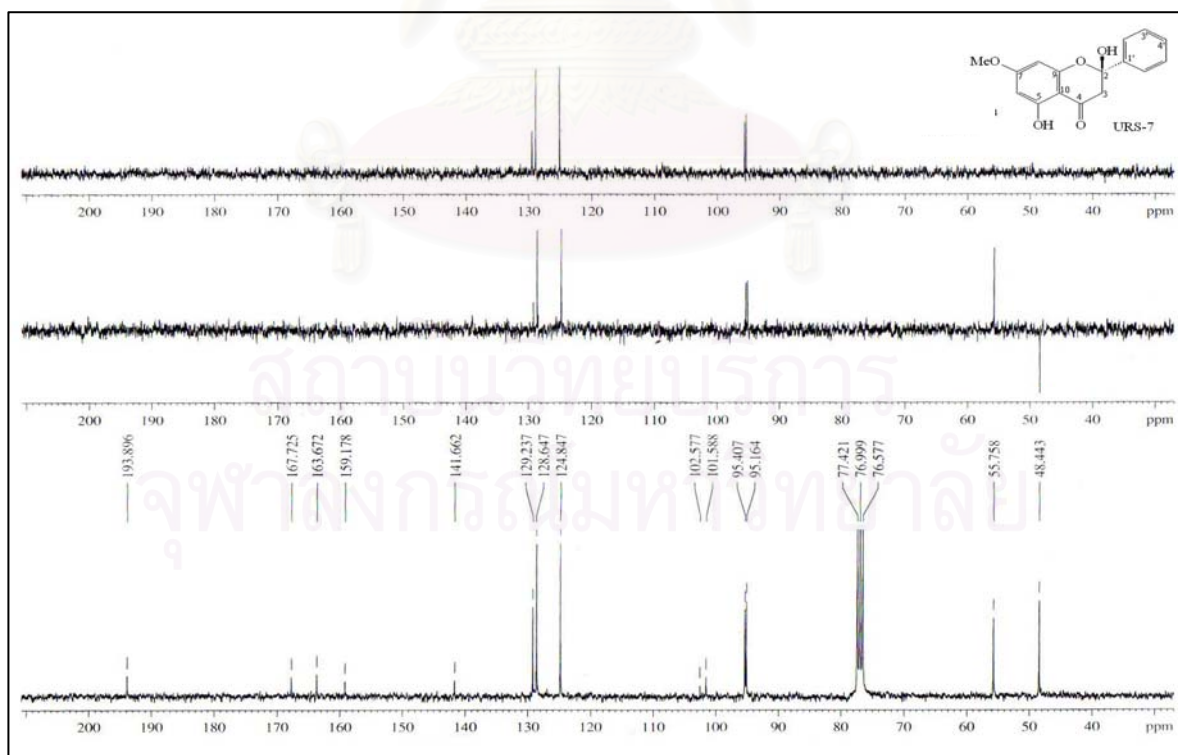
Figure 77. DEPT Spectra of compound URS-7 (in CDCl$_3$)
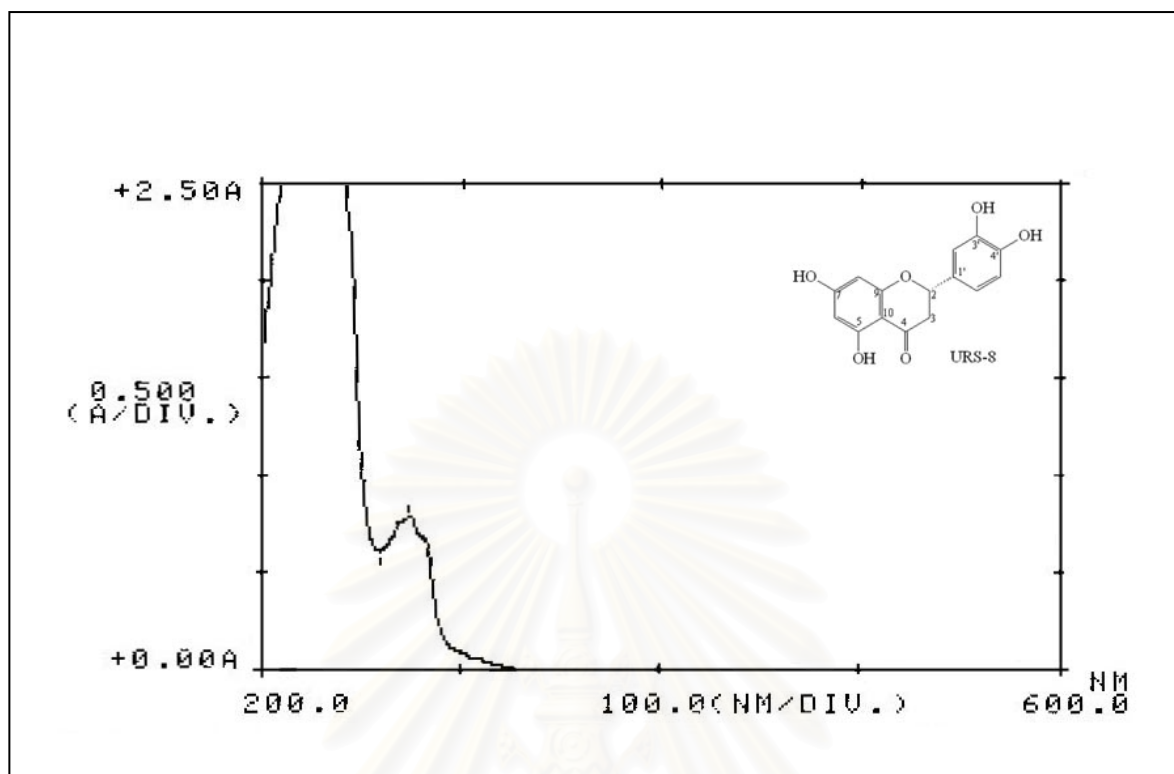
Figure 78. UV Spectrum of compound URS-8 (in MeOH)
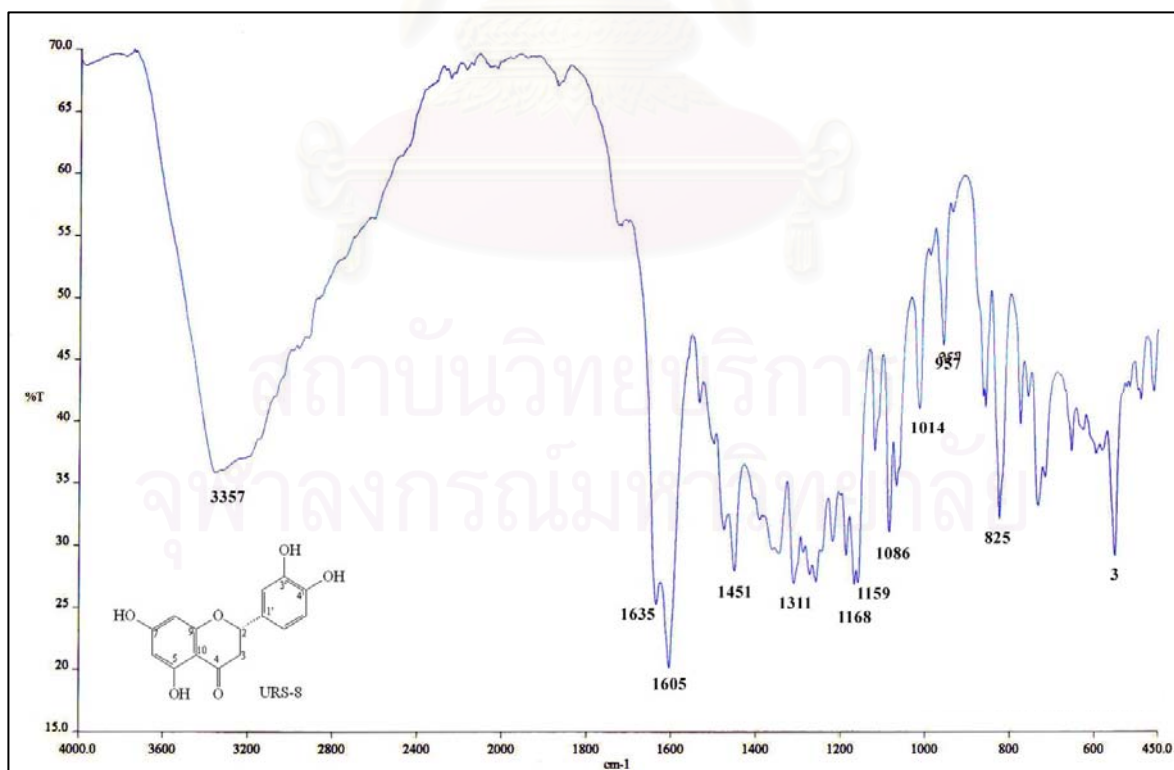
Figure 79. IR Spectrum of compound URS-8 (KBr disc)
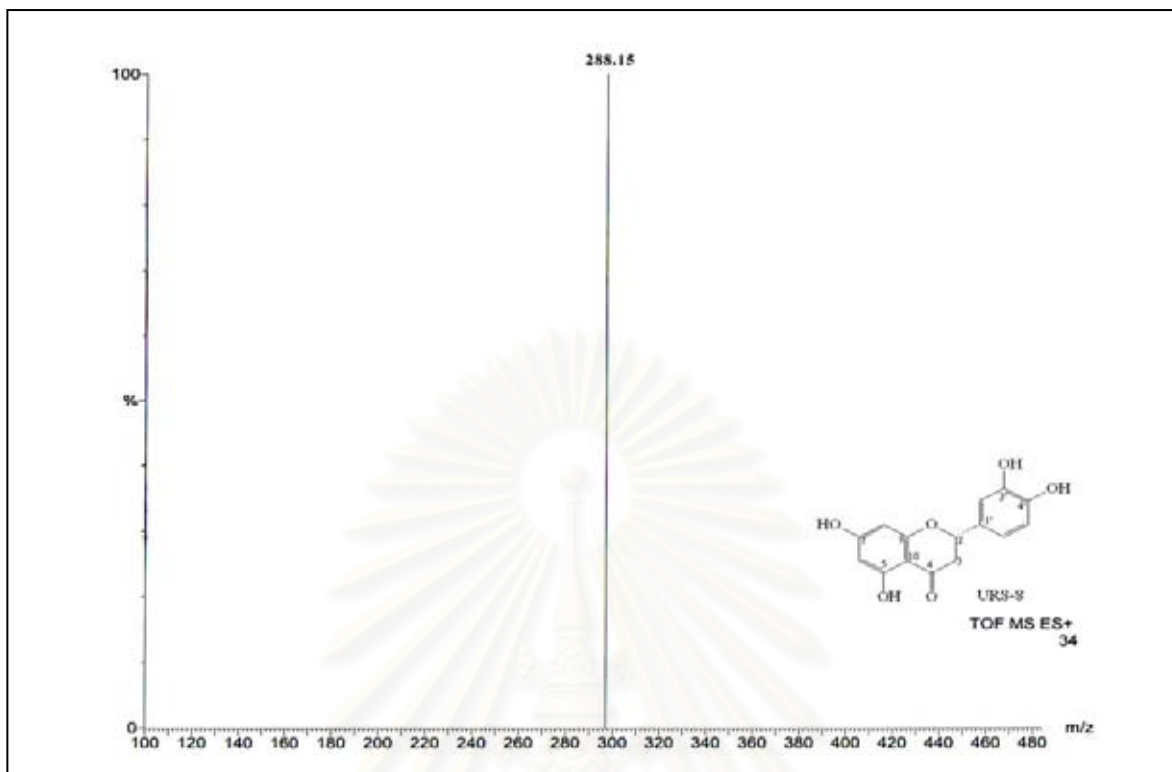
Figure 80. ESITOF Mass spectrum of compound URS-8
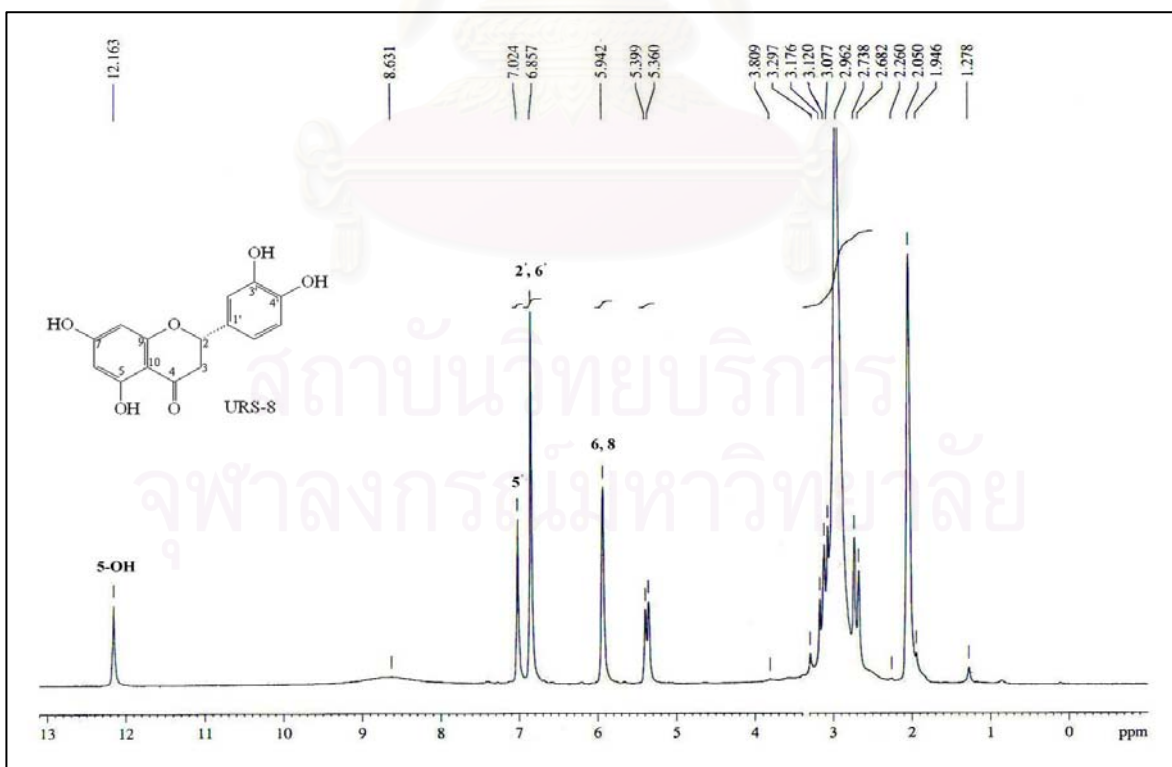
Figure 81. ^{1}H NMR (300 MHz) Spectrum of compound URS-8 (in acetone-d_6)

Figure 82. ^{13}C NMR (75 MHz) Spectrum of compound URS-8 (in acetone-d_6)
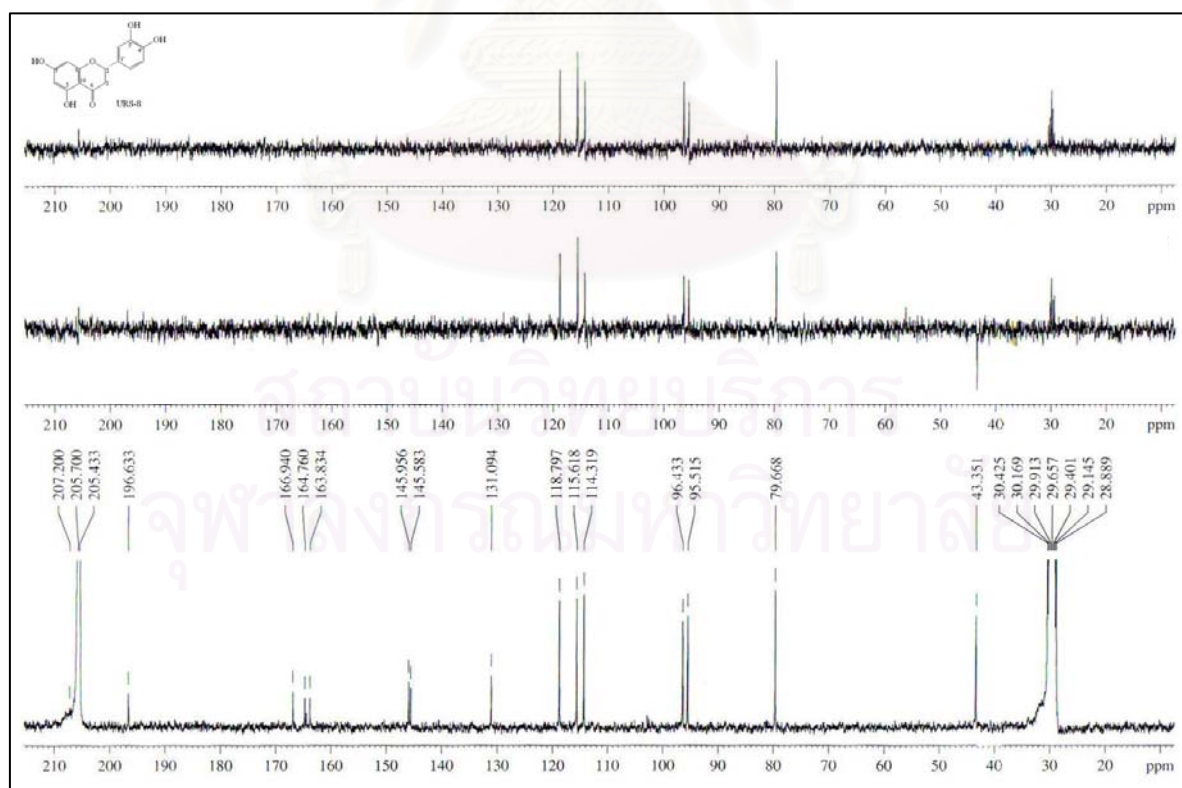
Figure 83. DEPT Spectra of compound URS-8 (in acetone-d_6)

Figure 84. UV Spectrum of compound MML-1 (in CHCl₃)

Figure 85. IR Spectrum of compound MML-1 (KBr disc)
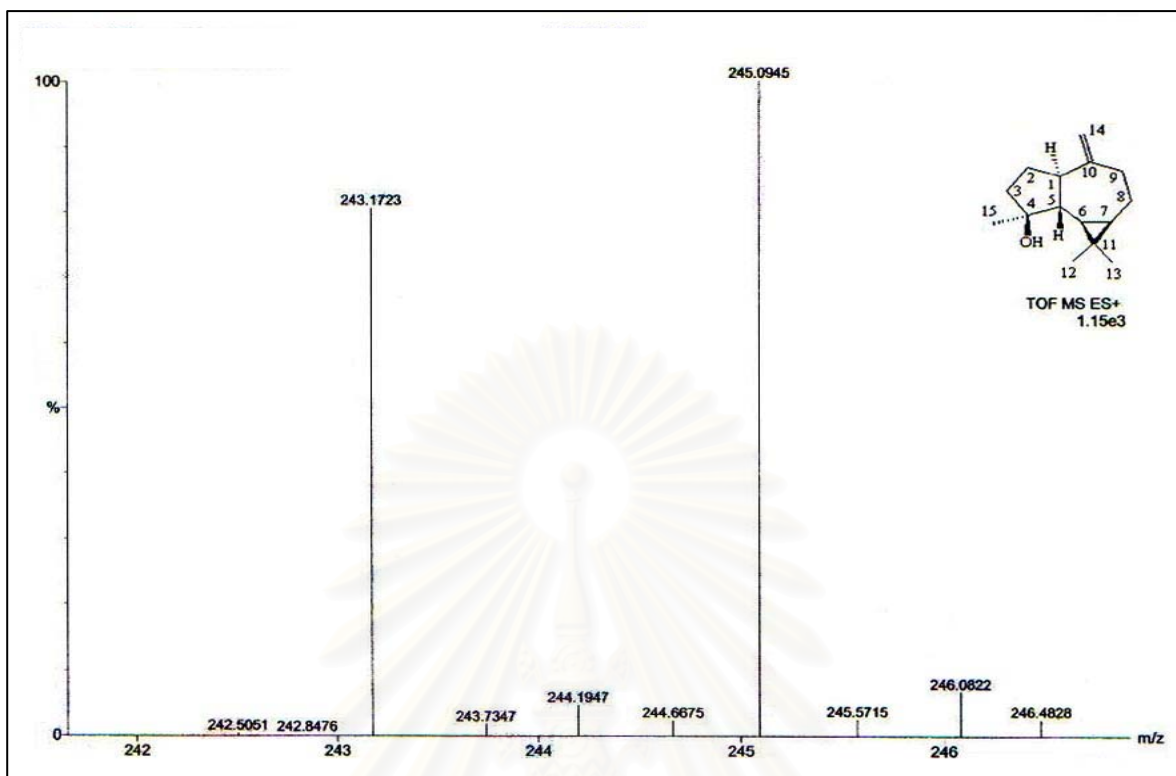
Figure 86. ESITOF Mass spectrum of compound MML-1

Figure 87. ^{1}H NMR (300 MHz) Spectrum of compound MML-1 (in CDCl$_3$)
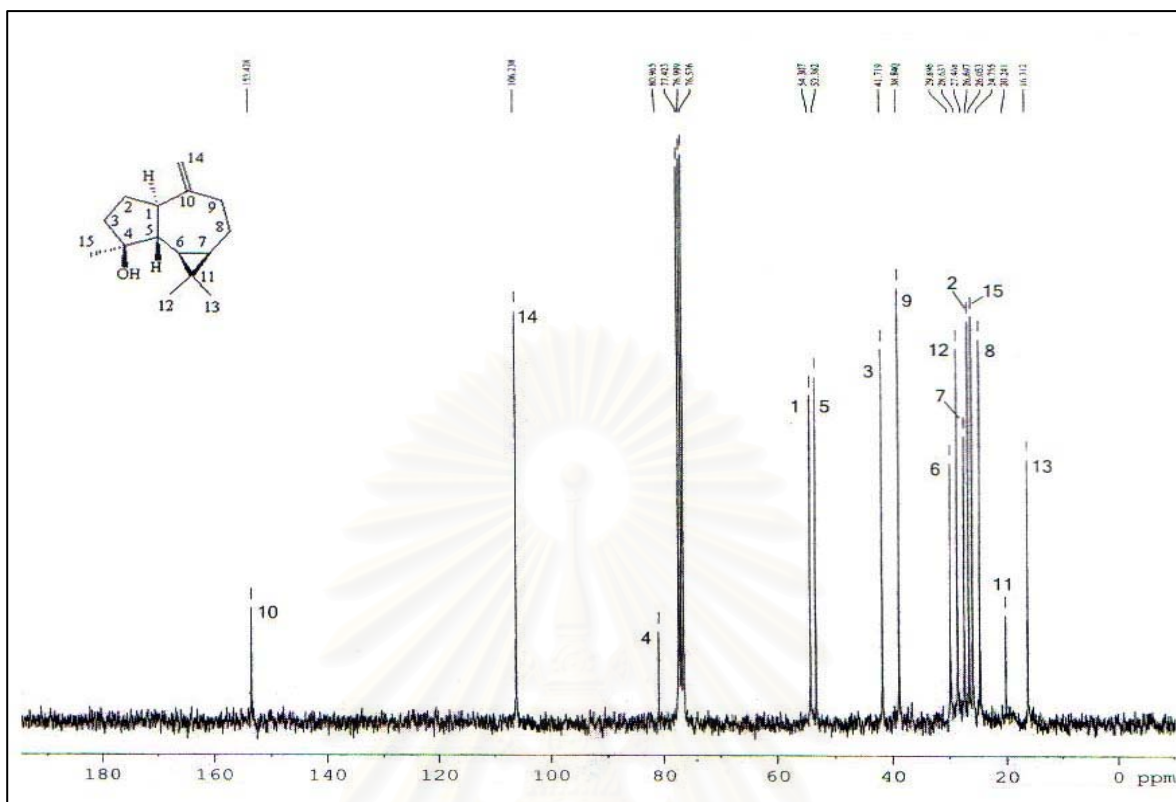
Figure 88. ^{13}C NMR (75 MHz) Spectrum of compound MML-1 (in CDCl$_3$)
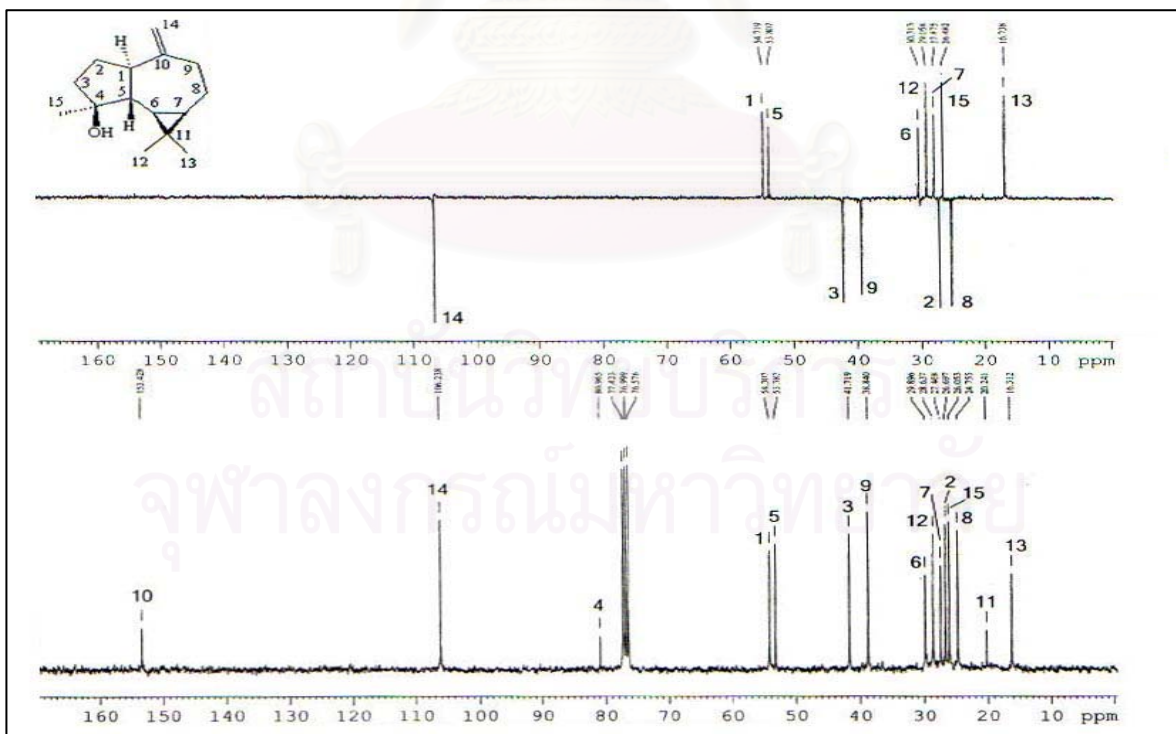
Figure 89. DEPT 135 Spectrum of compound MML-1 (in CDCl$_3$)
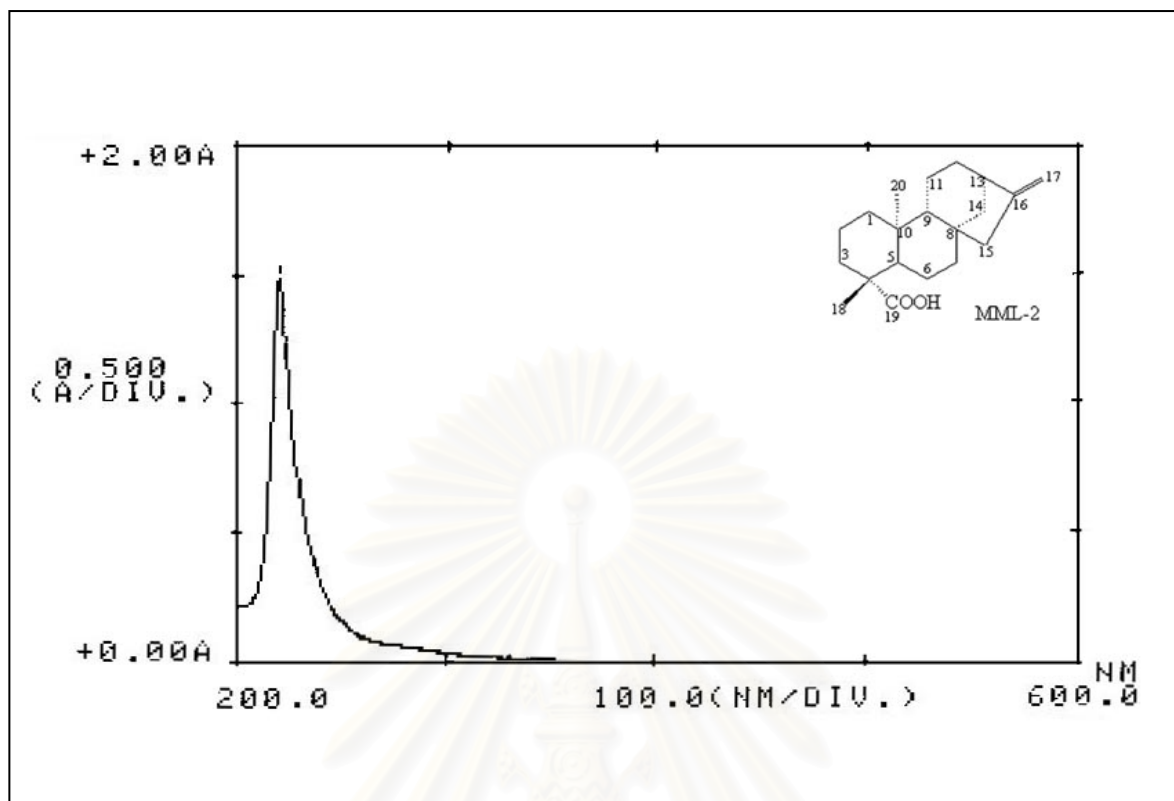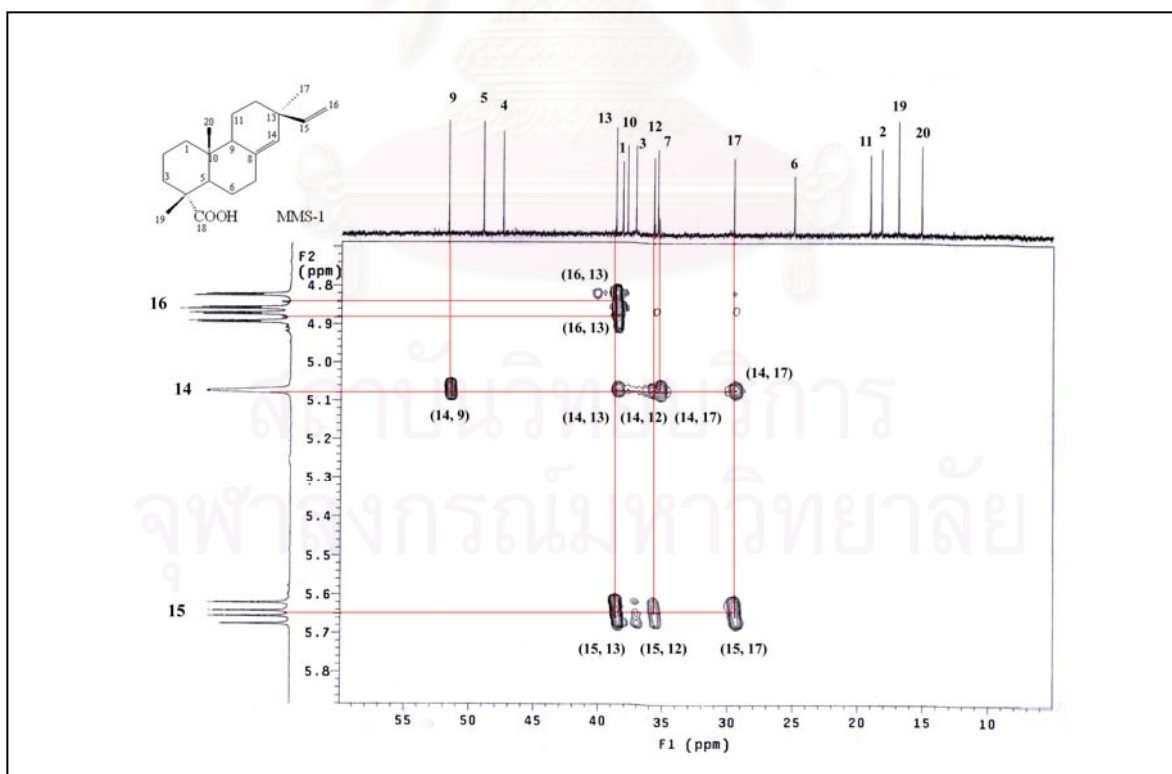
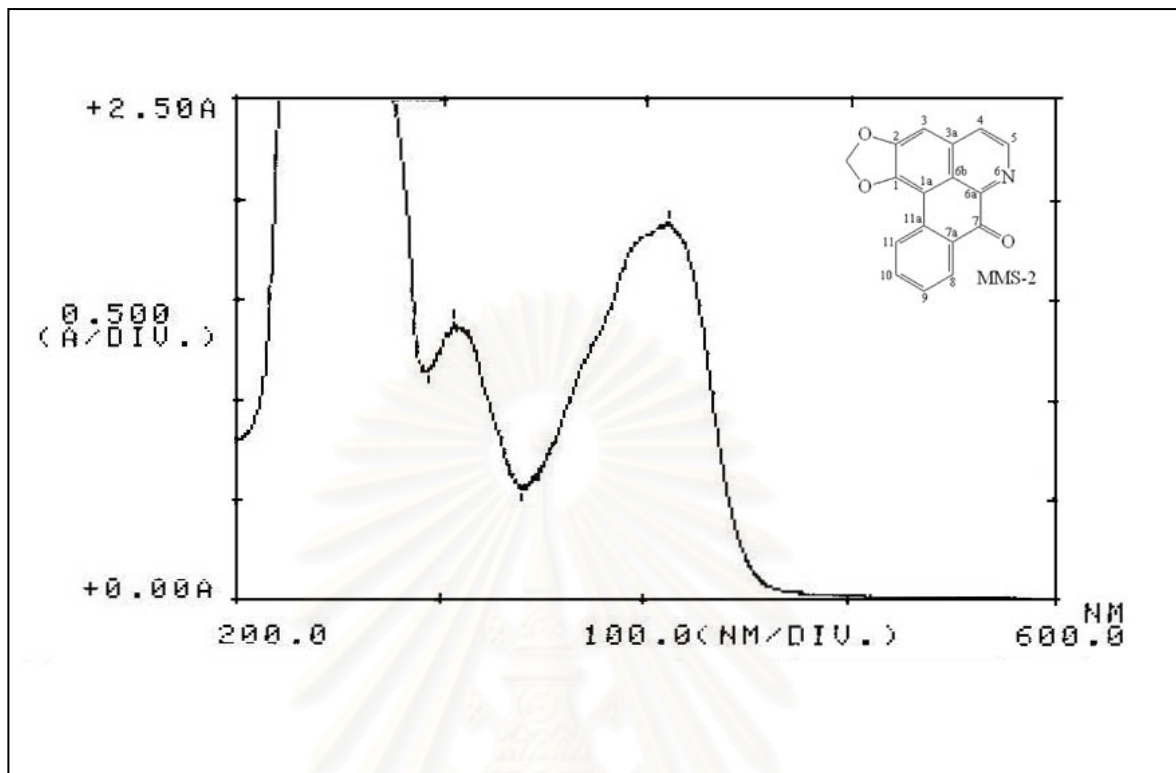**Figure 90.** UV Spectrum of compound MML-2 (in MeOH)

Figure 91. IR Spectrum of compound MML-2 (KBr disc)
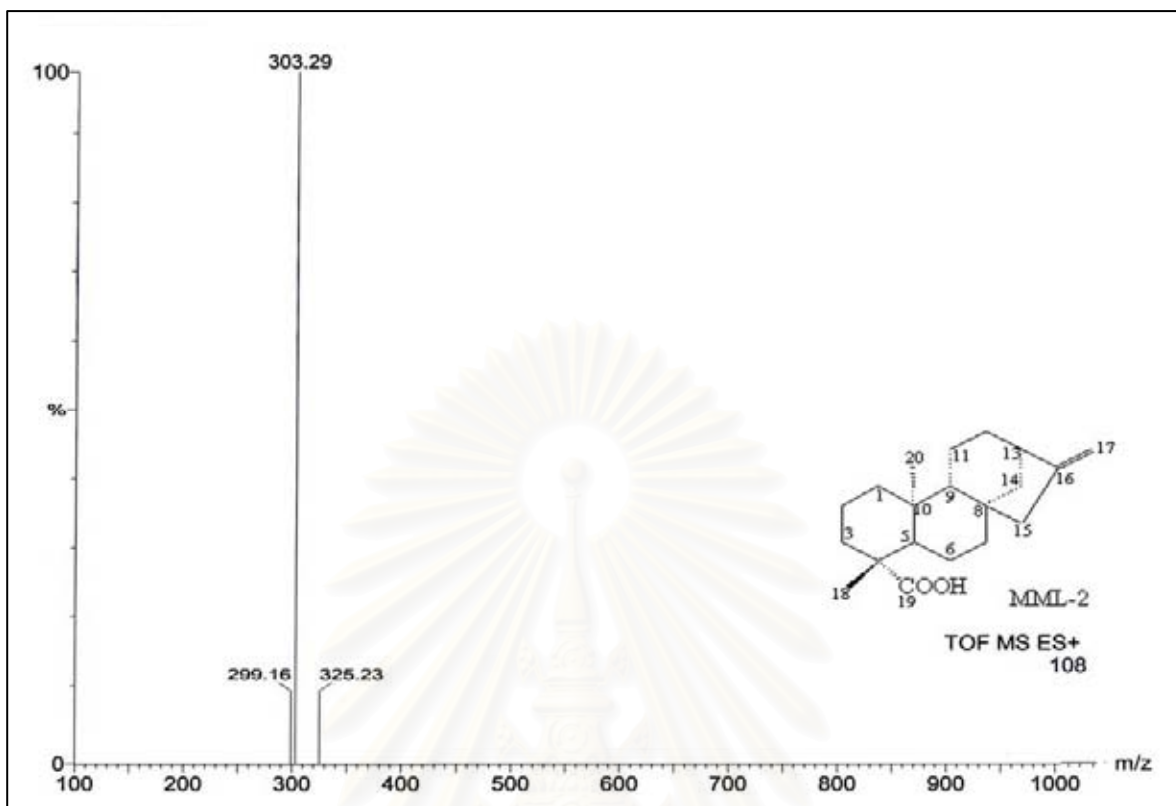
Figure 92. ESITOF Mass spectrum of compound MML-2
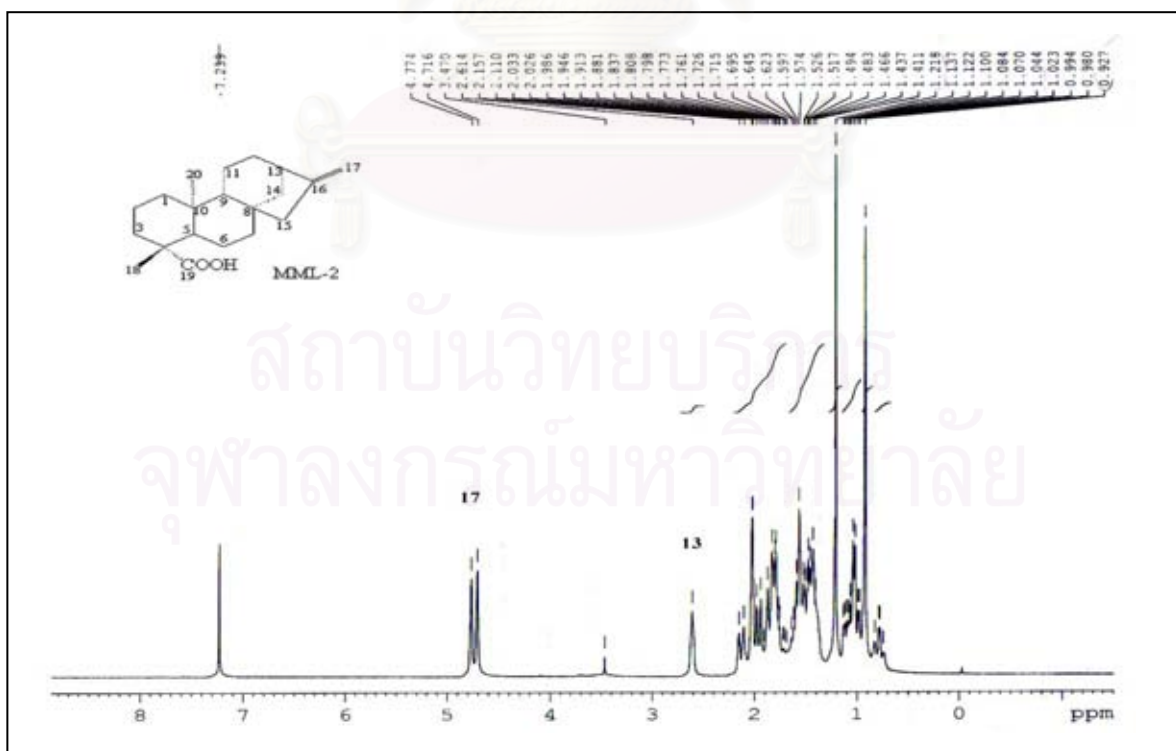
Figure 93. ^{1}H NMR (300 MHz) Spectrum of compound MML-2 (in CDCl$_3$)
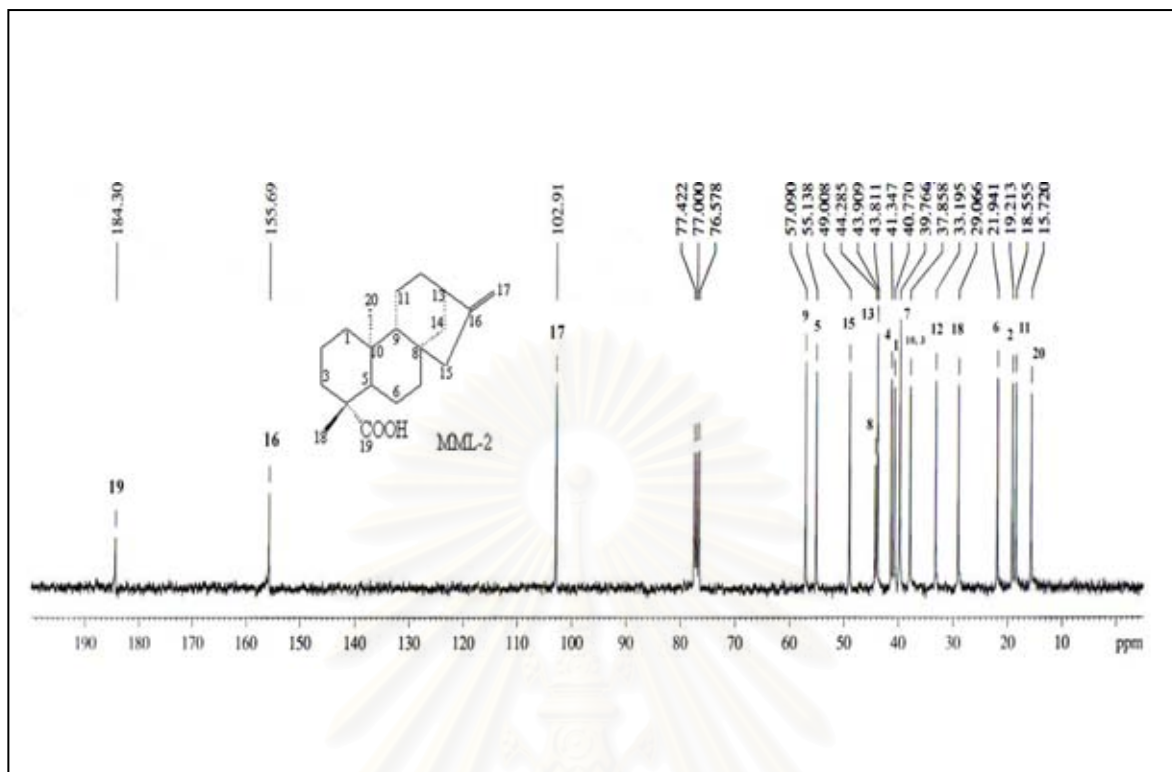
Figure 94. ^{13}C NMR (75 MHz) Spectrum of compound MML-2 (in CDCl$_3$)
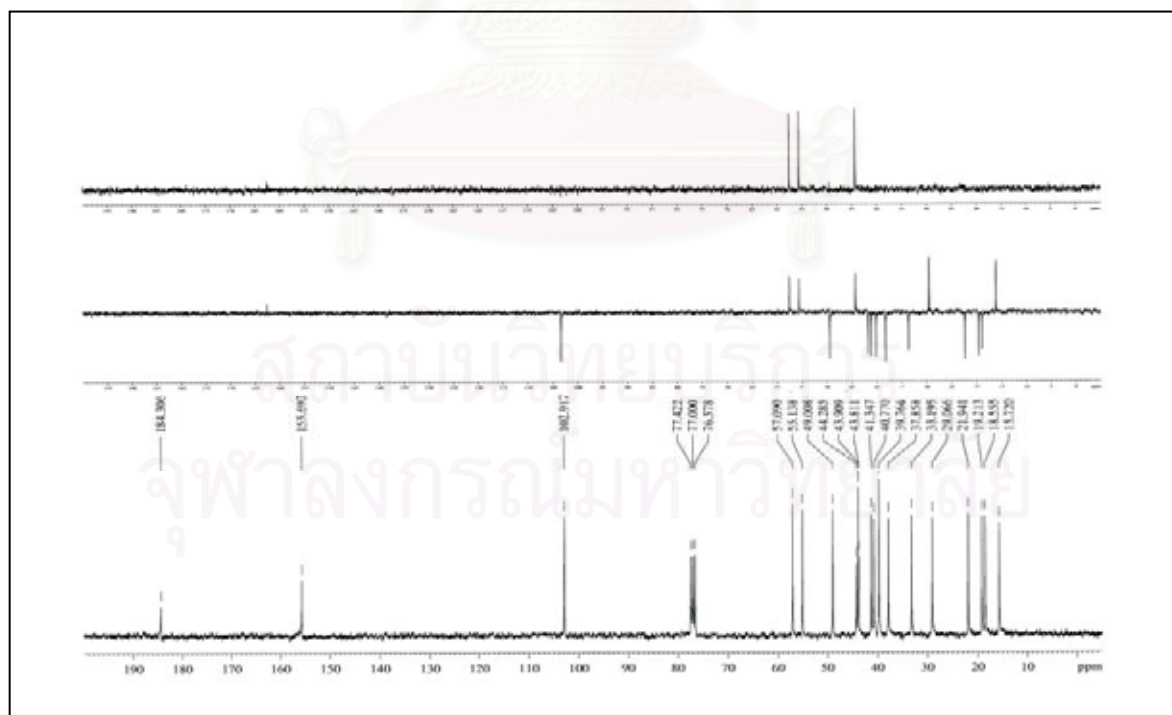
Figure 95. DEPT Spectra of compound MML-2 (in CDCl$_3$)
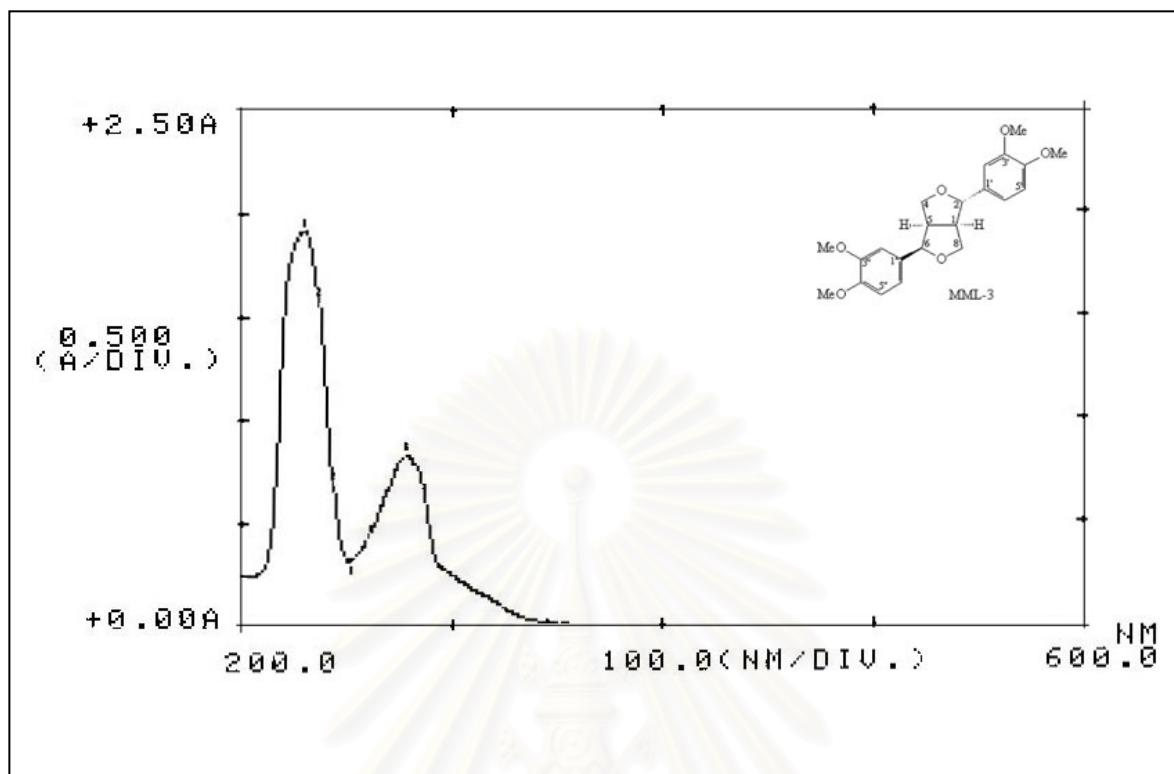
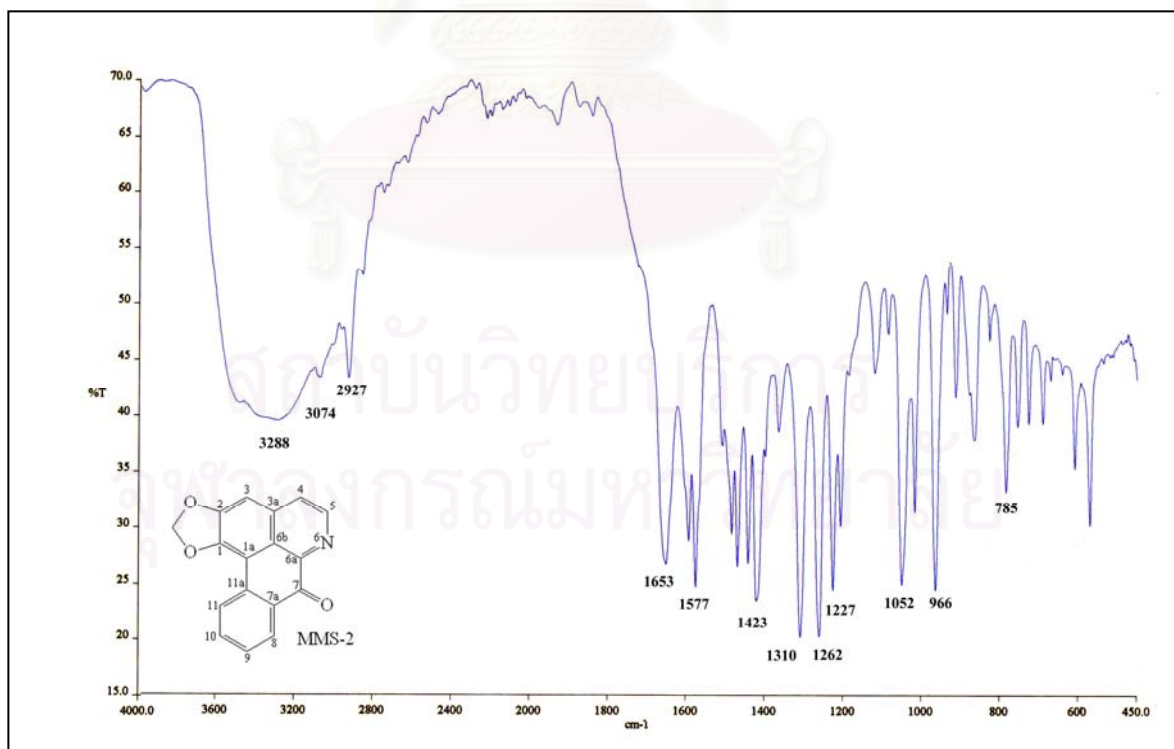**Figure 96.** UV Spectrum of compound MML-3 (in MeOH)
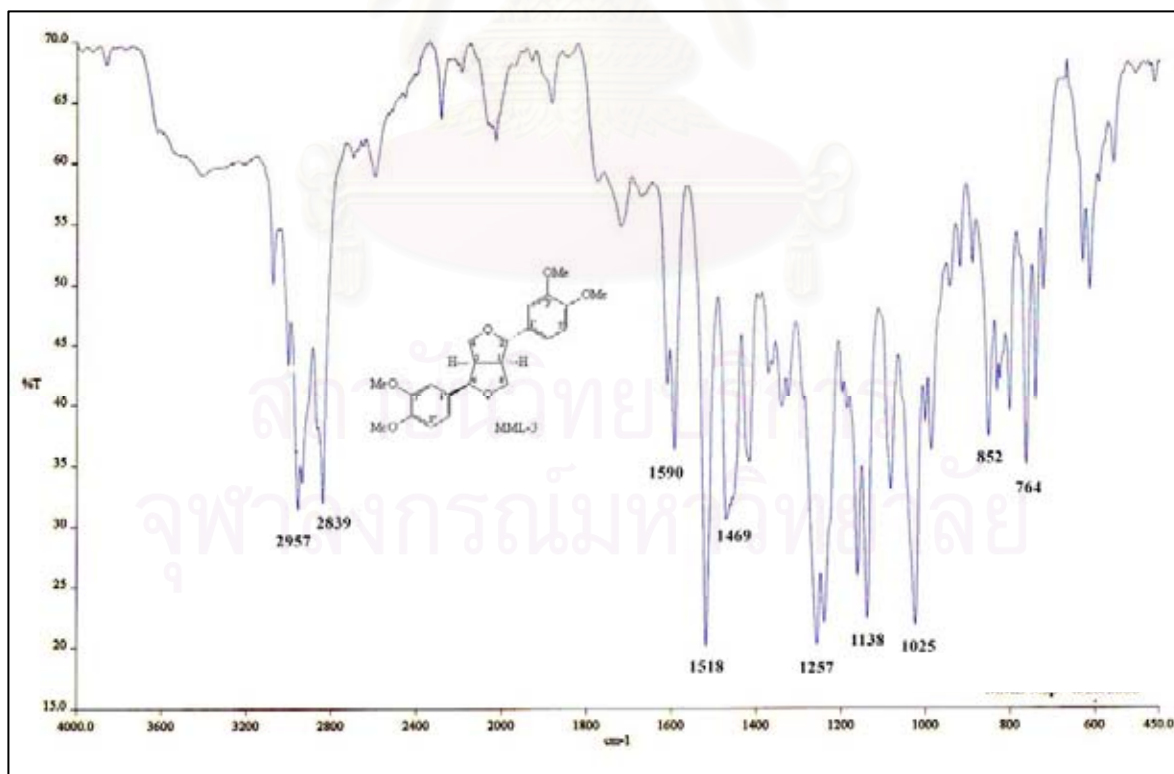
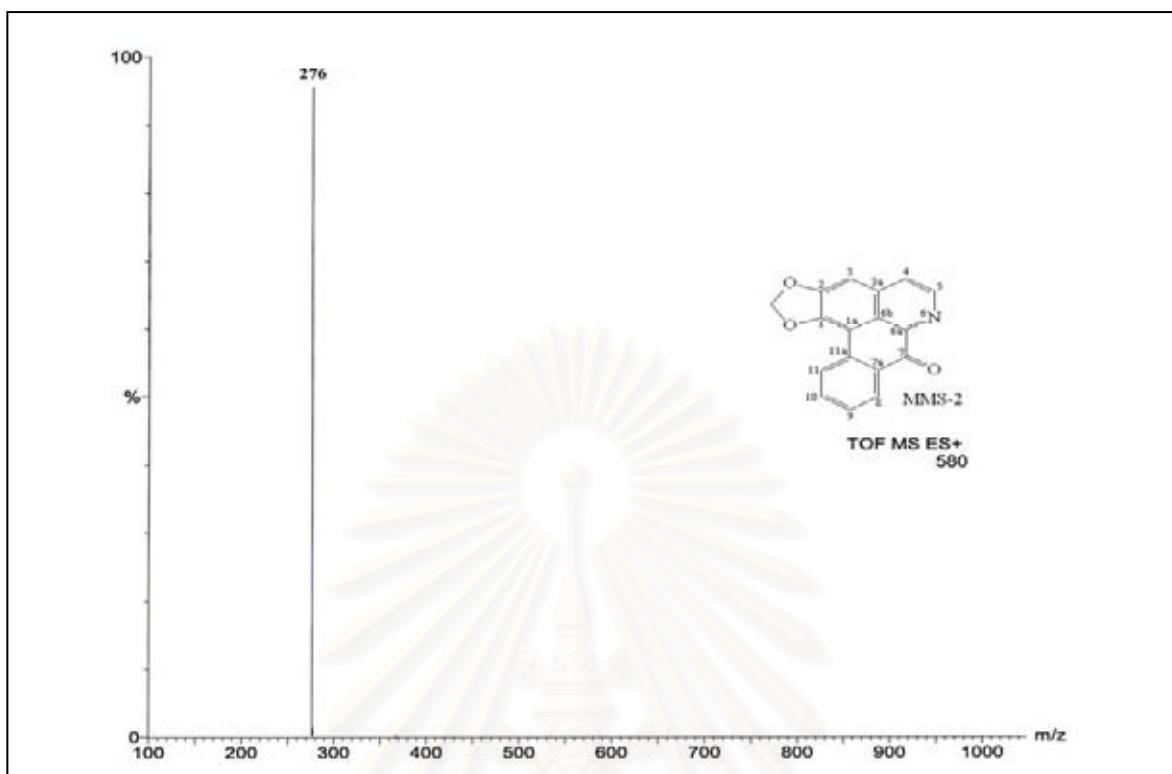**Figure 97.** IR Spectrum of compound MML-3 (KBr disc)
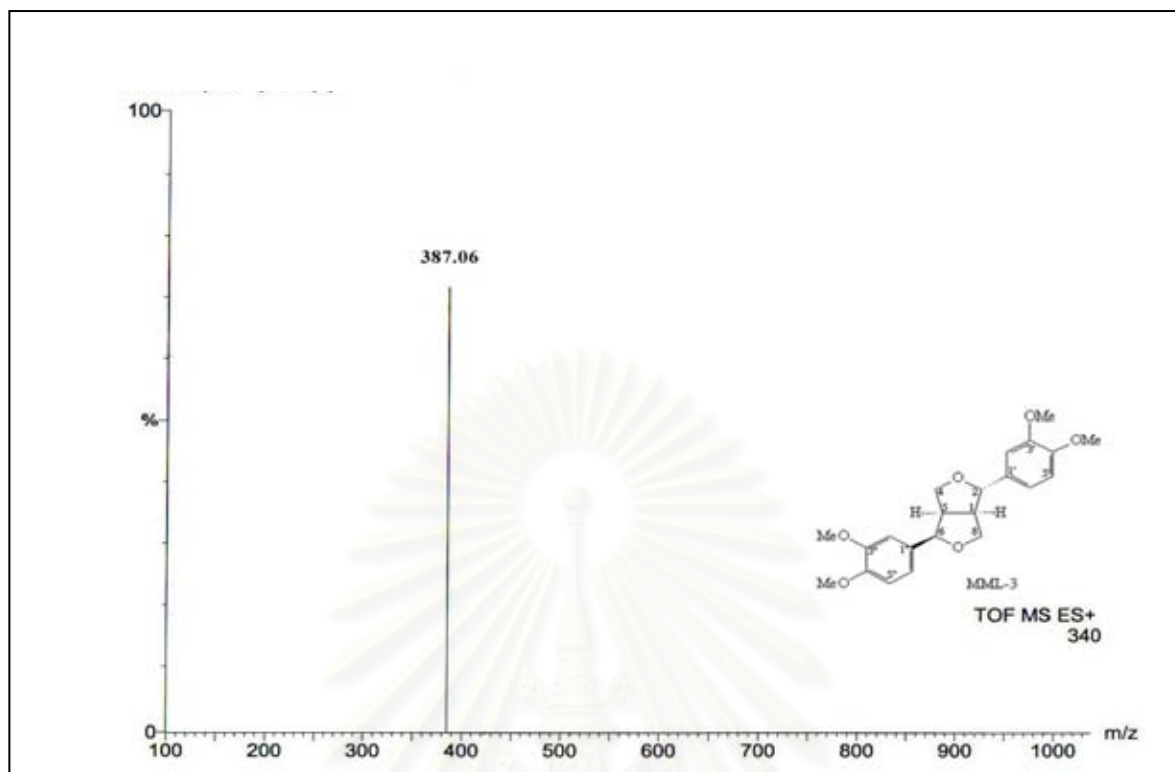
Figure 98. ESITOF Mass spectrum of compound MML-3
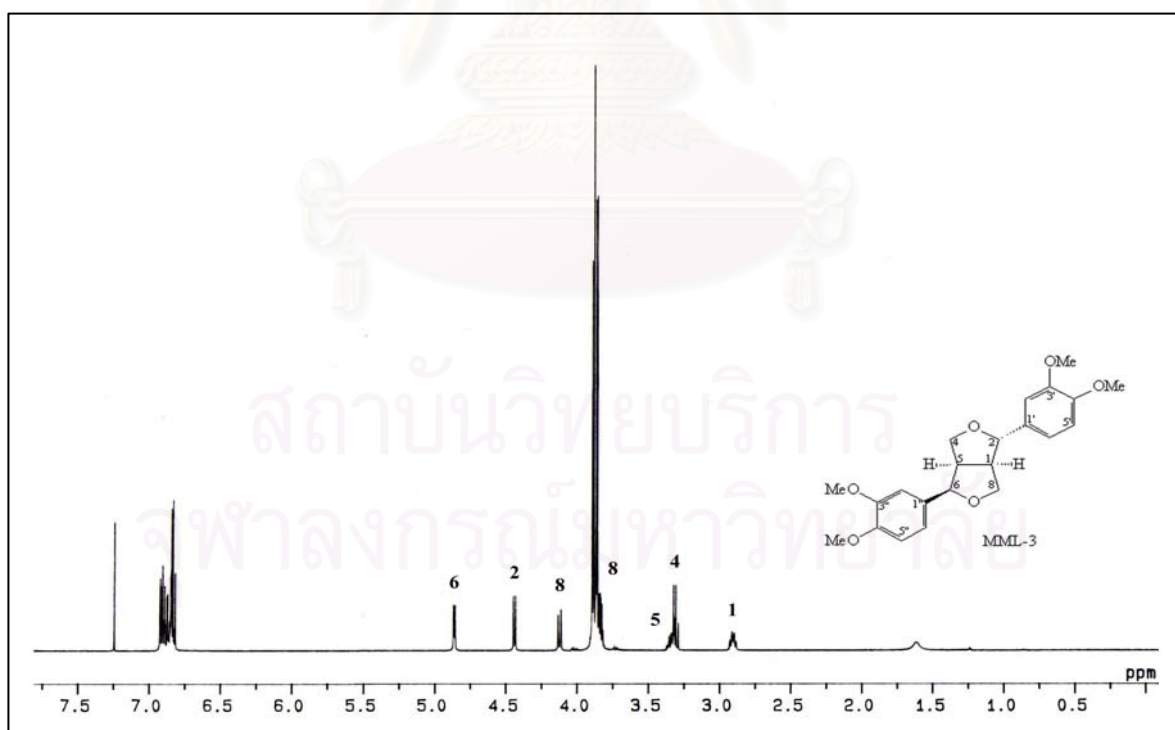
Figure 99a. ^{1}H NMR (500 MHz) Spectrum of compound MML-3 (in CDCl$_3$)

Figure 99b. ^{1}H NMR (125 MHz) Spectrum of compound MML-3 (in CDCl$_3$, expansion)

Figure 100. ^{13}C NMR (125 MHz) Spectrum of compound MML-3 (in CDCl$_3$)

Figure 101. IR Spectrum of compound MML-4 (KBr disc)
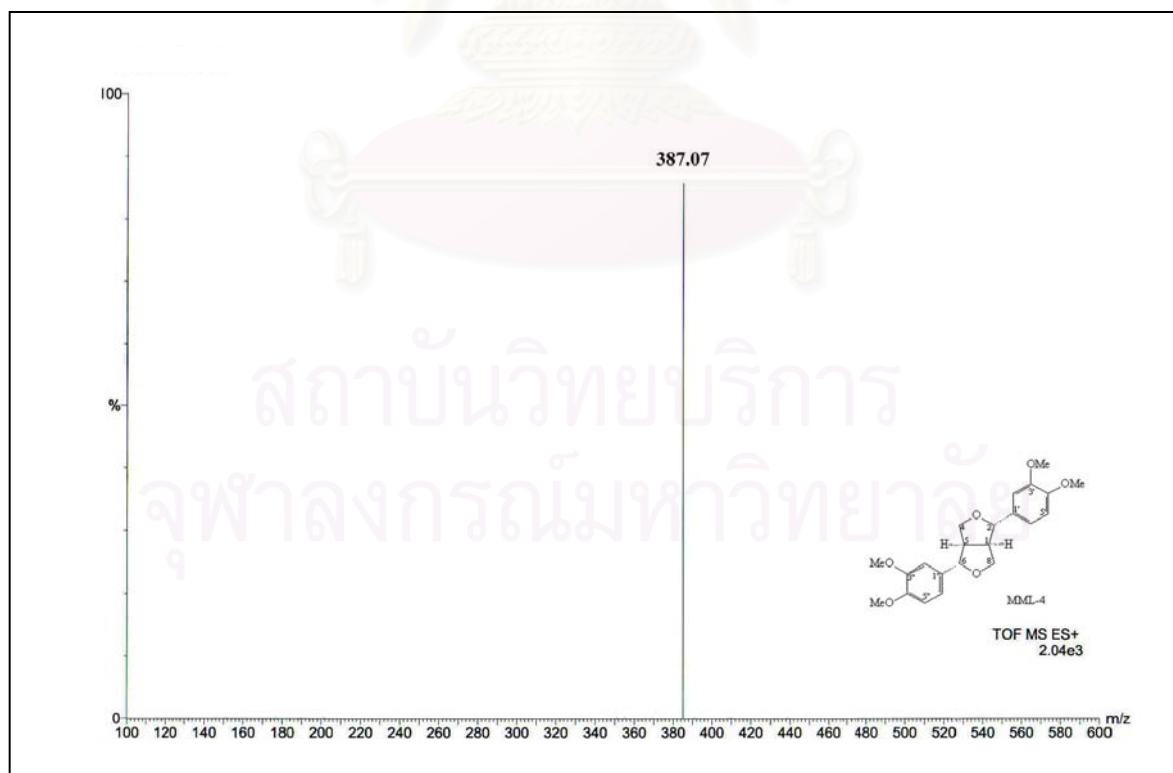
Figure 102. ESITOF Mass spectrum of compound MML-4

Figure 103. ^{1}H NMR (300 MHz) Spectrum of compound MML-4 (in acetone-d_6)
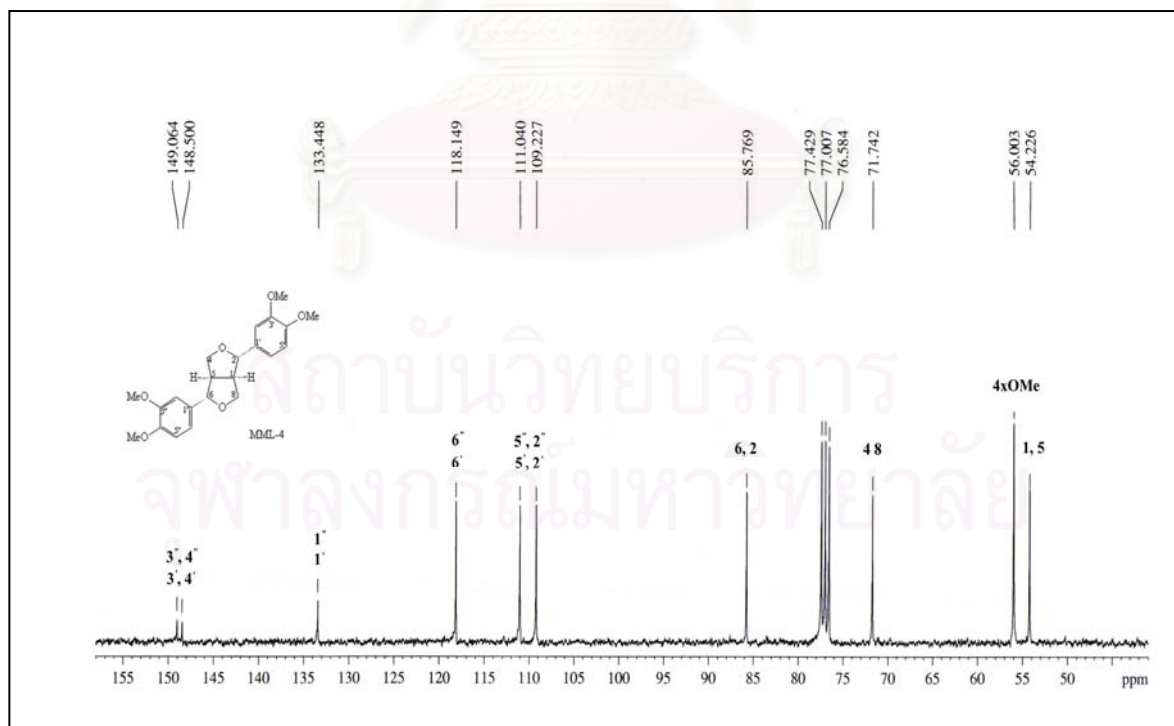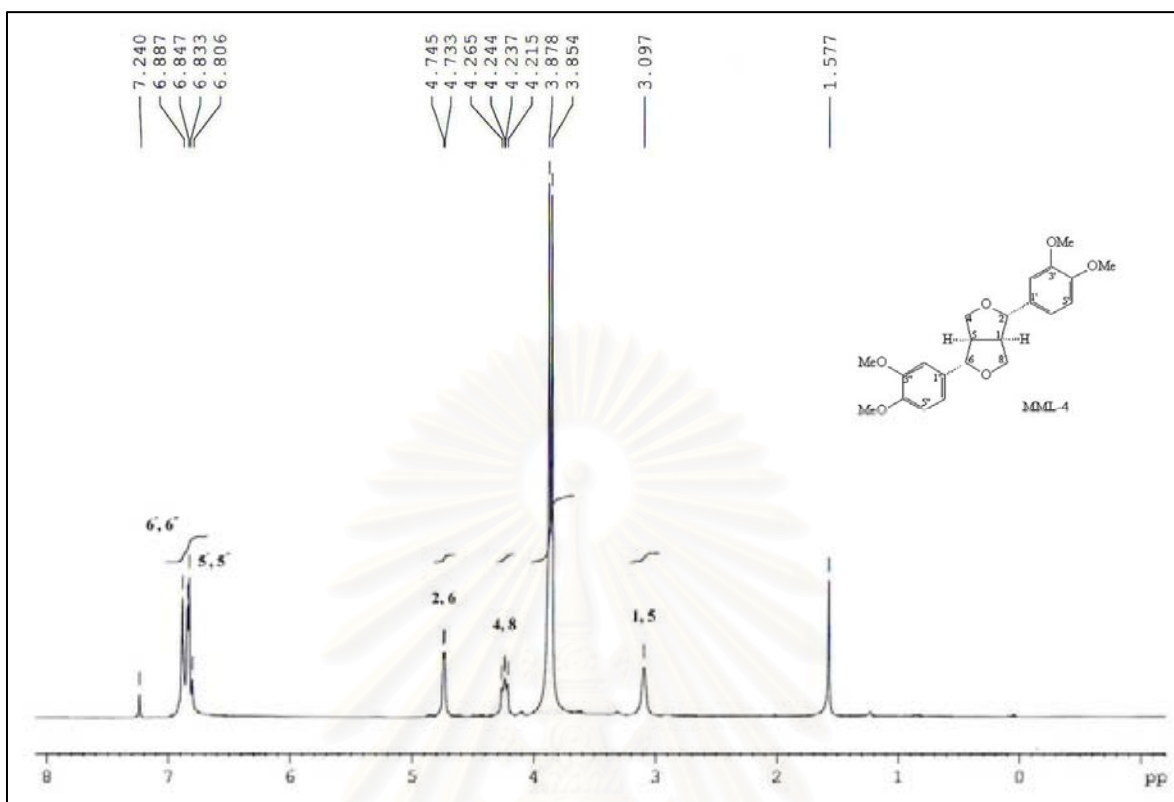
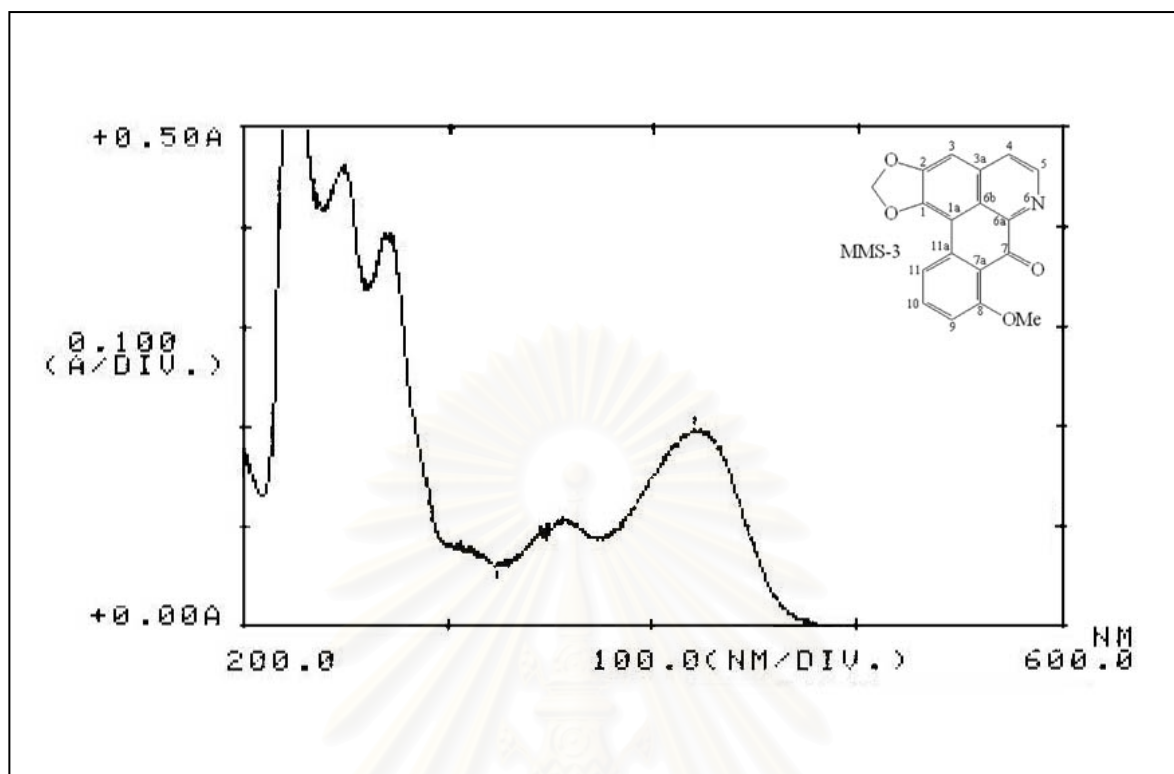**Figure 104.** ^{13}C NMR (75 MHz) Spectrum of compound MML-4 (in acetone-d_6)
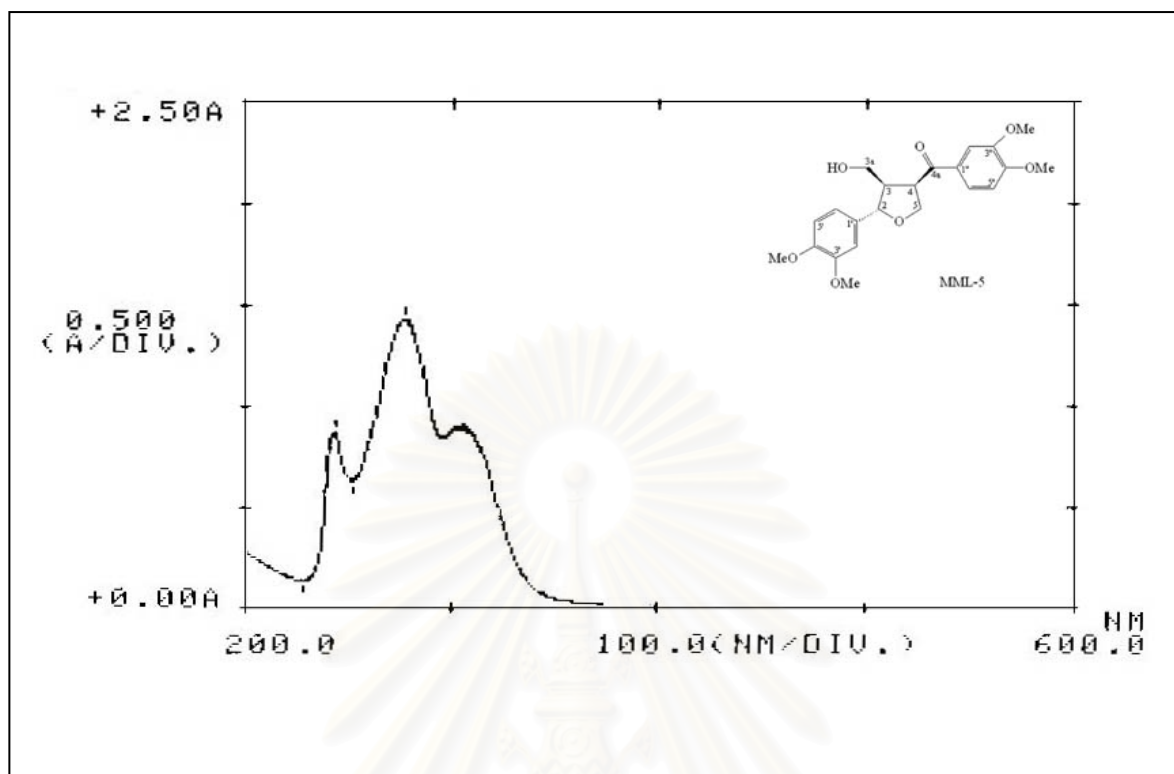
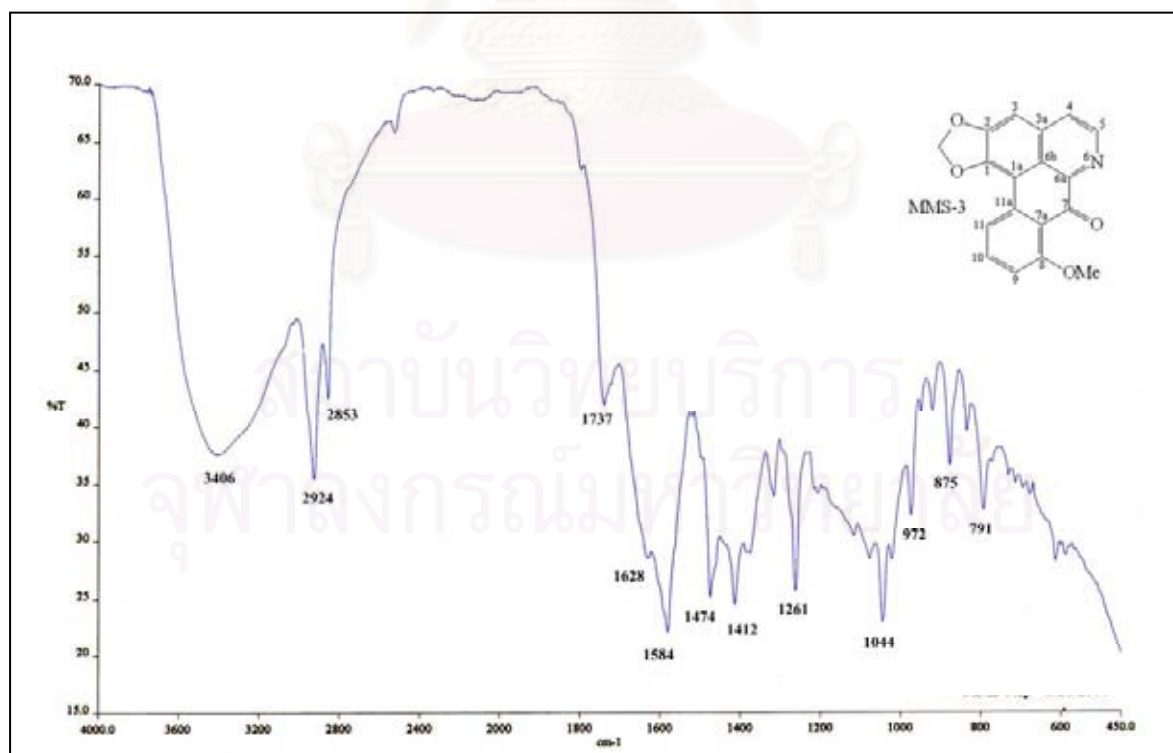**Figure 105.** UV Spectrum of compound MML-5 (in MeOH)
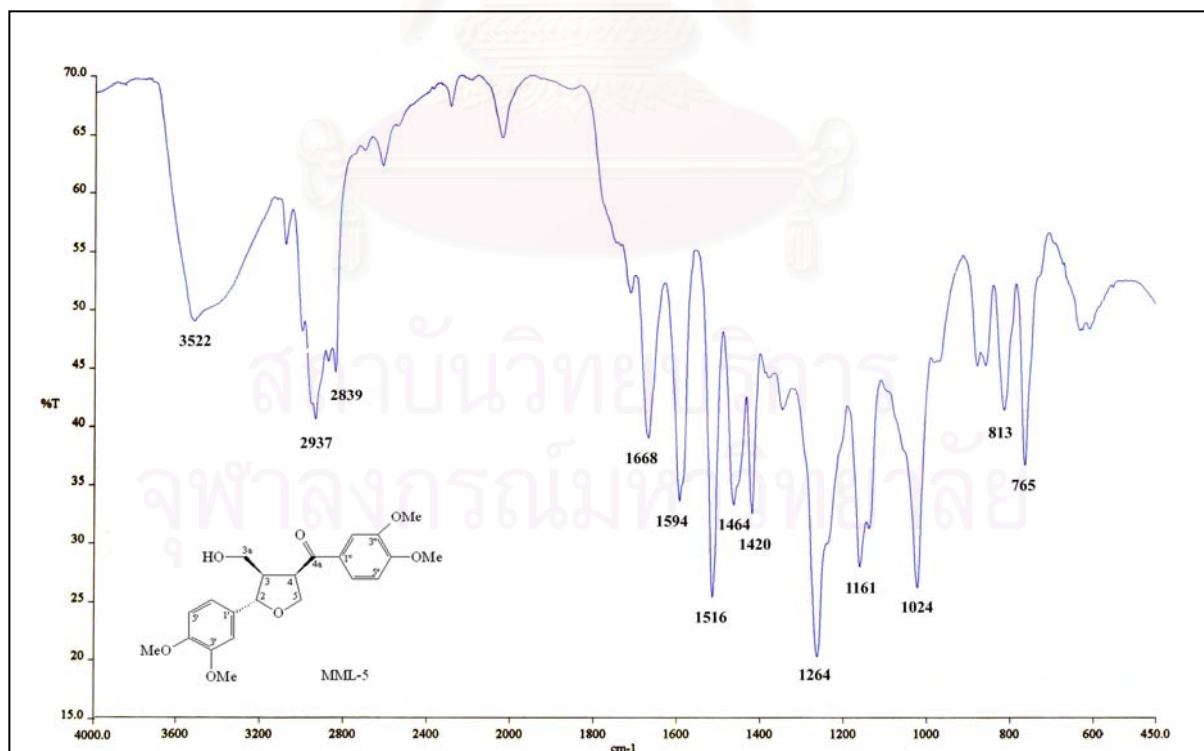
Figure 106. IR Spectrum of compound MML-5 (KBr disc)
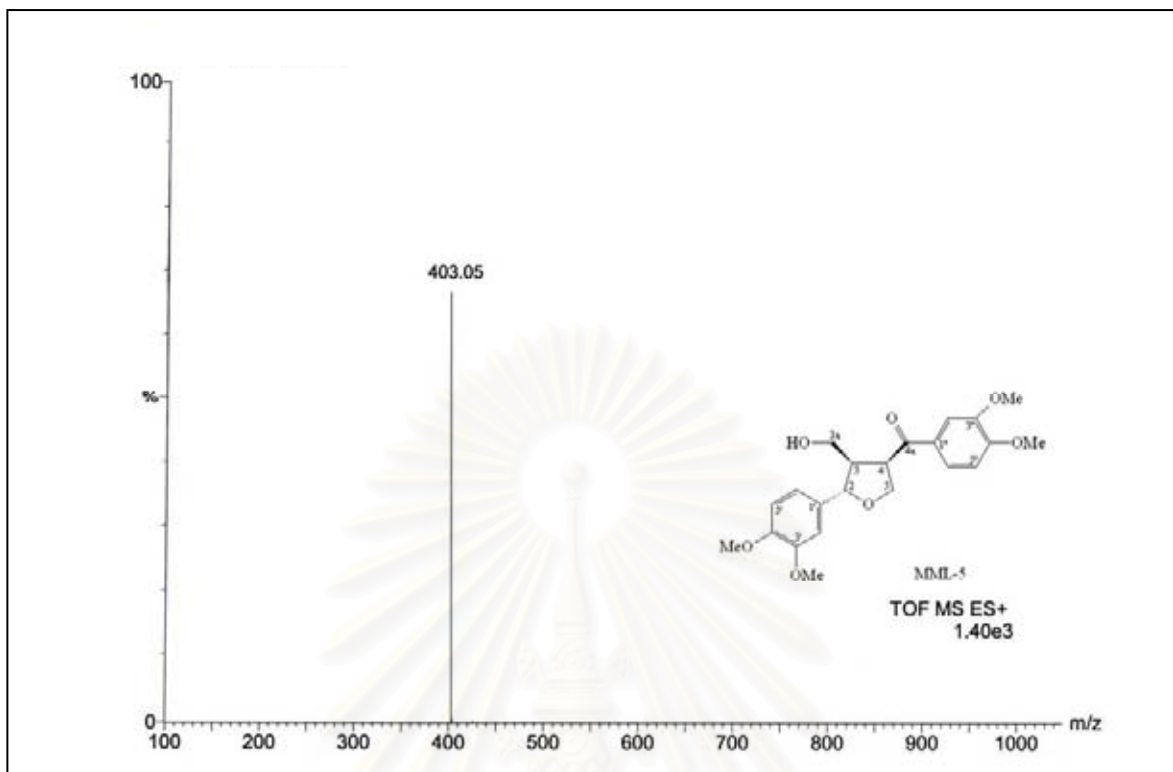
Figure 107. ESITOF Mass spectrum of compound MML-5
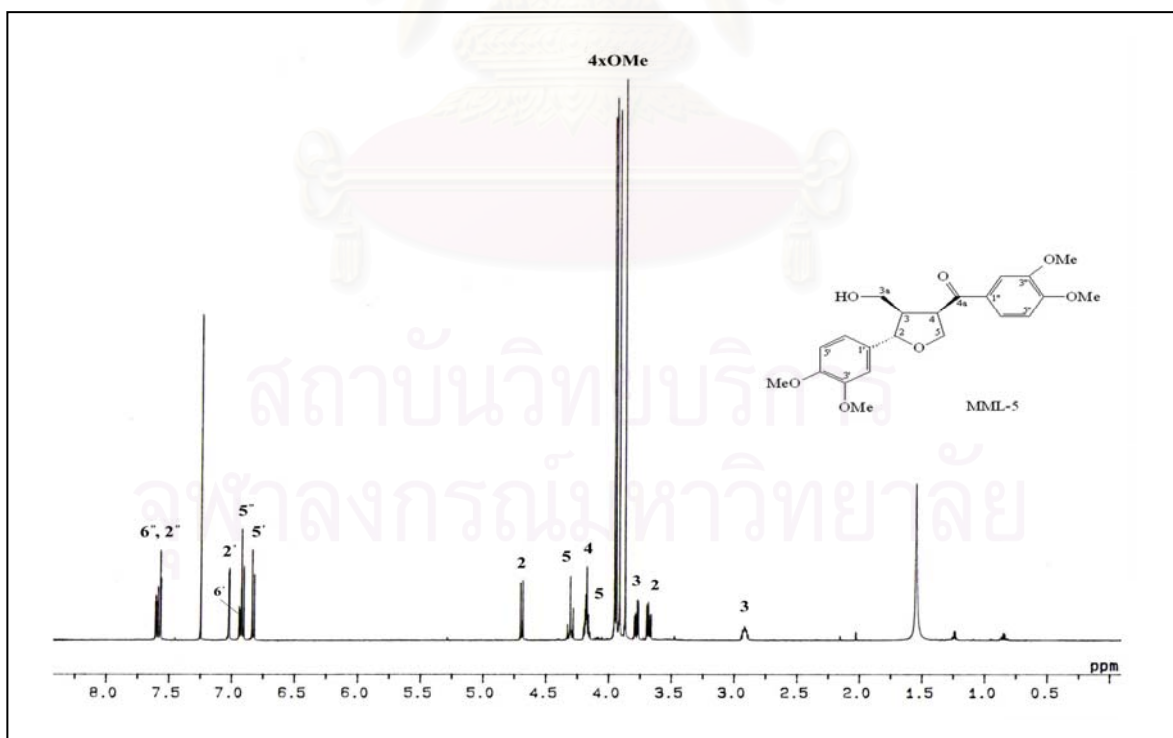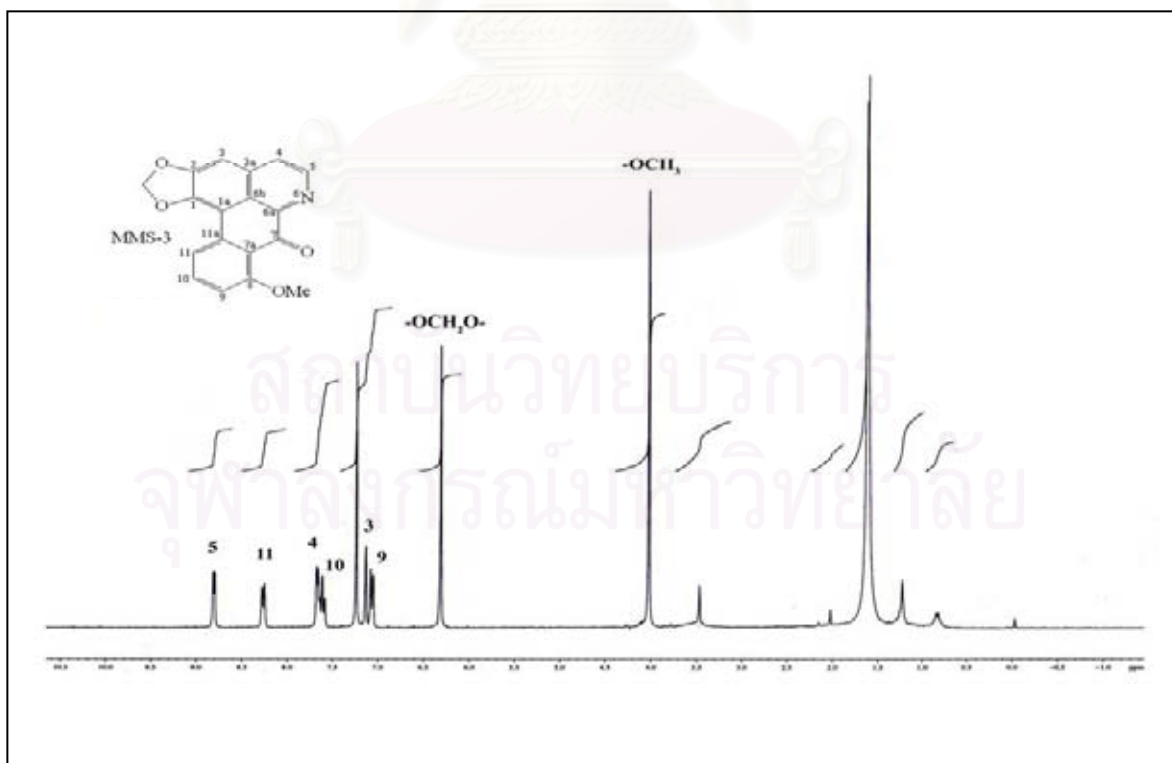

Figure 108. ^{1}H NMR (500 MHz) Spectrum of compound MML-5 (in CDCl$_3$)

Figure 109. ^{13}C NMR (125 MHz) Spectrum of compound MML-5 (in CDCl$_3$)

Figure 110. ^{1}H NMR (500 MHz) Spectrum of compound MML-6 (in acetone -d_6)
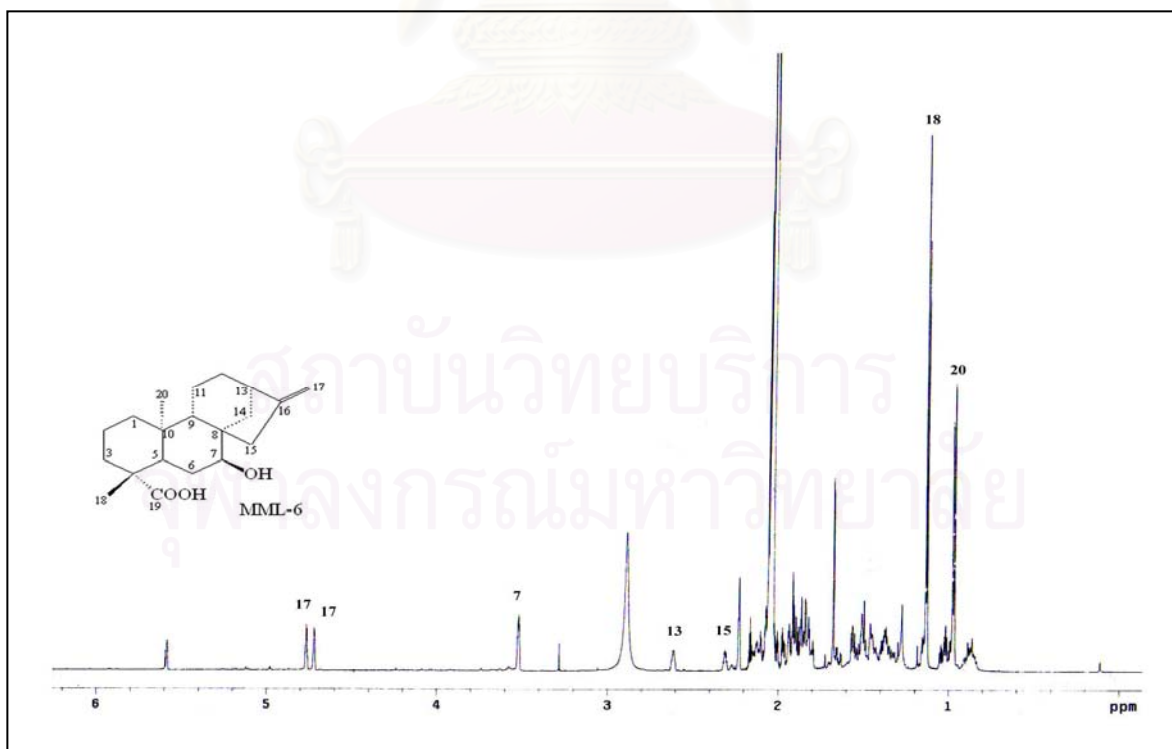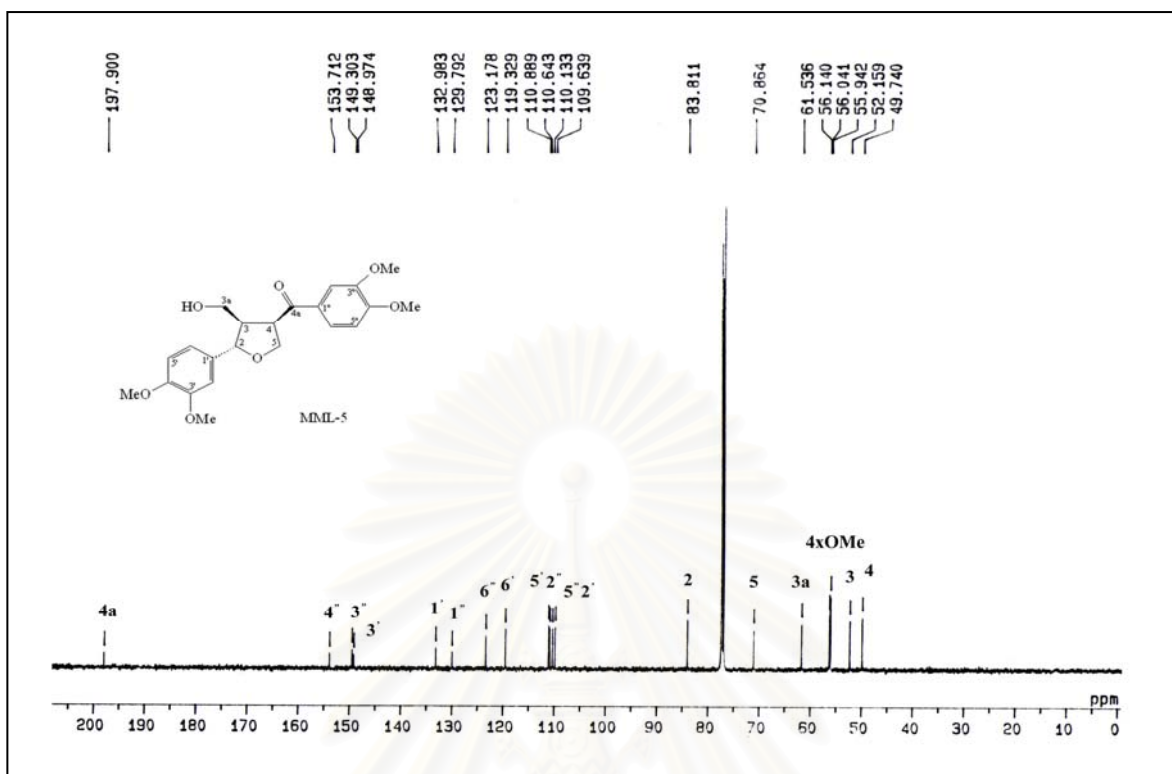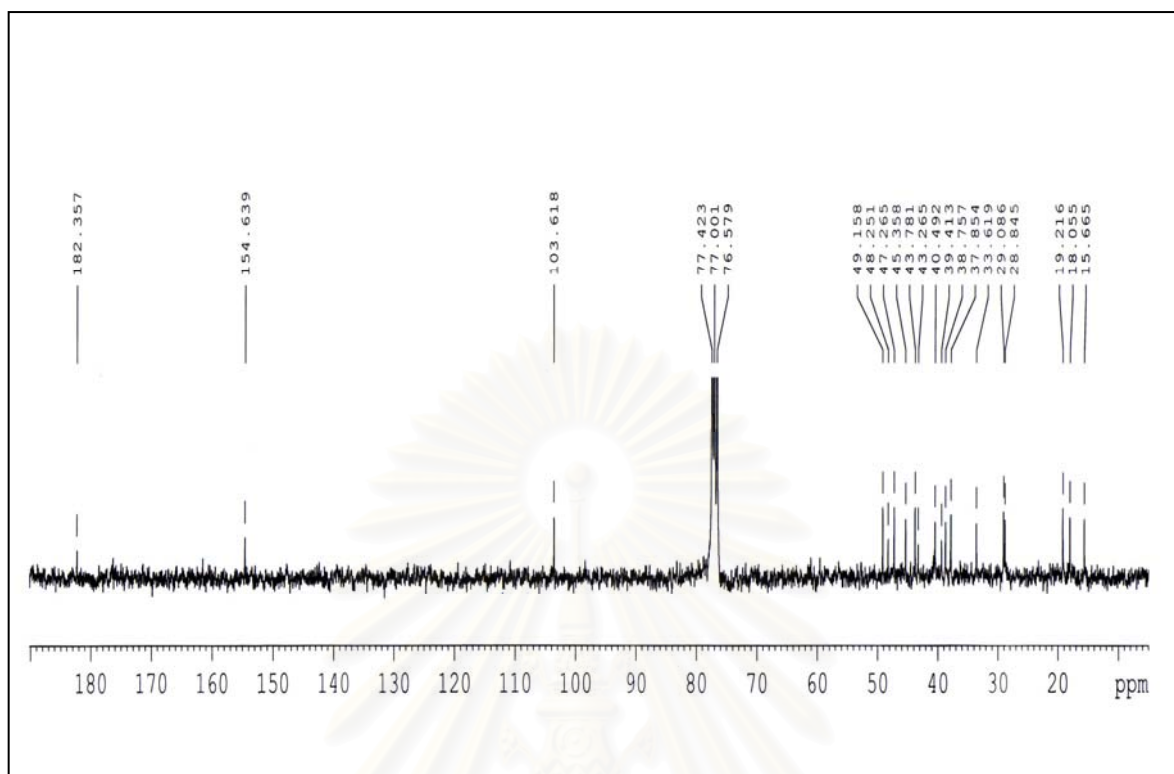
Figure 111. ^{13}C NMR (75 MHz) Spectrum of compound MML-6 (in CDCl$_3$)
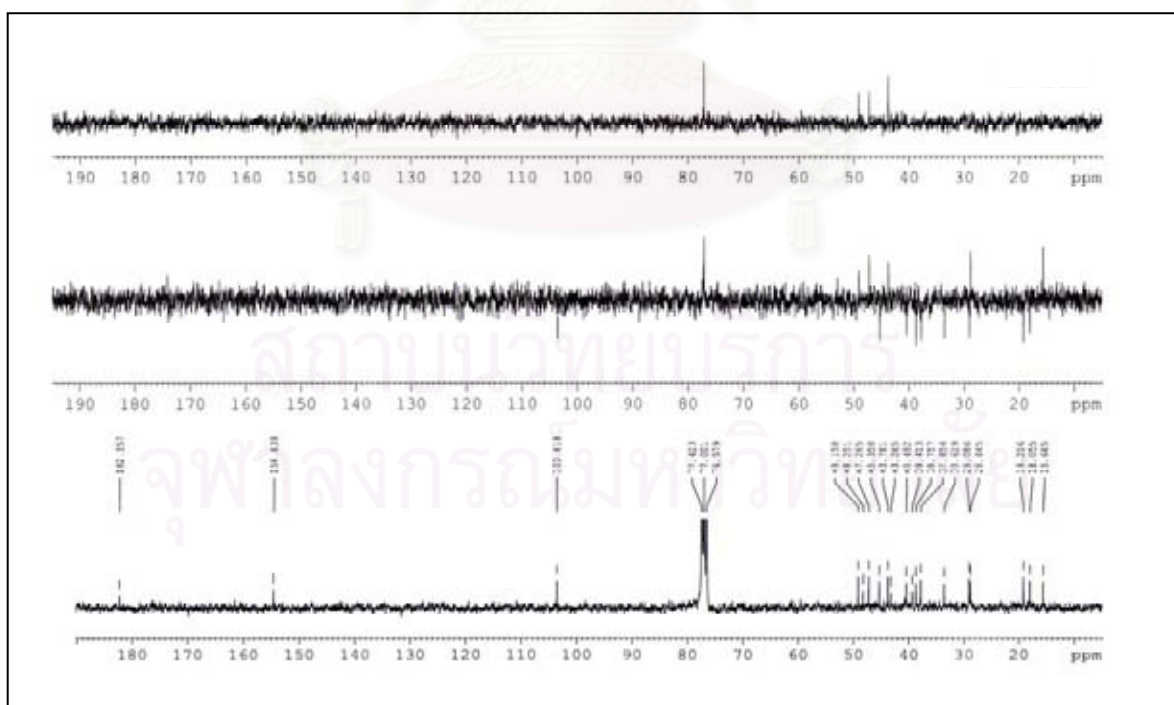
Figure 112. DEPT Spectra of compound MML-6 (in CDCl$_3$)
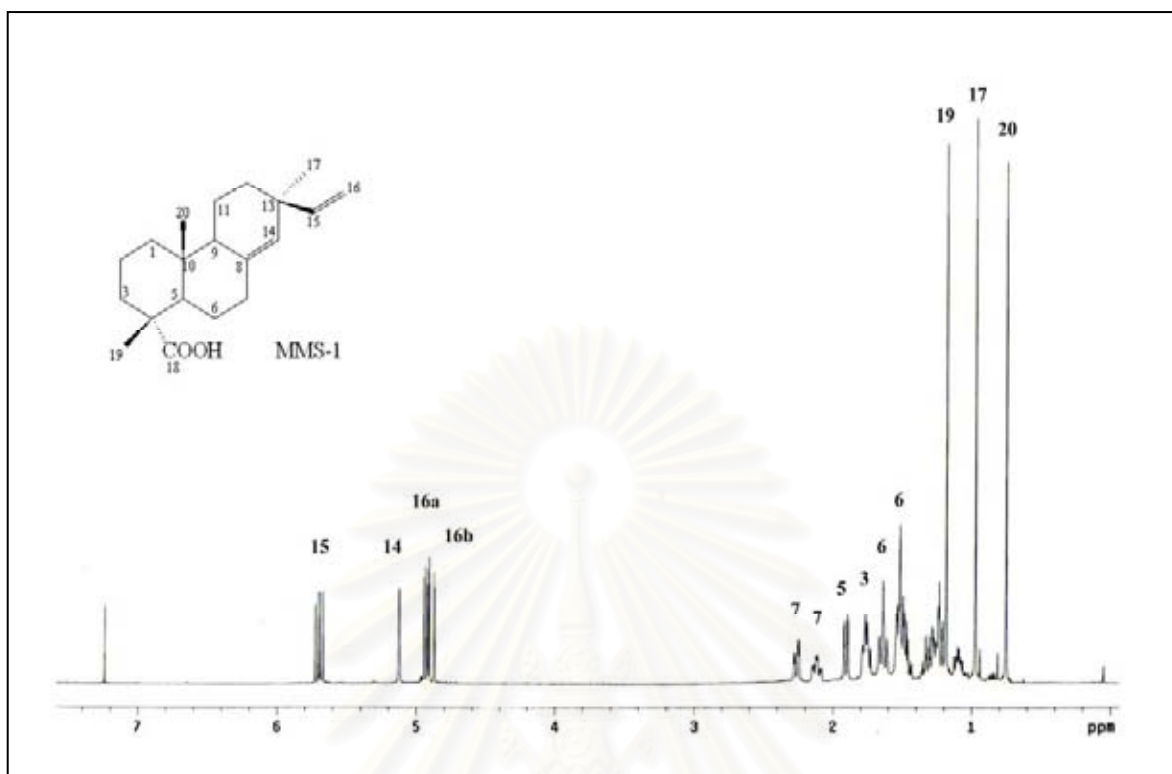
Figure 113a. ^{1}H NMR (500 MHz) Spectrum of compound MMS-1 (in CDCl$_3$)
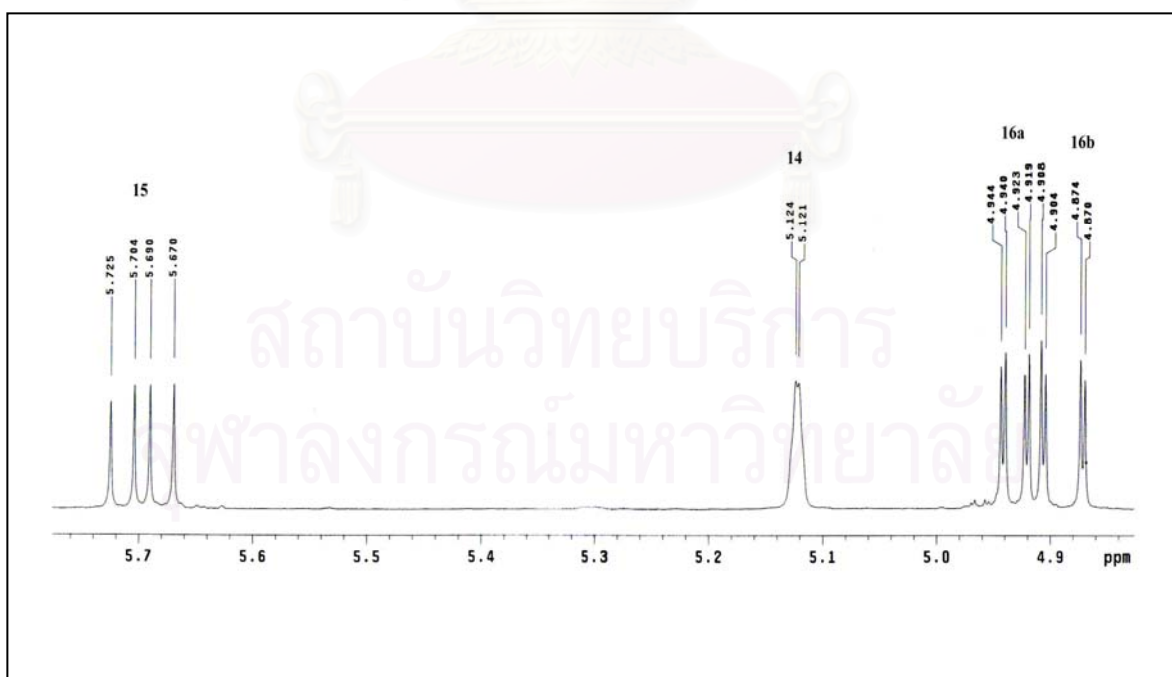
Figure 113b. ^{1}H NMR (500 MHz) Spectrum of compound MMS-1 (in CDCl$_3$, expansion)
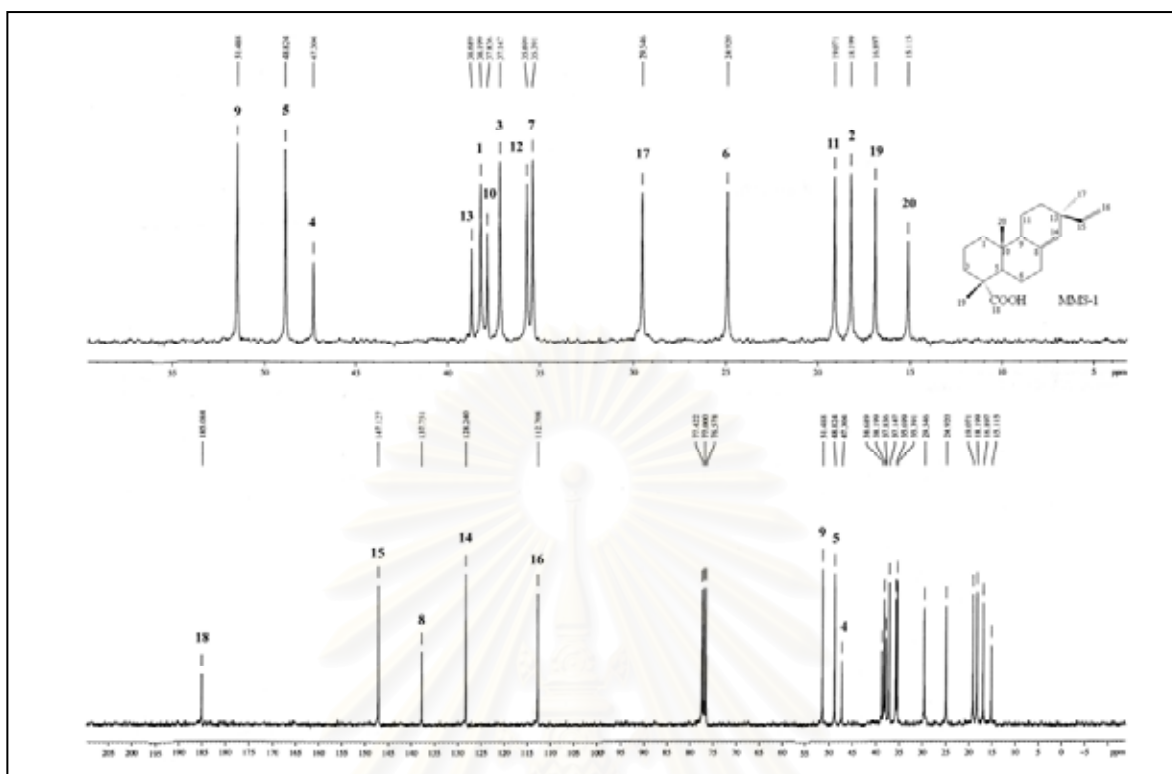
Figure 114. ^{13}C NMR (75 MHz) Spectrum of compound MMS-1 (in CDCl$_3$)
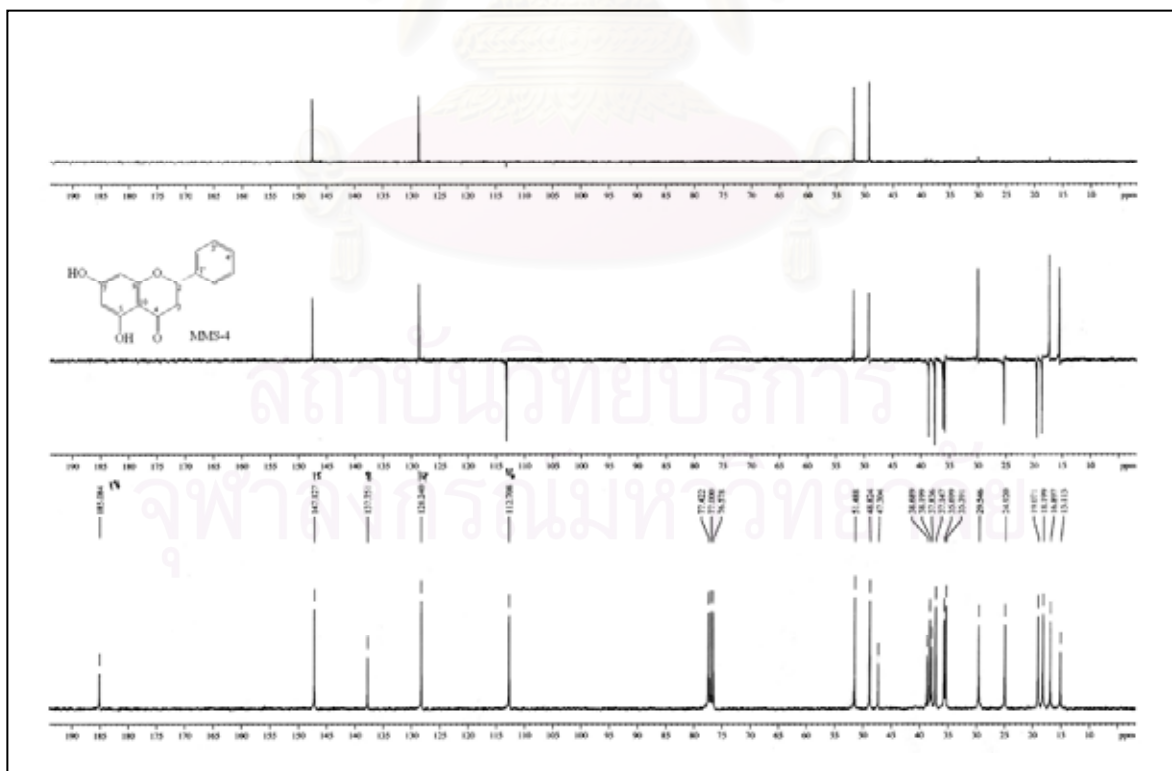
Figure 115. DEPT Spectra of compound MMS-1 (in CDCl$_3$)
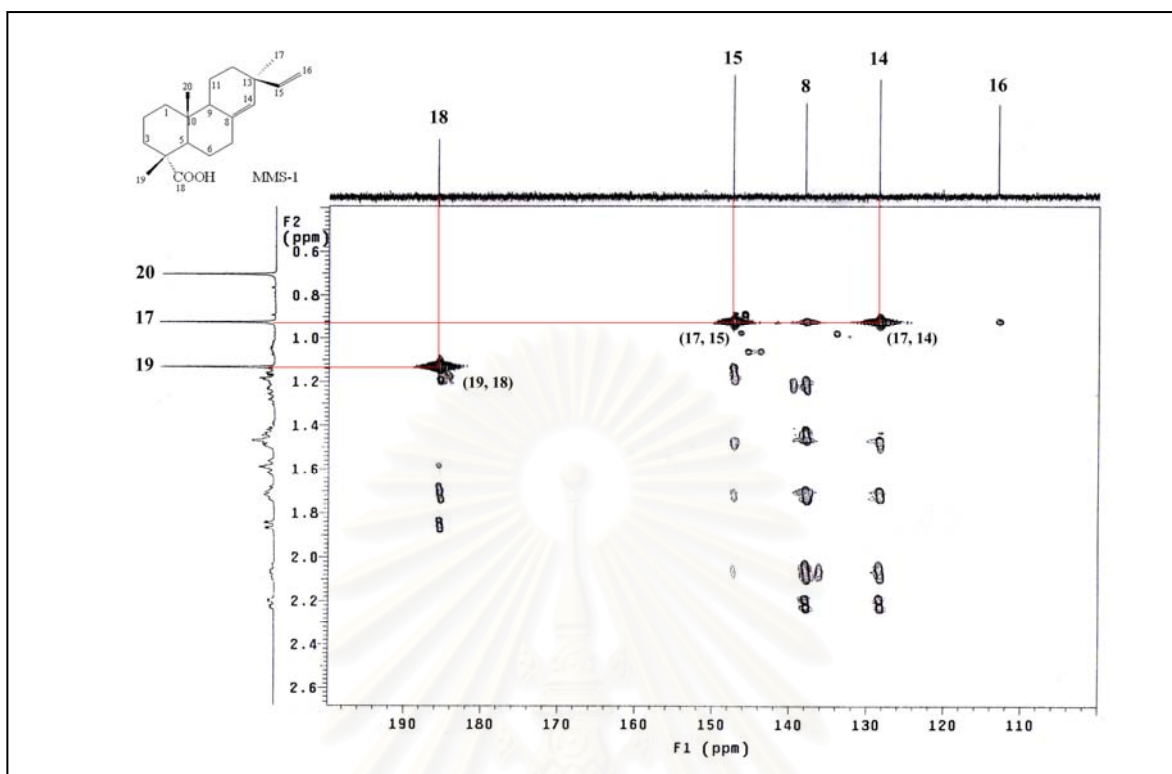
Figure 116a. HMBC Spectrum of compound MMS-1 (in CDCl₃)
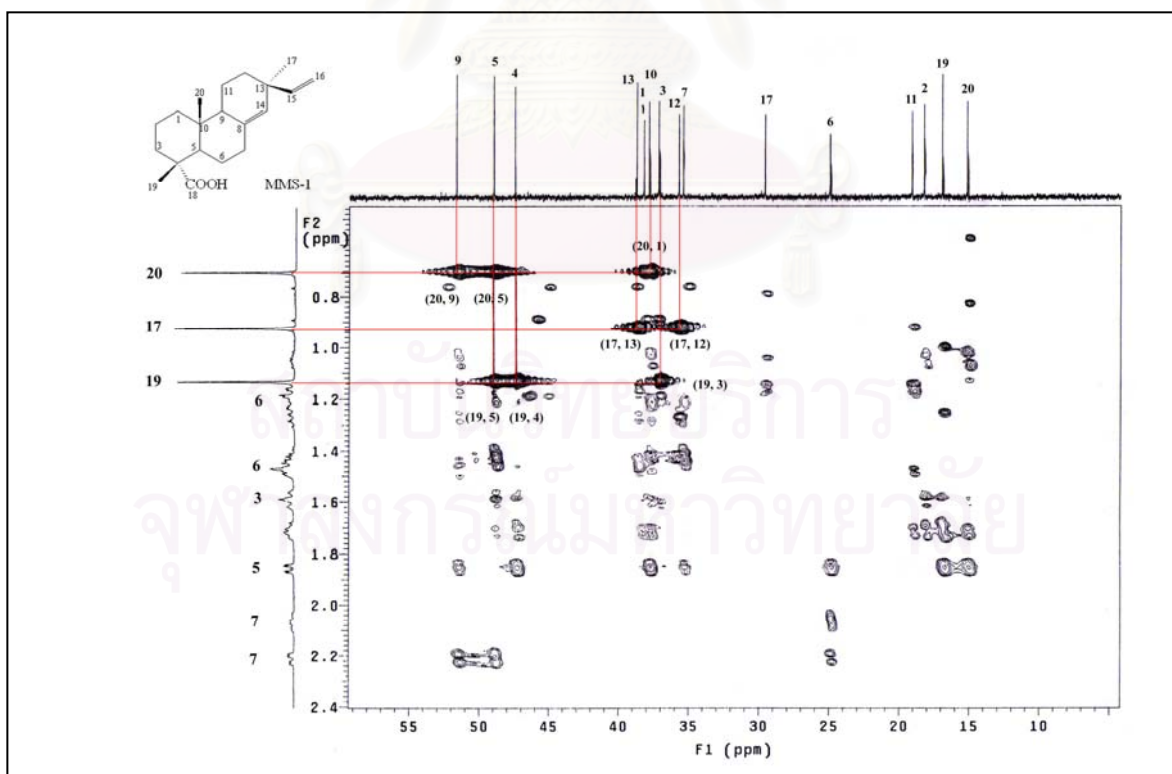
Figure 116b. HMBC Spectrum of compound MMS-1 (in CDCl₃)
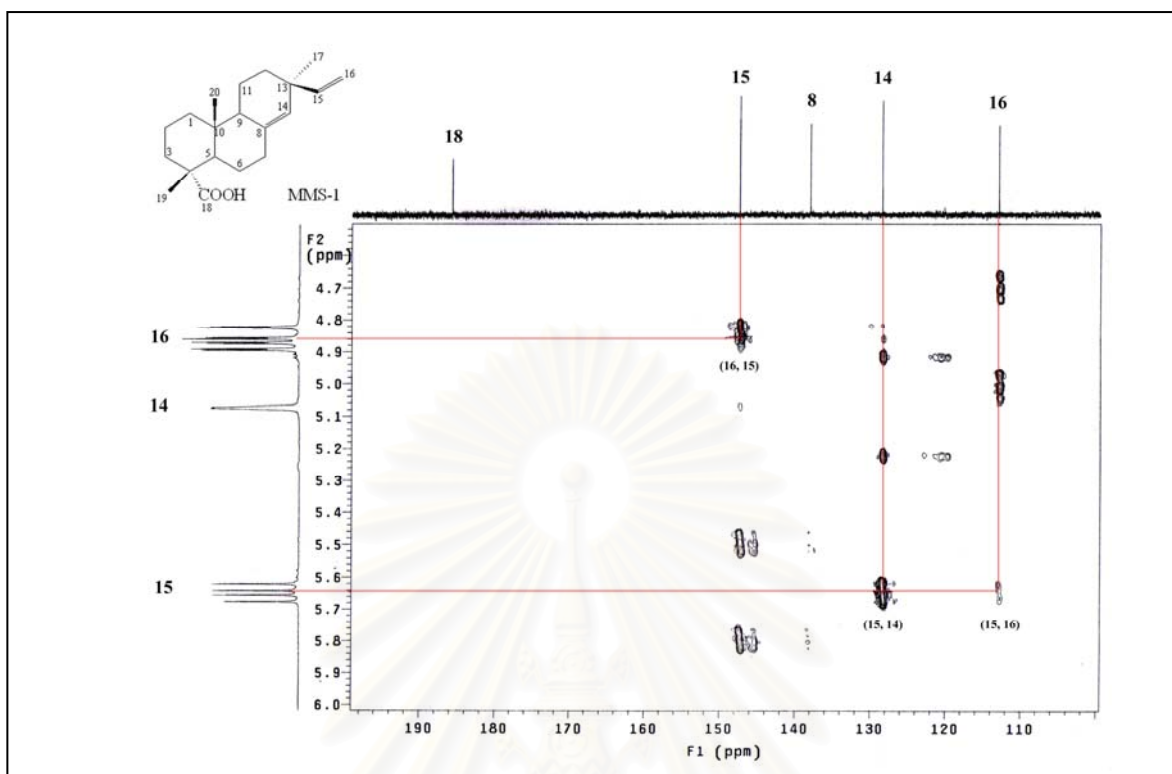
Figure 116c. HMBC Spectrum of compound MMS-1 (in CDCl$_3$)

Figure 116d. HMBC Spectrum of compound MMS-1 (in CDCl$_3$)

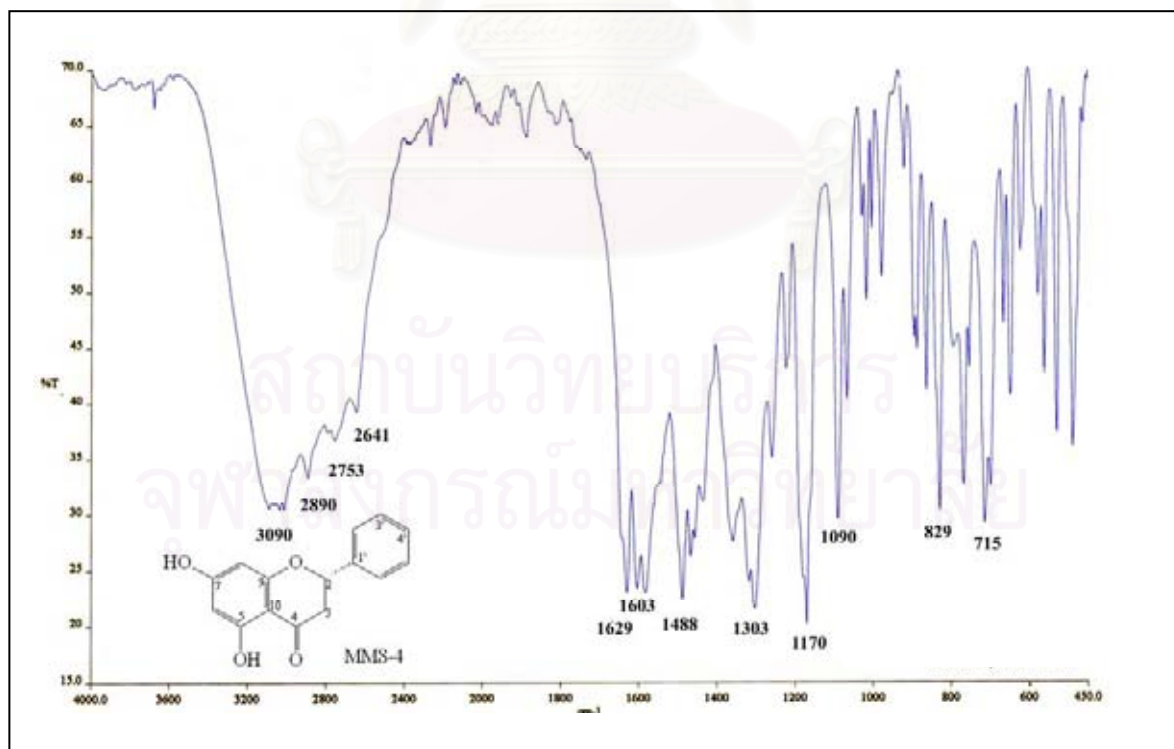**Figure 117.** UV Spectrum of compound MMS-2 (in MeOH)

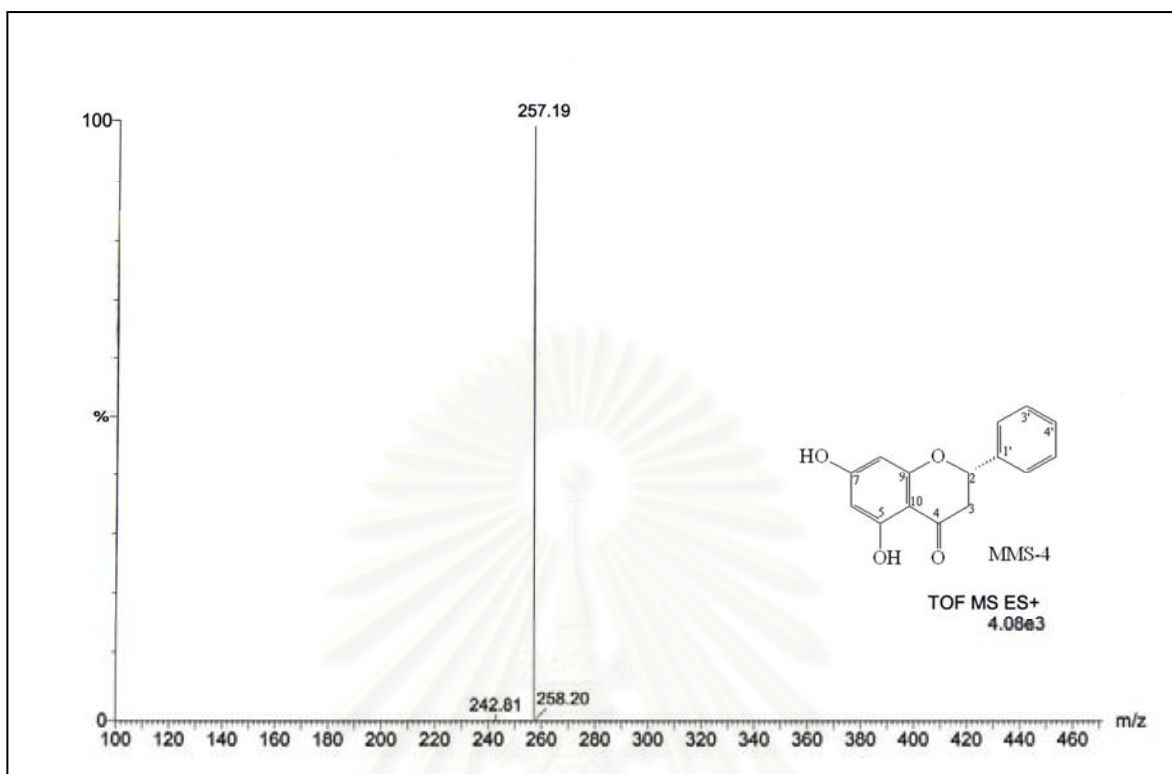**Figure 118.** IR Spectrum of compound MMS-2 (KBr disc)

Figure 119. ESITOF Mass spectrum of compound MMS-2
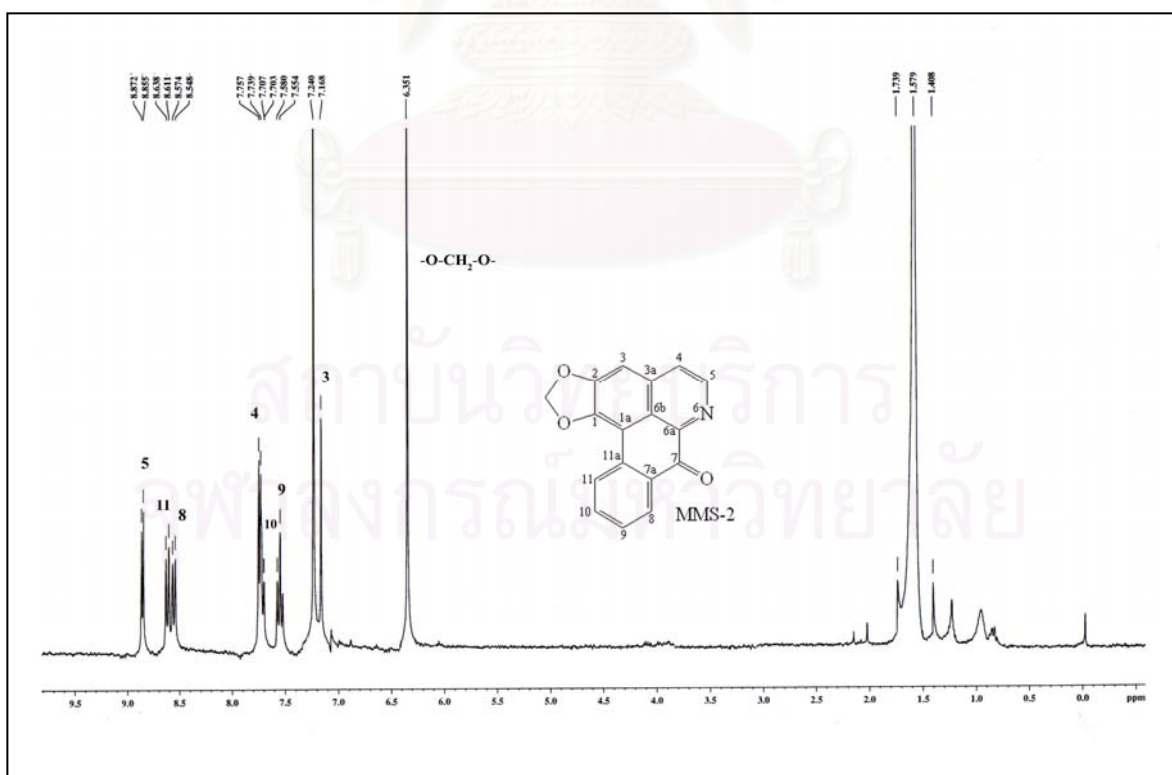
Figure 120. ^{1}H NMR (300 MHz) Spectrum of compound MMS-2 (in CDCl$_3$)

Figure 121. UV Spectrum of compound MMS-3 (in MeOH)

Figure 122. IR Spectrum of compound MMS-3 (KBr disc)
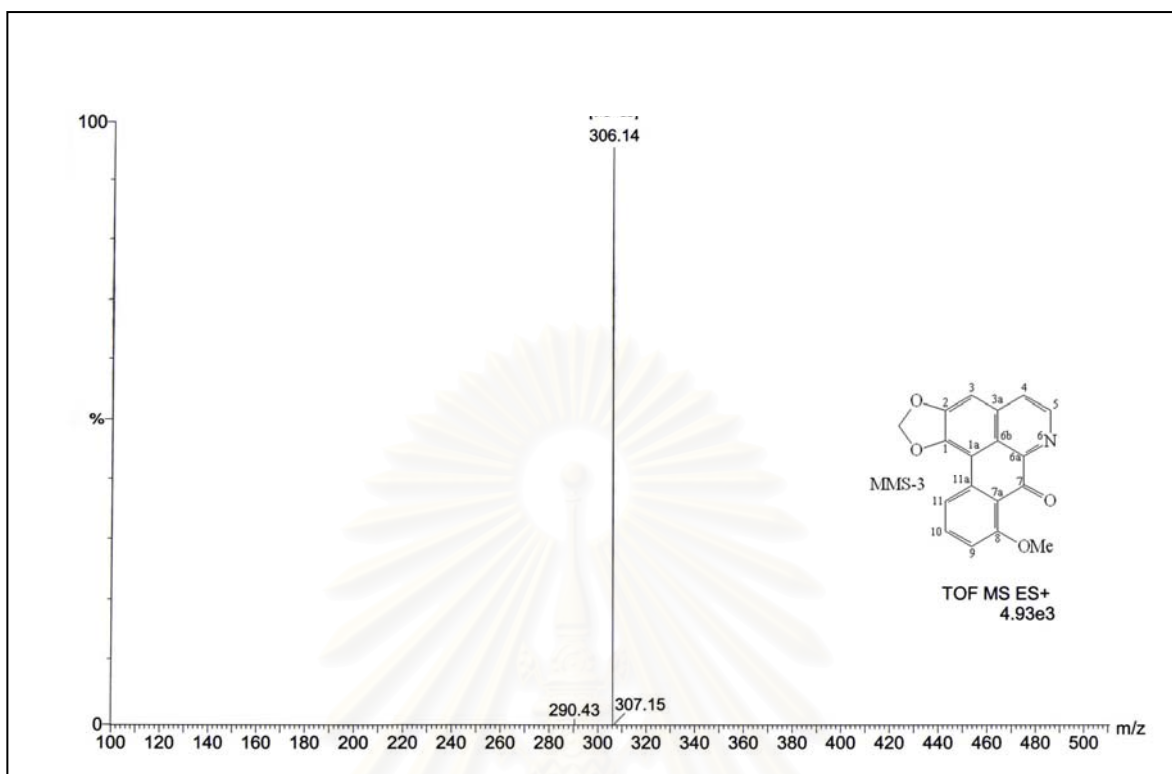
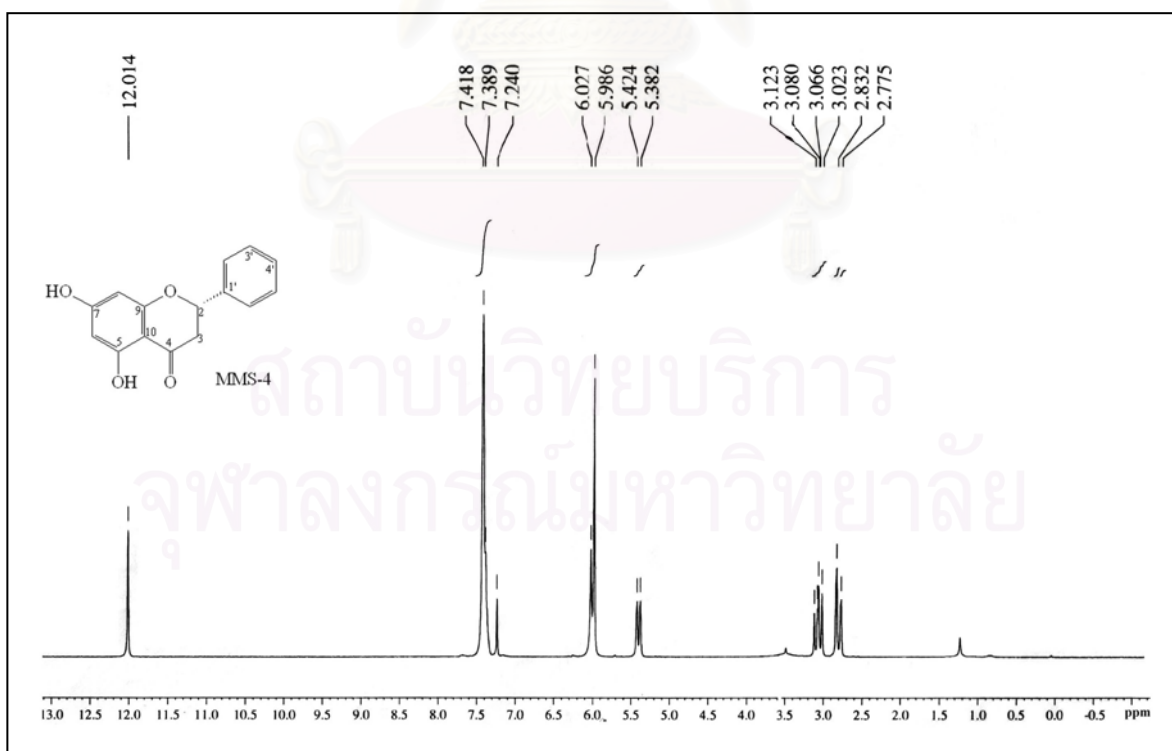**Figure 123.** ESITOF Mass spectrum of compound MMS-3

Figure 124. ^{1}H NMR (300 MHz) Spectrum of compound MMS-3 (in CDCl$_3$)
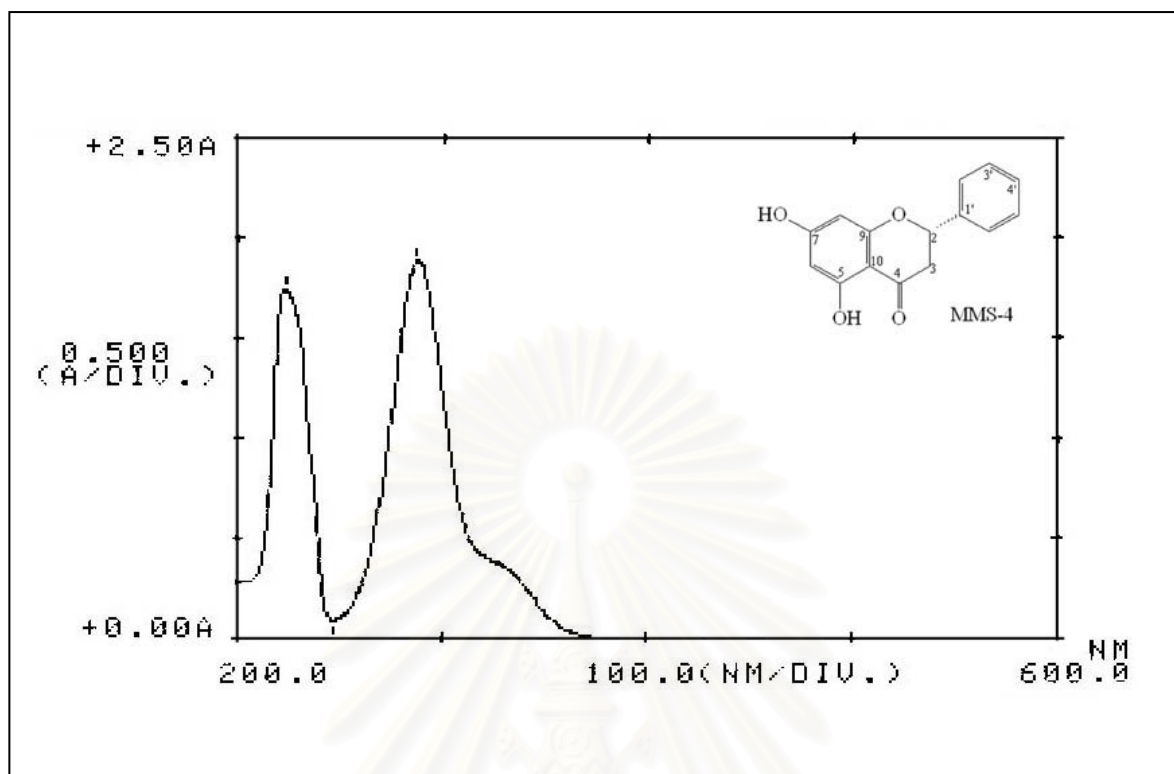
Figure 125. UV Spectrum of compound MMS-4 (in MeOH)

Figure 126. IR Spectrum of compound MMS-4 (KBr disc)
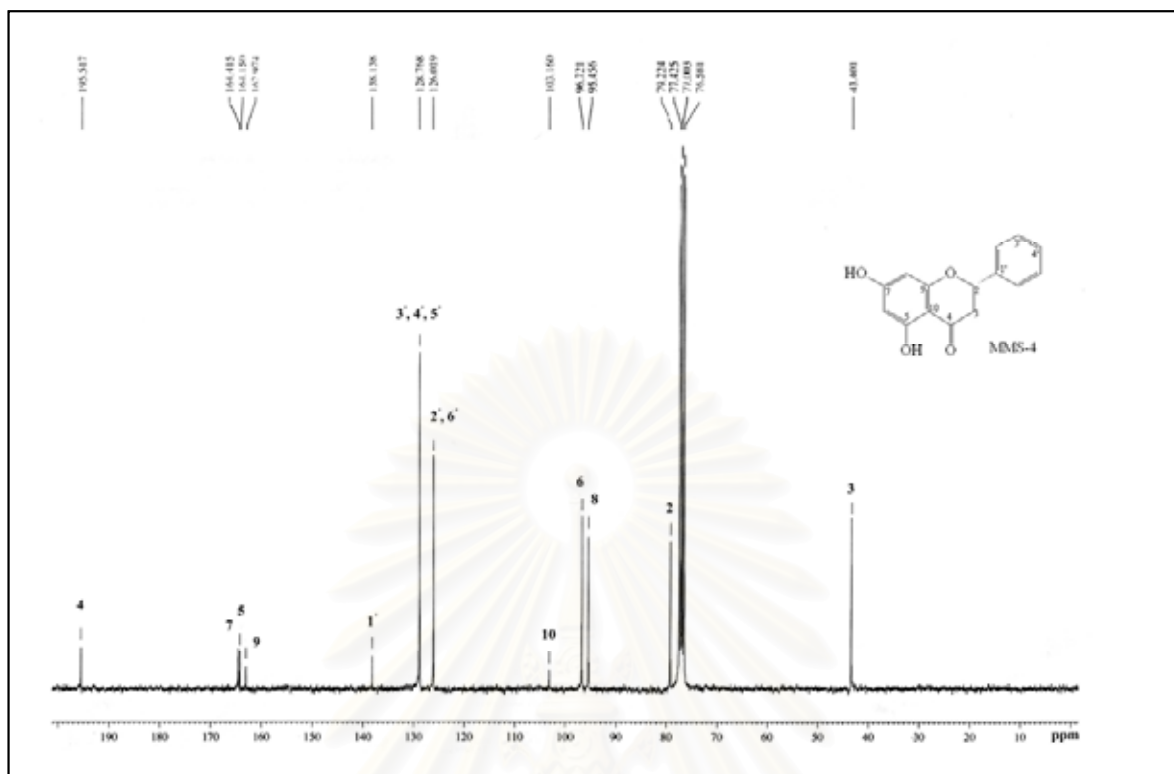
Figure 127. ESITOF Mass spectrum of compound MMS-4

Figure 128. ^{1}H NMR (300 MHz) Spectrum of compound MMS-4 (in CDCl$_3$)

Figure 129. ^{13}C NMR (75 MHz) Spectrum of compound MMS-4 (in CDCl$_3$)

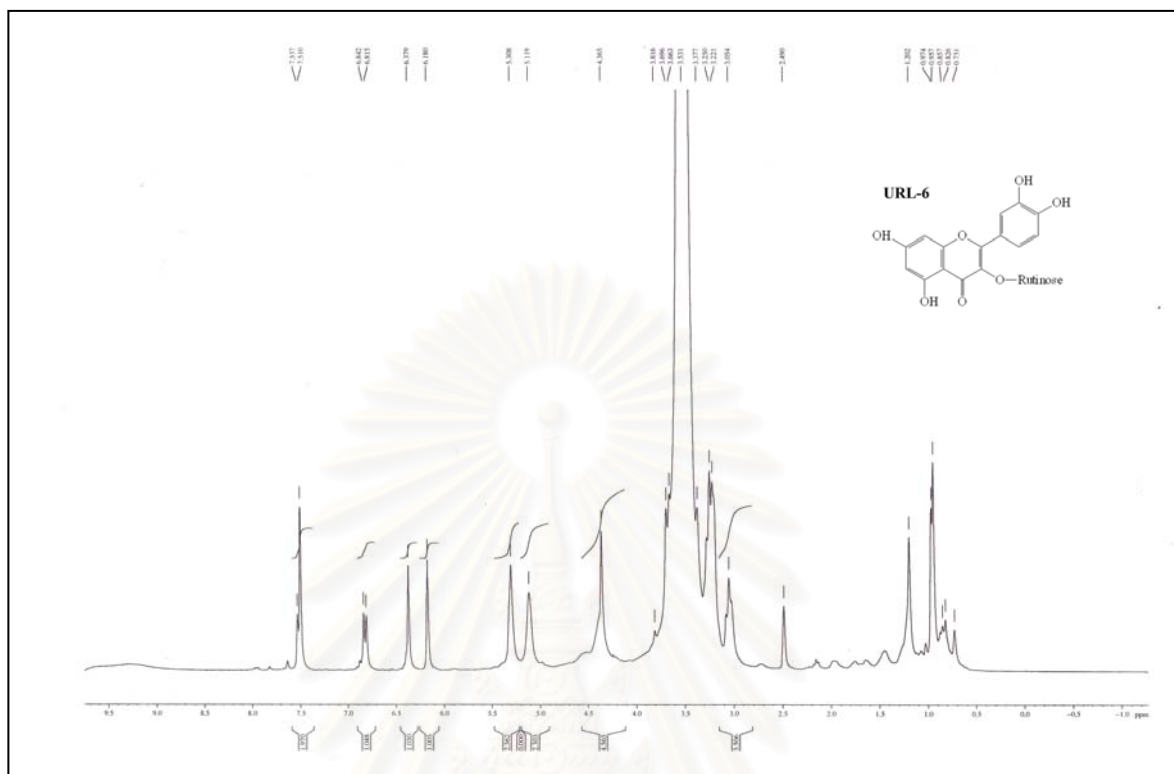**Figure 130.** DEPT Spectra of compound MMS-4 (in CDCl$_3$)
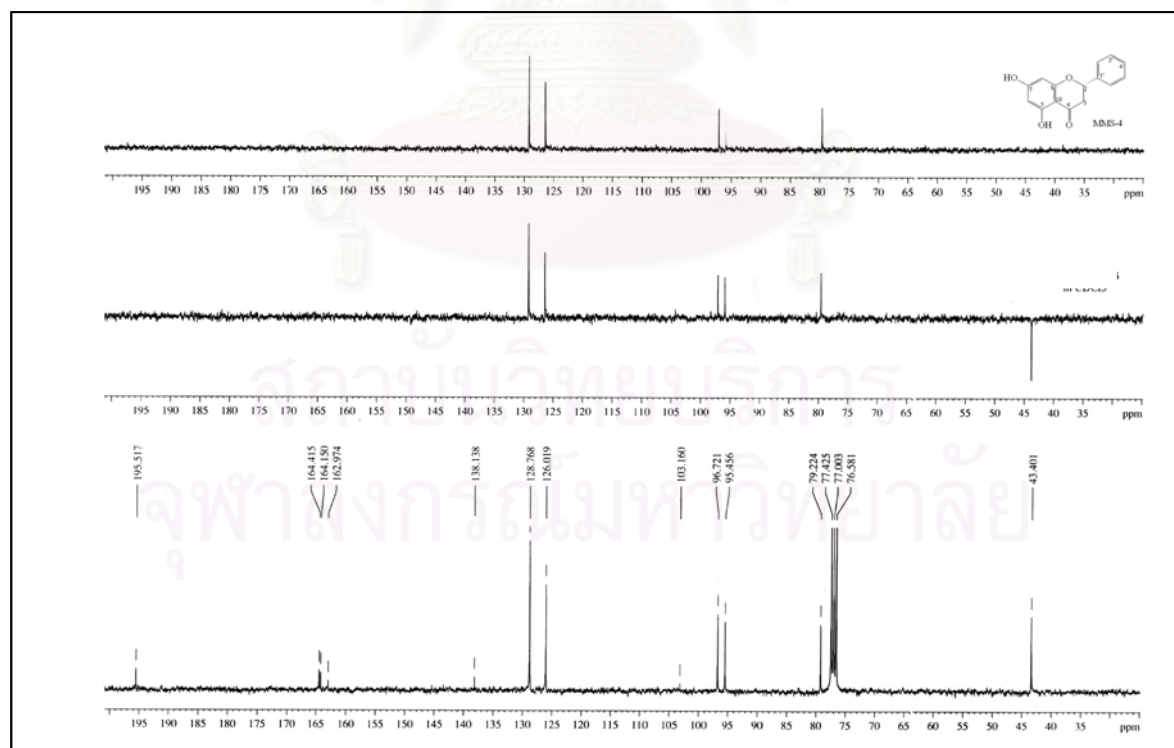
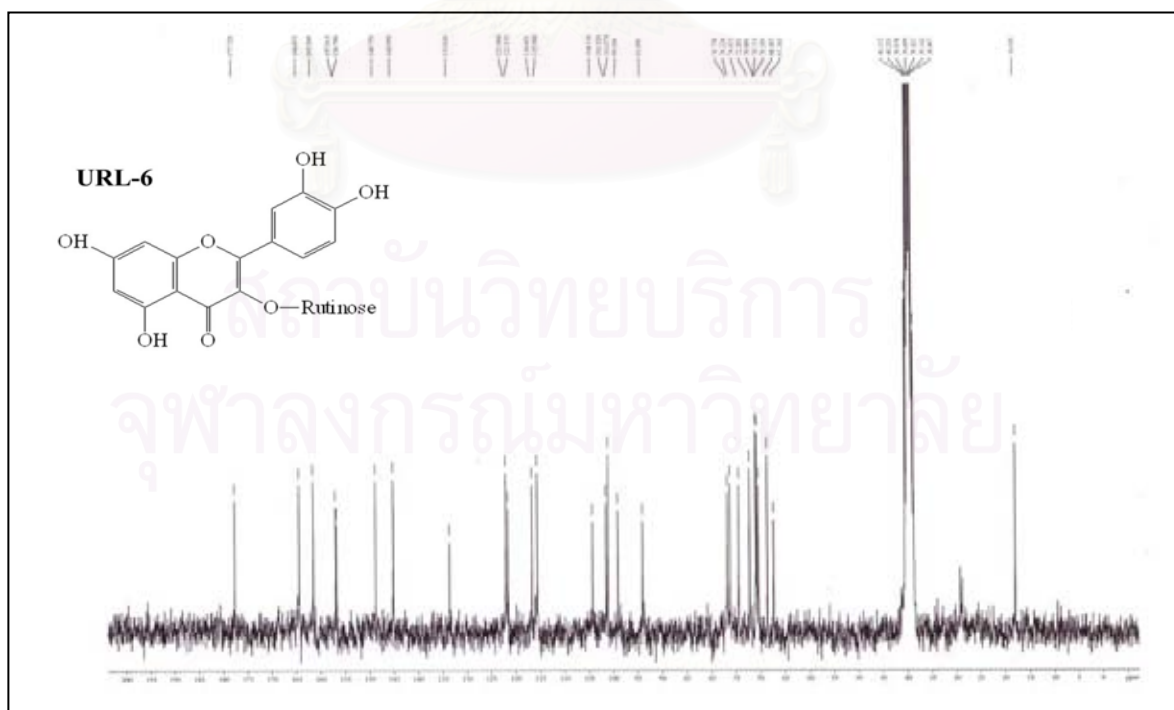**Figure 131.** ^{1}H NMR (300 MHz) Spectrum of compound URL-6 (in DMSO-d_6)

Figure 132. ^{13}C NMR (75 MHz) Spectrum of compound URL-6 (in DMSO-d_6)

Figure 133. ^{1}H NMR (300 MHz) Spectrum of compound URL-7 (in DMSO-d_6)

Figure 134. ^{13}C NMR (75 MHz) Spectrum of compound URL-7 (in DMSO-d_6)

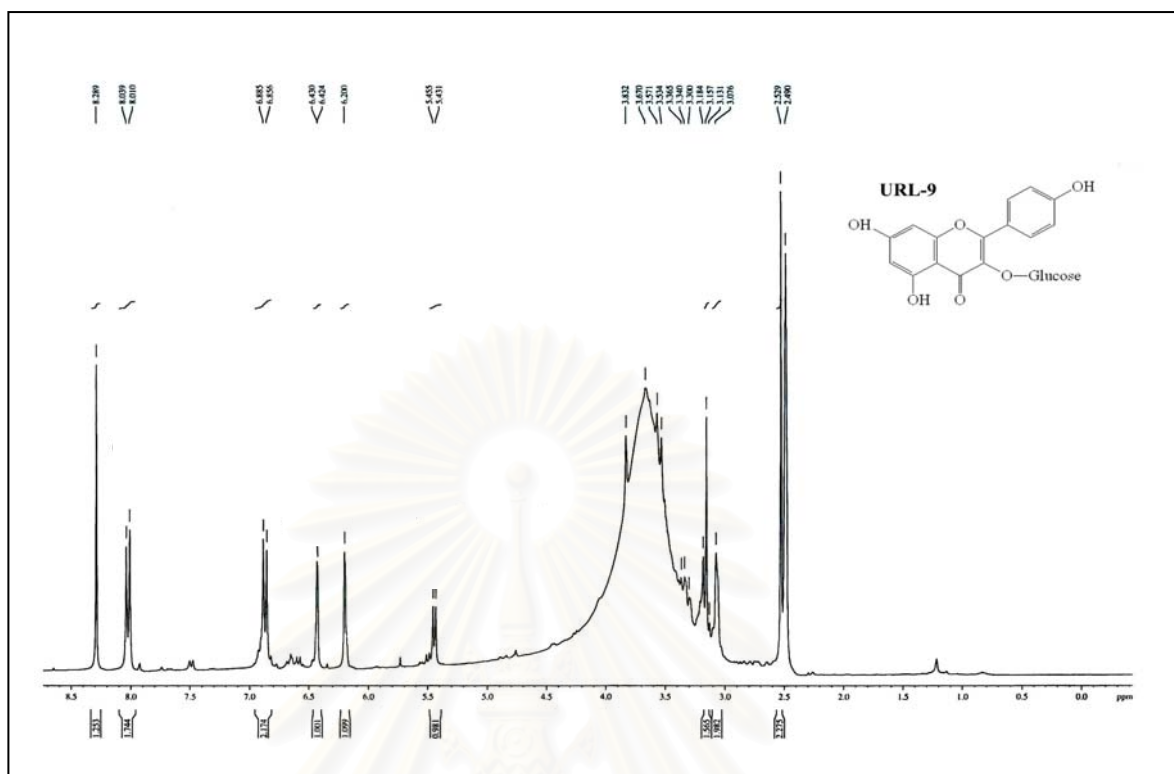**Figure 135.** ^{1}H NMR (300 MHz) Spectrum of compound URL-8 (in DMSO-d_6)

Figure 136. ^{13}C NMR (75 MHz) Spectrum of compound URL-8 (in DMSO-d_6)

Figure 137. ^{1}H NMR (500 MHz) Spectrum of compound URL-9 (in DMSO-d_6)

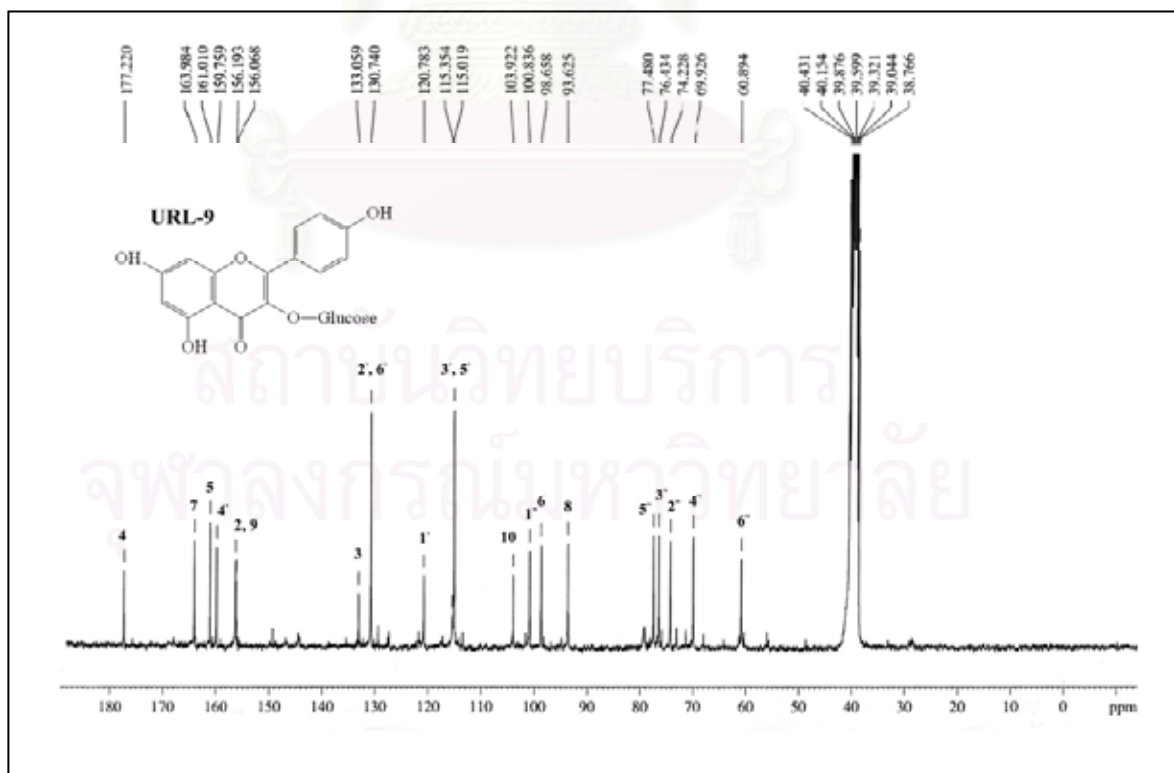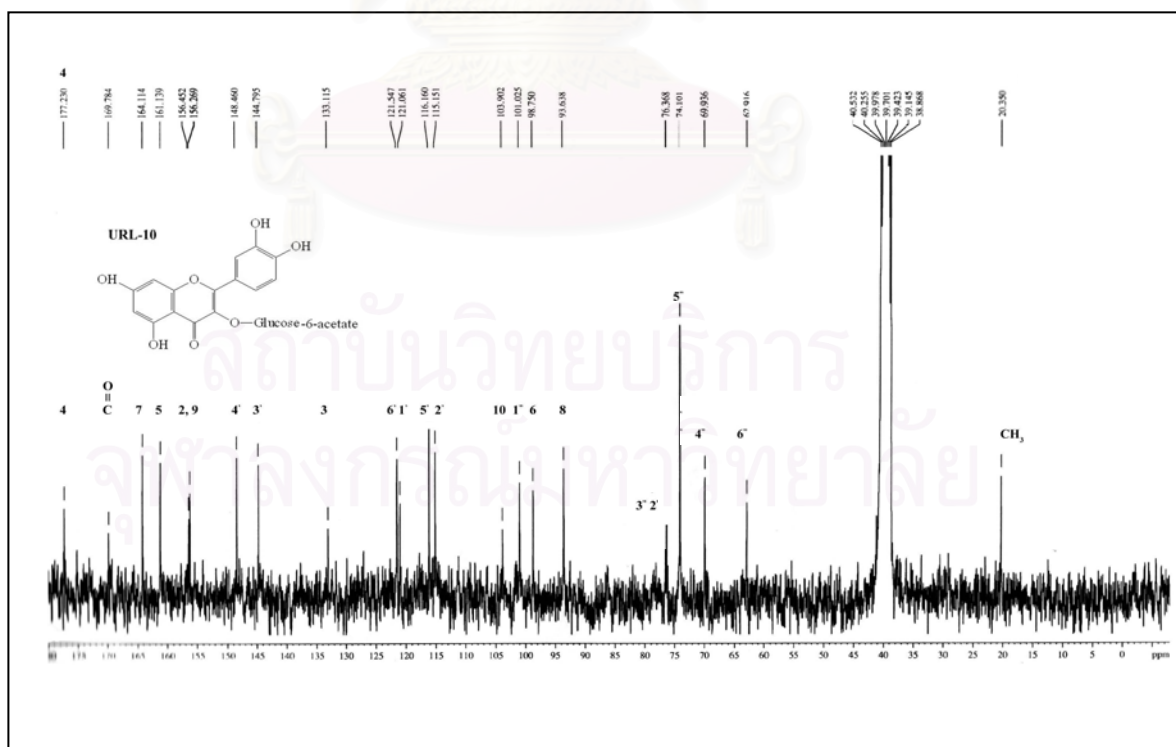**Figure 138.** ^{13}C NMR (125 MHz) Spectrum of compound URL-9 (in DMSO-d_6)

Figure 139. ^{1}H NMR (300 MHz) Spectrum of compound URL-10 (in DMSO-d_6)

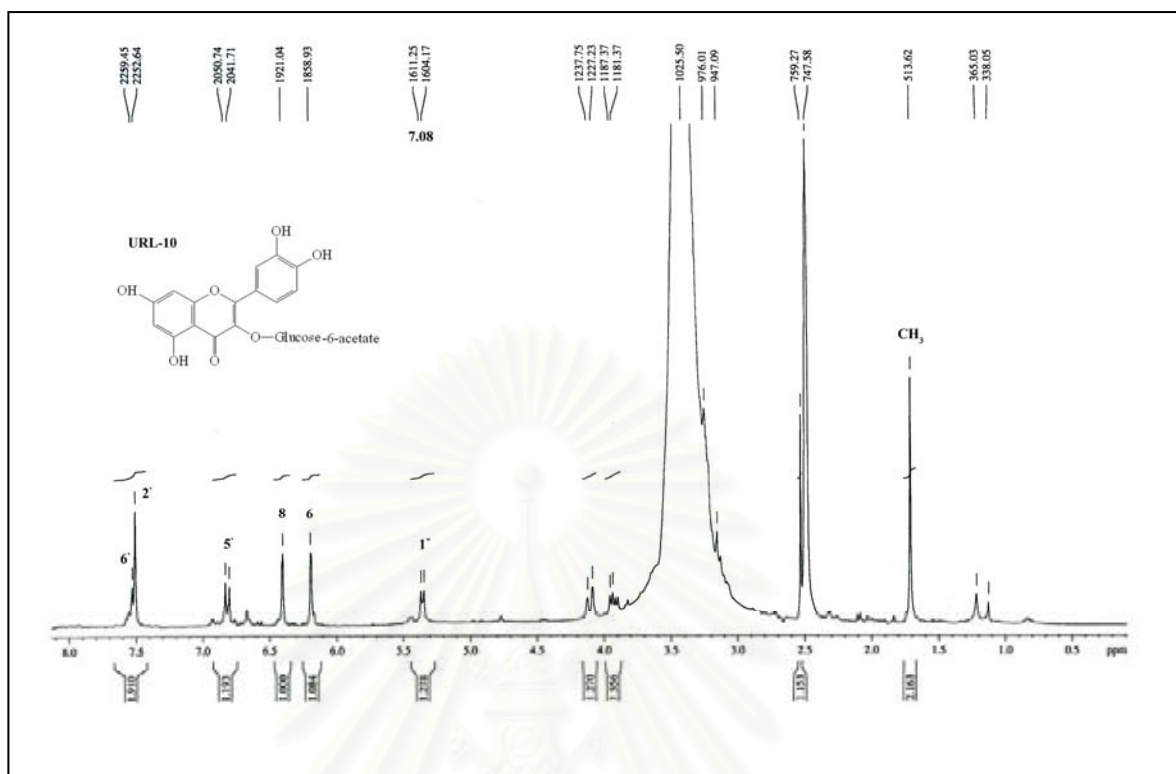**Figure 140.** ^{13}C NMR (75 MHz) Spectrum of compound URL-10 (in DMSO-d_6)

VITA

Miss Khanittha Deepralard was born on May 12, 1972 in Saraburi, Thailand. She received her Bachelor's Degree of Science (Botany) from Kasetsart University, Bangkok, Thailand in 1994. She was granted a scholarship from National Science and Technology Development Agency to pursue her Master Degree of Science in Pharmacy at the Department of Pharmaceutical Botany, Faculty of Pharmaceutical Sciences, Chulalongkorn University in 1997. After graduation, she worked as a researcher at the Institute of Biotechnology and Genetic Engineering, Chulalongkorn University. She was granted a Royal Golden Jubilee Ph.D. Scholarship from the Thailand Research Fund (TRF) in the year 2002.

Publication

1. Juntawong, N. and Deepralard, K. 1997. Effects of prehydration, sucrose concentration and development stage of anther on pollen germination of chili cv Kheenuu (*Capsicum frutescens* L. cv Kheenuu). Kasetsart J. (Nat. Sci.) 30: 373-377.

Poster presentation

1. Wirasathien, L., Deepralard, K., Boonarkard, C., Lipipan, V., Pengsuparp, T. and Suttisri, R. 2003. Lymphocyte proliferation stimulating compounds from two annonaceous plants. NRCT-JSPS CORE UNIVERSITY SYSTEM: The Sixth NRCT-JSPS Joint Seminar in Pharmaceutical Sciences: Drug Development Through Biopharmaceutical Sciences, December 2-4, 2003, Bangkok, Thailand.

2. Deepralard, K., Kawanishi, K., Moriyasu, M, Pengsuparp, T., and Suttisri, R. 2006. Inhibitors of advanced glycation end-products formation from *Uvaria rufa* Blume. RGJ-Ph.D. Congress VII, April 28-30, 2006, Chonburi, Thailand.